Experimental Investigations of the Multiple Impulse Energy Handling Capability of Metal-Oxide Varistors for Applications in Electrical Power Engineering

translation of

Experimentelle Untersuchungen zur Mehrfachimpulsbelastbarkeit von Metalloxidvaristoren für Anwendungen in der elektrischen Energietechnik

Vom Fachbereich Elektrotechnik und Informationstechnik
der Technischen Universität Darmstadt
zur Erlangung des akademischen Grades eines
Doktor-Ingenieurs (Dr.-Ing.)
genehmigte Dissertation

von
Dipl.-Ing. Maximilian Nikolaus Tuczek
Geboren am 14. Mai 1982 in Frankfurt am Main

Referent:	Prof. Dr.-Ing. V. Hinrichsen
Korreferent:	Prof. Dr.-Ing. S. Tenbohlen
Tag der Einreichung:	17. Juni 2014
Tag der mündlichen Prüfung:	12. November 2014

D17
Darmstadt 2015

Translated by Franziska Ospald (M. A.)

This is a translation of the above-mentioned dissertation. The translation has not been checked as thoroughly as the original text and therefore may contain mistakes. For citations and further use please refer to the original dissertation.

Please quote the original dissertation as follows:
URN: urn:nbn:de:tuda-tuprints-4339
URL: http://tuprints.ulb.tu-darmstadt.de/4339

This translation and the original dissertation is provided by tuprints,
e-publishing service of the TU Darmstadt.
http://tuprints.ulb.tu-darmstadt.de
tuprints@ulb.tu-darmstadt.de

Acknowledgements

Contents

List of Symbols

ΔI_{12}	A	difference of the currents flowing through specimen 1 and specimen 2
Φ_{B}	eV	height of potential barrier
α	1	nonlinearity exponent
α	1	first Weibull coefficient
β	1	second Weibull coefficient
ζ	eV	distance between conduction band and Fermi-Level at non-energized condition
θ	1	parameter of the maximum likelihood function
θ_1	1	maximum likelihood parameter for the expected value ($\hat{\theta}_1$ is the point estimator)
θ_2	1	maximum likelihood parameter for the standard deviation ($\hat{\theta}_2$ is the point estimator)
μ	1	expected value
σ	1	standard deviation
C	1	confidence region
C_{int}	F	capacity of an MOV
C_{D}	F	capacity of the double-exponential discharge current generator
C_{R}	F	capacity of the long-duration current impulse generator
d	m	width of potential barrier at non-energized condition
E_{C}	eV	conduction band
$E_{\mathrm{F_n}}$	eV	Fermi level of the boundary layer
E_{F}	eV	Fermi level
E_j	J	Energie stress of class j
E_{V}	eV	valence band
$F_{\mathrm{d}}(x)$	1	distribution function of the double exponential distribution
$F_{\mathrm{l}}(x)$	1	distribution function of the log-normal distribution
$F_{\mathrm{N}}(x)$	1	distribution function of the normal distribution
$F_{\mathrm{w2}}(t)$	1	distribution function of the two-parameter Weibull distribution
$F_{\mathrm{w3}}(t)$	1	distribution function of the three-parameter Weibull distribution

---

[1] The unit of the statistical quantity follows the unit of the investigated characteristic.

$f_\mathrm{d}(t)$	[1]	density function of the double exponential distribution
$f_\mathrm{l}(t)$	[1]	density function of the log-normal distribution
$f_\mathrm{N}(t)$	[1]	density function of the normal distribution
$f_\mathrm{w2}(t)$	[1]	density function of the two-parameter Weibull distribution
$f_\mathrm{w3}(t)$	[1]	density function of the three-parameter Weibull distribution
I	A	amperage
J	A/cm^2	current density
$\hat{J}_\mathrm{ch}$	mA/cm^2	peak value of the current density at which the characteristic voltage is measured
K	1	level of the maximum likelihood function
k_j	1	amount of failures of class j
L	[1]	maximum likelihood function
L_b	H	inductance of an MOV
L_D	H	inductance of the double-exponential discharge current generator
L_max	[1]	maximum value of the maximum likelihood function
$L_\mathrm{MLM}(\theta_1,\theta_2)$	[1]	maximum likelihood function for MLM
$L_\mathrm{PSM}(\theta_1,\theta_2)$	[1]	maximum likelihood function for PSM
L_R	H	inductance of the long-duration current impulse generator
M	[1]	likeliest distribution function
m_j	1	amount of test specimens of class j
n_t	1	density of the trapped charge carriers
R_g	Ω	series resistance of an MOV
R_int	Ω	voltage-dependent resistance of an MOV
R_D	Ω	resistance of the double-exponential discharge current generator
r	1	degree of freedom
T	°C	temperature
t	s	time
t_0	[1]	starting value of the three-parameter Weibull distribution
V	V	voltage
V_c	kV	continuous operating voltage of a surge arrester
V_ch	V	apparent root mean square $(\frac{\hat{U}}{\sqrt{2}})$ of the "characteristic voltage" at a peak value of the current density of $\hat{J}_\mathrm{ch} = 0.12\,\mathrm{mA/cm}^2$
V_COMP	V	voltage of the compensation coil
V_DVM	V	voltage that is transferred to the digital voltmeter
V_IND	V	voltage that is induced by the magnetic field of the main current path

---

[1]   The unit of the statistical quantity follows the unit of the investigated characteristic.

V_{Mes}	V	voltage at the low-voltage section of the voltage divider
V_{pk}	kV	voltage peak value
$V_{\mathrm{pk,\,res}}$	kV	peak value of the residual voltage at a stress with a lightning current impulse of the $8/20\,\mu s$ type at a current peak value of $10\,\mathrm{kA}$
W	J/cm^3	applied energy
w_j	1	amount of specimens of class j that withstood the energy injection

List of Abbreviations

AC	Alternating Current
CR	Cracking
DC	Direct Current
DEDC	Double-Exponential Discharge Current
EGLA	Externally Gapped Line Arrester
FACTS	Flexible AC Transmission System
FO	Flashover
GFRP	Glass-Fiber Reinforced Plastic
GIS	Gas-Insulated Switchgear
HVDC	High-Voltage Direct Current
IEC	International Electrotechnical Commission
IEEE	Institute of Electrical and Electronics Engineers
LabVIEW	Laboratory Virtual Instrumentation Engineering Workbench
LD	Long Duration Current Impulse
MF	Mechanical Failure
MLM	Multiple Level Method
MO	Metal Oxide
MOV	Metal-Oxide Varistor
NGLA	Non-Gapped Line Arrester
NTC	Negative Temperature Coefficient
PC	Personal Computer
PSM	Progressive Stress Method
PTC	Positive Temperature Coefficient
PU	Puncture
RMS	Root Mean Square
SA	Surge Arrester
TOV	Temporary Overvoltage
UHV	Ultra-High Voltage

Abstract

In this thesis, the results of the research on multiple impulse energy handling capability of metal-oxide varistors (MOVs) are described. The focus here is on repetitive impulse stresses with a high energy density where the specimens cool down to ambient temperature after each energy injection. The repetitive energy injection handling capability of MOVs is compared to their single impulse energy handling capability.

It is widely known that the single impulse energy handling capability of MOVs increases with the current density of the impulse stress. This is due to the homogeneous current distribution within MOVs when applying higher current densities. The findings described in this thesis suggest that the temperature dependence of electrical resistance causes a further homogenization of the current distribution within the material of the MOVs at higher current densities. However, the impact of this seems to be small as its influence on the single impulse energy handling capability of the MOVs is not measurable. Furthermore, the results of experiments conducted for this thesis show that short interruptions of long-duration current impulse stresses up to the range of seconds do not increase the impulse energy handling capability of MOVs.

Additionally, the research results illustrate that the repetitive impulse energy handling capability of MOVs does not correlate with their single impulse energy handling capability. Concerning repetitive energy injections at lower current densities, the stress handling capability is very close to the single impulse energy handling capability. However, repetitive impulse stresses with higher current densities cause a reduced stress handling capability compared to the single impulse energy handling capability. Nonetheless, the energy handling capability when applying repetitive energy injections does not drop below the characteristic volume-related nominal energy handling capability of standard surge arresters. With regard to these findings, it is also shown that a change in reference voltage due to prior repetitive stressing of the MOV is not a sure sign for a pre-damage that leads to a decrease in single impulse energy handling capability.

The results gained from this research are discussed with regard to routine tests of MOVs, the usage of surge arresters within electric power systems and the international standardization of surge arresters.

1 Introduction

Concerning the protection of electrical equipment in medium-voltage and high-voltage grids, surge arresters with metal-oxide varistors (MOVs) have become an international standard. As a result of increasing cost pressure and major challenges related to new network constellations (for example in ultra-high-voltage grids), surge arresters are being designed and operated near the limit of their energy handling capability[2] with increasing frequency. In order to guarantee the surge arresters' capability of repeatedly limiting overvoltages when stressed up to the limit of their energy handling capability, new findings on their behavior at limiting loads are required.

Overvoltages can be caused for instance by switching operations inside the grid, errors concerning the grid operation itself or atmospheric influences (such as lightning discharges). Depending on the type of incident, single or – as is very often the case with lightning discharges – multiple overvoltages can occur (see for example [Cig13a] and [Cig13b]). Since surge arresters have to repeatedly limit overvoltages while being operated, the single as well as the multiple impulse energy handling capability of MOVs matter. In addition to the changes within the metal-oxide varistors caused by energy input, heat is generated inside the surge arrester during the discharging process. As long as the heat has not been emitted to the environment, the increase in temperature inside the MOVs reduces their energy handling capability during subsequent stresses.

The strongly non-linear *V-I* characteristic (which is explained in detail in chapter 2.2) allows for a wide application range of MOVs usually without the need for serial spark gaps, which has a positive influence on the protective effect of surge arresters. However, a disadvantage of the strong non-linearity is that, when applying certain types of energy injections, the electric current is not distributed homogeneously inside the MOV. This can lead to a significantly reduced energy handling capability (as shown for example in [Bar01], [He07] and chapter 5.2). Additional factors, such as the temperature dependency of the *V-I* characteristic and microscopic changes in the distribution of charge carriers caused by energy injections (as described for example in [Stu87]), already change the electrical

---

[2] "Limit" in this case refers to the different types of energy handling capability as well as those types of energy stresses (such as temporary overvoltages) that cause a particularly low energy handling capability.

properties of the MOV even before macroscopic mechanical defects occur. Thus, a key characteristic of metal-oxide varistors, "the energy handling capability"[3], depends on many factors, some of which are yet unknown respectively the influences and interdependencies of which have not been sufficiently analyzed yet.

The conditions under which energy injections cause reversible or irreversible changes within MOVs or under which energy injections cause MOVs to fatigue are not only relevant for the design and the operation of surge arresters. They are also important for example for routine tests at the end of the production process during which MOVs with defects are to be identified reliably by applying a destructive energy injection while, at the same time, MOVs without defects must not be pre-damaged.

In previous experimental research (as described in chapter 2.5), the focus (along with the single impulse energy handling capability of MOVs) was on the mechanical fatigue of MOVs caused by current impulses at a high current density and a high current rise time. In this thesis, the experimental research is largely on energy injections at different current densities and low current rise times, but with energy injections up to the electrical overload of the examined MOVs. So far, this kind of energy injection has rarely been analyzed systematically. However, due to the difficulties previously mentioned, research in this field of study is of great relevance.

This thesis was developed in the context of the project "Impuls-Energieaufnahmevermögen von Metalloxidvaristoren für Überspannungsableiter in Hochspannungsnetzen" (English: "Impulse Energy Handling Capability of Metal-Oxide Varistors for Surge Arresters in High-Voltage Grids"), which is supported by the Deutsche Forschungsgemeinschaft (DFG; English: German Research Foundation). In addition to the faculty of "High Voltage Laboratories" (Prof. Dr.-Ing. Volker Hinrichsen), the project also involves the faculties of "Theory of Electromagnetic Fields" (Prof. Dr.-Ing. Thomas Weiland) and "Nonmetallic-Inorganic Materials" (Prof. Dr.-Ing. Jürgen Rödel). Furthermore, this thesis was supported by the Cigré working group A3.25 "MO varistors and surge arresters for emerging system conditions", of which the author of this thesis was a member.

Firstly, in this thesis the design and function of surge arresters and of the MOVs they contain are explained. Subsequently, a description of the state of scientific knowledge and standardization concerning the impulse energy handling capability is given, which leads to the derivation of the motivation for and aims of this thesis in the following section. After that, the test set ups used for this study are described (for detailed information on the

---

[3]   Due to their different effects, different types of energy handling capability are distinguished. They are introduced in chapter 2.3.

applied test set-ups, measurement technique and the resulting measuring uncertainties, see appendix chapter A). In the subsequent sections, the experimental research and the resulting scientific findings are presented. After having described the single impulse energy handling capability, the focus here is on the impact of repetitive multiple impulse stresses with different types of energy injections where the specimens cool down to ambient temperature after each injection. The behavior of the MOVs that could be observed is interpreted at the end of each section. The final part of this thesis consists of a summary of the research results and conclusions which can be drawn from these. In this section, the consequences of the research results are discussed and recommendations for a further development of the relevant international standards and future research are given, too.

In the appendix of this thesis, the test set-ups used are described in detail. It should be noted that the bibliography is split into four separate parts for reasons of clarity.

2 Energy Handling Capability of MOV—Current Scientific Knowledge

In this chapter, the characteristic design and the features of MOVs that are important for their use in surge arresters are described. Due to reasons of space limitations, this section cannot offer an all-encompassing illustration of the subject but has to be narrowed down to topics that become relevant as this thesis is being developed. Subsequently, different types of electric energy handling capability that occur in various practical applications are introduced. After that, the current state of scientific knowledge concerning single and multiple impulse energy handling capability is presented taking experimental studies as well as findings gained through simulation into account. At the end of this section, the current state of international standardization is depicted as it reflects the manufacturers' and users' recent discussions concerning energy handling capability.

2.1 The Use of MOVs in Surge Arresters

(see [ABB11], [Cig13a] and [Hin11])

In order to limit overvoltages, surge arresters must absorb electric energy and convert it into heat. In modern surge arresters, this task is accomplished by the active part of the surge arrester that consists of a column of MOVs. These MOVs are protected against sometimes extreme ambient conditions by a housing. It has to be noted that, depending on the field of application and voltage level, different designs of surge arresters have been established. Concerning air-insulated surge arresters, a basic distinction is made between *directly molded* surge arresters and surge arresters with *tube design*[4] (*gas-insulated* surge arresters are discussed at the end of this chapter). In *figure 2.1*, those two designs are shown next to each other[5]. Regarding the directly molded design, the housing consists

---

[4] Hybrids of both designs exist, too. However, it has been decided to refrain from describing them in this basic description.

[5] The sources were chosen randomly; Siemens as well as ABB produce surge arresters of both design types.

of a synthetic polymer, which is sprayed onto the MOVs. Concerning the tube design, however, the column of MOVs is enclosed by a tubular housing which typically consists of porcelain or glass-fiber reinforced plastic – in the following referred to as GFRP – with sprayed-on synthetic polymer. For the directly molded, the desired mechanical stability is achieved by using GFRP-rods and, according to the requirements, by additional bandages. Looking at the tube design, mechanical stability is guaranteed by the hollow insulator. The column of MOVs clamped with GFRP-rods, which is often fastened to a spring inside the housing, does not contribute to mechanical stability. The housing is supposed to protect the MOVs against environmental influences such as moisture and dirt. If the required arcing and creepage distances (see [IEC60099-4]) require a housing longer than would be necessary for the column of MOVs, the gap is usually filled with metal spacers[6]. One of the characteristics of the tube design is that there is a space between the column of MOVs and the housing, which is usually filled with nitrogen or dry air (rarely with solid material or sulfur hexafluoride (SF_6)) and has to be hermetically sealed off from the environment for its entire operational life span. At the same time, in case of an overload of the active part of the surge arrester and the resulting overpressure, the sealing system has to open up very quickly in order to prevent the housing from bursting.

Surge arresters for medium-voltage applications are produced across all manufacturers almost without exceptions in the cheaper directly molded design. Apart from the designs mentioned above, special international designs and applications should also be mentioned:

Gas-insulated surge arresters are used inside gas-insulated switchgear (GIS). A GIS is insulated by a gas or a mixture of gases, the main component of which is SF_6. This gas also surrounds the column of MOVs in gas-insulated surge arresters. Due to the lower flashover risk when MOVs are surrounded by SF_6, MOVs with higher electric field strength can be used. This can offer constructional advantages.

Line arresters are used to limit overvoltages in overhead transmission lines. A distinction is made between non-gapped line arresters (NGLA) and externally gapped line arresters (EGLA). Concerning externally gapped line arresters, the AC voltage at power frequency is not applied to the column of MOVs but instead almost solely to the serial spark gap. For that reason, there are no thermal stability problems (see chapter 2.3) in consequence of an overvoltage stress. Non-gapped line arresters without a serial spark gap behave like standard surge arresters but are often provided with ground lead disconnectors[7].

---

[6] In some particular applications, various metal spacers may be used specifically in order to increase the energy handling capability, see chapter 2.3.1.

[7] For further information on line arresters, [Cig10] is recommended.

Venting outlet
Sealing ring
Metal spacer
Supporting rod (GFRP)
MOV
Housing
Bandage (GFRP)
Aluminium flange
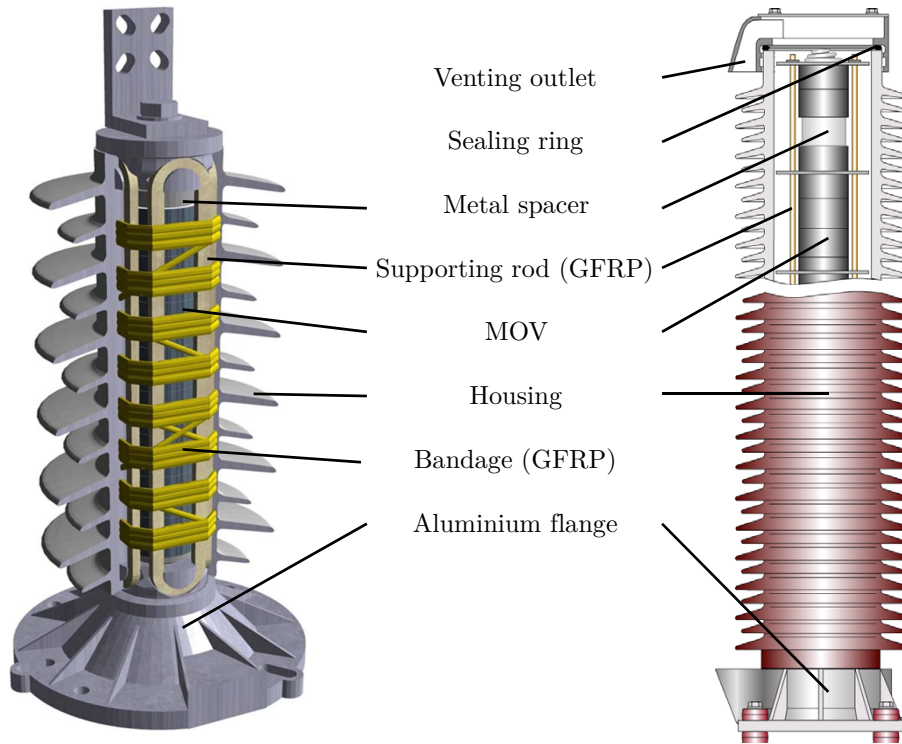
Figure 2.1: Example of surge arresters used at the high-voltage level. On the left, a *directly molded* surge arrester; on the right, a surge arrester in *tube design.* Source on the left: ABB ©ABB AG, Source on the right: Siemens ©Siemens AG

Separable arresters are used for example in switchgear for the medium- and high-voltage level and are characterized from a constructional point of view by a grounded housing and a connection system, which allows for an easy replacement of arresters.

Surge arresters in power-electronics applications have occasionally been stressed continuously with high peak currents of low energy density respectively with unconventional types of energy. For example, considering high-voltage direct current transmission (HVDC), surge arresters are used in converter stations to limit overvoltages inside the converter towers or inside the filter circuits[8].

Under-oil surge arresters are used in oil-insulated transformers, the insulating oil directly encompassing the column of MOVs. Thus, the surge arresters protect the regular windings of the transformers. In the USA and in Japan, these surge arresters additionally protect primary windings of transformers of the medium-voltage level (see [Cig13a] and [Ish04]). In both cases, the MOVs are operated at higher temperatures (at transformer oil temperature).

---

[8] Different fields of application and types of energy stresses can be found in [IEC-37/417/FDIS].

Surge arresters for the protection of capacitors are used for example in flexible AC transmission systems (FACTS). In case of an earth fault in a power system with a series compensation system, the serial capacitors have to be protected from the short circuit current at power frequency in the affected phase. This is achieved by surge arrester banks that are connected to the capacitors in parallel and contain several parallel columns of MOVs (in some cases up to one hundred). These columns of MOVs draw the energy until the earth fault is shut down (or until the short-circuiting of the capacitors) respectively they provide a parallel current path (see [IEC60143-2]). In this field of application, the MOVs are stressed almost exclusively with AC voltage energy injections at power frequency. Concerning this kind of usage, thermal stability (see chapter 2.3) is not a design criterion. However, especially in this field of application, MOVs are often stressed up to the limit of their energy handling capability.

2.2 Behavior and Production Process of MOVs

(see [Cig13a], [Cla99], [Eda89], [Gre90], and [Gup90])

MOVs are used for limiting overvoltages due to their strongly non-linear *V-I* characteristic. An example of such a *V-I* curve is given in *figure 2.2*. In this characteristic, the voltage peak value is plotted above the logarithmically depicted current peak value. For the voltage peak value, a voltage peak value at a discharge current impulse of the $8/20\,\mu s$ type with a current peak value of $10\,kA$ is assumed. Only the resistive parts of current and voltage are shown here; the capacitive and inductive components are usually compensated by means of measurement procedures (see [IEC60099-5] and [Rei08]).

The section of the *V-I* characteristic that shows very small amperages is called "range of leakage current" and is characterized by its relatively linear behavior. The nonlinearity exponent α is defined by the equation:

$$I \sim V^{\alpha} \tag{2.1}$$

At these current densities, α is in the low single-digit range (for example, [Kle04] assumes $\alpha \approx 1$, [ABB11] $\alpha \leq 5$ and [Lev76] also assumes $\alpha \approx 1$). The continuous operating voltage V_c of a standard surge arrester typically lies within this range. According to [IEC60099-5], it is supposed to be about $5\,\%$ higher than the highest continuously applied phase-to-ground voltage of the grid.
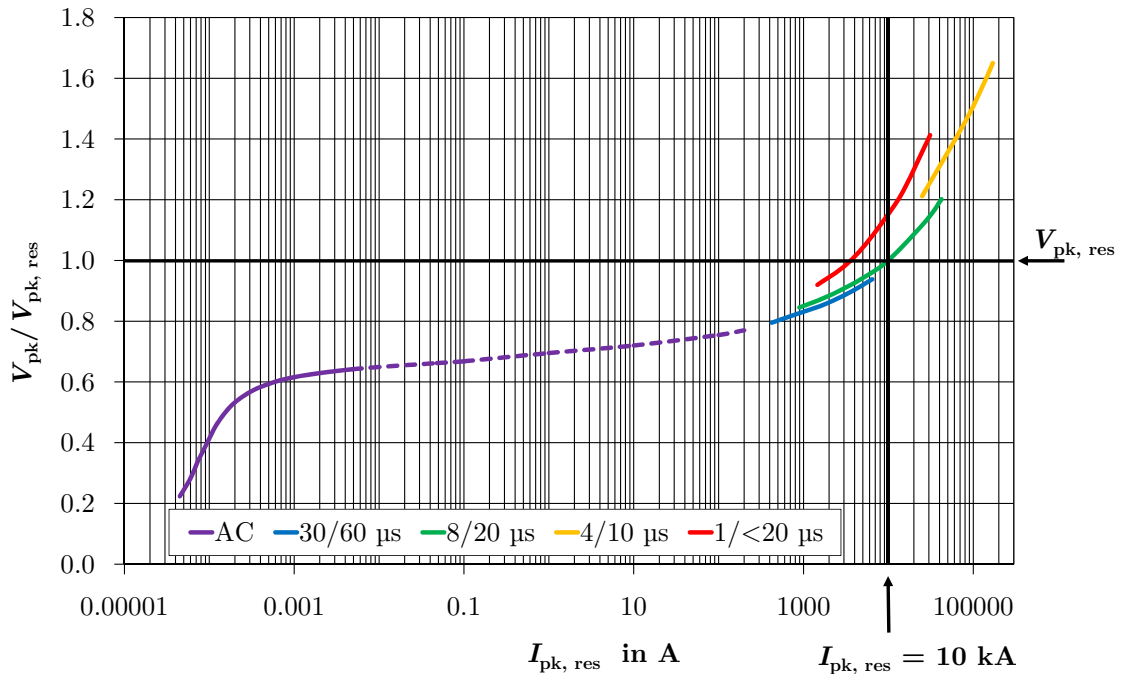
Figure 2.2: Schematic diagram of a resistive *V-I* characteristic of an MOV as it could be applied in a surge arrester at high-voltage level. The voltage peak values are scaled to a residual voltage at a current peak value of 10 kA.

In the adjacent dashed section showing the largest nonlinearity in the *V-I* characteristic, α is in the double-digit range (for example, [Kle04] assumes $\alpha \approx 30$ to 70, [Sch94] assumes up to $\alpha = 150$, [ABB11] $\alpha \leq 50$, and [Lev76] also assumes $\alpha \approx 50$). As has also been done here, the values in this range of *V-I* characteristics are often approximated as the attempt to specify these by AC or DC measurements would lead to a destruction of the MOVs. Moreover, double-exponential discharge current circuits (see chapter 4.4) often cannot produce such small amperages. Surge arresters are only operated in this range of the *V-I* characteristic if temporary overvoltages (TOVs) at power frequency occur or for some half-waves at power frequency when protecting series compensation systems.

Within the range of higher currents, α decreases again and approaches low single-digit values (for example, [Kle04] assumes $\alpha \approx 1$, [ABB11] $\alpha \leq 5$ and [Lev76] also assumes $\alpha \approx 1$). In this range, the values of the *V-I* characteristic are usually identified by double-exponential discharge currents. It can be seen that the voltage peak values measured are dependent on the type of the impulse (current rise time), which will be discussed later in this chapter. Amperages within this range can be caused during actual operation for example by lightning discharges or switching operations.
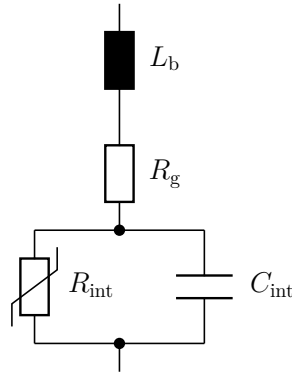
Figure 2.3: Equivalent circuit diagram of an MOV (see [Lev76]).

Figure 2.3 shows a simple equivalent circuit diagram[9] of an MOV, with the help of which wide ranges of the *V-I* characteristic can already be illustrated. The capacitance C_{int} is connected in parallel to the voltage-dependent resistor R_{int}. These two components primarily represent the characteristic features of the grain boundaries inside the MOV, as will be discussed later in this chapter. The capacitance is voltage-, temperature- and frequency-dependent. An overview of several publications on this topic is given for example in [Had90]. The resistor R_g and the inductance L_b are serially connected to the parallel connection of R_{int} and C_{int}. R_g and the L_b are also necessary in order to describe the characteristic features of an MOV and must not be confused with equivalent components for connection wires or the like [Lev76]. Instead, the serial components R_g and L_b reflect the characteristics of the grains of the ceramic as will be described later.

The main component of MOVs is zinc oxide (ZnO) with approximately 90 % of the overall mass. The remaining approx. 10 % consist of oxidic additives that adjust the nonlinearity of the *V-I* characteristic, regulate grain growth, ensure electrical stability of the MOV, or support the production process. The best known additives and their published effects and functions are shown in *table 2.1* (it is not claimed that this table is exhaustive).

Not all of the additives mentioned in *table 2.1* are being used in recent MOVs. The exact composition is, among other things, adjusted to the production process of the respective manufacturer, which is why it differs for the various MOVs currently obtainable. The process of production of modern MOVs (which will be described subsequently according to [Kle04], [Mic70] and [Cig13a]) differs from manufacturer to manufacturer. However, the main features are identical and will be introduced in the following.

---

[9]   An overview of the various equivalent circuit diagrams mentioned in scientific publications can be found for example in [Had90].

Table 2.1: Overview of the best known additives and their effects/functions in MOVs

Additive	Effect and Function
Al_2O_3	• improves conductivity of the $ZnO-Al_2O_3$ grain [Car82] • increases non-linearity of the *V-I* characteristic [Stu90]
Ag, B_2O_3, Ni and molten glass	• improve stability [Eda88]
Pr_6O_{11}, SrO and U_3O_8	• generate or change potential barrier like Bi_2O_3 does (but not with the same intensity) [Eda88]
BeO and TiO_2	• support grain growth [Eda88]
Bi_2O_3	• surrounds the ZnO grain and causes the nonlinearity of the *V-I* characteristic due to the formation of the grain boundary [Eda88] • increases grain growth [Won80] • as a flux, it supports liquid phase sintering [Sch94] • causes homogeneous distribution of the dopants [Kle04] • is not responsible for a strong nonlinearity [Kle04]
CoO and MnO	• considerably improve nonlinearity [Eda88]
Cr_2O_3	• improves nonlinearity [Eda88] • increases stability [Eda88] • limits grain growth [Fl08]
Ga	• improves nonlinearity by providing charge carriers for ZnO [Eda88]
Nb_2O_5	• improves nonlinearity [Aso88] • increases energy handling capability [Aso88]

Table 2.1: Overview of the best known additives and their effects/functions in MOVs *(continued)*

Additive	Effect and Function
Sb_2O_3	- reduces grain growth [Eda88] - supports merging of ZnO and Bi_2O_3 [Eda88] - increases stability against impulse stresses [Eda88] - improves microstructure [Sch94]
SiO_2	- reduces grain growth [Eda88] - improves microstructure [Sch94]

(a)	(b)	(c)	(d)	(e)	(f)	(g)
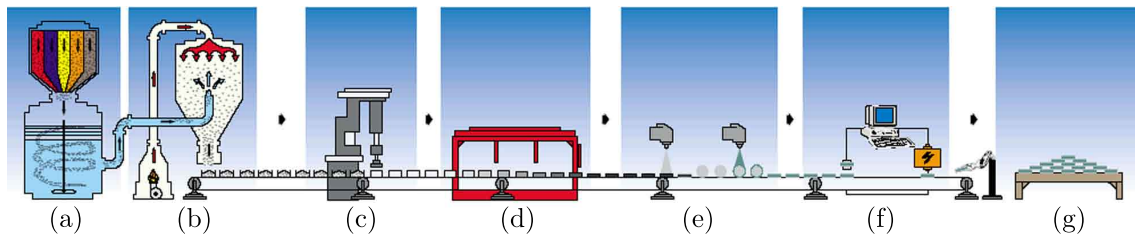
Figure 2.4: The production process of MOVs in strongly simplified terms (according to [ABB11] ©ABB AG).

The production process as shown in simplified terms in *figure 2.4* is divided into seven steps. The main component of MOVs is ZnO with approximately 90 % of the overall mass. The main additives currently used are Bi_2O_3[10], Sb_2O_3, CoO und MnO according to [Cig13a]. Sometimes other additives are added within the ppm range. The first step of the production process involves that, depending on the manufacturer's formula, the additives that are used are weighed, mixed and in some cases grounded in order to achieve a more homogeneous mixing (a). The mixing process is often carried out wetly while adding solvents and binders since this leads to a more homogeneous distribution[11] of the additives. In this case, the mass must be dehumidified (b) in order to lose a large part of the liquid before the next step of the process. This can be done for example in a spray drying process. Subsequently, the powder obtained is pressed into shape[12] in a dry pressing process (mostly uniaxial). At that moment, the product called green block has already

---

[10] There is evidence that some manufacturers use Pr_6O_{11} instead of Bi_2O_3.

[11] Achieving a homogeneous distribution of additives is a complex task as the percentage volume of the additives in some circumstances is within the ppm range. However, a homogeneous distribution of additives is crucial for the quality of the end product [Cig13a].

[12] Cylindrical shapes are common for MOVs used in surge arresters at the high-voltage level. Considering the low-voltage level, other shapes are used, too.

reached 50 % to 60 % of the theoretically attainable density (c). After a pyrolyzing process during which organic solvents and binders are removed, the green blocks are sintered in air. The temperature profile depends on the manufacturer and can reach peak values of up to 1450 °C (d). During the sintering process, grains and grain boundaries are shaped by diffusion processes. Thus, grain sizes[13] in the range of 10 µm to 20 µm are achieved for MOVs in high-voltage applications.

After a defined cooling process, the current-carrying front surfaces of the varistors are smoothed and grinded plane parallel. Moreover, metal electrodes with good electrical conductivity are applied (e). For this step, aluminum has gained a higher acceptance compared to the silver mentioned in [Mic70]. The typical thickness of the aluminum layer is about 0.1 mm (see [Bog00]). In addition to that, a passivation layer is applied to the lateral surface, which is supposed to protect the varistor against environmental influences (for example during storage) and to improve the flashover behavior at high discharge currents. Generally, glasses are used here. It has to be mentioned though that the temperature effects during the baking process might change the structure of the lateral surface of the MOV. This is why glasses that melt at low temperatures are used. However, according to [Dar97], a temperature of 500 °C is needed for the application of metallization and coating. Thus, the required low melting point is often achieved by the addition of lead, which at the same time is undesirable due to reasons of environmental compatibility in terms of waste disposal. Occasionally, varnishes are also used as passivation layers.

At the end of the production process, quality and electrical characteristics of the MOVs are checked in a routine test[14] (f). In order to test the electrical characteristics, depending on the manufacturer, AC and/or DC reference voltages[15], AC and/or DC power losses (depending on the manufacturers' definitions) as well as the residual voltage are measured and mostly imprinted onto a varistor front surface in an encoded form. In order to test the quality, which is essentially defined by the homogeneity of the ceramic, long-duration current impulses, high-current impulses (both defined in [IEC60099-4]) or sinus half-waves at power frequency are applied. The series of impulses are carried out with or without cooling of the MOVs between the impulses and, in some circumstances, with polarity

---

[13] For particular applications of surge arresters, so-called "high-field varistors" have been developed that are characterized by small grains and high a breakdown field strength per height of the MOV. They are used for example in gas-insulated surge arresters (see *Kapitel 2.1*; see for example [Kle04]). For applications of the low-voltage level (for example in automation electronics), MOVs with only few volts breakdown voltage are needed. For these applications, extra-large grains achieved in respective production processes are used [Cla99].

[14] Across all manufacturers, certain tests are carried out only for individual varistors of the production lot due to their negative impacts on the MOV or the high effort required. One example for this is the accelerated aging test according to [IEC60099-4].

[15] The AC reference voltage is defined in [IEC60099-4].

reversals between the impulses. MOVs with defects are supposed to fail during the routine test for example by cracking mechanically in consequence of the energy injection. After having passed the test, the MOVs are packed and stored. In doing so, the humidity is controlled / reduced in most cases (g).

The microstructure of an MOV resulting from the sintering process is depicted in *figure 2.5*. The image was taken with a scanning electron microscope and shows a breakage of a commercially available MOV of the high-voltage level as used in *chapter 5*. Due to the fact that a cracking of the material primarily occurs along the grain boundary (see [Den98]), the image shows the comparatively large ZnO grains and the brightly depicted Bi_2O_3 triple points (see for example [Gre86] and [Stu87]). The bismuth-rich boundary layer[16] between the ZnO grains is responsible for the varistor effect (explained in great detail for example in [Gre90]) that is described in the following. Inside the triple points, so-called spinel phases can be seen (described for example in [Cig13a]). Moreover, the MOV shown in this figure obviously contains air inclusions like those described in [Cig13a].

└──── 30 µm ────┘
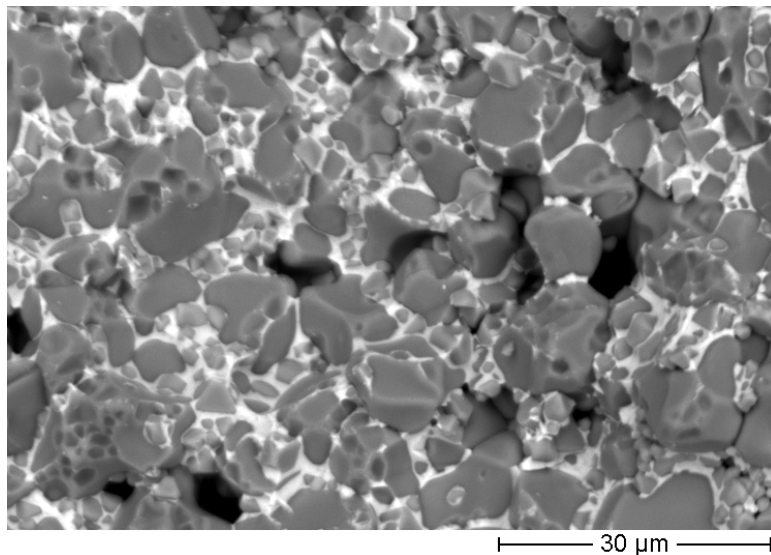
Figure 2.5: Scanning electron microscope image of a fractured surface of an MOV as described in *chapter 5* (at 1000x magnification).

Each boundary layer[17] between two ZnO grains has a breakdown voltage of $3.2\,V$ or $3.6\,V$ depending on the structure (see for example [Ols89a] and [Ols89b]). In order to achieve the desired breakdown voltage for the whole varistor for a given application, MOVs have

---

[16] This boundary layer cannot be seen in an image of this kind of resolution as it is only $1\,nm$ to $2\,nm$ thick.

[17] It has to be mentioned that not all grain boundaries inside an MOV are active or generate a varistor behavior (see for example [Sch94].

to be provided with the appropriate amount of serial grain boundaries. Due to reasons of production and testing, the height of the MOVs is limited to a value of about 45 mm across all manufacturers. Thus, in surge arresters for high-voltage applications, many individual MOVs are stacked on top of each other (see *chapter 2.1*). In order to obtain the desired energy handling ability or a specific residual voltage at impressed currents, there has to be the right amount of parallel paths through the MOV for the current flow. This is achieved by choosing the appropriate diameter of the MOVs. For constructional reasons, the diameter of MOVs is limited to about 110 mm. If a higher energy handling capability is required, several columns of MOVs (inside one or more surge arrester housings) are operated in parallel.

It is often assumed that the *E-J* curve as an electrical characteristic is the same for equally manufactured MOVs of different geometric dimensions. Therefore, the *E-J* characteristic is derived from a measured *V-I* characteristic divided by the geometric dimensions of the MOV. Since the current flow inside the MOV is not distributed homogeneously in all sections of the *V-I* characteristic (see [Bar96b]), it has to be considered that, depending on the respective section of the characteristic, the current density differs from the calculated average value of the whole MOV. Moreover, the distribution of grain sizes varies for different diameters of MOVs due to reasons of production, limiting the scalability when a calculated *E-J* characteristic is assumed.

As already mentioned, the structure of the boundary layer is defined by the composition of materials[18] and the sintering process. During the sintering process, ZnO grains grow due to diffusion processes. These grains are surrounded[19] by a bismuth-rich liquid phase. Due to the outer shape of the ZnO grains, the extent of the boundary layer is inconstant, as depicted in [Eda89] and in figure 2.5. In the gussets between the grains, spinel and pyrochlore phases accumulate. According to [Sch94], they do not contribute to the electrical behavior of the MOV and thus will not be considered in the following. Bi is not directly responsible for the varistor effect. However, there is no varistor effect without Bi doping or doping with an equivalent additive [Gre90]. Bi^{3+} activates the grain boundary as its defect states can trap electrons[20]. If there is Bi^{3+} between two ZnO grains, electrons move from the ZnO grains to the boundary until the thermodynamic equilibrium is reached

---

[18] As described above, it is assumed that ZnO is the main component of the MOV with approximately 90 % of the overall mass (see [Cig13a]) and that the MOV discussed here consists mainly of the common additives used nowadays(Bi_2O_3, Sb_2O_3, CoO and MnO).

[19] According to [Gre90], the necessary amount of Bi in order to generate the varistor effect inside an MOV is only slightly higher than the amount that would be needed to surround all ZnO grains with an atomic layer of Bi^{3+}. [Kle04] assumes that a reason why the Bi^{3+} ions are not built into the ZnO lattice could be their size.

[20] According to studies by [Stu87], the defects are compensated or overcompensated by O^{2-} [Sch94].

[Cla99]. The electrons that are moving away from the ZnO grains leave a section with ionized impurities[21], which is called "depletion zone" and has a thickness in the range of $\approx 100\,\text{nm}$ ([Ein79] assumes a thickness of $34\,\text{nm}$ per ZnO grain whereas for example [Cig13a] mentions a total width of $\approx 200\,\text{nm}$). The double Schottky barrier thus created prevents a current flow and is depicted in *figure 2.6* (see for example [Cla99]).

Concerning the conduction mechanisms, there are various models for the different current ranges. An overview of this is given for example in [Eda89]. In the following, only the basic models are introduced. In figure 2.6(a), the energy levels of the grains on both sides of the grain boundary are depicted. Since ZnO has an excess[22] of Zn^{2+} (respectively O^{2-} vacancies), it has the electrical properties of an n-type semiconductor and electrons are the majority charge carriers (see for example [Kle04] and [Cig13a]). The Fermi level E_F inside the grain is located only slightly below the conduction band edge E_C. The grain boundary containing Bi^{3+} is a p-type semiconductor and can trap electrons. This is why the Fermi level inside the grain boundary is only slightly above the valence band edge E_V (see [Gre90] and [Cla99]).

Figure 2.6(b) shows the band diagram after the "recombination" of the electrons along the grain boundary. The Fermi level E_F is balanced across the whole section and the negative charge n_t has shifted into the grain boundary. The symmetrical[23], positive depletion region with a width of $2 \cdot d$ forms a potential barrier with a height of Φ_B, which can be surmounted for example by thermally activated electrons or by quantum tunneling (though the probability of this to happen is very low at ambient temperature) [Gup90].

If a voltage V is applied to the boundary layer, the bands are bent accordingly. The result of this is depicted in *figure 2.7*. Conduction band, Fermi level and valence band shift according to the voltage applied. Electrons of a higher energy level can pass the grain boundary. The potential barrier continues to exist[24] when small voltages are applied, causing only a small leakage current flow [Cig13a].

In order to explain the behavior of the MOV within the strongly non-linear section for $\alpha > 20$, another effect is needed: the "hot electron" effect (see [Pik81], [Bla86] and [Gre90]), which is depicted in figure 2.7(b). If voltages above breakdown voltage are applied, the

---

[21] For the sake of completeness it has to mentioned that, as depicted in [Cla99], the height of the potential barrier also depends on the conductivity of the grain. He points out that if the electrical conductivity is too high, the height of the barrier is reduced and that if the electrical conductivity is too low, there is no potential barrier. Thus, there is an electrical conductivity optimum.

[22] According to [Kle04], this excess can even be enhanced by other dopants (deep donors) that can be easily integrated into the ZnO lattice.

[23] Symmetry is the basis for the varistor effect being independent of polarity [Gup90].

[24] The trapping of electrons in initially unfilled interface states (the so-called "pinning") is the reason for this behavior [Cig13a].
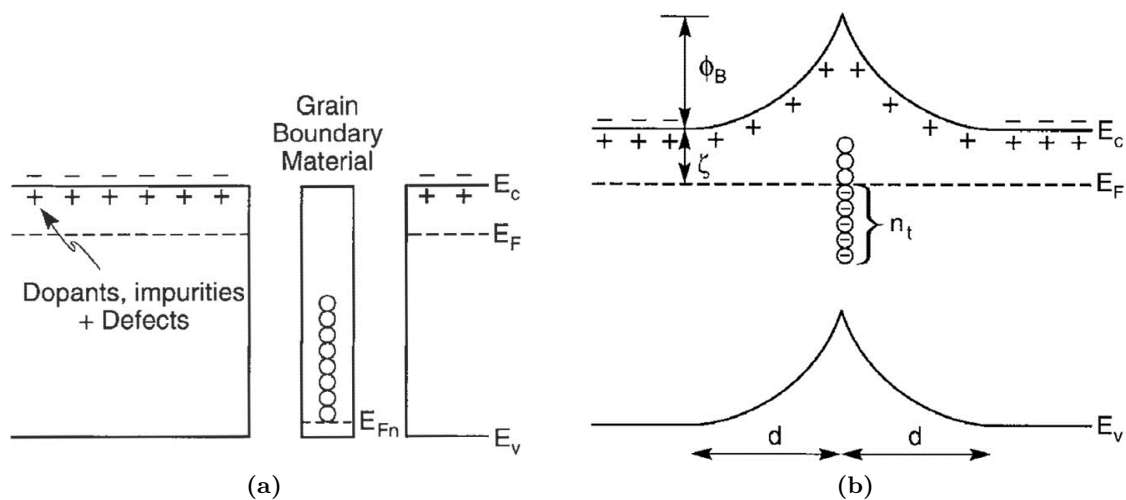
Figure 2.6: Band diagrams for grain boundary sections (according to [Cla99] ©1999 AIP, see also [Pik81] and [Gre90]); (a) before and (b) after the charge balancing (for a definition of the symbols see *table 2.2*).

Table 2.2: Definition of the symbols used in figure 2.6 (see also [Hal12])

Symbol	Description
d	width of the potential barrier at a non-energized condition (in m)
E_C	conduction band (in eV)
E_F	Fermi level (in eV)
E_{F_n}	Fermi level of the boundary layer (in eV)
E_V	valence band (in eV)
n_t	density of trapped charge carriers / interface charge
ζ	distance between conduction band and Fermi level at a non-energized condition (in eV)
Φ_B	height of potential barrier (in eV)
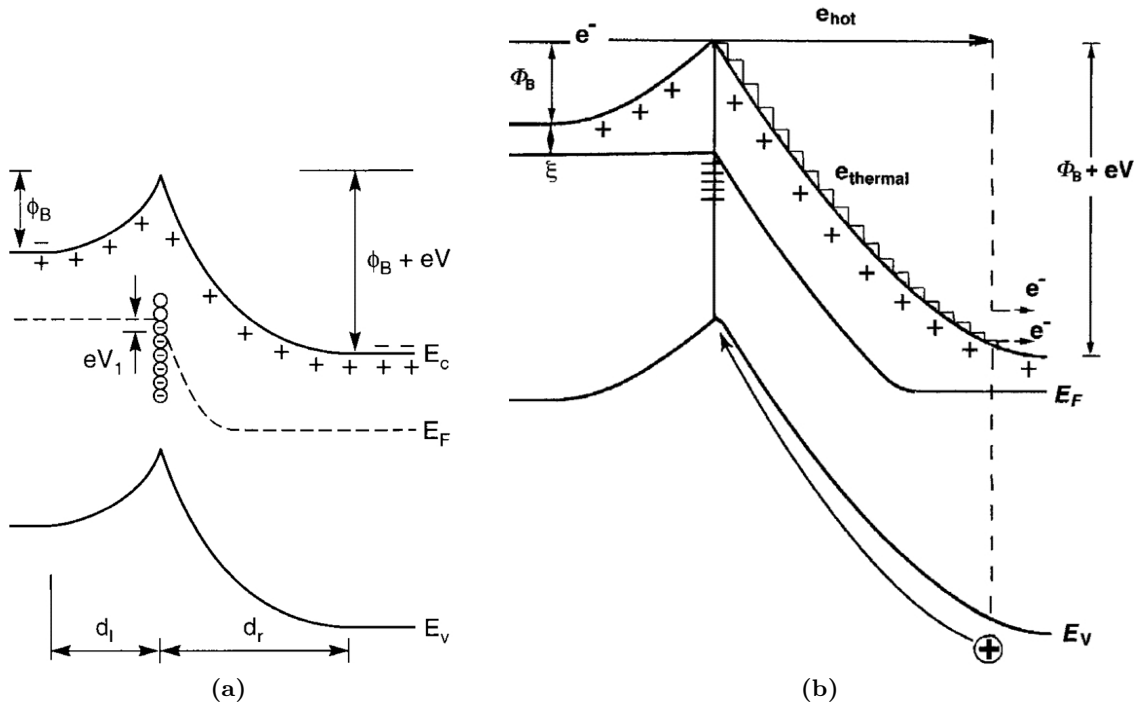
Figure 2.7: Band diagrams for grain boundary sections at applied voltage (according to [Cla99] ©1999 AIP, see also [Pik81] and [Gre90]); (a) effect of the applied voltage concerning the band structure and (b) depletion of the potential barrier by "hot electrons" (for a definition of the symbols see *table 2.3*)

Table 2.3: Definition of the symbols used in figure 2.7 in addition to table 2.2 (see also [Hal12])

Symbol	Description
d_l	width of the potential barrier on the left side of the grain boundary at an applied voltage "eV" (in m)
d_r	width of the potential barrier on the right side of the grain boundary at an applied voltage "eV" (in m)
e	elementary charge of an electron
e^-	abbreviation for electron with the elementary charge e
e_hot	electron with sufficient amount of energy to release minority charge carriers through impact ionization
e_thermal	electron the energy of which is reduced by the emittance of phonons
eV	acceleration energy for electrons at voltage "V"
V	applied voltage from right to left

electrons that are in a thermally activated state can be accelerated to such a great extent inside the electric field that their kinetic energy is sufficient for their generating minority charge carriers through impact ionization (see [Pik81], [Bla86]). These electrons are called "hot electrons". The emitted electrons flow away from where they were emitted whereas the holes move towards the grain boundary[25], which is supported by Bi_2O_3 a very good oxygen ion conductor [see for example [Den98]]. When reaching the grain boundary, the emitted electrons recombine with the electrons trapped there, thus lowering the barrier height. This leads to an increasing amount of "hot electrons" because now also thermally activated electrons with lower energy can surmount the potential barrier. This causes an avalanching reduction of the potential barrier[26] [Cig13a].

With increasing current density (referring to the whole MOV surface), the voltage of the MOV is slowly rising at first. Thus, steadily more parallel paths with a slightly higher breakdown voltage are used [Gup90]. At very high current densities, the nonlinearity α decreases notably (as already described), due to the fact that, with rising current density, more and more potential barriers are reduced and the current flow is increasingly influenced by the limited conductivity of the grains [Gup90].

The reason why an "inductive" behavior of MOVs can be observed at high current densities and high current rise times (provided that the length-dependent inductivity of an MOV, as shown for example in [Rei08], is compensated) is explained in various ways. While [Eda89] states that the reason for this behavior is the switching time of Bi_2O_3, [Bla86] mathematically demonstrates that it can be explained with the conduction mechanism which switches from conduction of electrons to a recombination of holes when the breakdown voltage is exceeded (see also [Sch94]). In first-order approximation, this behavior is often taken into consideration by introducing the inductivity L_b, which is shown in figure 2.3 (see also [Cig13a]).

Finally, the temperature dependence of the *V-I* characteristic needs to be mentioned. Within the pre-breakdown region, a negative temperature coefficient behavior of the conductivity results from the conduction mechanism (see for example [Eda84]) since more electrons are able to surmount the potential barrier at higher temperatures. Compared to this effect, the temperature dependence in the high-current region is only very small [Sch94]. Within this range (as already mentioned above), the behavior is mainly determined by the metallic conductivity of the grain. This is why there is a positive temperature coefficient behavior within this range, shown for example in [Had05] and [FH03].

---

[25] For this, according to [Cig13a], they need less than 1 ns; [Ein82] talks about "some nanoseconds".

[26] This effect distinguishes MOVs from Zener diodes [Cla99].

Based on this microscopic view of the inside of an MOV, its macroscopic behavior can now be better interpreted.

2.3 Types of Energy Handling Capability

Surge arresters are supposed to limit overvoltages[27] and thus reduce the voltage stress for electrical equipment which makes the production of the latter cheaper. As described in chapter 1, overvoltages can occur for example due to switching operations or defects inside the grid or due to lightning discharges. During the discharging process (combined with the design-dependent voltage drop[28]), electric energy is converted into heat. This heat as well as the occurring forces (for example resulting from the heating) can damage the MOV. Moreover, the current flow can cause reversible or irreversible changes inside the MOVs that can impair the continuation of their being operated. The limit of the energy handling capability of a surge arrester is considered to be reached when the applied energy has damaged the surge arrester or its MOVs so much by primary or secondary effects that an operation of this surge arrester is no longer possible. Thus, in this thesis, a difference is made between thermal and impulse energy handling capability. The focus of this thesis is mainly on the impulse energy handling capability.

2.3.1 Thermal Energy Handling Capability

The thermal energy handling capability is limited by the temperature MOVs in surge arresters can adopt without the increased power loss (at applied system voltage) exceeding the amount of heat that can be dissipated (as described for example in [Cig13a] and [Kle04]). Due to the fact that the V-I characteristic of an MOV in the pre-breakdown region is strongly temperature-dependent and has the characteristics of a negative temperature coefficient thermistor[29], a higher leakage current at applied system voltage than before flows through the MOV after a heating caused by an energy injection. If the energy

---

[27] The term "surge arrester" suggests that the equipment would conduct away overvoltages. Strictly speaking, surge arresters in high-voltage grids discharge overvoltages to the ground (for example as a result of lightning discharges), thus making sure only small overvoltages can occur at the equipment which is to be protected (for example transformers). Hence, they prevent (at assumed impressed currents) the development of overvoltages.

[28] As already described, the V-I characteristic is design-dependent (varying for MOVs from different manufacturers) and thus, the voltage drop across the MOV at an impressed current is design-dependent, too. As a consequence, the energy that must be handled by the MOV at an impressed current is also design-dependent.

[29] At higher temperatures, the V-I characteristic within the pre-breakdown region shifts to the right towards higher currents at the same applied voltage.

injection is so high that the injected energy causes the temperature of the MOVs to rise to such an extent that the power loss at the applied voltage is higher than the amount of heat that can be dissipated, the temperature inside the MOVs is constantly rising due to the negative feedback until they are mechanically destroyed ("thermal runaway") [ABB11]. The design of the surge arrester – especially its transient heat dissipation ability – is of major importance for the amount of heat that can be dissipated. Furthermore, system voltage and temperature characteristics of the V-I characteristic of the MOVs are of major importance for their thermal stability. Since the V-I characteristic can be negatively influenced by an energy injection (see [Hei01] und [Kle04]), the type of energy injection (the history) can also be crucial for the thermal stability of the surge arrester. The temperature of MOVs after an energy injection of a defined intensity can be controlled by constructional methods, for example by the volume of the MOVs or heat sinks inside the surge arrester such as metal spacers [Hin11]. The heat dissipation behavior (and with it the amount of electric power that can be added without causing thermal instability) can also be influenced by the construction of the surge arrester (see [Cig13a]). The thermal energy handling capability is the design criterion for surge arresters in standard applications and is verified by the so-called operating duty test (for example in [IEC60099-4]).

2.3.2 Impulse Energy Handling Capability

"Impulse energy handling capability" describes the energy which can be injected by an impulse energy injection without damaging the MOV. In many publications on this subject (for example in [Bar99] and [Rin97]), solely the different types of mechanical damages of the MOV are taken into consideration. Changes within the V-I characteristic of the MOV that are caused by impulse stresses and thus can influence the further operation of the MOV (and, as already described, its thermal stability) constitute another damage criterion (see for example [Kle04] and [Rei08]). The common feature of all of these criteria is that they primarily depend on the MOVs and only secondarily on the construction[30] of the surge arrester. The various damage criteria might in some circumstances be intensified by the application of repetitive stresses. This is why, in this thesis, a distinction is made between single and multiple impulse energy stresses, the latter being divided into multiple and repetitive stresses.

---

[30] Apart from the flashover phenomena at the coating of the MOV that can be influenced by constructional criteria. Moreover, if the contact pressure of the contact electrodes is too low, the energy handling capability can be influenced [Rei08].

Single Impulse Energy Handling Capability

"Single impulse energy handling capability" describes the energy handling capability at one single[31] energy injection. The single impulse energy handling capability depends on the duration and the current density of the energy injection (see for example [Rin97] and [Cig13a]) and is examined in detail in chapter 5.1. Since energy injections occurring in the field can have very short impulse durations and high current amplitudes (see [Cig13b]), the energy injection leads to an immediate heating. Combined with inhomogeneities due to constructional reasons (see [Hin11]) as well as uneven current sharing (see for example [Bar96b]), this leads to thermomechanical tensions inside the MOV, which can cause its cracking (see [Kle04]). If the energy injections are prolonged, the melting of one single current path can be observed, which leads up to a puncture (see [Cig13a]). This damage symptom also appears after a thermal runaway of an MOV. The type tests of the impulse energy handling capability in [IEC60099-4] or [IEC-37/416/FDIS] and [IEEEC62.11-2012] represent a hybrid of multiple impulse energy handling capability and handling of repetitive impulses, as is described in chapter 6.2.

Multiple Impulse Energy Handling Capability

The multiple impulse energy handling capability expands this type of stress by several subsequent (so-called multiple) impulse stresses where the intervals between the energy injections are so small that no considerable amount of energy can be emitted by the MOV. Thus, mechanical fatigue can occur due to the increased amount of impulses. However, due to the high thermal conductivity of the MOV (see for example [Lat83]), this can also lead to thermal balancing processes inside the volume which improve energy handling capability. Since there are only small intervals between the energy injections, the temperature inside the MOV or in the active current paths rises after each impulse. This is the reason why the mechanisms that lead to a breakdown at very short intervals between the energy injections can be compared to those of single impulses. In chapter 5.3, new findings concerning double impulse energy handling capability at long-duration current impulses are introduced.

---

[31] It has to be mentioned that, due to its waveform, an AC energy injection at power frequency AC voltage cannot unambiguously be defined as single or multiple stress. Strictly speaking, it is a multiple stress with alternating polarity. However, since there are only idle times in the range of milliseconds during the current flow, an AC energy injection as a whole will be defined as a single impulse. At the same time, since this definition is also used in earlier publication such as for example [Rin97], [Rei08], [Cig13a] etc., it simplifies comparison.

Energy Handling Capability Regarding Repetitive Impulses

The energy handling capability regarding repetitive impulses describes the capability of the MOV to repeatedly withstand stresses where the intervals between the stresses are long enough to allow the stressed MOV to cool down to ambient temperature. Thus, the sum of energy of the individual stresses is not relevant, but only the amount of repetitive stresses of a certain energy level. This kind of stress can lead to mechanical fatigue inside the MOV, though not only energy injections but also the cooling process can influence mechanical fatigue[32]. Also, changes of the *V-I* characteristic of the MOV have to be observed because reversible changes can be intensified due to repeated stresses. In chapter 5.4, new findings regarding repetitive stresses are introduced.

2.4 Mechanical Damages

Different kinds of energy stresses can lead to different kinds of damages inside the MOV. Changes within the microstructure (see for example [Stu90]) that lead to a change of the *V-I* characteristic are one example for this. Moreover, due to high energy injections, thermomechanical tensions can occur inside the MOV (as already mentioned) that can lead to its cracking or individual current paths can melt if they are thermally overloaded. In addition, not only can the varistor ceramics be damaged and cracked in consequence of the thermal shock, but also the coating. This significantly increases the probability of flashovers in subsequent operation (see [Kle04]). An overview of characteristic symptoms of mechanical failure as well as crack formations is given in *figure 2.8.*

Mechanical tensions can lead to a cracking of the varistor ceramics or the coating, which can result in the damage symptoms shown in figure 2.8 (a)–(c) and (g)–(i) depending on the cause. If a current path is thermally overstressed to such an extent that the melting temperature and subsequently the boiling temperature is reached, a melting channel can develop through a part of the MOV as shown in figure 2.8 (e) or through the whole varistor as shown in figure 2.8 (d). In experimental tests, if the melting channel is eccentric, the evolving gas pressure often leads to a bursting of the ceramics, which can result in damage symptoms such as in figure 2.8 (b). If the dielectric stress along the MOV is so high as to trigger a flashover, the damage symptom of figure 2.8 (f) can be observed. In this case, under some circumstances a further operation of the MOV can be rendered impossible due

---

[32] Very fast cooling can lead to thermal tensions, which can mechanically damage the MOV. In contrast, if the cooling is done very slowly (similar to tempering or resintering), the high temperature that is kept for a long time can have a positive effect on the charge carrier distribution inside the MOV [Gre90].
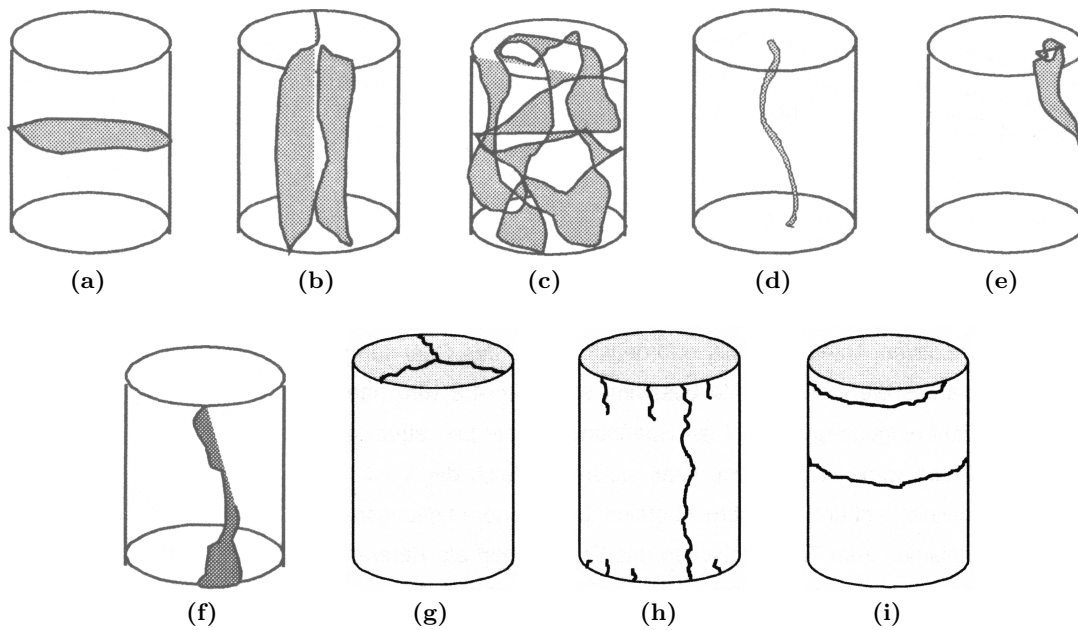
Figure 2.8: Characteristic damage symptoms of MOVs resulting from energetic and impulse stresses [Kle04] ©2004 Shaker Verlag.

to conductive accumulations (see [Kle04]). Additionally, the coating can be ripped due to the selective heat exposure, which can lead to the damage symptom in figure 2.8 (h).

2.5 Current Scientific Knowledge Regarding Single and Multiple Impulse Energy Handling Capability

In the following, an overview of the current scientific knowledge regarding single and multiple impulse energy handling capability of MOVs is given. However, the amount of independent research findings is small compared to other fields of research since specific costly test facilities are necessary to generate relevant energy injections for the investigations described below. In the following, mostly experimental and simulative tests are introduced that were conducted with MOVs of medium- and high-voltage level applications. Research findings concerning MOVs of the low-voltage level can only be limitedly adapted to MOVs of the medium- and high-voltage level because their mechanical construction differs significantly regarding the macroscopic as well as the microscopic level. The differences in grain size, the external diameter to height ratio of the MOV, the macroscopic contacting, and the volume (to name but a few examples) influence the energy handling capability, as described for example in [Eda84] and [Bar01].

In the publication of [Hie74], the capability of the earlier MOVs to withstand stresses is depicted and to that end, the author elaborates on energy handling capability, too. The MOVs described (with a diameter of 56 mm) were stressed on the one hand with a series of 20 long-duration current impulses with a virtual duration of 2 ms, on the other with two high-current impulses of the 4/10 µs type with a current peak value of 150 kA or 100 kA. During the repetitive energy stresses, the author observed changes within the *V-I* characteristic, which are shown in the diagram given in *figure 2.9*. It can be seen that, with the increasing amount of impulses, the *V-I* characteristic is changed more and more within the pre-breakdown region (measured at an impressed direct current of 1 mA with similar or reverse polarity corresponding to the impulse energy injection). Compared to other scientific publications, the amount of energy stresses with up to 100 stresses with a current peak value of 40 kA at a high-current impulse of the 4/10 µs type or 1,000 energy stresses at long-duration current impulses with a virtual duration of 2 ms and current peak values of 400 A or 600 A was very high. One has to be critical about the fact that the author does not comment on the failure probabilities for the different stresses. The observations made are limited solely to the changes of the *V-I* characteristic (probably of one single MOV). Presumably, the reason for this is the early stage of development of MOVs at the time of the publication.

Almost ten years later, [Kan83] explored the factors influencing the energy handling capability in systematic experiments. He equally stressed 10 to 20 MOVs (with a diameter of about 100 mm), modifying the impulse duration (double-exponential discharge currents of about 3 ms to 40 ms), the initial temperature (around 50 °C to 200 °C), the amount of impulses for a long-duration current impulse with a virtual duration of 2 ms (single impulse stresses compared to multiple and repetitive stresses) as well as the length of AC energy injections (duration of the energy injection about 0.1 s to < 100 s). It has to be mentioned that [Kan83] – unlike subsequent publications of other authors – does not observe a difference in energy handling capability regarding different types of stresses or durations of the applied stresses (three impulses within a time interval of 2 min were applied). The MOVs also failed at the same failure energy in a wide range of the duration of the energy injection when stressed with AC energy injections as it was the case when stressed with impulses. According to [Kan83], the change of the *V-I* characteristic within the pre-breakdown region caused by impulse or AC stresses is negligible except for high currents of the 4/10 µs type where changes can be observed at high current densities. [Kan83] notices a decrease of energy handling capability at rising initial temperatures[33] if the MOVs are preheated, but not until an initial temperature of 100 °C. The differences in energy handling capability at stresses succeeding each other without letting the MOVs

---

[33] The type of impulse applied here was a long-duration current impulse with a virtual duration of 2 ms.

(a)

(b)
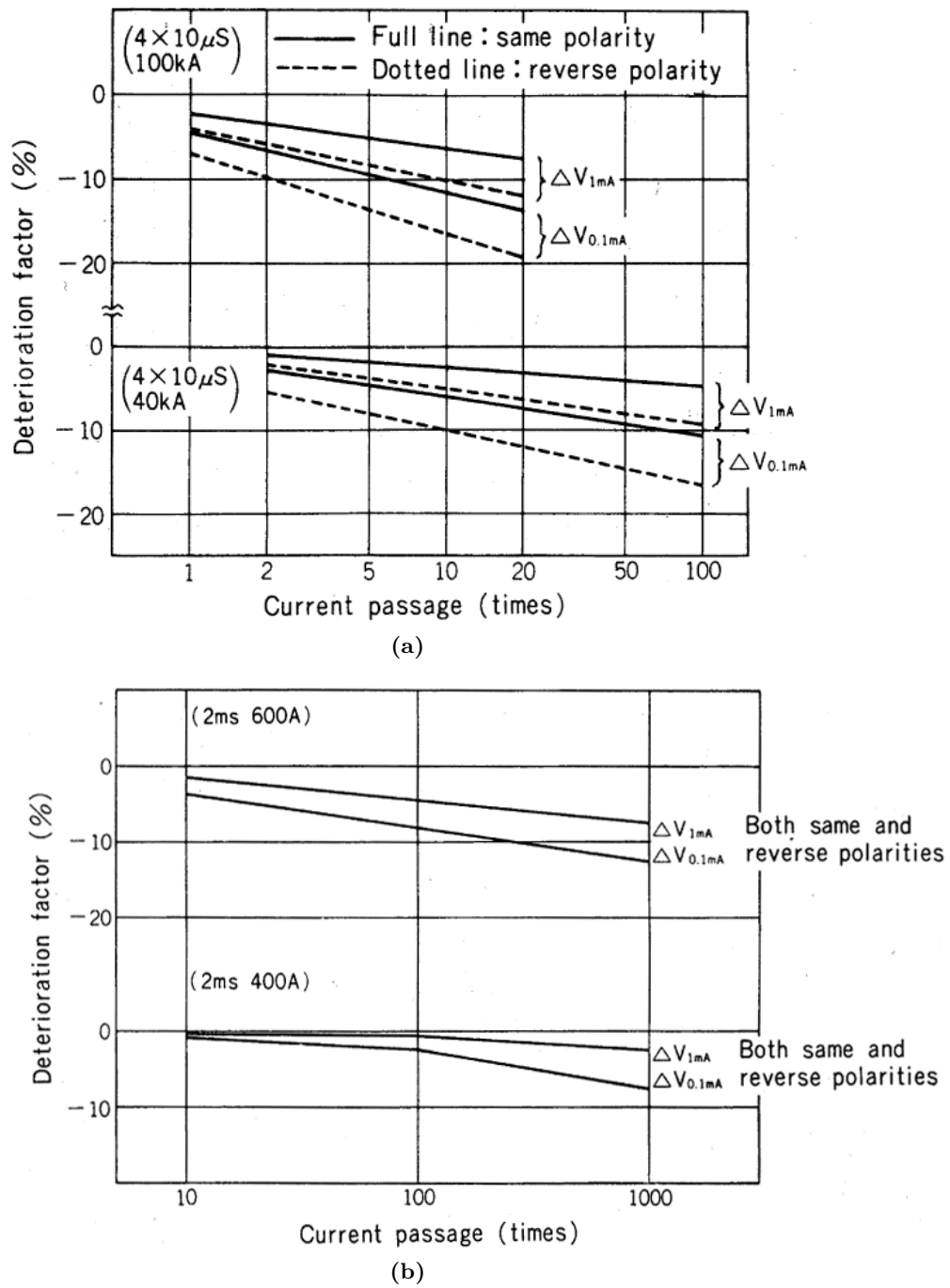
Figure 2.9: Aging of the *V-I* characteristic of MOVs due to repetitive stresses [Hie74] ©1974 Meidensha
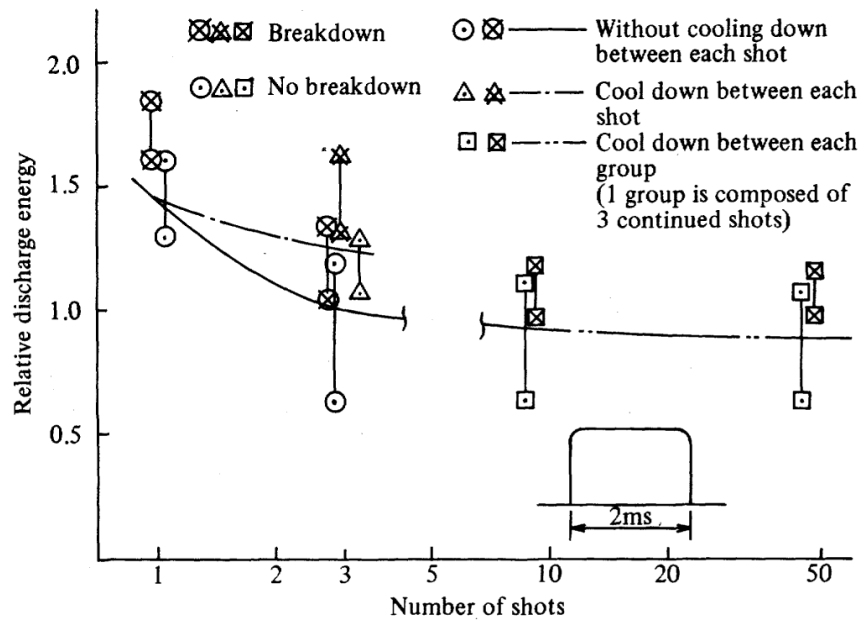
Figure 2.10: Energy handling capability for long duration current impulses with a virtual duration of 2 ms depending on the amount of impulses [Kan83] ©1983 IEEE.

cool down[34] and at stresses when letting them cool down[35] are depicted in *figure 2.10*. A difference concerning the energy handling capability[36] at multiple and repetitive stresses can be observed. Moreover, [Kan83] concludes that the applicable energy does not decrease any further after an amount of about six impulses.

Within the same time period, [Eda84] published his study on the failure mechanisms of MOVs caused by impulse stresses. In the practical tests he carried out with MOVs (with a diameter of 10 mm to 115 mm and a height of 1 mm to 20 mm) manufactured by himself, he evaluated the current density of the energy injection depending on the duration of the energy injection. In doing so, he was the first to observe the approximately linear decrease (in the double-logarithmic diagram) of the amount of time until an MOV fails when the impressed current density increases[37]. Moreover, he stated that the volume-related energy handling capability decreases with increasing diameter (but the same height, thus increasing volume) of the MOVs. According to [Eda84], this can be explained by the

---

[34] Multiple stresses as described in chapter 2.3.

[35] Repetitive stresses, see chapter 2.3.

[36] It is not clear whether this publication refers to failure energy as being the energy content of a single impulse or the sum of energy injected by the three subsequent impulses when the MOV is stressed by a group of three impulses. Neither can one derive which of these is referred to as failure energy since the author does not comment on the contacting of the MOVs in the specimen fixture, hence there is no information on the heat dissipation between the impulses.

[37] However, he carried out this investigation only with varistors of the low-voltage level with a diameter of 14 mm and a height of 1.3 mm.

increasing inhomogeneity of the MOVs at an increased diameter. Finally, he analyzed the failure behavior of MOVs with the help of computer simulations and found out that the destruction energy is determined by and can be estimated based on the homogeneity of the test specimens.

In his publication, [Swe89] describes the developing of an MOV (with a diameter of 50 mm to 109 mm and a height of 18.5 mm in serial production) with an energy handling capability[38] of 1000 J/cm^3 used for the protection of capacitors (see chapter 2.1). This is why [Swe89] tested the single impulse energy handling capability by applying AC energy injections at current densities[39] of about 0.04 A/cm^2 to 0.2 A/cm^2. He concludes that such a high single impulse energy handling capability can be achieved as peak value for MOVs with a lower volume. However, he also states that, in serial production, the energy that can be specified with a low risk lies significantly below this value[40].

Another broad study regarding multiple impulse energy handling capability of MOVs respectively surge arresters of the medium-voltage level was carried out by Darvenzia and published for example in [Dar94], [Dar97], [Dar98] and [Dar00]. In his investigations, he generated single and multiple impulse stresses (the impulses were generated at intervals of 15 ms to 150 ms) with impulse currents of the 8/20 μs type (current peak values of 5 kA to 10 kA) as well as the 4/10 μs type (current peak values of 65 kA to 100 kA at single stresses and 15 kA at multiple stresses). Darvenzia noted that the *V-I* characteristic is not changed measurably[41] by these stresses. However, he observed that if multiple stresses are applied, flashovers through (or between MOV and) the coating occur more frequently. He states that these flashovers are independent of the surrounding gas (his studies involved SF$_6$ as surrounding medium), its pressure as well as its humidity content. He also explained that only optimization of the coating or direct molding of the MOVs with a polymer can improve the flashover behavior. [Dar98] assumes that these flashovers are initiated by pre-discharges at the electrodes which is why close attention should be paid to the contacting respectively the design of the electrodes regarding impulse current stresses. Besides, he observed that MOVs that are stored in rain water or MOVs that are tested wetly do not show a higher failure risk. Darveniza did not assess energy handling capability, but he noted that, at

---

[38] Currently, the specified energy handling capability is 200 J/cm^3 to 300 J/cm^3 across all manufacturers [Hin12].

[39] Subsequent studies have shown that the single impulse energy handling capability at low current densities is lower than at high current densities.

[40] Moreover, he describes that a relatively high energy handling capability of the MOVs of 500 J/cm^3 was specified eventually when constructing the application.

[41] He tested the *V-I* characteristic within the pre-breakdown region with a direct current of 1 mA, the residual voltage at 5 kA within the high-current region and the power loss at continuous operating voltage. Changes under 10 % were considered to be uncritical.

multiple stresses, there is a risk of thermal instability (due to the sum of energy of the individual impulses).

In the publication of [Mar96], the author examines the single impulse energy handling capability with double-exponential discharge currents with durations of $860\,\mu s$ to $18\,000\,\mu s$. He tested 20 to 25 MOVs per waveform and evaluated the findings statistically. He also observed that the energy handling capability depends on the impressed current density.

Another comprehensive and internationally acknowledged study was conducted by [Rin97]. He examined the single impulse energy handling capability of MOVs of the high-voltage level by applying AC energy injections and long-duration current impulses up to mechanical failure within a wide current range (current peak values from $0.84\,A$ to $35\,200\,A$). In doing so, he tested 19 to 55 MOVs per current density and evaluated the results with different distribution functions. However, none of the used distribution functions covered all instances; thus he pursued the normal distribution. [Rin97] also notes an increase in energy handling capability as the current density of the energy injection rises as well as a linear dependency (within the double-logarithmic diagram) of current density and duration of the impulse up to the mechanical failure of the MOV. Here, the kind of mechanical failure (puncture, cracking or flashover) of the MOV depends on the current density of the energy injection.

In the same time period, the findings of simulation tests carried out by Bartkowiak were published for example in [Bar96b], [Bar96a], [Bar99] and [Bar01]. He simulated grain size distributions, distributions of grain boundaries with different electrical properities[42] as well as different voltage stresses (leading to current flows of different values) of MOVs of the medium- and high-voltage level. In doing so, he took a failure of the MOV as given if limiting values of mechanical tensions[43] (different for axial and tangential directions), the temperature inside a channel or the mean temperature of the MOV (due to thermal stability) were exceeded. He observed that the reason for a mechanical failure[44] depends on the current density of the energy injection (these findings are compared to studies by [Rin97]), the homogeneity of the MOV, its *V-I* characteristic (which can be improved by the addition of a higher amount of Al_2O_3 according to Bartkowiak) and the geometry of the MOV. According to his simulations, if the nonlinearity is very distinct, a very distinct

---

[42] One has to be critical about the fact that it was assumed that the electrical characteristic is temperature-independent within the high-current region.

[43] [Rei08] comments critically that Bartkowiak assumes that the MOV can expand freely in axial direction, which does not have to be true for all MOVs in surge arresters (see chapter 2.1) but influences the mechanical tensions inside the MOV.

[44] For applications of the medium-voltage level, he predicts a melting of individual channels (puncture) for low current densities, whereas he states that a cracking of MOVs is more probable at high current densities.
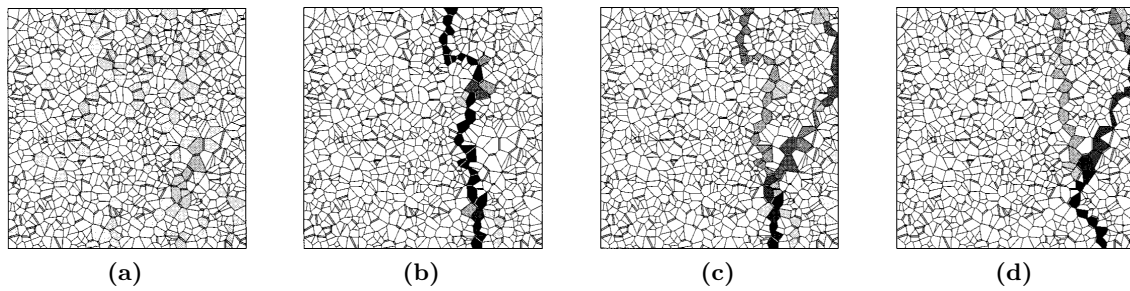
Figure 2.11: Simulated distribution of current of an MOV at different voltage stresses (increasing from (a) to (d)) from the pre-breakdown region to the breakdown region of the *V-I* characteristic [Bar96b]. Within dark surfaces, a higher current flows. All current densities were scaled to the total current ©1996 AIP Publishing LLC

current path formation occurs (as shown in *figure 2.11*), which depends on the sum of the *V-I* characteristics of the individual current paths. Thus, the formation of the most distinct current paths occur when voltage stresses within the range of the biggest nonlinearity of the *V-I* characteristic are applied. For an MOV of the medium-voltage level, he calculates a minimum energy handling capability of about $300\,\mathrm{J/cm^3}$ at a current density of about $1\,\mathrm{A/cm^2}$. Furthermore, he concludes that the current distribution at high-current impulses of the $4/10\,\mathrm{\mu s}$ type is very homogenous and thus this kind of stress is unsuitable for the testing of the energy handling capability (for quality assessments) [Bar01].

In the dissertation of [Den98], the author analyzes the impulse aging of MOVs of the medium- and high-voltage level by applying double-exponential discharge currents of the $0.5/80\,\mathrm{\mu s}$, $1/20\,\mathrm{\mu s}$, $4/10\,\mathrm{\mu s}$, and $8/20\,\mathrm{\mu s}$ type. In doing so, he also takes effects of the AC voltage that is applied while the MOV is in service into consideration. One focus here is on repetitive stresses with mostly 400 and up to 1,500 impulses. Analyzing all these variations of stresses, he notes that the residual voltage is not influenced measurably by the stresses, whereas the *V-I* characteristic is influenced within the pre-breakdown region (he identified the changes within the pre-breakdown region by measuring the power loss at continuous operating voltage). Moreover, he observed that impulse currents with a higher current rise time generate a higher increase in power loss at the same current density peak value. Dengler showed that the first impulse of repetitive stresses generates the biggest change (the power loss increases more strongly at monopolar stresses than at alternating polarity of the impulse stresses) but did not observe a saturation effect. He could not determine whether the energy content of the impulse influences the changes within the *V-I* characteristic. Dengler carried out the repetitive stresses in sequences of several impulses, letting the MOV cool down between the impulses (for about 5 min). Partly, a number of days lay between the sequences. According to his findings, however, the duration of the intervals

between the impulses had no influence on the increase in power loss. Dengler also observed flashovers in the consequence of repetitive stresses[45] and that, comparing various impulse types, when it comes to slower impulses (with the same energy content), flashovers can already be observed when lower amounts of impulses are applied.

In [Bog00], the author examines the influence of the edge margin (difference between the MOV radius and the radius of the metallization applied to the MOV) on the energy handling capability by means of simulations. If the edge margin is too big, the current density at the edge of the metallization rises strongly, which leads to a local heating and thus, at high energy inputs, to a melting of the metal oxide. However, an edge margin that is too small can cause flashovers along the MOV at high impulse stresses. [Bog00] concludes that an optimum size for the edge margin for the geometry he analyzed (with a diameter of 46 mm and a height of 23 mm) would be 0.3 mm to 0.6 mm[46].

In the dissertation of [Kle04], the author analyzes the influences of single and multiple impulse currents of the 4/10 µs, 8/20 µs, and 30/60 µs type on the *V-I* characteristic of MOVs of the medium- and high-voltage level. Concerning the multiple stresses, six individual impulses with variable polarity in time intervals of 0.05 s to 10 s could be generated. As was already known, high current rise times and high current peak values of the current density cause changes within the pre-breakdown region of the *V-I* characteristic. [Kle04] additionally notes that the energy content of the impulse current also affects the *V-I* characteristic negatively. However, he also observed that the increase in temperature inside the MOV may lead to regeneration processes that can reduce the asymmetry[47] of the reference current. He also notes that, concerning multiple stresses, the first current impulse causes the biggest change within the pre-breakdown region of the *V-I* characteristic. However, he also demonstrates that polarity reversals can reverse these changes. This is the reason why, at multiple stresses, the order of polarities influences the reference voltage changes of the impulse sequence. The author could not verify that the length of the time interval between the impulses had any influence on the change in reference voltage. He concludes that multiple stresses with impulse currents are less crucial than a single energy injection (at a similar sum of energy of the injection) because the current density is lower at multiple stresses. Regarding the flashover behavior, he states that multiple stresses can be more crucial because here the behavior of the coating respectively its dielectric strength at higher temperatures is essential. He notes that, as the heating of the coating can take

---

[45] If an MOV failed due to a flashover or breakdown in consequence of an impulse stress, this failure was not preceded by a change in power loss.

[46] The MOVs analyzed in chapter 5 predominantly do not have edge margins.

[47] Current asymmetry is defined as the difference between positive and negative current amplitude when applying AC voltage at power frequency.

several 10 ms ([Kle04]), the risk of a flashover along the coating rises with increasing time intervals between the stresses of a sequence of impulse currents.

In his investigation, [He07] exemplarily determines the single impulse energy handling capability by applying AC energy injections, long duration current impulses with a virtual duration of 8 ms and 2 ms, as well as an impulse current of the 8/20 µs type. Furthermore, simulations regarding current distribution and energy handling capability that are dependent on the impressed current, the inhomogeneity of the microstructure and the inhomogeneity of the electrical and thermal characteristics are introduced. In his publication, [He07] mentions astonishingly low average single impulse energy handling capability values of 216 J/cm^3 to 575 J/cm^3 for MOVs with a height of 10 mm and a diameter of 32 mm. The lowest energy handling capability occurred at a long-duration current impulse with a virtual duration of 2 ms. Obviously, this low energy handling capability is due to the very inhomogeneous material (of commercial origin[48]).

Very comprehensive findings on single impulse energy handling capability of MOVs are published in the dissertation [Rei08] and also in [Cig13a]. Since these studies are essential for this thesis and will be elaborated on in the following, the findings are presented in the main section (in chapter 5.1).

2.6 Current State of International Standardization Regarding Surge Arresters in IEC and IEEE

In this subchapter, a short overview of the current state of international standardization concerning the energy handling capability of surge arresters of the medium- and high-voltage level will be given. In doing so, the standardization in the IEC (International Electrotechnical Commission) as well as, due to its relevance[49], the IEEE (Institute of Electrical and Electronics Engineers) will be taken into consideration. Regarding the IEC, the [IEC60099-4] is to be considered and regarding the IEEE, the [IEEEC62.11-2012]. At the moment, the [IEC60099-4] is being revised based on current research findings mainly of the TU Darmstadt in cooperation with the Cigré working groups A3.17 and A3.25. Due to the fact that the new version will presumably contain basic changes for the tests regarding

---

[48] It can be assumed due to the authors of the publication, the location of the university where the tests were carried out and the received funding that the sole manufacturer is Chinese.

[49] The IEEE standard is a standard that is interesting for international manufacturers due to the size and the openness of the market. Since it is very different from the IEC standard (which is not the case with other national standards such as for example the European, Australian, Japanese standard etc.(see for example [Hin07])), it will be discussed separately in this subchapter.

energy handling capability, the current state of the discussion will also be presented by reference to the [IEC-37/416/FDIS].

Since the above mentioned standards primarily cover standard applications of surge arresters, the testing of the thermal energy handling capability plays a key role. Moreover, the impulse energy handling capability is verified in additional tests[50]. The standards differentiate between tests for surge arresters of the medium-voltage level and tests for those of the high-voltage level because, for these different applications, the stresses occurring during operation can differ[51]. As already described, the interaction between the housing and the MOVs is important for the thermal energy handling capability. However, degradation symptoms of the MOVs (that cause an increased power loss at continuous operating voltage) can also influence the test negatively. For this reason, [IEC60099-4] as well as [IEC-37/416/FDIS] and [IEEEC62.11-2012] include conditioning stresses of the MOVs previous to the thermal stability tests. For surge arresters of the high-voltage level, this is achieved in [IEC60099-4] for one thing by 20 nominal discharge currents of the 8/20 μs type (at defined intervals) that overlap with the AC voltage at power frequency (at about 20 % increased continuous operating voltage). Additionally, the test specimens are stressed with two high-current impulses of the 4/10 μs type with a current peak value of maximum 100 kA ($\pm 10\,\%$)[52]. This very complex test (the influence of the discharge current impulses of the 8/20 μs type can be questioned on the basis of the findings of for example [Den98] and [Kle04]) was reduced to the high-current impulses in [IEC-37/416/FDIS]. In the current [IEEEC62.11-2012][53], a conditioning with 18 long-duration current impulses (at defined intervals) as well as two high-current impulses of the 4/10 μs type with a current peak value of 65 kA is compulsory for the testing of surge arresters of the high-voltage level.

For each of the three standards, the impulse energy handling capability is verified by a different test. In the older one [IEC60099-4], it is assumed that a impulse energy handling capability higher than the thermal energy handling capability is only of minor relevance. For this reason, the energy handling capability is tested by applying nominal energy. To this end, three MOVs are stressed separately with 18 long-duration current impulses with a virtual duration of 2 ms to 3.2 ms (depending on the line discharge class) in six sequences with three impulses each. The time interval between each impulse is 50 s to 60 s and the

---

[50] Naturally, standard tests verify the manufacturer's data for critical operating conditions. Limiting values concerning stresses are not determined, which distinguishes these tests from scientific research.

[51] As an example, the shielding of overhead lines is treated differently internationally for the medium-voltage and high-voltage level.

[52] It is possible to choose lower current peak values for surge arresters of the medium-voltage level. Furthermore, the second high-current impulse simultaneously serves as the energy injection for the testing of the thermal stability of these surge arresters.

[53] The [IEEEC62.11-2012] is also applicable to surge arresters with spark gaps.

MOVs are cooled down to ambient temperature between the sequences[54]. The test is considered to be passed if none of the MOVs fails (is mechanically damaged) or if their change in residual voltage does not exceed 5 %.

This test has been improved significantly in [IEC-37/416/FDIS]. It is now carried out for ten MOVs in a first run[55]. The impulse duration is limited (long duration current impulses with a virtual duration of 2 ms to 4 ms or monopolar sinus half-waves of the same total duration)[56] and the series of impulses is limited to ten sequences at two impulses whereas the time interval between the impulses of a sequence is still 50 s to 60 s and the MOVs are still cooled down to ambient temperature between the sequences. The statistical significance is improved due to the fact that the test is passed even if an MOV should fail. If two out of ten MOVs fail, the test has to be repeated and none of the MOVs must fail. If more than two MOVs fail in the first run, the whole test is failed. The MOV is considered to have failed if it shows mechanical damages (except for damages of the metallization), if the change in reference voltage or in residual voltage exceeds 5 % in consequence of the stresses or if it fails mechanically in consequence of the two following discharge current stresses of the 8/20 µs type with increased current density ($0.5\,\text{kA/cm}^2$ or double nominal current; the lower value is used). The change of the definition of the type of applied stress from energy stress to charge transfer (each stress must be applied with 110 % of this value[57]) is even more far-reaching. Moreover, the charge transfer capability specified by the manufacturer is not linked to the thermal energy handling capability[58].

The standard [IEEEC62.11-2012], which was published earlier[59], pursues the same approach as [IEC-37/416/FDIS], but it only allows long-duration current impulses (of the same length as in [IEC-37/416/FDIS]) and does not introduce a high-current impulse of the 8/20 µs type with increased current density for the exit measurement. Furthermore, surge arresters of the medium-voltage level are excluded from this test. It has to be mentioned again that the thermal stability test for surge arresters of the high-voltage level includes a conditioning with 18 long-duration current impulses (equivalent to those used in the

---

[54] For surge arresters of the medium-voltage level, virtual durations of 0.5 ms or 1 ms of the long-duration current impulses and very low current peak values of 50 A or 75 A (depending on the type) are demanded. Line arresters (without spark gap) are stressed with a double-exponential discharge current with a total duration of 200 µs to 230 µs.

[55] The dimensions of the MOVs are defined in more detail in the standard.

[56] For surge arresters of the medium-voltage level, double-exponential discharge currents of the 8/20 µs type can be applied; for line arresters, double-exponential discharge currents with a duration of 200 µs to 230 µs.

[57] This takes into account that, though the test is only carried out for individual MOVs, it is still supposed to verify the specified value for the whole surge arrester.

[58] Regarding surge arresters of the medium-voltage level, the thermal charge transfer capability.

[59] The working groups that are responsible for the standards coordinate their work regularly. However, no complete alignment could be achieved yet regarding the surge arrester standards in IEC an IEEE.

testing of thermal stability). For surge arresters of the medium-voltage level, long-duration current impulses as conditioning are not included in the thermal stability test; hence the ability to discharge long-duration current impulses is verified in a separate test.

3 Motivation and Aims of This Thesis

As shown in chapter 2.6, the testing of impulse energy handling capability is changing fundamentally in international standardization (and it was changing while the investigations for this dissertation were carried out, too). In the studies on energy handling capability of MOVs published up to now, repetitive and multiple energy stresses have only been researched very rarely and scarcely systematically (as described in chapter 2.5). The multiple stresses examined have been limited mainly to impulse stresses with high current peak values and high current rise times but low energy content although the impact of the applied energy on the change of the V-I characteristic has already been observed (for example by [Kle04]).

Impulse stresses with low energy content are not always applicable to stresses with higher energy content as can be seen for example by closely looking at the microstructure of an MOV. Fundamental differences exist concerning the damage behavior caused by impulse stresses of different current density and rise time due to the fact that high current rise times change the charge carrier distribution along the grain boundary, whereas higher energy densities can lead to local thermal overloads. Furthermore, secondary effects of high energy inputs can lead to a change for example in flashover behavior. [Kle04] observed a higher flashover risk for multiple stresses with higher time intervals. He states that this is due to a higher temperature of the coating (which is supposed to reduce the dielectric strength). Moreover, this increase in temperature after stresses with high energy inputs could lead to regeneration symptoms inside the MOV similar to "tempering" (see for example [Stu90]).

In conclusion, it can be said that multiple impulse stresses with high energy inputs have not been evaluated systematically yet but that physical effects suggest that they differ from multiple impulse stresses with lower energy density (which have already been examined). Since possible interdependencies between different types of energy injections, polarity effects, amounts of impulses, material dependencies, duration of time intervals between the energy injections etc. have only been examined insufficiently so far, there is much space for further research. Unfortunately, the test facilities for relevant energy injections in MOVs of the medium- and high-voltage level are entailed with high costs and require a

lot of space; moreover, tests concerning multiple stresses are very time-consuming. This limits the possibilities of testing significant samples which is why, while planning the tests, a compromise has to be found between the amount of test specimens with the same types of stresses (to statistically support the validity of the findings) and the amount of different types of stresses (in order to evaluate the impact of as many influencing factors as possible).

In order to narrow down this issue, elaborating on the following influencing factors or questions concerning the multiple impulse energy handling capability of MOVs seems sensible and thus they become the aims of this thesis:

- How does the energy handling capability change concerning multiple stresses that succeed each other quickly depending on the duration of the time interval between the stresses? Starting with what length of the time interval between the stresses can these be regarded as separate?

- How does the temperature behavior of the *V-I* characteristic of MOVs influence the internal current distribution and how does this affect the impulse energy handling capability?

- How is the single impulse energy handling capability related to the resistance against repetitive stresses? Is this correlation independent of current density, duration and the type of the impulse of the pre-stress?

- Can failures of MOVs / surge arresters as a result of repetitive energy injections be predicted by analyzing the changes in the *V-I* characteristic of the MOV?

By clarifying these questions, firstly, the above mentioned international standards can be developed further with regard to more significant tests concerning the impulse energy handling capability. This could be supported by clarification of the question on how the length of the time interval between the energy injections and the duration or current density of the energy injection influence the impulse energy handling capability or how much they are to be limited in the relevant standard. The question whether failures of MOVs at repetitive stresses are preceded by changes of the *V-I* characteristic is of interest for the definition of exit measurements in standards (after corresponding stresses).

For manufacturers and operators of MOVs, the influence of pre-stresses on the features of the MOV, such as for example on the *V-I* characteristic and on the impulse energy handling capability, is important, too. A suitable routine test at the end of the production process is supposed to unambiguously detect MOVs with defects (by failure of the MOV

when stressed with a high energy input) with minimum effort[60]. At the same time, the MOVs without defects that can be used further are to be changed or pre-damaged as little as possible. Thus, information on what kinds of energy injections cause very little pre-damages and at the same time are able to detect MOVs with a low energy handling capability can help manufacturers of MOVs to choose suitable test loads.

For manufacturers of surge arresters, scientific knowledge concerning multiple impulse energy handling capability can be useful for the design of surge arresters particularly in special applications. Regarding these special applications (for example the protection of capacitors in series compensation systems), some types of stresses with a high energy input can occur at large numbers. This is why the information drawn from the above mentioned questions can be easily applied here.

For operators of surge arresters of the medium- and high-voltage level, the answers to the above mentioned questions could offer useful suggestions as to whether specifications of surge arresters in special applications need to be refined. Moreover, indications as to how failures can be predicted after repetitive energy injections are of great interest in order to, for example, assess the state of operating surge arresters.

---

[60] The question whether a completely different method, for example a non-electric method, would be more appropriate to detect MOVs with defects is a separate issue, which cannot be answered with the help of the above mentioned questions and thus cannot be discussed in the context of this thesis.

4 Test Facilities Used

In the following chapter, the test facilities used for the investigations described in chapter 5 are introduced. Further information on the design, the measuring equipment etc. can be found in appendix A of this thesis. Except for the aging test set-up, the test facilities have existed already since the study described in [Rei08] and were modified and optimized for the investigations shown in this thesis.

4.1 Specimen Fixture

The specimen fixture is of big importance as it is directly connected to the specimens and thus is affected immediately by impulse stresses, many replacements and failures of specimens. Moreover, parameters such as contact force of the electrodes, heat flow in axial and radial direction, surrounding medium and ambient temperature are adjusted with the specimen fixture. The aim for the adjustment of the specimen fixture is that it is able to simulate not the best or the most critical case of the design of a surge arrester, but a realistic case in order to achieve results that are as practice-oriented as possible.

The specimen fixtures inside the AC energy injection test set-up and inside the long-duration current impulse generator are identically constructed; an inside view of this test chamber is depicted in *figure 4.1*. In order to prevent a movement of the electrodes during an energy injection, the contact electrodes are pressed[61] against the specimen with a surface load of $3\,\mathrm{N/mm^2}$ (which is generated by a pneumatic actuator). [Rei08] demonstrates that, for an equivalent test fixture, this surface load suffices to prevent a lifting of the electrodes even at a high-current impulse of the $4/10\,\mathrm{\mu s}$ type with a current peak value of $100\,\mathrm{kA}$.

In order to reduce a heat flow in axial direction away from (or, after the replacement of specimens, towards) the specimen, a thermal insulation is applied between the test fixture and the contact electrode. The insulation consists of the fiber silicate "Contherm FS 650"

---

[61] The clamping force of MOVs in surge arresters lies, according to information of a manufacturer, within a similar range. For the directly molded design, it can be higher in some circumstances, otherwise lower than the clamping force applied in the specimen fixture.
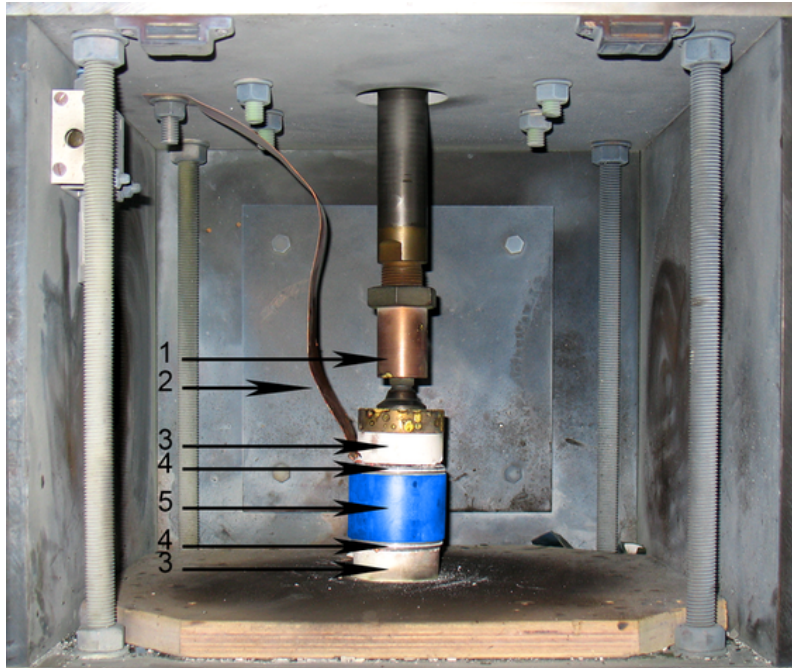
Figure 4.1: Specimen fixture inside the AC energy injection test set-up and long-duration current impulse generator (1 application of force of the pneumatic actuator, 2 test current feeder, 3 thermal insulation, 4 aluminum electrode, 5 test specimen (The specimen has been colored by image editing due to reasons of anonymization.)).

and has a thickness of 19.1 mm and a thermal conductivity of 0.3 W/(K·m). In radial direction, no insulation is applied. The air surrounding the specimen is replaced after each energy injection in order to reduce the influence of combustion residues (after failures of MOVs) and of the heating of the air. In doing so, the installation situation of an MOV for example in the middle of the active part of a surge arrester in tube design (see capter 2.1) is simulated[62].

For the contacting, aluminum electrodes with smooth surface and rounded edges are used. They are 5 mm high and their diameter is 1 mm to 2 mm smaller than the diameter of the respectively used specimen. Before each energy injection, the contact electrodes are replaced in order to prevent temperature and damaging influences.

The specimen fixtures for special investigations such as for example for energy injections at increased ambient temperature or for aging tests are depicted in the respective sections.

---

[62] Concerning directly molded surge arresters, the heat flow is higher in radial direction which is not of relevance for the examined short energy injections. The flashover risk is lower for directly molded MOVs (see for example [Dar98]).

4.2 AC Energy Injection Test Set-Up

With the help of the AC energy injection test set-up, specimens can be stressed with energy injections applied by AC voltage at power frequency. The equivalent circuit diagram of this test set-up is shown in *figure 4.2* . The test circuit is supplied directly by the 6-kV grid and its main component is a Thoma type regulator transformer with a downstream high-voltage transformer. With this test set-up, it is possible to infinitely adjust the voltage, which is especially important for applying energy injections to MOVs within the range of high nonlinearity of the *V-I* characteristic. The RMS value of the voltage that can be maximally applied is 10 kV due to the downstream high-voltage transformer. Thus, energy injections with current peak values of up to 300 A can be achieved for the tested MOVs.
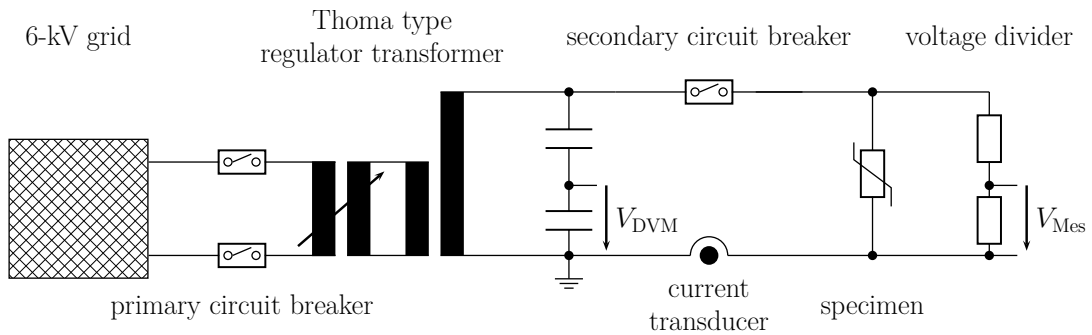
Figure 4.2: Equivalent circuit diagram of the AC energy injection test set-up. V_{DVM} is the voltage that is transferred to the digital voltmeter for the adjustment of the target voltage; V_{Mes} is the voltage transferred to the PC data acquisition card.

After the adjustment of the target voltage, the energy injection is started by closing the secondary circuit breaker. The voltage drop across the specimen is measured by means of an ohmic voltage divider, the current flowing through the specimen by means of a Hall effect current transducer. The measuring signal is transferred via an optical transmission system and is recorded by a PC data acquisition card. With the help of a LabVIEW[63]-program, the energy injection is evaluated and recorded. The end of an energy injection is either determined by the expiration of the adjusted test duration or by a failure of a specimen, which automatically leads to an opening of the secondary circuit breaker as soon as the short circuit current is perceived by the system. Since the secondary circuit breaker is a circuit breaker in vacuum technology, the current flow cannot be immediately stopped but only disconnected during a current zero-crossing. The consequence of this is that the duration of the current flow can spread for one half-wave. During the course of the

---

[63] "LabVIEW", short for "Laboratory Virtual Instrumentation Engineering Workbench", is a graphic programming system by National Instruments.

investigations, the primary circuit breaker was extended by a semiconductor switch with the help of which a phasing-oriented switching of the unstressed transformer and a switching off immediately after the subsequent current zero-crossing of the current (after a perceived overcurrent) was rendered possible.

An example oscillogram of current and voltage during the stressing of an MOV with an AC energy injection[64] is shown in *figure 4.3*. While the current flows, the voltage waveform only roughly matches a sine. This is due to the internal resistance of the transformer (see [Rei08]). The peak values of current flow differ from half-wave to half-wave, which is also a result from the changes of the tested MOV. In the experiments described in chapter 5, the lowest current peak value of one complete half-wave is taken as current peak value of the energy injection. In the depicted case, the MOV was destroyed by the energy injection which can be identified by the most distinct increase of the current at 360 ms.
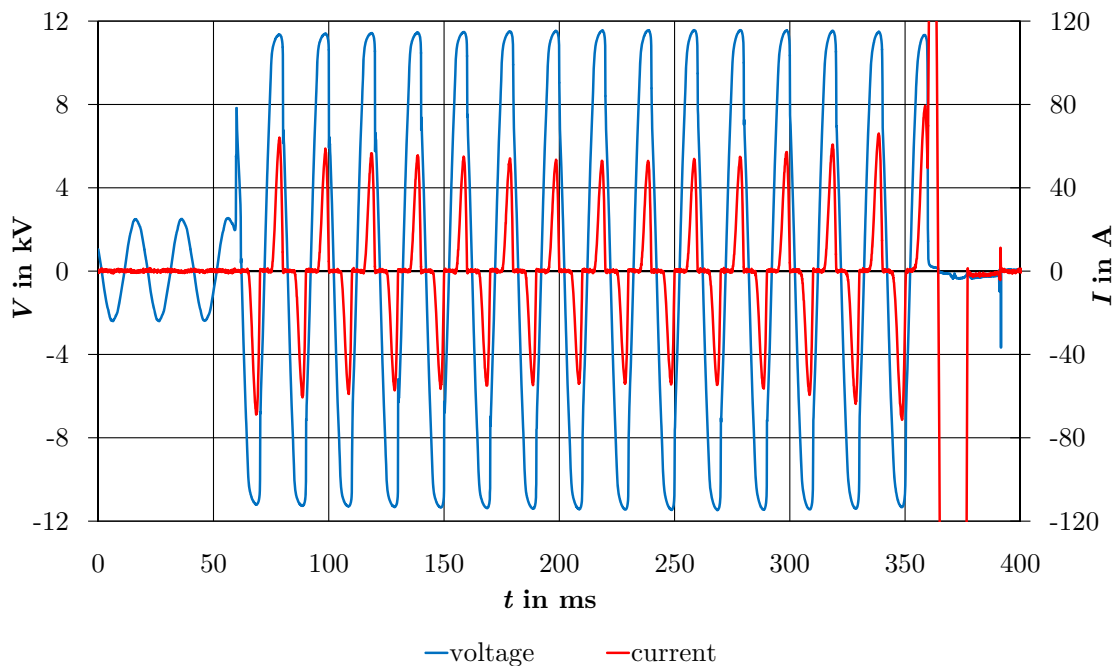
Figure 4.3: Oscillogram of voltage and current when stressing an MOV up to mechanical failure by means of the AC energy injection test set-up.

Further information on this test set-up is given in chapter A.1.

---

[64] The oscillograms depicted in the following were partly taken of MOVs of different manufacturers and geometries. For this reason, amplitudes of the different current and voltage waveforms cannot be directly compared to each other.

4.3 Long-Duration Current Impulse Generator

By means of a long-duration current impulse generator, long-duration current impulses[65] with various virtual durations can be generated. The equivalent circuit diagram of the test set-up is depicted in *figure 4.4*. The test set-up mainly consists of 34 capacitors[66] with a capacity of $10\,\mu\text{F}$ each and a nominal voltage of at least $40\,\text{kV}$, as well as 34 coils with different taps that lead to inductivities of $250\,\text{mH}$ to $3920\,\text{mH}$.
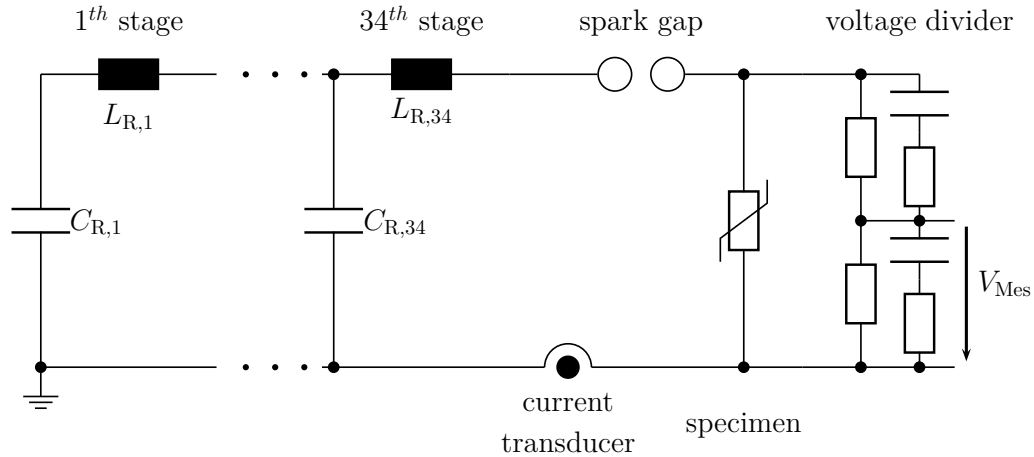
Figure 4.4: Equivalent circuit diagram of a long-duration current impulse generator. V_{Mes} is the voltage that is transmitted to the oscilloscope.

After charging the capacitors to the selected charging voltage, the long-duration current impulse can be triggered by actuating the spark gap. During the course of the investigations, the spark gap was replaced by a semiconductor switch consisting of serial thyristors. This switch enables a triggering independent of the charging voltage and suppresses a possible current reversal after the primary long-duration current impulse. The current that is impressed in the MOV is measured by means of a Rogowski coil and the voltage drop across the MOV by means of a universal voltage divider and captured by a digital storage oscilloscope. The data is transported to a PC which evaluates and documents it automatically with a LabVIEW program.

An example for an oscillogram of current and voltage when stressing an MOV with a

---

[65] According to [IEC60099-4], a long-duration current impulse is a "rectangular impulse which rises rapidly to a maximum value, remains substantially constant for a specified lenght of time and then falls rapidly to zero." Virtual duration is defined as "time during which the amplitude of the impulse is greater than 90 % of its peak value."

[66] In the course of the investigations, the long-duration current impulse generator has been extended from 20 stages to 34 stages. This was necessary in order to determine the mechanical failure energy of MOVs of the high-voltage level by one single energy injection. At this point, we thank the Deutsche Forschungsgemeinschaft for its financial support.

long-duration current impulse is given in *figure 4.5*. This oscillogram shows the current waveform that is quickly rising, staying approximately constant for a time interval of about 1.9 ms and then is quickly dropping to zero. The voltage waveform, which is characteristic for this type of impulse[67], is increasing during the stress, which is supposedly due to the increase in temperature within the MOV (see chapter 5.2.1).
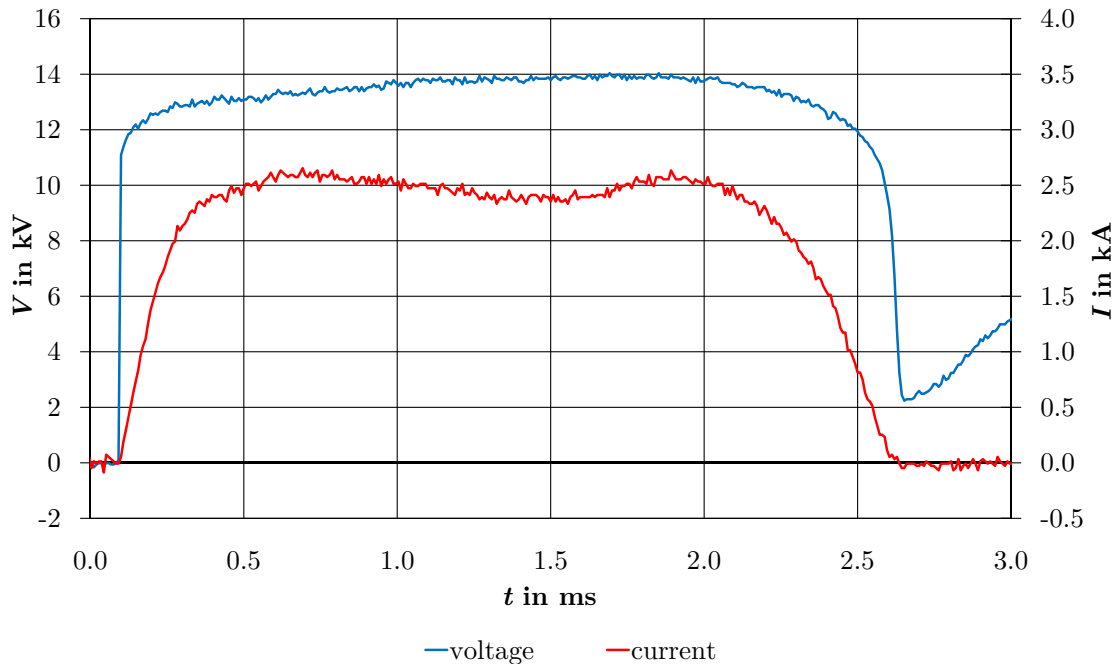
Figure 4.5: Oscillogram of voltage and current when stressing an MOV with the long-duration current impulse generator.

For long-duration current impulses with a high virtual duration, all 34 stages are operated serially, whereas, for short stresses or double impulses, the long-duration current impulse generator is divided into two parallel generators (the equivalent circuit diagram is shown in figure A.4). In addition to the long-duration current impulses, double-exponential discharge currents[68] of the 90/200 µs type are generated. For this stress, 20 capacitors are connected in parallel and the current waveform is shaped by means of a central inductivity of 24 µH.

An example of an oscillogram of current and voltage when stressing an MOV with a double-exponential discharge current of the 90/200 µs type is given in *figure 4.6*. The energy injection lies within the range of the single impulse energy handling capability of

---

[67] The fluctuation of the current waveform is only reflected to a much lower degree in the voltage waveform due to the nonlinearity of the *V-I* characteristic in the stressed range.

[68] This impulse current refers to the double-exponential discharge current as it is described in the annex of the [IEC60099-4]: it is supposed to be higher than 5 % of the current peak value for a time interval of 200 µs to 230 µs.

the stressed MOV and thus leads to its intense heating. In the oscillogram, the current peak is prior to the voltage peak, which is presumably due to the temperature dependence of the *V-I* characteristic of the MOV (see chapter 5.2).

Figure 4.6: Oscillogram of voltage and current when stressing an MOV with a double-exponential discharge current of the 90/200 µs type.

Further information on this test set-up is given in chapter A.2.

4.4 Double-Exponential Discharge Current Generator

With the double-exponential discharge current generator, double-exponential discharge currents[69] for the identification of the *V-I* characteristic within the high-current region are carried out as well as double-exponential energy injections of the 4/10 µs type. The generator, the equivalent circuit diagram of a section of which is shown in *figure 4.7*, consists of up to eight parallel sections. Each of these sections consists of a capacitor with a capacity of 2 µF and a nominal voltage of 100 kV as well as an inductance-resistor combination (the technical data of which can be found in *table A.10*) for the adjustment of the waveform.

---

[69] The specific values and criteria for the identification of the time parameters etc. are defined in [IEC60099-4].
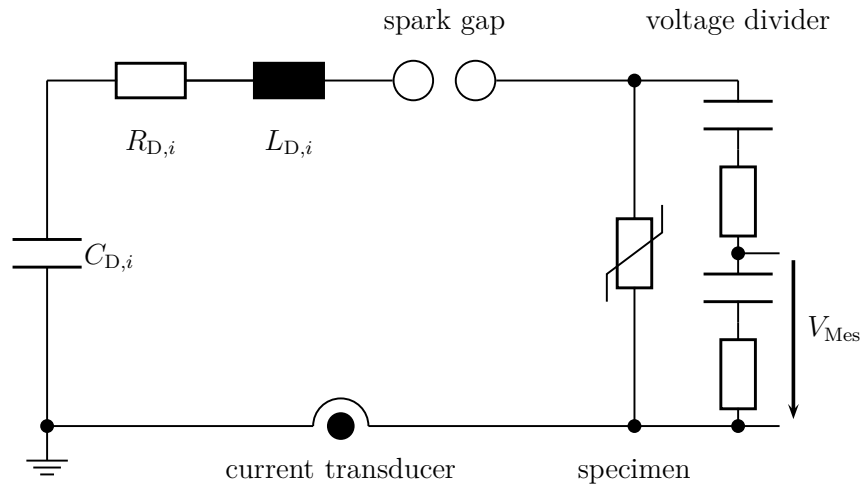
Figure 4.7: Equivalent circuit diagram of the double-exponential discharge current generator. V_{Mes} is the voltage that is transmitted to the oscilloscope.

The current flowing through the specimen is measured with the help of an inductive current transducer and the voltage drop[70] across the specimen with the help of a damped capacitive voltage divider. Both flowing current and voltage drop across the specimen are recorded by the same oscilloscope used for the long-duration current impulse generator and are thus evaluated and documented with a PC.

An exemplary oscillogram of an unfiltered lightning current impulse of the $8/20\,\mu s$ type can be found in *figure 4.8* and one of a high-current impulse of the $4/10\,\mu s$ type in *figure 4.9*. It can be seen that the double-exponential current curve leads to a drop of a non-double-exponential voltage waveform across the tested MOV due to the non-linear *V-I* characteristic. Moreover, during the lightning current impulse, the voltage reaches its peak value prior to the current peak value although the inductive regions of the voltage curve, which are caused by the geometry of the specimen, are compensated[71]. Considering the depicted high-current impulse, the energy content of which lies in the range of the single impulse energy handling capability of the tested MOV, the voltage curve is bent much stronger than this is the case for the lightning current impulse stress and only reaches its peak after the current peak. From the stronger bending it can be concluded that the MOV is stressed in a range of the *V-I* characteristic with a lower nonlinearity exponent. The shift of the voltage peak now occurring after the current peak is presumably due to the temperature dependence of the *V-I* characteristic. As is shown in *figure A.8*, regarding

---

[70] It has to be mentioned that the inductive regions of the voltage curve are compensated by a compensation coil (see [Rei08] or chapter A.3).

[71] According to [Sch94], this is due to the protons transmission mechanism prevalent within the high-current region.

a lower current peak value for another stressed MOV (with a bigger diameter), the voltage peak lies before the current peak. This behavior is discussed in more detail in chapter 5.2.

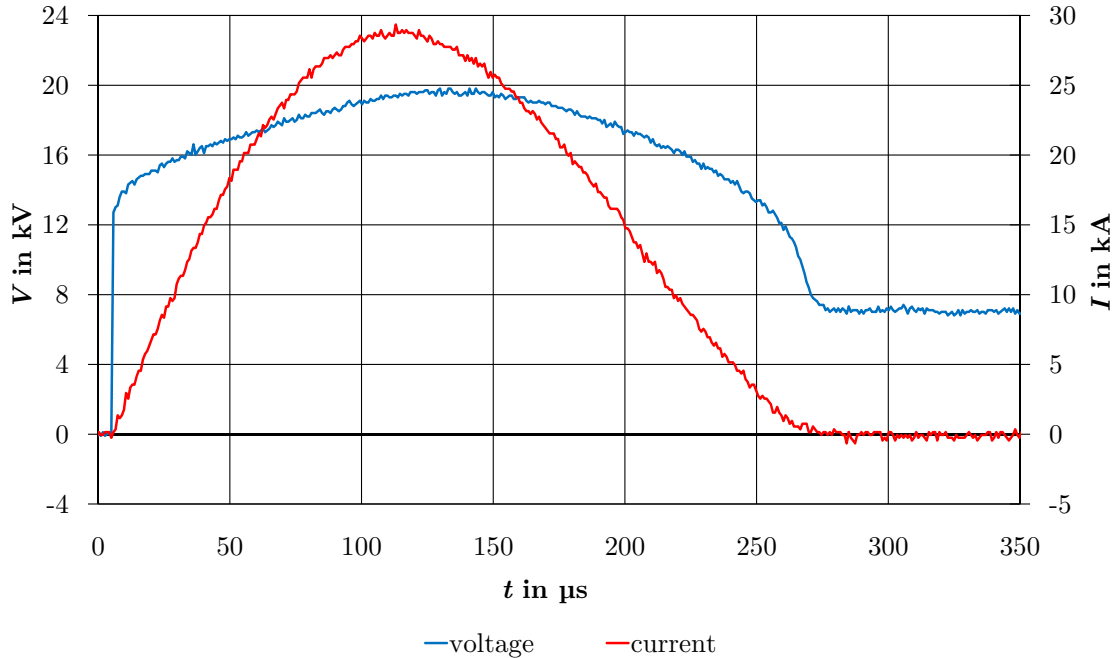**Figure 4.8:** Oscillogram of voltage and current when stressing an MOV with a double-exponential discharge current of the 8/20 µs type.

Due to the high energy injections, the stressed MOVs are thermally decoupled from the test fixture for stresses with high-current impulses of the 4/10 µs type by thermal insulation (with the help of the already mentioned fiber silicate) with a centered current feeder. Between thermal insulation and specimen, an aluminum contact electrode (see chapter 4.1) is used on each side.

In order to characterize the MOVs within the high-current region of the *V-I* characteristic, the specimens are tested by means of a rotating magazine, which is depicted in *figure 4.10*. In this case, the test fixture is used without thermal insulation since the energy content of the characterization discharge currents is relatively low and does not lead to a significant heating of the specimens. Above and below the specimens, aluminum contact electrodes (see chapter 4.1) are used.

Further information on this test set-up is given in chapter A.3.
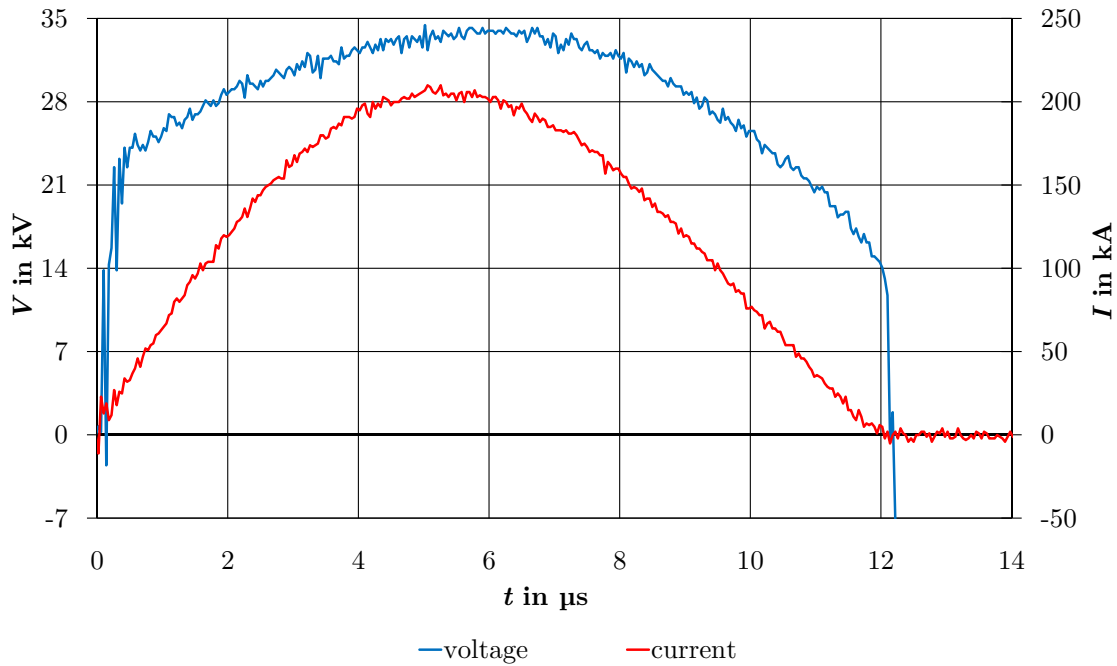
Figure 4.9: Oscillogram of voltage and current when stressing an MOV with a double-exponential discharge current of the 4/10 µs type.
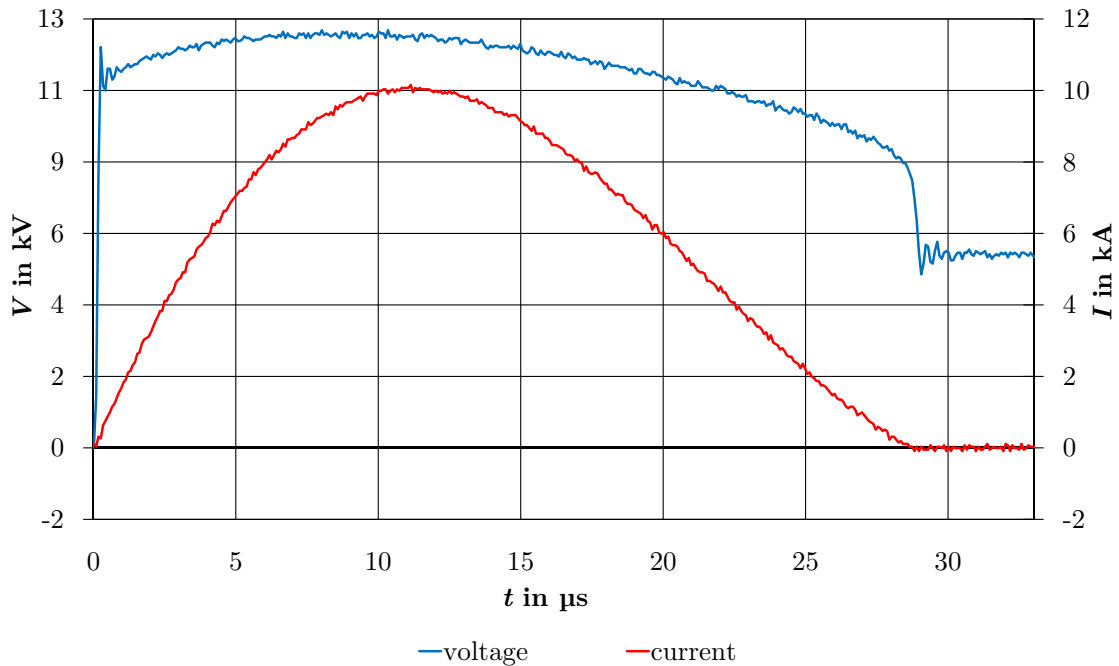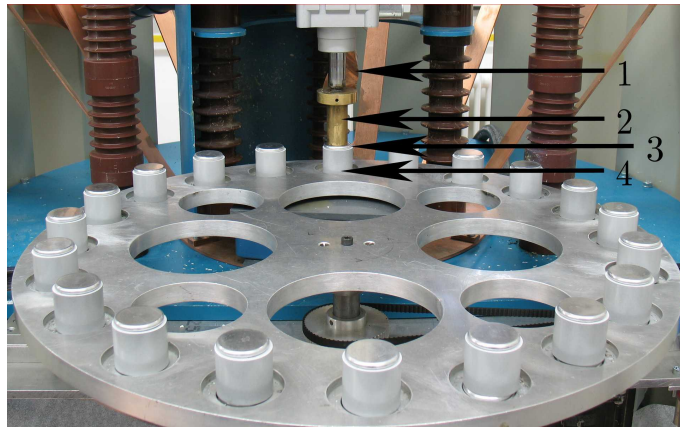

Figure 4.10: Test fixture of the double-exponential discharge current circuit for the characterization within the high current region (1 test current feeder, 2 application of force from the pneumatic actuator, 3 aluminum electrode, 4 test specimen).

4.5 Reference Voltage Test Set-Up

The reference voltage test set-up is used to determine the "characteristic voltage"[72] (as $\frac{V_{pk}}{\sqrt{2}}$) at a current density peak value of mostly $0.12\,\mathrm{mA/cm^2}$. The equivalent circuit diagram of the test set-up is shown in *figure 4.11*. The test voltage is generated by a PC data acquisition card, intensified by a power amplifier and stepped up by a high voltage transformer. The voltage across the test specimen is measured by means of an ohmic voltage divider and the current is measured by means of an ohmic shunt. Both are recorded by a PC data acquisition card and evaluated and documented automatically by a LabVIEW program. The bigger value of the current peak value of positive or negative amplitude is detected and the voltage peak within the same half-wave is analyzed. Due to the fact that the signal is generated at the PC data acquisition card, an automated adjustment of the current (or voltage) level is possible. Moreover, an identification of the measurement parameters at the exact same moment (for the tests described here: $5\,\mathrm{s}$ after the application of the voltage) is rendered possible, which increases reproducibility. Due to the principle of providing the test voltage with a power amplifier, voltages of a defined frequency with low harmonic content can be guaranteed, which is of big importance for the identification of the measurement parameters within this range of the *V-I* characteristic.
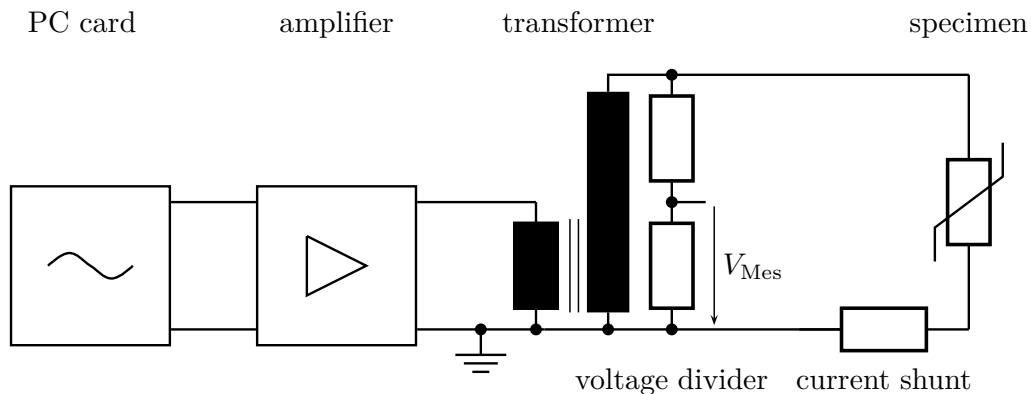
Figure 4.11: Equivalent circuit diagram of the reference voltage test set-up. V_{Mes} is the voltage that is transferred to the PC data acquisition card.

An example of an unfiltered voltage and current waveform within the range of the current densities that will be referred to later on is depicted in *figure 4.12*. It can be seen that, despite the stress, the voltage waveform is very close to an ideal sine[73]. The current is

---

[72] It lies within the range of typical reference voltages of surge arresters. However, since the current density for the measurement of the reference voltage is not defined in [IEC60099-4], but instead varies between the different manufacturers, the term "characteristic voltage" is used here (as has been done in other publications).

[73] According to [IEC60099-4], the ratio of peak value and RMS value must not differ more than $2\,\%$ of

displaying a distinctly capacitive component, which in this case is superimposed by an asymmetrical resistive component due to the pre-stress.
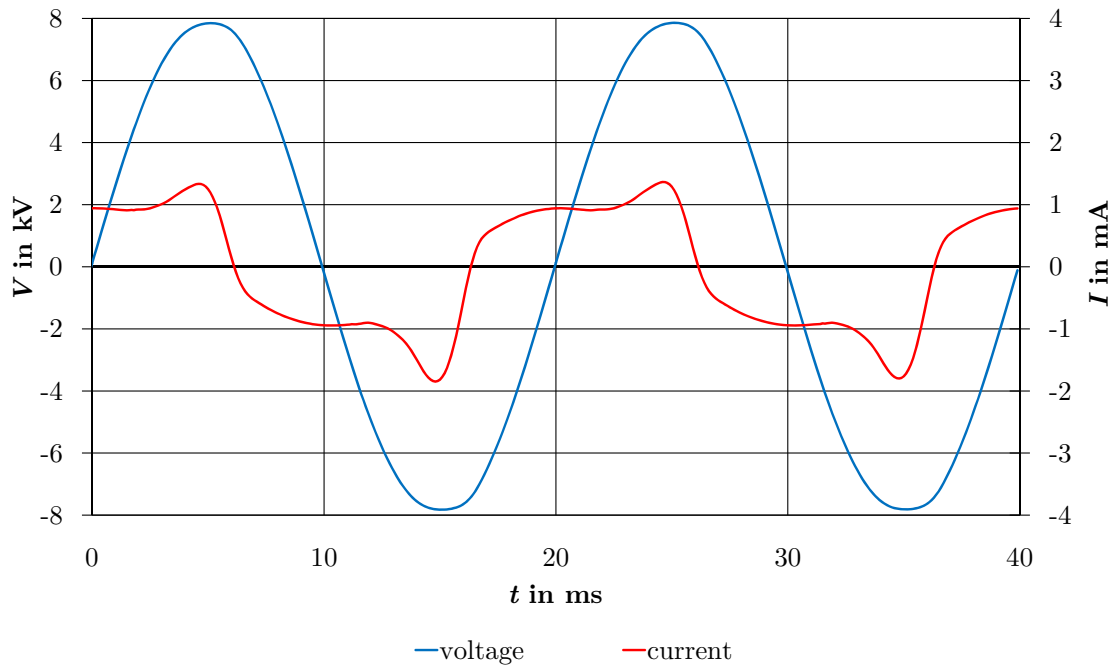
Figure 4.12: Oscillogram of voltage and current within the pre-breakdown region of the *V-I* characteristic of an MOV.

The test specimens are measured in a pneumatic test fixture at a clamping force of 314 N. The ambient temperature is measured and documented[74].

Further information on this test set-up is given in chapter A.4.

4.6 Aging Test Set-Up

In the aging test set-up[75], specimens are stressed with AC voltage at increased ambient temperature over long periods of time (e.g. 1000 h). There are three temperature chambers available in each of which up to five specimens can be operated at temperatures of up

---

$\sqrt{2}$. In [IEC60060-1], only 5 % are demanded for AC voltages at power frequency, which, however, does not lead to reproducible results for the strongly nonlinear *V-I* characteristic of the MOVs. For this reason, the limiting value of 2 % is used. This limiting value has not been exceeded in neither of the measurements described in the following.

[74] As is shown in [Rei08], the expectable error rate within the considered current region and at a fluctuation of the ambient temperature of 20 °C to 30 °C is lower than 1.5 %.

[75] This test set-up has been developed and built up in the context of this thesis (see [Tsc11].

to 200 °C with voltages of up to 10 kV. The equivalent circuit diagram resembles the one in figure 4.11 with the exception that, in the aging test set-up, more than one specimen can be simultaneously stressed by the central voltage supply. The voltage waveform is generated by a PC data acquisition card, intensified by a power amplifier and stepped up by a high voltage transformer. The voltage drop across the test specimens is measured by means of an ohmic voltage divider and the current flowing through each of the specimens is measured by means of an ohmic shunt. Both are recorded by a PC data acquisition card and evaluated and documented by a LabVIEW program. The power loss is averaged over three cycles and is measured two times per minute at the beginning of the test and only every five minutes at the end of the test (due to the significantly lower gradient). The LabVIEW program also takes over the adjustment of the central test voltage and the adjustment of the temperature inside each of the temperature chambers. The temperature of each of the test specimens is monitored by a temperature sensor inside of the aluminum contact electrode that is connected to the ground. This temperature functions as control variable.

In *figure 4.13*, the power loss behavior of an MOV is shown that was stored at a voltage (within the range of typical continuous operating voltages) for 1000 h at 115 °C inside the aging test set-up. It can be seen that voltage as well as temperature are kept very constant[76] by the test set-up and that the power loss of the MOV steadily decreases during the test duration.

The inside view of a temperature chamber in which an MOV is inserted is depicted in *figure 4.14*. The MOV is fixed between two aluminum contact electrodes by the weight force of the upper brass contact. The temperature sensor is integrated into the bottom aluminum contact electrode. The bottom electrode is put up insulated to be able to measure the current waveform inside the ground connection by means of a shunt.

Further information on this test set-up is given in chapter A.5.

---

[76] According to [IEC60099-4], the voltage must not change more than 1 % and the temperature no more than ±1 K. Moreover, the value of the peak to RMS value ratio of $\sqrt{2}$ must not deviate more than 2 %. This has been monitored for the whole test duration; a bigger deviation than 2 % occurred in none of the described investigations.
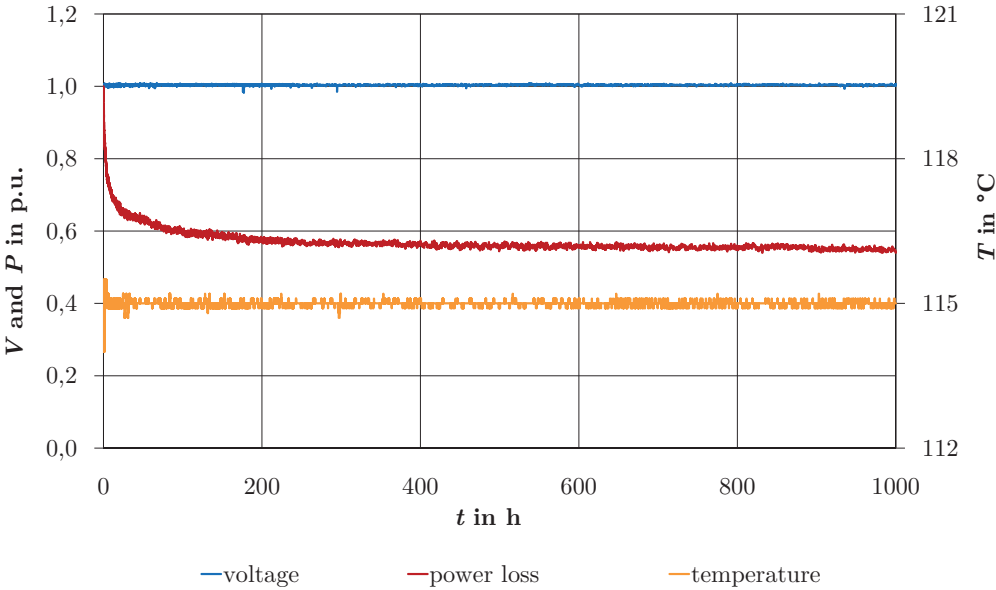
Figure 4.13: Recording of voltage, power loss and temperature for an MOV inside the aging test set-up where power loss and voltage are depicted scaled to the initial value.
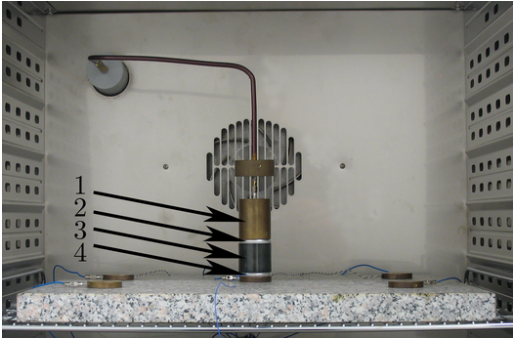
Figure 4.14: Inside view of one of the three temperature chambers of the aging test set-up (1 brass contact, 2 upper aluminum electrode, 3 test specimen, 4 temperature sensor inside bottom aluminum electrode).

5 Impulse Energy Handling Capability of MOVs

In the following paragraphs, the results of the experimental investigations are introduced and interpreted. In the first section, the investigations on the single impulse energy handling capability[77] are presented that have been published for the most part in [Rei08] and will be supplemented in this thesis by further investigations. The results serve as reference for the subsequent investigations concerning multiple impulse energy handling capability.

There is a difference between single and multiple impulse energy handling capability, as is shown in chapter 5.4. For one, previous impulses cause microscopic and macroscopic changes within the MOV. Moreover, they cause a rising of the temperature inside the MOV. In order to separate these effects, investigations on how temperature influences the energy handling capability of MOVs are introduced in chapter 5.2. In the subsequent section, the single impulse energy handling capability is compared to the energy handling capability at two successive long-duration current impulse stresses with a short interval between the stresses ($< 3\,\text{s}$).

The focus of this thesis is on the investigations on repetitive[78] impulse energy handling capability where the difference between several types of stresses (current densities of the stresses) and the influence of the energy density of each stress can be differentiated. Since these investigations are especially relevant for routine tests following the manufacturing process, a conventional routine test is compared to a recommended new routine test procedure in chapter 5.4.4.

Finally, investigations on the single impulse energy handling capability after a pre-stressing of the MOV are introduced in chapter 5.5. Due to their high practical relevance, investigations that identify the influence of changes of the $V\text{-}I$ characteristic on the energy handling capability are introduced here as well as investigations on the energy handling

---

[77] The different types of energy handling capability are compared in chapter 2.3
[78] The test specimens are cooled down to ambient temperature between the stresses.

capability of MOVs that were being operated for several years in real surge arresters inside the electric power system.

An overview of the aims for the investigations described in the following is given in *table 5.1*.

For all of the investigations (with the exception of those in chapter 5.5.3), brand-new MOVs were used which had not been exposed to electric stresses except for the routine test[79] at the end of the production process. In order to prevent a contamination of the surfaces of the MOVs, they were touched with white cotton gloves only.

The MOVs were provided by different international manufacturers on condition that the published results of the investigation would be anonymized. For this reason, neutral labels are used for the different varistor ceramics and different varistor types by different manufacturers and the coating is colored blue in photographic depictions. Each label represents a group of MOVs of the same type, the same manufacturer and the same production lot[80]. On the explicit request of the manufacturers, new symbols are introduced in each section as to make deciphering harder. There is no direct relation between the labels S to Z (of the size 1 and 2), ceramic 1 and 2, I to III, α to γ, type 1 and 2 as well as SA1 to SA9 used in the different sections. Partly, different sections involve MOVs of the same production lot, which have not been labelled equally for the stated reasons. If any new insights that exceed the individual investigations can be gained resulting from cross connections between the different investigations, they are described explicitly. Within the same section, no two similar MOVs by one manufacturer but separate production lots are labelled differently. The production lots that are labelled differently usually differ in the manufacturer of the MOVs. In exceptional cases, different types of MOVs (where not only the geometric dimension but also the recipe differ) of one manufacturer are distinguished.

Two sizes of MOVs were analyzed:

Size 1:   The MOVs of "size 1" are $55\,\text{mm}$ to $65\,\text{mm}$ in diameter and $40\,\text{mm}$ to $45\,\text{mm}$ in height[81]. This size of the MOV is normally used in surge arresters of high-voltage grids with line discharge class 2 or 3 (according to [IEC60099-4]).

---

[79] It can be assumed that the MOVs used here resemble those that the respective manufacturers use for the production of their surge arresters. However, since an undercover purchase of the necessary amount of MOVs was not possible, it cannot be ruled out (although this is not to be expected) that the specific manufacturers used special recipes or routine tests in the production process of the MOVs that were provided for the investigations.

[80] With exception of the labels in chapter 5.1: here, the labels used in the investigations of [Rei08] are continued, each manufacturer is given a label and the types of MOVs are distinguished based on their "size".

[81] One of the manufacturers provided MOVs with a height of only $26\,\text{mm}$.

Table 5.1: Overview of the investigations of MOVs introduced in the following

Chapter	Aim of the Investigation
5.1	**single impulse** energy handling capability depending on the current density of the stress
5.2.1	**temperature dependence of the V-I characteristic** within the range of current densities that are relevant concerning energy injections
5.2.2	Influence of the **temperature dependence of the V-I characteristic** on the **single** impulse energy handling capability
5.2.3	Change in the **single impulse** energy handling capability due to an **increased initial temperature**
5.3	Distinction between **single and multiple impulse energy handling capability**
5.4.1	Determination of energy handling capability with **repetitive AC energy injections**
5.4.2	Determination of energy handling capability with **repetitive long-duration current impulses**
5.4.3	Comparative investigations concerning energy handling capability with **repetitive energy injections of the same energy density** but different current density Comparison of the impact of **repetitive** pre-stresses on **AC energy and long-duration current impulse energy injections** Definition of energy handling capability with long-duration current impulses with **alternating polarity**
5.4.4	Comparison of selectivity and pre-damaging behavior of a **routine test** with long-duration current impulses or AC energy injections
5.5.1	Investigation on the correlation between the **change of the V-I characteristic** (due to pre-stresses) and the **change of the single impulse** energy handling capability
5.5.2	Investigation on the **reversal of the changes of the V-I characteristic** (after a pre-stress) by applying continuous operating voltage at increased ambient temperature
5.5.3	Determination of the **influence of actual stresses** in electric power systems on single impulse energy handling capability

Size 2: The MOVs of "size 2" are approx. 40 mm in diameter and 30 mm to 40 mm in height. They are normally used in surge arresters of medium-voltage grids with 10 kA nominal discharge current.

5.1 Single Impulse Energy Handling Capability of MOVs

Large parts of the results concerning the single impulse energy handling capability presented in the following were obtained during the investigations of [Rei08]. In the context of this dissertation, these investigations have been extended and supplemented.

For the investigations of single impulse energy handling capability, over 3,000 MOVs of seven internationally established manufacturers were analyzed. In order to anonymize the results, a representative letter (S, T, U, V, W, X, Y and Z) is allocated to each manufacturer of MOVs. If a manufacturer provided MOVs of both of the distinguished sizes, the same letter is allocated to both sizes. In one case, one of the manufacturers provided two different types of MOVs (differing in recipe) of the same size. For these two types, two different letters are used.

Due to the limits concerning the test facilities as well as for reasons of practical relevance, the single impulse energy handling capability is analyzed with three different types of energy stresses for the MOVs of "size 1" (see above). In doing so, AC energy injections at a current peak value of 10 A, 100 A, and 300 A, long-duration current impulses with a virtual duration of 1.2 ms, 1.9 ms, and 3.9 ms as well as stresses with the double-exponential discharge current of the 90/200 μs type are used. On the other hand, MOVs of the "size 2" are stressed with long-duration current impulses with a virtual duration of 1.2 ms, 1.9 ms, and 3.9 ms or with double-exponential discharge currents of the 90/200 μs or the 4/10 μs type.

For the investigation of single impulse energy handling capability at stresses with AC energy injections, these injections are carried out up to the mechanical failure of the respective test specimen. Thus, the results can be compared very easily with previous investigations for example by [Rin97]. The simplicity of the failure criterion "stressing up to mechanical failure" involves the disadvantage that failure mechanisms cannot be differentiated any further. Since changes in the *V-I* characteristic and pre-damages of MOVs can occur especially when stressed with high current densities (which is explained in chapters 2.2 and 2.5), a "complex failure criterion" that takes pre-damages into account is chosen for the investigations with long-duration current impulses. A flowchart showing a testing of an MOV with this "complex failure criterion" is given in *figure 5.1*.
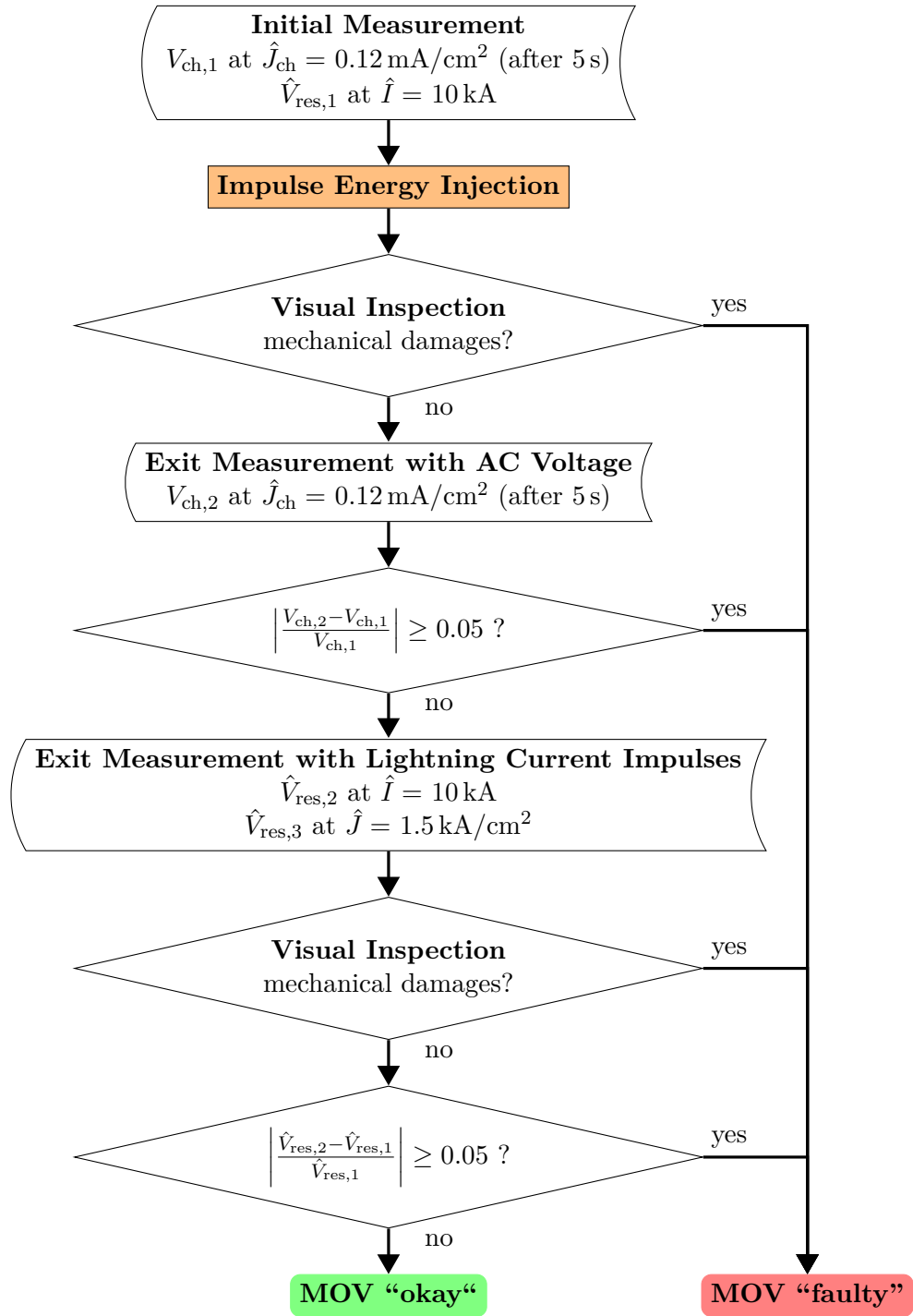
Figure 5.1: Flowchart of the determination of the single impulse energy handling capability taking the "complex failure criterion" into consideration (according to [Rei08]).

At the beginning of the investigations, an initial measurement is carried out for each MOV. Here, the "characteristic voltage" V_{ch}[82] at a peak value of the current density of $\hat{J}_{ch} = 0.12\,\text{mA/cm}^2$ ($\pm 2\,\%$) is determined after the voltage has been applied for $5\,\text{s}$. Furthermore, the residual voltage for a lightning current impulse of the $8/20\,\mu\text{s}$ type at a current peak value of $10\,\text{kA}$ ($\pm 1\,\%$) is determined.

After the initial measurement, the energy injections within the range around the mean failure energy of the respective type of energy injection of the MOV type of the investigated manufacturer are carried out. In doing so, 40 MOVs[83] of the same MOV type of a production lot are investigated for each type of energy injection (for example impulse duration). Within this group, five to 20 (very often ten) MOVs are stressed with the same energy density in order to determine the failure probability for this particular energy density.

If the MOV fails during the energy injection (which can be gathered from the oscillogram of the current), a visual inspection of the MOV is carried out. In the process, the failure symptoms mechanic cracking, puncture and flashover are distinguished. If the MOV does not fail mechanically due to the energy injection, the MOV is cooled down to ambient temperature and an exit measurement is carried out where the "characteristic voltage" and the residual voltage are measured again. Moreover, the MOV is stressed with an additional double-exponential discharge current of the $8/20\,\mu\text{s}$ type with a current density peak value of $\hat{J} = 1.5\,\text{kA/cm}^2$ in order to classify pre-damages even better. [Rei08] defined that a varistor is regarded as having failed if an energy injection leads to its mechanical failure, if "characteristic voltage" or residual voltage change by at least $5\,\%$ due to an energy injection or if the double-exponential discharge currents of the exit measurement lead to its mechanical failure. This definition is adapted in this dissertation for all investigations with "complex failure criterion".

If a mechanical failure of a specimen happens during the energy injection, the waveform of the energy injection matches the defined waveform only up to the failure. The resulting shortening of the impulse duration in case of failure amounts to an average of about $10\,\%$ due to the fact that the investigations are carried out within the narrow range around the mean failure energy. Due to the limited variation and in order to choose the labels failure-independent, the prospective waveform is constantly used as label in the following sections. The current density of the energy injection represents the less intuitive, yet physically more

---

[82] It lies within the typical reference voltage range of surge arresters. However, since the current density for the measurement of the reference voltage is not defined in [IEC60099-4] but differs between manufacturers, the term "characteristic voltage" is used here (as has been done in other publications).

[83] If this amount of MOVs does not lead to a clear result, the group is expanded to up to 80 MOVs.

exact description of the stress and is thus used for the purpose of evaluation (for example in diagrams).

The results of the investigation are statistically evaluated. In doing so, the mean failure energies during destructive analyses (AC energy injections) are evaluated with the "progressive stress method" and those during investigations with "complex failure criterion" (using impulse energy injections) are evaluated with the "multi-level method". The processes of statistical evaluation are explained in the appendix of chapter B.

The mean failure energies[84] above the amplitude of the current density as well as approximate values for the duration of the energy injections for MOVs of "size 1" are shown in *figure 5.2*[85]. Each mark in the diagram is determined by stressing at least 40 MOVs of one production lot. For the investigations within the range of current peak values of about $0.3\,\mathrm{A/cm^2}$ to $10\,\mathrm{A/cm^2}$, AC energy injections are used where the test specimens are stressed up to mechanical failure. Within the range of current peak values of about $60\,\mathrm{A/cm^2}$ to $300\,\mathrm{A/cm^2}$, the MOVs are stressed with long-duration current impulses. Within the range of the highest current densities investigated (up to $2500\,\mathrm{A/cm^2}$) the MOVs are stressed with the double-exponential discharge current of the $90/200\,\mathrm{\mu s}$ type. For these impulse energy injections, the "complex failure criterion" is applied. Hence, they are not directly comparable to the results of [Rin97], which are depicted in the diagram for reasons of comparison[86]. [Rin97] stressed all MOVs up to mechanical failure; this is why only the results within the range of the AC energy injections can be directly compared to the results in this thesis.

The failure mechanisms of the investigated MOVs of "size 1" are depicted in *figure 5.3* for the different types of energy stresses. In doing so, failure symptoms that lead to a cracking of the MOV are labeled "CR", as is shown in figure: 2.8(a) to (c), (e), (g), and (i). Flashovers such as in figure: 2.8(f) are labeled "FO"; punctures that do not cause a tearing of the MOV such as in figure: 2.8(d) are labeled "PU". For "100 %", all failures of one type of energy injection of one MOV by one manufacturer are assumed. The test series that are not depicted (regarding "Z") were not carried out.

---

[84] The AC energy injections of "S", "U" and "X" were carried out by [Rei08]. The impulse stresses of "S", "U" and "X" as well as the AC energy injections of "Z" were carried out by the author of this thesis in cooperation with [Rei08] and are contained in [Rei08]. All of the remaining investigations (except for those labeled [Rin97]) were carried out by the author of this thesis subsequent to the investigations by [Rei08]. All of the investigations are contained in [Cig13].

[85] For reasons of clarity, the standard deviations of the single mean values measured are not depicted here. On average, the standard deviation is less than 10 % of the mean value of the failure energy.

[86] The effects of both failure criterions on the determined energy handling capability of one production lot are depicted in *figure 5.6*.
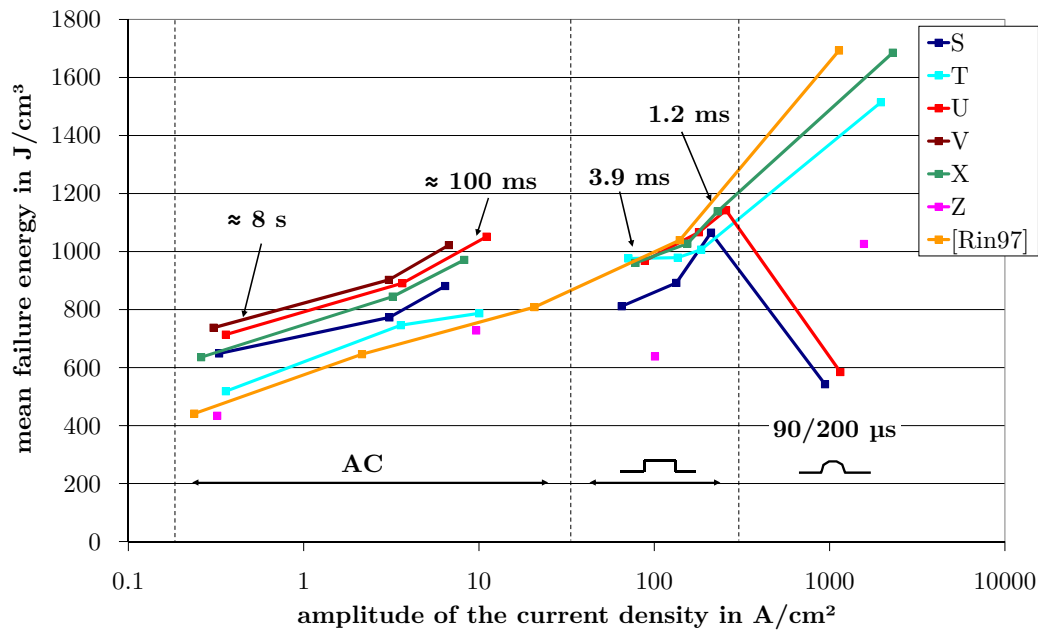
Figure 5.2: Mean single impulse failure energy above the peak value of the current density of the energy injection for MOVs of "size 1" (according to [Cig13]).

The following results can be deduced from the investigations of the single impulse energy handling capability (as for the most part published in [Cig13], [Hin09], [Tuc13a] and [Tuc09] and discussed in detail in [Rei08]):

- The single impulse energy handling capability increases with increasing current density[87] from about $400\,\mathrm{J/cm^3}$ to $1200\,\mathrm{J/cm^3}$. Here, the failure symptoms of the MOVs that are stressed with high current densities show a lot of residues on the front surface caused by local thermal overloads, presumably beginnings of punctures. On the other hand, those MOVs that were stressed with low current densities show only one single puncture channel and no additional incomplete melting channels. This observation seems to confirm the simulation results by for example [Bar96b], according to which more parallel current paths are used during stresses with high current densities than during stresses with low current densities, increasing the energy handling capability.

- By means of further evaluations, it could be shown that not only the energy increases with increasing current peak value of the energy injection, but also the charge that can be transferred.

---

[87] It has to be mentioned again that these values must not be mistaken for the thermal energy handling capability of standard surge arresters (which normally lies within the range of $200\,\mathrm{J/cm^3}$ to $300\,\mathrm{J/cm^3}$ according to [Hin12]).

CR	<u>cr</u>acking.
FO	<u>f</u>lash<u>o</u>ver
PU	<u>pu</u>ncture
MF	<u>m</u>echanical <u>f</u>ailure
Vch	change of "<u>ch</u>aracteristic voltage" exceeding 5 %
Vres	change of <u>res</u>idual voltage exceeding 5 %
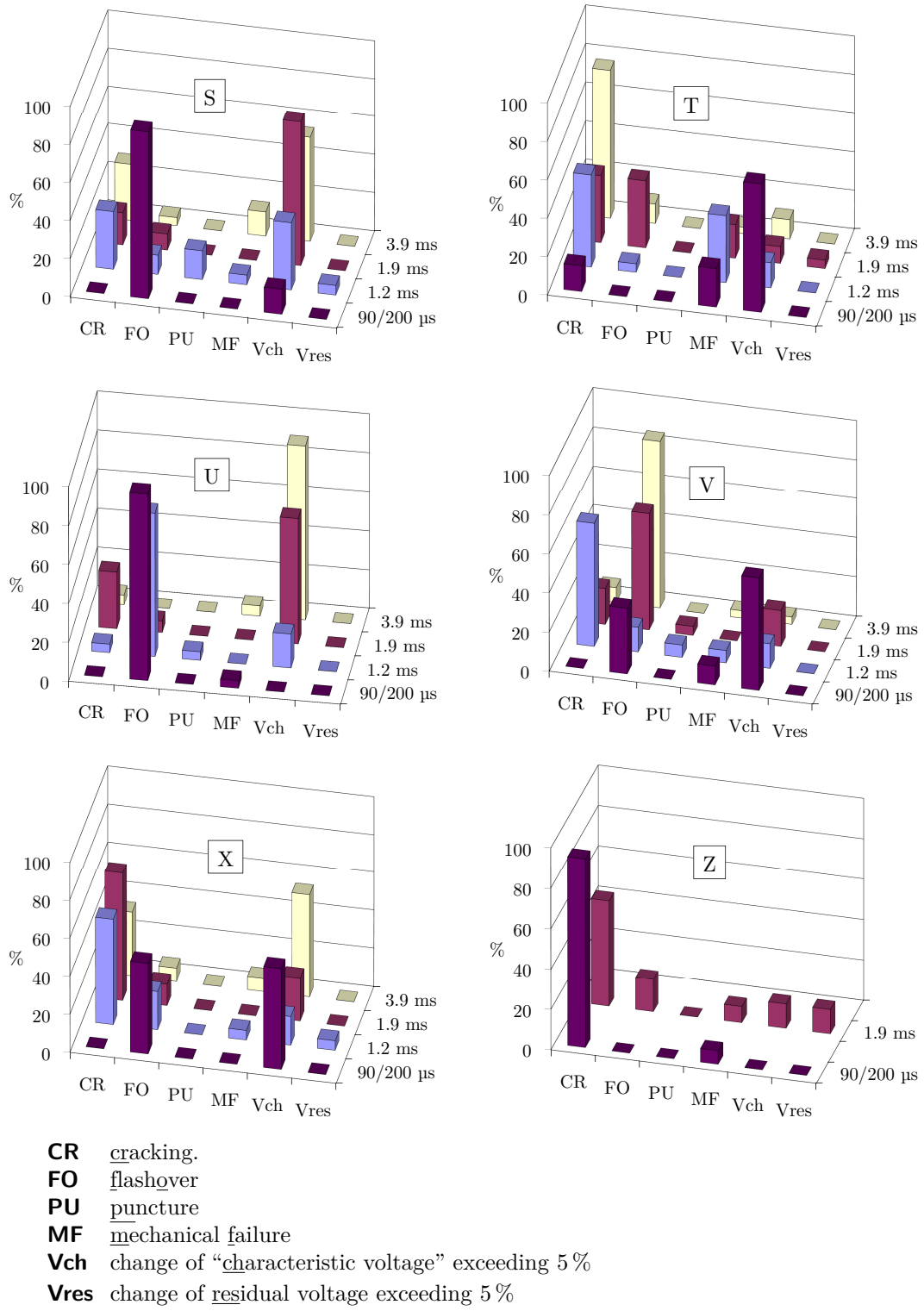
Figure 5.3: Failure mechanisms of the impulse energy injections of MOVs of "size 1" (according to [Cig13]), based on the "complex failure criterion".

- The increase of the mean failure energy at very high current densities is no longer limited by the ZnO ceramic but for example by the dielectric strength[88] of the coating (as it is the case for production lots "S" and "U"). However, it has to be taken into consideration that, also within this range, the single impulse energy handling capability lies above the usual thermal energy handling capability.

- The residual voltage is influenced only very rarely by an energy injection (as is already mentioned for example in [Dar97]) whereas the "characteristic voltage" seems to be more sensitive.

- The energy handling capability of the MOVs investigated here is – within the range of AC energy injections – about 30 % higher than it was the case with the MOVs investigated in [Rin97][89]. This is possibly due to the further development of the production processes, which led to an improved quality in MOVs despite the increased cost pressure.

Furthermore, it is noted by [Rei08] that, when testing the single impulse energy handling capability with AC energy injections for several hundreds of specimens, there are one or more MOVs (so-called outliers) within almost every production lot that show a considerably lower energy handling capability than the other MOVs. In *figure 5.4*, an example of a measurement series with 50 MOVs is depicted. It can be seen that the MOV with the number 31 shows a considerably lower energy handling capability than the rest of the MOVs. It is possible that recent routine tests used by manufacturers cannot reliably detect outliers for this type of stress.

The outliers can indicate inhomogeneities or inclusions inside the MOV, which can have varying effects depending on the different types of stresses. In *figure 5.5*, the failure energies of 37 MOVs per production lot are depicted. The failure energies were determined by an energy injection up to mechanical failure with an alternating current (at a current density of $0.35\,\mathrm{A/cm^2}$ or $3.5\,\mathrm{A/cm^2}$) or with a long-duration current impulse (at a current density of $185\,\mathrm{A/cm^2}$). It becomes clear that the failure energies for AC energy injections at a current density of $3.5\,\mathrm{A/cm^2}$ are much more dispersed than those for AC energy injections at a current density of $0.35\,\mathrm{A/cm^2}$ and those for long-duration current impulses at a current density of $185\,\mathrm{A/cm^2}$. When stressing the MOVs at a current density of $3.5\,\mathrm{A/cm^2}$, the failure energies spread around two energy levels: one of them around 60 % of the mean failure energy, the other at around 120 %. It can be assumed that the MOVs that fail

---

[88] [Rei08] demonstrated that the puncture happens between "MOV" and coating.

[89] The reason why the energy handling capability appears to be almost equal for the range of impulse energy injections is that different failure criteria were applied. A comparison of the mean failure energies for different failure criteria is shown in figure 5.6
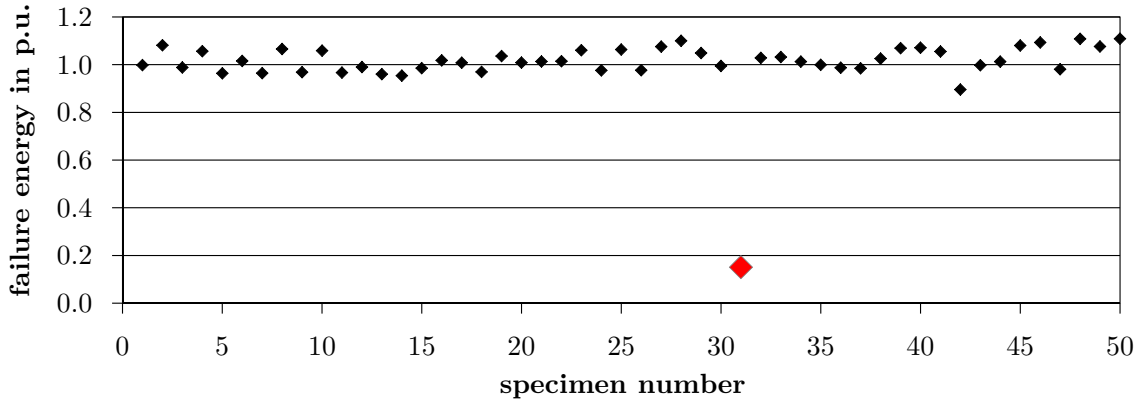
Figure 5.4: Overview of the scaled failure energies when stressing the MOVs of one production lot with the same AC energy injection (according to [Rei08]).

at the lower energy level contain defects that have a large impact on the mean failure energy for this type of stress[90]. It is possible that the stressing current flow concerning AC energy injections at a current density of $3.5\,\text{A/cm}^2$ is most strongly focused on the current path with the lowest resistance[91] until this path is overloaded and fails. If this applies, mechanical defects in MOVs can be detected more sensitively with this type of stress than with other types of energy injections (current densities, durations of the energy injection).

A comparison between the single impulse energy handling capability while using the two different failure criteria for long-duration current impulse energy injections and the investigations of [Rin97] is depicted in *figure 5.6* for "T" of "size 1". As can be seen in figure 5.3, most of the MOVs of this production lot fail during a long-duration current impulse energy injection with a virtual duration of $3.9\,\text{ms}$ and not during the exit measurement[92]. For this production lot, the amount of MOVs that fail during the energy injection decreases when the durations of the energy injections are decreasing (higher current densities of the energy injection). Accordingly, the difference of the mean failure energies between the two failure criteria that were investigated increases with increasing current density of the energy injection within the observed range. From a current density of about $250\,\text{A/cm}^2$ onwards (determined by long-duration current impulses with a virtual duration of about

---

[90] Since the simulation results in [Bar01], it has been known that, at higher current densities, defects within the MOVs do not affect the energy handling capability to such a great extent as they do at lower current densities.

[91] Concerning the formation of current paths, it is likely that the duration of the energy injection and the thermal conductivity of the ZnO ceramic matter.

[92] MOVs fail during the exit measurement due to a change of "characteristic voltage", a change of residual voltage or mechanical failure during the exit measurement resulting from the stress of the main energy injection.
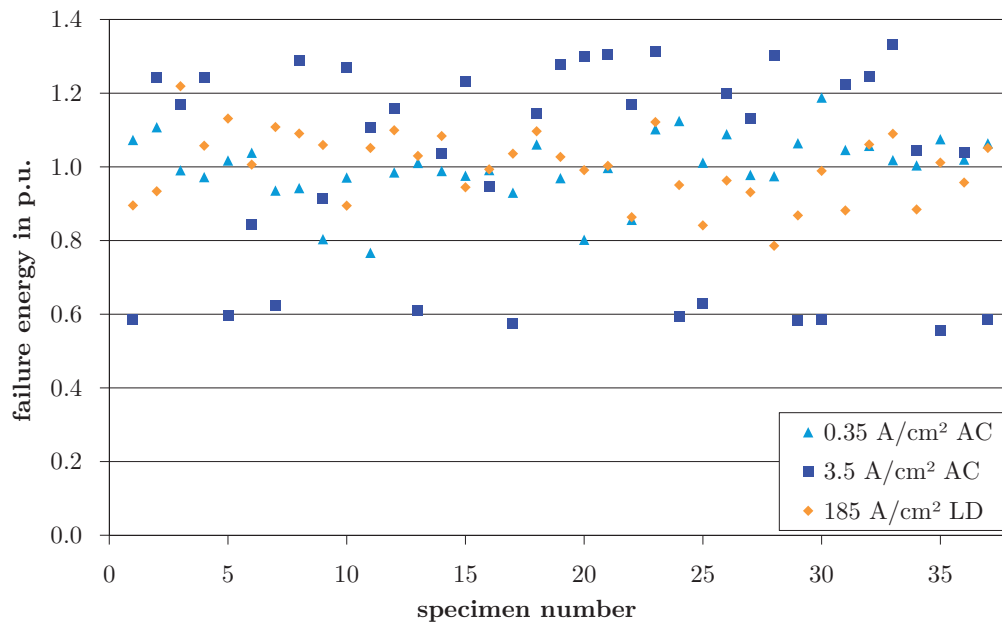
Figure 5.5: Overview of the failure energy for stresses at different current densities. The failure energy for the different current densities is scaled to the mean failure energy of the respective current density. The current densities $0.35\,\text{A/cm}^2$ and $3.5\,\text{A/cm}^2$ are determined by AC energy injections ("AC") and $185\,\text{A/cm}^2$ by long-duration current impulses ("LD").
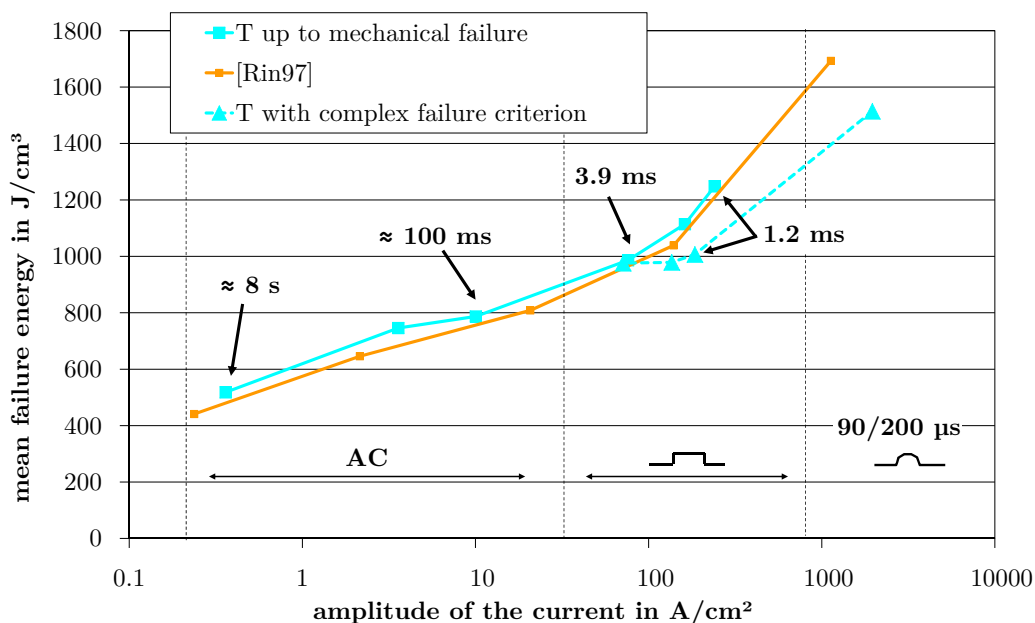
Figure 5.6: Comparison of the mean single impulse energy handling capability of MOVs labelled "T" ("size 1") at investigations with "complex failure criterion" or stresses up to mechanical failure, compared to the investigation results of [Rin97] (according to [Cig13]).

1.2 ms), the complex failure criterion seems to lead to a failure energy decreased by 20 %.

It can be assumed that it is different for those production lots where the energy handling capability at short energy injections is mainly limited by mechanical failure and not by a change within the *V-I* characteristic. One example for this is production lot "U" (see figure 5.3), where more MOVs fail due to a change within the *V-I* characteristic during long-duration current impulses than it is the case when applying short energy injections (which is probably due to the coating). In such cases, for short energy injections there will be just a minor difference or none between the mean energy handling capabilities when applying the two failure mechanisms. As becomes clear with this example, there is no general correlation between the failure energy when applying the "complex failure criterion" and failure energy for stresses up to mechanical failure. If one failure energy is to be deduced from the other, the failure causes must be taken into consideration.

For the MOVs of "size 2", the mean failure energies[93] are shown in *figure 5.7* and the failure mechanisms of each energy injection in *figure 5.8*. Concerning these MOVs, only impulse energy injections were carried out. However, for reasons of relevance, double-exponential discharge currents of the $4/10\,\mu s$ type were carried out for MOVs of "size 2", too.

As a result from the investigation of the MOVs of "size 2", the following statements (which are also given in the publications mentioned for the investigations of MOVs of "size 1") can be made:

- Within the range of the stresses with long-duration current impulses, the volume-related mean energy handling capability lies between $600\,J/cm^3$ and $1000\,J/cm^3$ and thus is about 15 % to 25 % lower than that of the MOVs of "size 1". As described below, MOVs with a smaller diameter generally show a higher energy handling capability. In this case, however, the difference can be explained by taking the different failure mechanisms into consideration. The MOVs of "size 2" fail relatively often due to flashovers. Apparently, the coating is not designed for such high stresses.

- Regarding double-exponential discharge currents of the $90/200\,\mu s$ type, the mean energy handling capability does not rise as much as for the MOVs of "size 1". The amount of failures caused by flashovers during the energy injections rises for the MOVs of individual production lots. This can of course be expected due to the increased voltage stress; nonetheless, this offers potential for optimization.

---

[93] The investigations concerning the single impulse energy handling capability for stresses with long-duration current impulses were carried out by [Rei08] for the production lots of the manufacturers "S", "U", "V", "W", and "Y". The investigations with double-exponential discharge currents were carried out in a cooperation of both authors and are contained in [Rei08]. All investigations are presented in [Cig13].
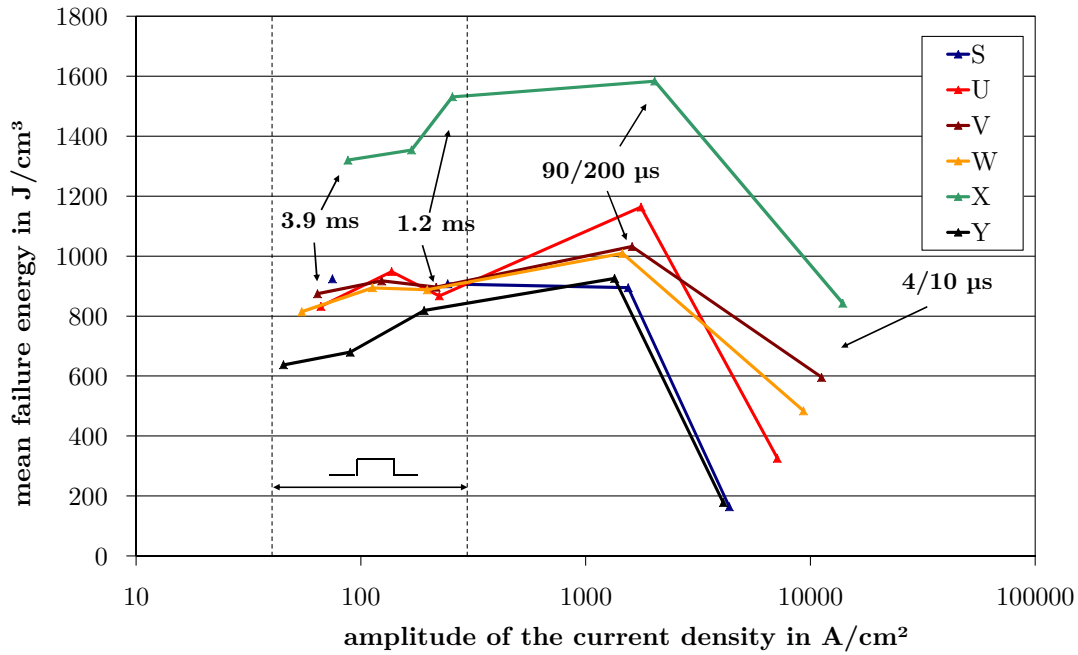
Figure 5.7: Mean single impulse failure energy above the peak value of the current density of the energy injection for MOVs of "size 2" (according to [Cig13]).

- Regarding double-exponential discharge currents of the $4/10\,\mu s$ type, the energy handling capability decreases again. This is due to an increase in failures caused by a change of the "characteristic voltage". However, this change does not influence the single impulse energy handling capability for stresses up to mechanical failure, as is described in chapter 5.5.1.

- The MOVs "X" stand out due to a very high single impulse energy handling capability, which was true for MOVs of "size 1", too. Here, the coating obviously seems to be designed for higher voltage stresses. Moreover, this manufacturer seems to be able to achieve a very high homogeneity of the produced MOVs.

The change of the "characteristic voltage" resulting from energy injections of the $4/10\,\mu s$ type are further evaluated in [Rei08]. The depiction of the change of the "characteristic voltage" above the current peak value[94] of the energy injection is shown in *figure 5.9*. Each mark within this diagram[95] represents a pre-stressed MOV of one production lot. It can be seen that the dispersion among individual MOVs is varyingly distinct for the different

---

[94] Due to the fact that the diameters of the MOVs of "size 2" differ only marginally, the absolute presentation is used here.

[95] Above which current range of the respective energy injection the change of the "characteristic voltage" is depicted depends on experimental, not specimen-related reasons.

CR	cracking.
FO	flashover
PU	puncture
MF	mechanical failure
Vch	change of "characteristic voltage" exceeding 5 %
Vres	change of residual voltage exceeding 5 %
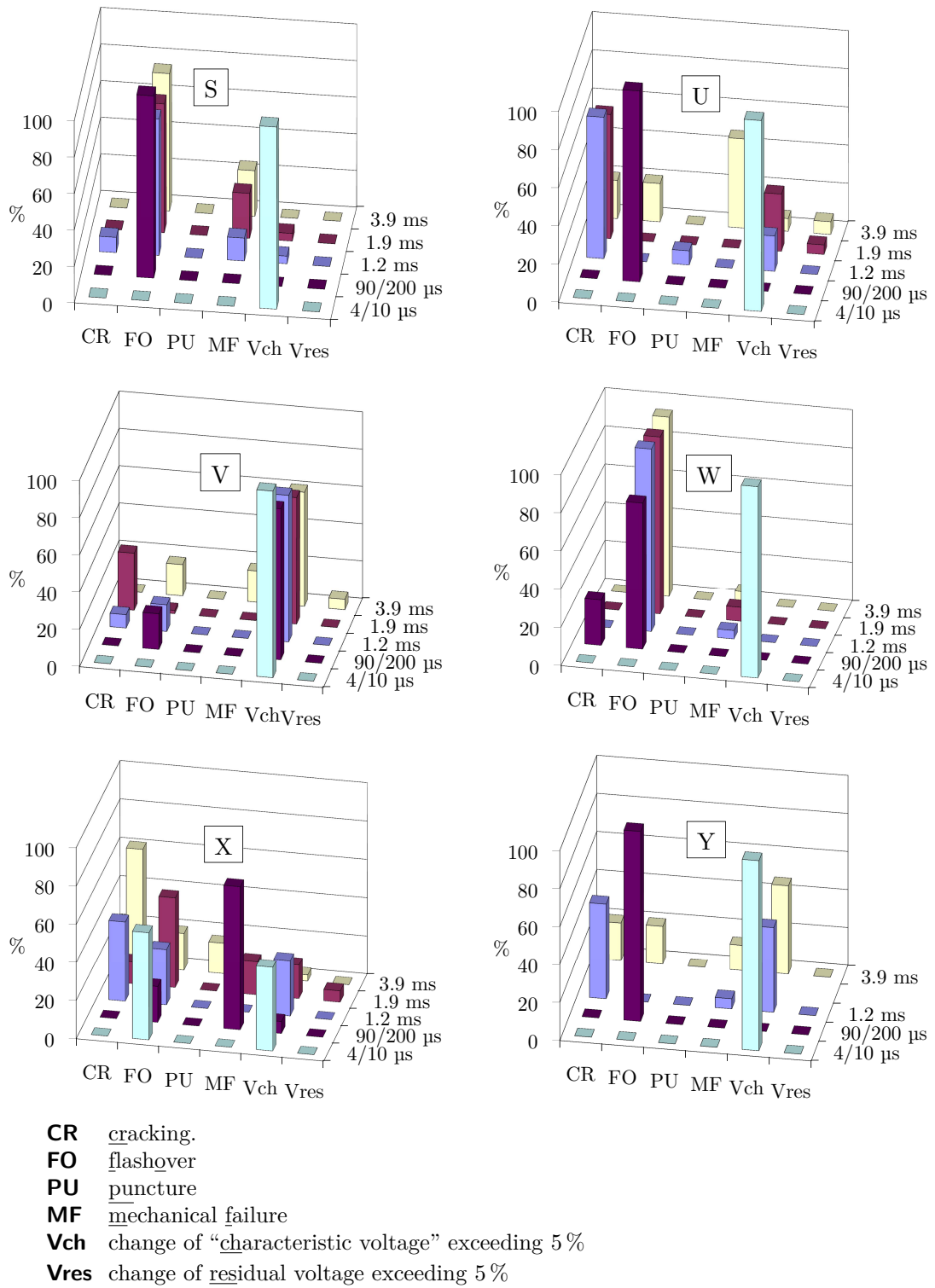
Figure 5.8: Failure mechanisms of the impulse energy injections of MOVs of "size 2" (according to [Cig13]), based on the "complex failure criterion".
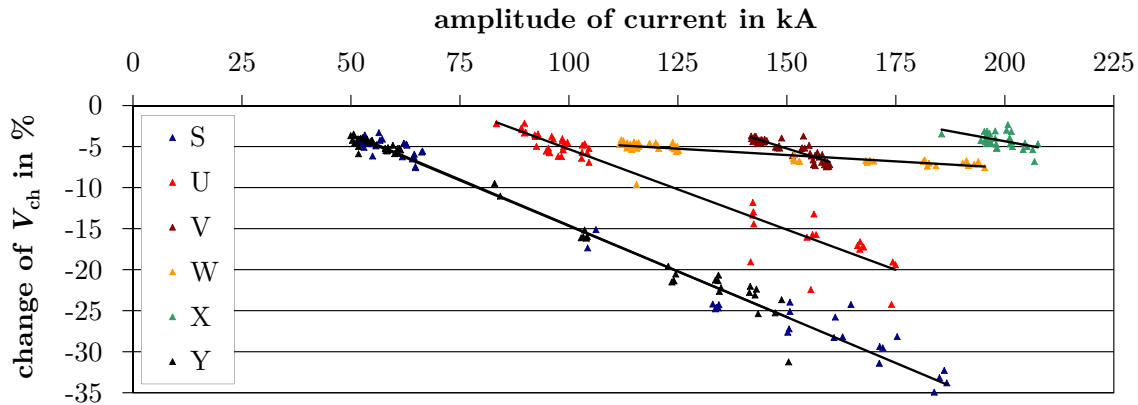
Figure 5.9: Change of the "characteristic voltage" V_{ch} resulting from a double-exponential discharge current of the $4/10\,\mu s$ type for MOVs of "size 2" (according to [Cig13]).

production lots. However, for all production lots the change of the "characteristic voltage" chiefly seems to be linearly[96] dependent on the current peak value of the energy injection. Some production lots already show a strong change of the "characteristic voltage" at a current peak value of $100\,kA$ of the energy injection. According to [IEC60099-4], this test is used for the verification of the thermal stability of surge arresters that typically contain this size of MOVs. Further investigations of the influence of the change of "characteristic voltage" on the energy handling capability and on the reversal at applied continuous operating voltage and at increased temperature are described in chapters 5.5.1 and 5.5.2.

The single impulse energy handling capability of the MOVs of "size 1" and MOVs of "size 2" differs even for one single manufacturer. This might be due to the different manufacturing processes or optimizations of the MOVs for different application fields. [Rei08] investigated the single impulse energy handling capability of MOVs of one manufacturer at AC energy injections. These MOVs had different diameters and, according to the manufacturer, were built using equal production processes. The results are shown in *figure 5.10*. Despite the dispersion of these results, it can be seen that the mean failure energy decreases with increasing diameter of the MOV, which matches the findings of [Eda84]. According to [Cig13], this cannot solely be attributed to the bigger volume, which generally leads to an increased failure probability, but presumably also to a higher degree of inhomogeneity (which is also presumed by [Eda84]).

---

[96] It can be assumed that, due to physical reasons, the trend crosses the abscissa only for very low current peak values of the energy injection.
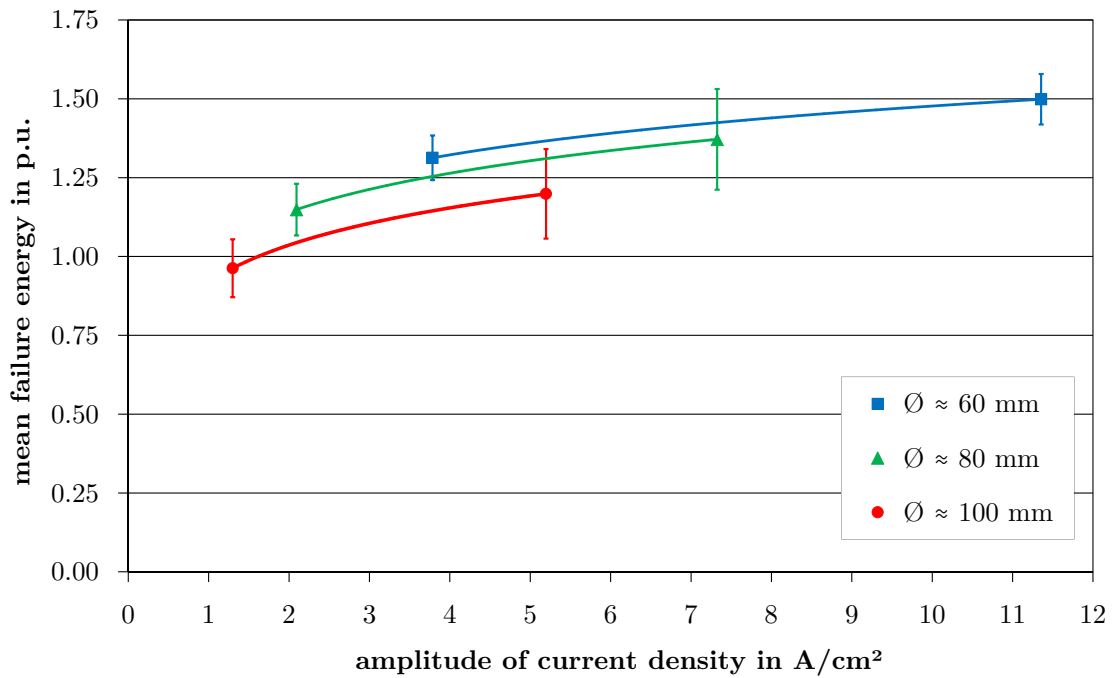
Figure 5.10: Single impulse energy handling capability of MOVs of different diameters but equal production processes at stresses with AC energy injections (according to [Rei08]).

5.2 Influence of Temperature Dependencies on the Energy Handling Capability

Energy injections can cause changes within the MOV because the current flow can change the charge distribution along the grain boundary (see chapter 2.2). Moreover, the heat converted inside the MOV leads to thermal tensions that can cause micro- or macroscopic cracks or, at worst, a partial melting of the ceramic. The focus of the investigations of impulse energy injections of a very short duration (within the range of less than 10 ms), which were carried out often in the past, was on changes caused by the current flow or on the dielectric strength of the coating. However, the focus of investigations of longer energy injections with bigger energy content is on the influence of heat on the MOV. For multiple energy stresses (with short time intervals between the stresses), not only the changes in charge distribution that are triggered by the current flow of prior impulses are relevant, but also the temperature or temperature distribution inside the MOV.

It is possible that an unbalanced distribution of the current flow during an energy injection leads to differences in temperature not only inside the MOVs, but also between parallel columns of MOVs. Furthermore, direct sunlight /shading might cause differences in

temperature between spatially divided columns of MOVs inside spatially extended surge arrester banks (for example used for the protection of capacitors, see chapter 2.1). This can lead to an unbalanced current distribution between the columns during an energy injection. These examples help clarify the fact that not only formations of current paths inside an MOV are of practical relevance, but also the macroscopic current distributions between MOVs. In the following sections, the influence of temperature on the current distribution between MOVs is elaborated on and, in turn, conclusions concerning the formation of current paths inside an MOV are drawn from these investigations. Finally, investigations of the temperature dependence of the single impulse energy handling capability are presented.

5.2.1 Determination of the Temperature Dependence of the *V-I* Characteristic within the Breakdown Region

It is known that the resistance of MOVs shows a negative temperature coefficient (NTC) behavior within the pre-breakdown region of the *V-I* characteristic (see for example [Eda89]). Moreover, it is assumed that, within the high-current region, a weakly marked positive temperature coefficient (PTC) behavior of the resistance predominates (see for example [Sch94] and [FH03]). This is explained by taking into consideration that, within this region, the overall conductivity of the MOV is determined not so much by the conductivity of the grain boundaries as by the conductivity of the grains themselves. This behavior is depicted in *figure 5.11*.
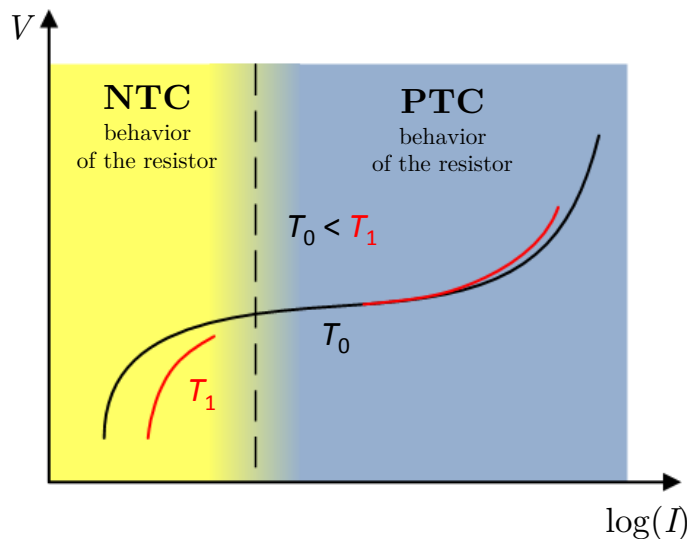
Figure 5.11: Chart showing the temperature dependence of the *V-I* characteristic of MOVs (according to [Hal12]).

The exact knowledge of the temperature behavior within the breakdown region of the *V-I* characteristic is of great interest when it comes to modeling the energy handling capability by computer-aided simulations. In order to support this interest, to answer the question in which part of the *V-I* characteristic the temperature behavior changes and to better classify thermal effects, the investigations concerning the determination of the temperature dependence within the breakdown region of the *V-I* characteristic of MOVs are introduced in this section.

To quantify the temperature dependence within the range of high non-linearity of the *V-I* characteristic is a big challenge because the change in voltage (at constant current density) at temperature jumps in the range of several 10 K varies only in the percent range and thus lies within the measuring uncertainty of commonly used measuring systems. For this reason, [Had05] suggests applying the current sharing measurement in order to determine the temperature dependence within this range of the *V-I* characteristic. This measurement technique is used for the investigations[97] introduced in the following.

The equivalent circuit diagram of the test set-up for the current sharing measurement is shown in *figure 5.12* and a picture of the applied specimen fixture in *figure 5.13* . For the investigation, two MOVs, "specimen 1" and "specimen 2", are simultaneously stressed with a discharge current. In doing so, the voltage[98] along the specimens as well as the single current[99] and differential current[100] through both specimens are measured.

The investigation is carried out for two different production lots of MOVs that are labelled ceramic 1 and 2 in the following. In doing so, the respective current sharing between two MOVs (of the same ceramic) is measured, specimen 1 being stressed at a defined increased temperature[101] inside the tempered test chamber and specimen 2 being stressed at ambient temperature[102]. Due to the mechanical setup as well as the different ohmic

---

[97] These investigations are also documented and evaluated in the diploma thesis [Hal12].

[98] For the measurement of the voltage, the voltage divider described in table A.8 is applied.

[99] For this measurement, the current transducer by "Pearson Electronics Inc.", model "410", with a frequency range of 0.120 kHz to 20 000 kHz and an accuracy of the transmission ratio of 1 % and the current transducers of the "CWT30" and "CWT150" type shown in table A.7 are used depending on the measurement range.

[100] For this measurement, the current transducer by "Pearson Electronics Inc.", model "110", with a frequency range of 0.001 kHz to 20 000 kHz and an accuracy of the transmission ratio of 1 % is used for all the investigations.

[101] The temperature is controlled by the temperature measurement system described in table A.14 with the temperature sensors described in table A.15 and are kept constant inside the range of ± 1 % around the target value for the investigation. The MOVs are preheated for at least eight hours inside a conventional temperature chamber.

[102] Due to the fact that the discharge currents used for this investigation only contain energy densities of a few J/cm^3 and that the specimens are not stressed thermally insulated, it is only very rarely necessary to externally cool down specimen 2. Furthermore, a 60-seconds wait is kept between the discharge currents.
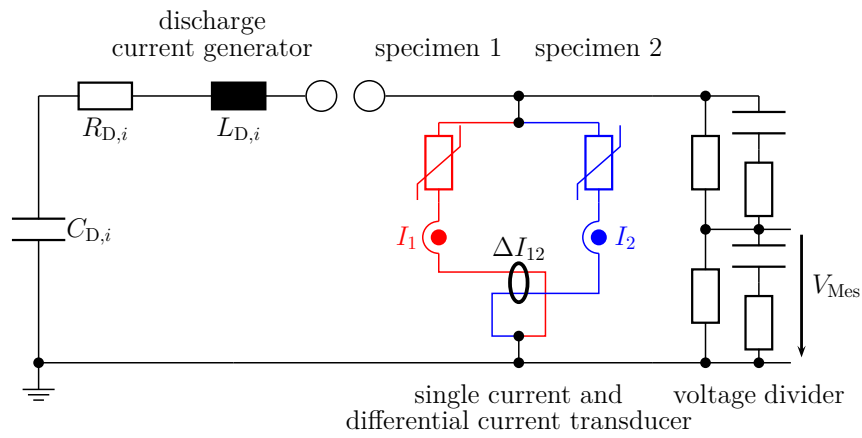
Figure 5.12: Equivalent circuit diagram of the current sharing measurement. I_1 and I_2 show the single currents through the specimens, ΔI_{12} the differential current and V_{Mes} the voltage that is transferred to the oscilloscope.

Figure 5.13: One side of the symmetrical specimen fixture for the current sharing measurement that is used for investigations of the temperature dependence within the breakdown region of the V-I characteristic.

resistances of the connection wires (at different temperatures), the two parallel strands of the specimen fixture show impedance differences. As could be demonstrated, regarding comparatively high-ohmic MOVs, these differences are negligible and thus influence the measuring uncertainty only secondarily. Changes of the MOVs due to discharge current stresses can largely be compensated by using the same comparison specimen 2 in a specimen pair and applying conditioning impulses prior to the evaluated discharge currents.

The results of the investigation are shown in *figure 5.14(a)* for ceramic 1 and in *figure 5.14(b)* for ceramic 2. In both diagrams, the percentage of the current difference at ambient temperature between the tempered specimen 1 and specimen 2, both being stressed simultaneously with a discharge current[103] of the 30/60 µs type, is plotted on the ordinate. On the abscissa, the current density of the MOV with ambient temperature (specimen 2) is plotted. The investigated current density range extends from $0.3\,\mathrm{A/cm^2}$ to $200\,\mathrm{A/cm^2}$. The nonlinearity exponent (see chapter 2.2) drops from about 60 to 30 within this range of the *V-I* characteristic. The temperature range of the respective specimen 1 lies between $20\,^{\circ}\mathrm{C}$ and $200\,^{\circ}\mathrm{C}$. Further investigations have shown that the discharge currents for the investigations of the *V-I* characteristic condition the MOV once the temperature rises above $200\,^{\circ}\mathrm{C}$, leading to an irreversible change of the current difference of the specimen pair of more than $5\,\%$ at ambient temperature. For this reason, the temperature range of this investigation is not extended any further.

Regarding the MOVs of ceramic 1, it can be seen that the difference in current density between the tempered specimen 1 and specimen 2, which is at ambient temperature, initially increases with rising temperature. Here, the depicted reduction of the current density by $50\,\%$ is equivalent to a halving of the current inside the warmer MOV caused by the increased temperature. The percentage of the current density difference between the two specimens drops with increasing current density of the current that flows through specimen 2 (with ambient temperature). This comes close to a vertical shift of the *V-I* characteristic due to the higher temperature, the nonlinearity exponent decreasing at higher current densities. This can be seen in the depiction of the temperature-dependent *V-I* characteristic in *figure 5.15*. At high temperatures, a minor change in the reduction of the current density between the temperature levels can be observed.

According to figure 5.14(b), the investigated ceramic 2 initially shows a rise in current difference with increasing current density of the stress for all temperatures, up to the moment where a slight declining tendency can be observed for the highest investigated

---

[103] For metrological reasons, the measurement points with the highest current density were determined by measurement with a discharge current of the 8/20 µs type. It could be shown that the influence of the current waveform is negligible within the observed range.

(a)

(b)
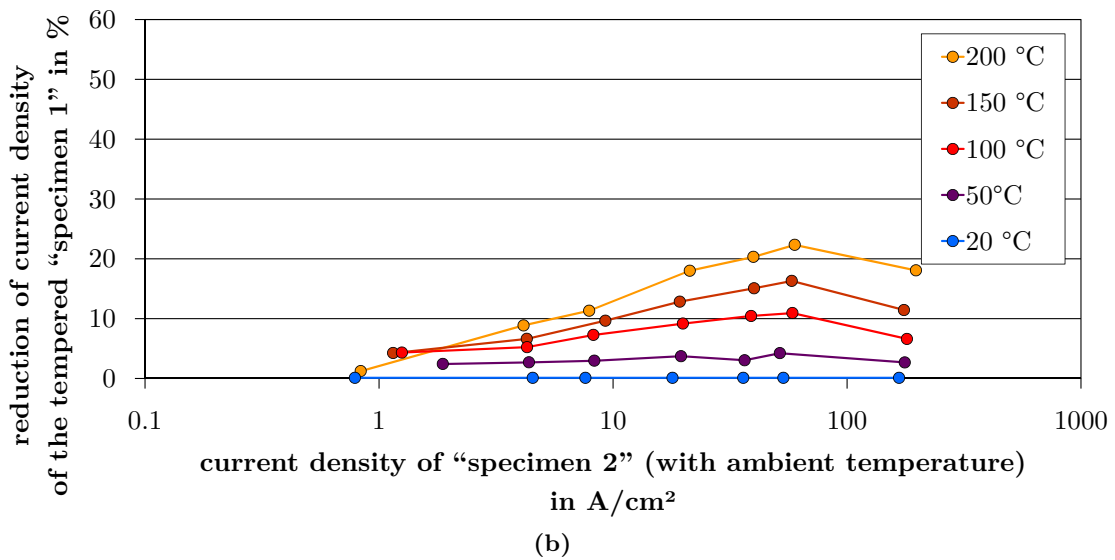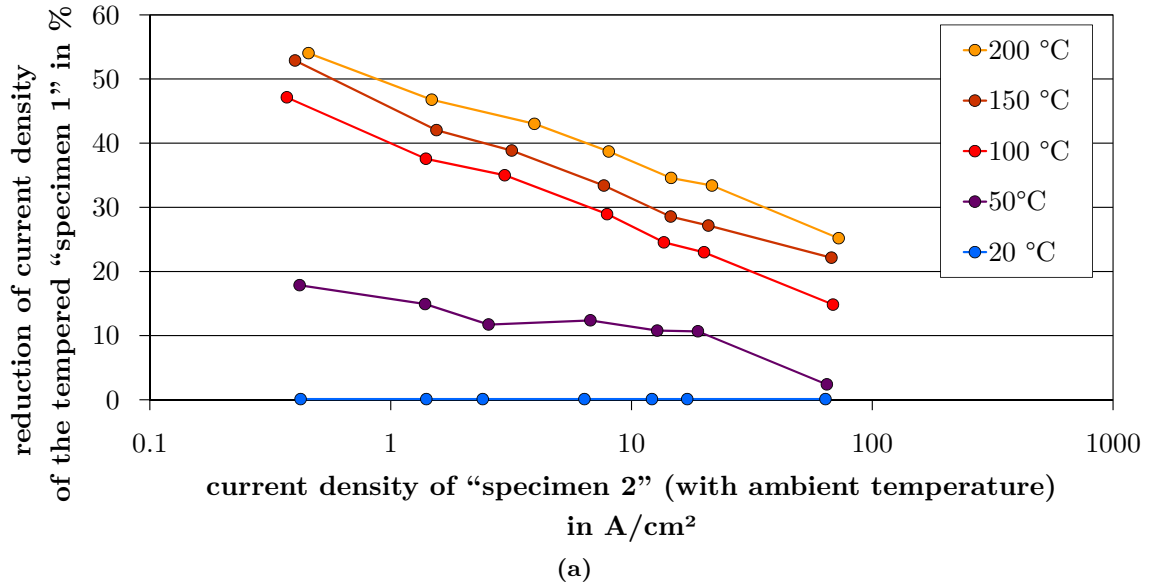
Figure 5.14: Change of current difference at different temperatures for the MOVs of ceramic 1 (a) and ceramic 2 (b).
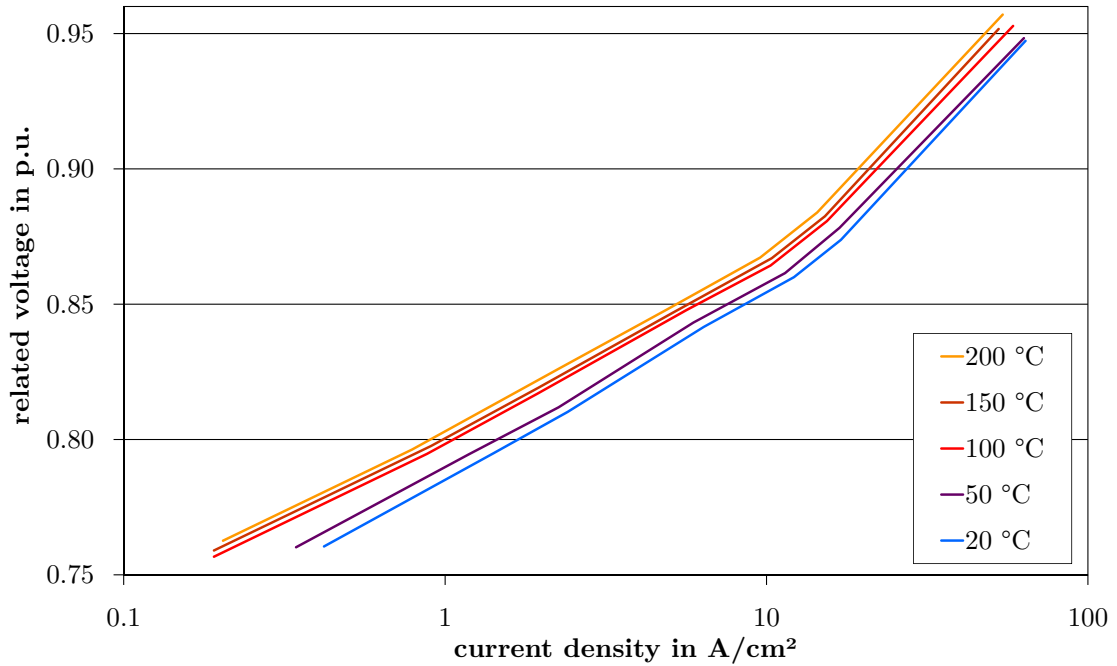
Figure 5.15: Depiction of the temperature dependent *V-I* characteristic of ceramic 1 within the investigated current density range.

current density. The temperature dependence within the investigated current range is less marked for this ceramic than for MOVs of ceramic 1.

Both ceramics show a negative temperature coefficient of the resistance within the pre-breakdown region of their *V-I* characteristic. For this reason, it can be presumed that, at low current densities, a sign conversion and a subsequent rise in change of the current density takes place for MOVs of ceramic 1 as can be observed for the investigated current density range of ceramic 2. It cannot be verified by the investigations carried out here whether both MOV ceramics follow the same tendency that shifts according to the current density or whether different mechanisms take effect.

Within the investigated range of current density and temperature, a positive temperature coefficient of the resistance of the MOVs can be noted for both ceramics. This could be explained by the increasing influence of the positive temperature coefficient behavior of the grain but also by a rising of the potential barrier (as is also described in [Hal12]). Concerning the latter, free charge carriers could be generated due to the temperature rise; the negative charges compensating defect states inside the grain boundary and the positive charges staying inside the grain. With rising temperature, the remaining positive charges expand the depletion region and thus the potential barrier. Hence, with rising temperature,

a higher voltage is necessary for the charge carriers to surmount the potential barrier. On a macroscopic level, this generates a PTC behavior of the resistance[104]. There is only a limited number of defect states within the grain boundary, hence the changes are becoming less frequent with rising temperature and finally come to a halt at high temperatures. For MOVs of ceramic 1, this can be observed at 200 °C. For MOVs of ceramic 2, it cannot be verified within this investigation whether almost all defect states are already entirely filled and thus another mechanism takes effect or, on the contrary, not all defect states are filled until 200 °C is reached and thus no saturation effect can be observed.

It must be pointed out that not only does the density of free charge carriers inside the MOV increase at higher temperatures, but that there is also a decrease in mobility concerning the charge carriers, which leads to a rise in resistance (see for example [FH03]). This could be a reason for the decrease in current difference within the range of $100 \, \text{A/cm}^2$ of the MOVs of ceramic 2. Moreover, the amount of free charge carriers does not only rise with the temperature, but also with the applied voltage (and thus with the current density of the stress), which is another indication for the effect that the temperature dependence must decrease with increasing current density.

The results of the investigation confirm that, within the breakdown region of the *V-I* characteristic, there is a sign conversion in the temperature coefficient of the resistance and, with this, the MOV changes from NTC to PTC behavior. Furthermore, the temperature dependence of the current density is not a constant, but depends heavily on the MOV ceramic and probably on temperature, as the investigations for ceramic 2 and additional investigations at higher temperatures show.

If further investigations confirmed the temperature dependence of the *V-I* characteristic and the zero-crossing of the temperature coefficient are dependent on the MOV ceramic, this could offer another indication for the explanation of the differences in the single impulse energy handling capability of MOVs of different manufacturers. A ceramic with a distinct positive temperature coefficient of the resistance should be more able to even out an inhomogeneous current distribution than a ceramic with a lower positive temperature coefficient. The energy handling capability of the investigated ceramics points into the same direction. However, the sample is too small to interpret this any further.

---

[104] Within the pre-breakdown region of the *V-I* characteristic, a higher leakage current develops due to the increased amount of free charge carriers. This is interpreted macroscopically as NTC behavior of the resistance.

5.2.2 Current Sharing between Parallel Stressed MOVs

So far, changes of the MOVs due to an energy injection (such as the above mentioned temperature dependence within the breakdown region of the *V-I* characteristic) are not considered in computer-aided simulations of current distributions inside MOVs, as for example in [Bar96b] (see chapter 2.5). An experimental measurement of individual current channels inside a single MOV during an energy injection is possible only with a lot of effort. However, an impression of the development of the current distribution between parallel current paths inside an MOV can be gained by observing the current sharing between parallel stressed MOVs. Also, this set-up is of practical relevance because, in some circumstances, several parallel columns of MOVs (with production-related uneven current sharing of up to 10 %) are used in surge arresters in order to enhance the energy handling capability. So far, the development of the current sharing during an energy injection inside such a set-up is unknown and is to be analyzed with the following investigation[105].

In this investigation, three MOVs of "size 1" of one production lot are stressed simultaneously with a long-duration current impulse. The current sharing during the energy injection is evaluated. Production-related, the three MOVs show small differences regarding the *V-I* characteristics that lead to an uneven current sharing between the MOVs. This way, three parallel current paths with slightly different *V-I* characteristics are simulated macroscopically.

The modified test fixture with three clamped MOVs can be seen in figure 5.16. The current flow through the MOVs is recorded by a separate current transducer[106] for each MOV. It could be demonstrated that small impedance differences between the current paths of the test fixture only have a minor influence on the current sharing.

The current characteristic of three simultaneously stressed MOVs of "size 1" when stressing them with a long-duration current impulse with a virtual duration of 1.2 ms is shown in *figure 5.17*; the characteristic when stressing the same MOVs with a virtual duration of 5 ms is depicted in *figure 5.18*[107]. In both figures, the arrows indicate the tendency of the amperage characteristic during the energy injections. During the energy injection with the virtual duration of 1.2 ms, about 220 J/cm^3 are applied to MOVs 1 and 2 and about 340 J/cm^3 are applied to MOV 3. This leads to temperature rises of the MOVs (taking the

---

[105] This investigation is also documented and evaluated in the bachelor thesis [Böl10].

[106] Each of the three currents is recorded by a current transducer of the type "HAT 1500-S", manufactured by "LEM", with a precision of ±1 %, linearity of ±1 % and a frequency range of 0 kHz to 25 kHz.

[107] The same three MOVs are stressed with a long-duration current impulse with a virtual duration of about 1.2 ms and 5 ms. In order to better illustrate the effects, higher differences in current density between the MOVs were applied than it would be the case in practical set-ups where differences in current density can amount to 10 % between the columns of MOVs.
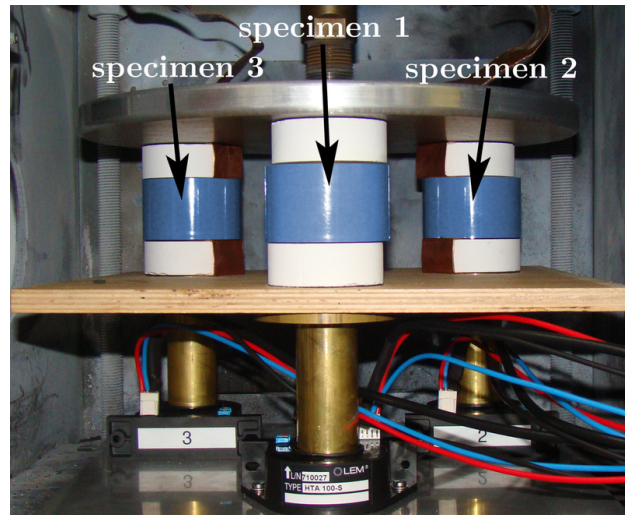
Figure 5.16: Test set-up for the parallel stressing of three MOVs.

material parameters according to [Lat83] as a basis) of about 77 °C or, concerning MOV 3, 116 °C. On the other hand, due to experimental reasons, for the longer energy injection with a virtual duration of 5 ms only about 150 J/cm^3 are applied to MOV 1, 170 J/cm^3 to MOV 2 and 290 J/cm^3 to MOV 3. This leads to temperature rises of about 54 °C or, concerning MOV 3, 100 °C. It can be seen in both diagrams that the current sharing between the MOVs changes during the energy injection. The current density through MOVs 1 and 2 shows an increasing tendency during the energy injection (see figure 5.17), whereas the current density through MOV 3 displays a slightly decreasing tendency. It can be seen in figure 5.18 that, here, the current density inside MOVs 1 and 2 only increases a little during the energy injection, whereas the current density inside MOV 3 clearly declines, which is also the case for the current sum provided by the long-duration current impulse generator.

Looking at the converted energy[108] in the individual sectors of the energy injection, it becomes clear that 80 % more energy is converted inside MOV 3 compared to MOV 1 within the first quarter of the long-duration current impulse depicted in figure 5.17 whereas only 45 % more energy is converted inside MOV 3 compared to MOV 1 within the last quarter. The energy intake during the long-duration current impulse shown in figure 5.18 changes similarly. Here, about 117 % more energy is converted inside MOV 3 compared to MOV 1 within the first quarter whereas only about 52 % more energy is converted inside MOV 3 compared to MOV 1 within the last quarter.

---

[108] It must be taken into consideration that (as can be seen in figure 4.5) the voltage inside an MOV rises during an energy injection with a long-duration current impulse.
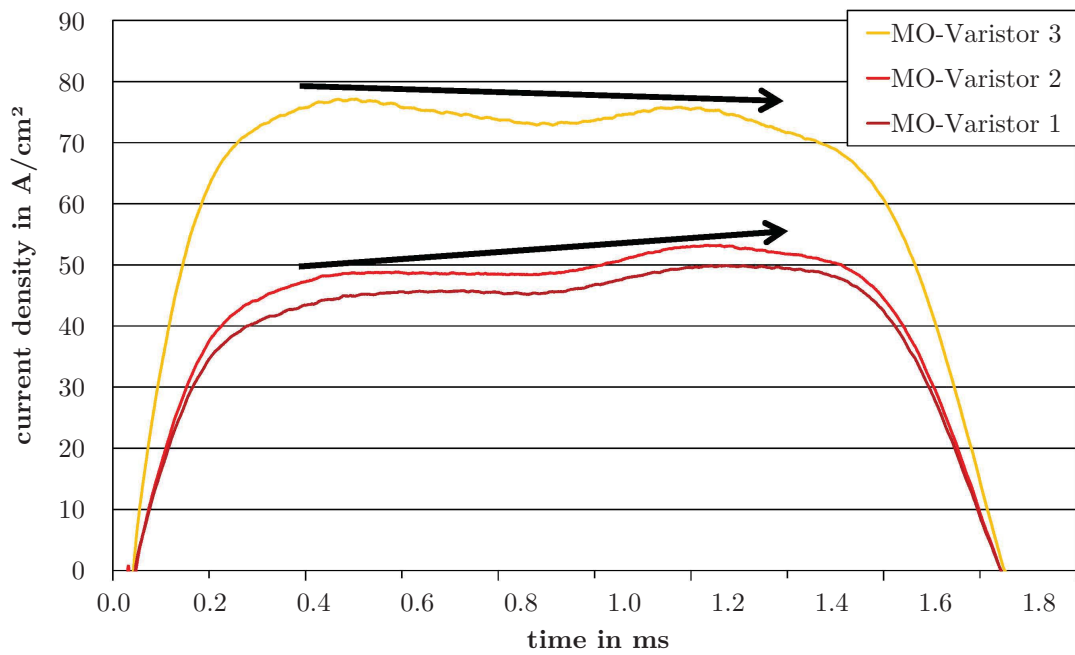
Figure 5.17: Current characteristic of three parallel stressed MOVs at a long-duration current impulse with a virtual duration of 1.2 ms.
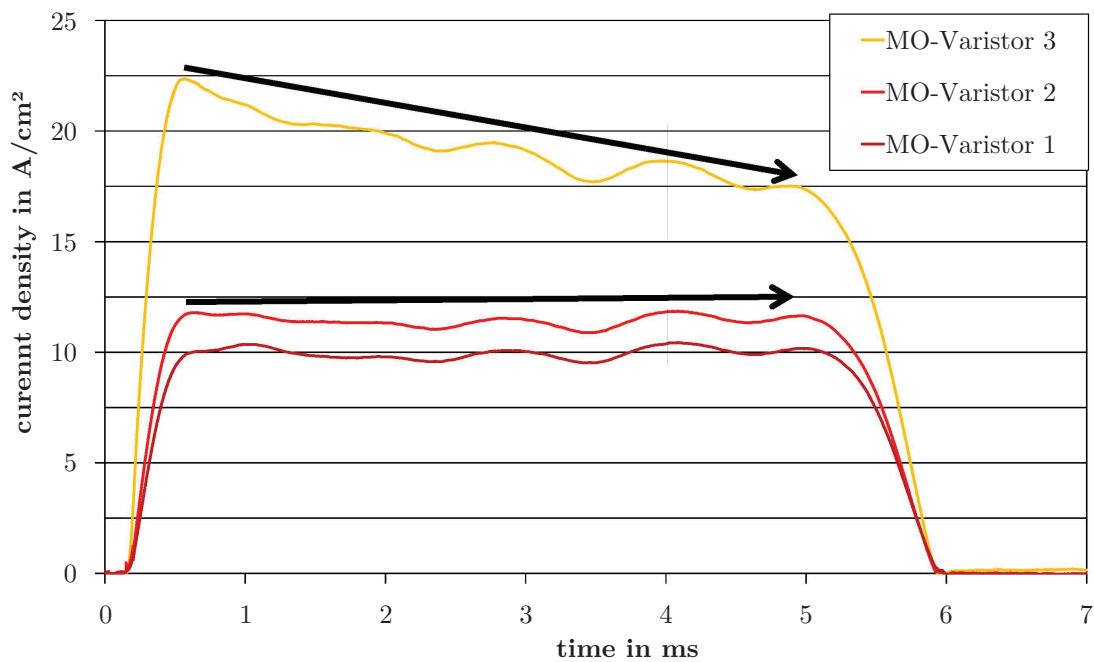
Figure 5.18: Current characteristic of three parallel stressed MOVs at a long-duration current impulse with a virtual duration of 5 ms.

Obviously, the difference between the current densities of MOV 1 (or MOV 2) and MOV 3 becomes smaller in the course of the investigated energy injections. It must be observed that the rise of the current density of MOVs 1 and 2 presumably cannot be attributed to a negative temperature coefficient of the resistance, but rather to the changed resistance behavior of the MOVs among themselves. Since the current density decreases inside the hotter MOV 3, the percentage of current density inside the colder MOVs 1 and 2 increases. Depending on the total current impressed by the long-duration current impulse generator, this can lead to an absolute increase of the current inside the MOVs with a lower temperature rise.

The results of this investigation support the findings of chapter 5.2.1, according to which higher voltages are necessary within the breakdown region of the *V-I* characteristic in order to impress the same current on a heated MOV as it would be the case for the same MOV in a cool state. This effect can be observed independent of whether the thermal energy is applied from the outside (as it was the case in chapter 5.2.1) or, as it is the case in this chapter, by an electrical energy injection that also induces other changes inside the MOV. However, this cannot be seen as being a distinct "self-protection effect" where small current differences would be balanced by the temperature effect during an energy injection as the temperature effect has too little impact on the *V-I* characteristic. Thus, it can be assumed that the temperature dependence of the *V-I* characteristic only has a small positive impact on the energy handling capability when several parallel columns of MOVs or several parallel paths inside an MOV are operated.

5.2.3 Single Impulse Energy Handling Capability of MOVs at Increased Ambient Temperature

In addition to the influence of the temperature dependence on the current distribution inside the MOV during an energy injection, the influence of the prevailing temperature of an MOV on the energy handling capability matters. Surge arresters can take several hours to cool down again to ambient temperature after a high energy injection[109], which reduces the ability to withstand multiple stresses. In order to be able to estimate the influence the initial temperature of the MOV has on the energy handling capability depending on the current density of the energy injection, the following investigation[110] is carried out.

---

[109] In [ABB11], a cool-down time of 45 min to 60 min is assumed for surge arresters of the medium-voltage level, depending on the construction and the ambient conditions. The cool-down time for surge arresters at higher voltage levels is much longer, as is suggested in the student papers [Mus09], [Dür10], [Kac11] and [Nur11].

[110] This investigation is also documented and evaluated in the bachelor thesis [Sch13].
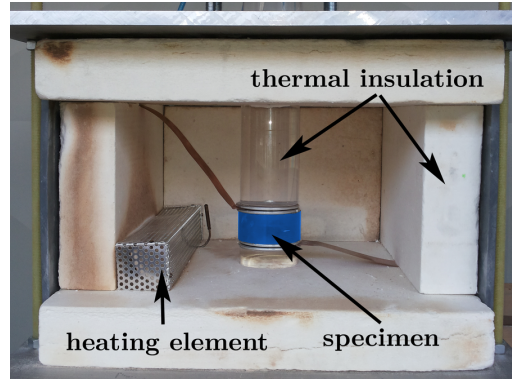
Figure 5.19: Test fixture for the investigation of the single impulse energy handling capability of tempered MOVs.

The single impulse energy handling capability is determined for three different initial temperatures (27 °C, 126 °C, and 213 °C) and two current densities: at $3.6 \,\text{A/cm}^2$ with an AC energy injection and at $177 \,\text{A/cm}^2$ with a long duration current impulse. The temperature levels are selected in such a way that the difference of the heat energy[111] stored inside the MOVs always amounts to the same value of $290 \,\text{J/cm}^3$ between two subsequent temperature levels.

$$27 \,°\text{C} \xrightarrow{+290 \,\text{J/cm}^3} 126 \,°\text{C} \xrightarrow{+290 \,\text{J/cm}^3} 213 \,°\text{C}$$

All energy injections are carried out up to mechanical failure of the MOVs. For each temperature level of one current density, 24 MOVs are stressed. The MOVs (as well as the aluminum contact electrodes) are pre-heated in a conventional temperature chamber for at least eight hours and stressed in the tempered specimen fixture, which is shown in *figure 5.19*. Inside the specimen fixture, the temperature of the specimen is controlled with an infrared sensor[112] (in figure 5.19, the sensor is hidden by the specimen). The energy injections are carried out when the air temperature of the specimen fixture as well as the specimen temperature lies within an interval of $\pm 5 \,\text{K}$ around the target value.

In *figure 5.20*, the results of this investigation are compared to the results concerning the MOVs of production lot "T" (using the same failure criterion) that were introduced in chapter 5.1. The standard deviation of the failure energies at increased initial temperature lies within the range of $10 \,\%$ of the respective mean failure energy. It can be seen that the

---

[111] In order to determine the heat stored inside the MOV, the heat capacity (the material parameters are taken from [Lat83]) of the MOVs is integrated via the temperature range of the pre-heating phase of the investigation.

[112] The infrared sensor used here (type "optris CS", manufacturer "Optris") has an accuracy of $\pm 1.5 \,\%$ respectively $\pm 1.5 \,°\text{C}$.

mean failure energy decreases with increasing initial temperature. Thus, as was expected, pre-heated MOVs can handle less electric energy of a single impulse energy injection than colder MOVs. Moreover, it can be observed that the mean failure energy for an initial temperature of the MOVs of 213 °C is reduced by about half during an AC energy injection with a current density of 3.6 A/cm². On the other hand, the mean failure energy is only reduced by around 20 % during a long-duration current impulse energy injection with a current density of 177 A/cm². These results are similar to the results of [Kan83], where there was no reduction of the single impulse energy handling capability detectable for long-duration current impulses with a virtual duration of 2 ms up to 100 °C and a reduction of about 40 % between 100 °C and 200 °C could be observed.

For comparison, the mean failure energy plus the thermal energy stored inside the MOV (starting from ambient temperature) is shown in *figure 5.21* for both types of energy injection[113]. As already mentioned, the stored thermal energy is determined by integration of the heat capacity of the MOVs (according to [Lat83]) via the temperature range starting from ambient temperature. It can be seen that the sum of thermally stored and electrically applied energy in all cases exceeds the single impulse energy handling capability that has been determined for ambient temperature. For AC energy injections with a current density of 3.6 A/cm², the sum of thermally applied and electrically applicable energy at an initial temperature of 213 °C is about 28 % higher than the electric energy that can be applied at ambient temperature. For the long-duration current impulse energy injection with a current density of 177 A/cm², this value amounts to about 33 %. The failure symptoms of the stressed MOVs are not significantly different from failure symptoms regarding investigations with different initial temperatures.

If the MOV is thermally heated constantly for several hours, the energy is distributed evenly inside the MOV, whereas the distribution of energy is inhomogeneous for electrical energy injections due to current path formation etc. The duration of the energy injections is very short with a virtual duration of 1.9 ms for the long-duration current impulse and about 100 ms for the AC energy injection, leading to a very limited heat equalization[114] inside the MOV. The percentage difference between the sum of the thermally applied energy plus the additionally electrically applicable energy at an initial temperature of 213 °C as well as the electrically applicable energy at ambient temperature lies within the same range (28 % or 33 %) for both investigated current densities. It can thus be concluded from the investigations in this section that, concerning the single impulse energy handling capability,

---

[113] In figure 5.20 and 5.21, the colors of the edges mark the temperature of the specimens before the energy injection and the colors of the surfaces mark the respective type of energy injection.

[114] By computer-aided simulations, it could be shown that a heat front can only spread distinctly less than 1 mm in 100 ms inside an MOV.
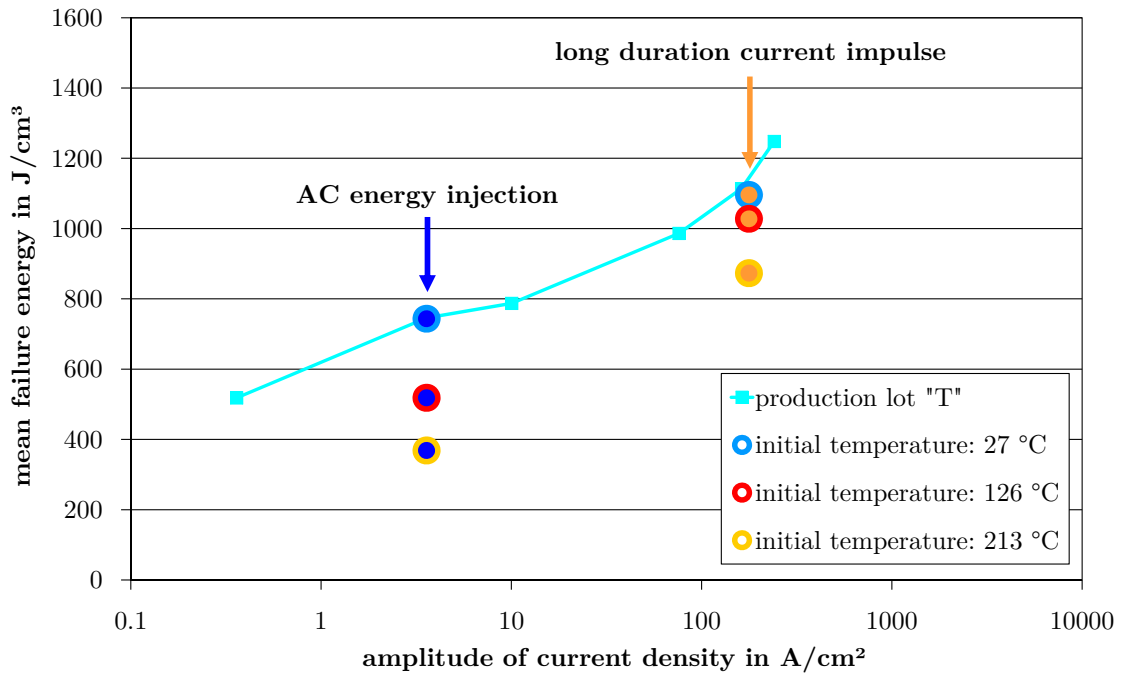
Figure 5.20: Mean failure energies of the tempered MOVs compared to earlier investigations (see chapter 5.1) at ambient temperature.
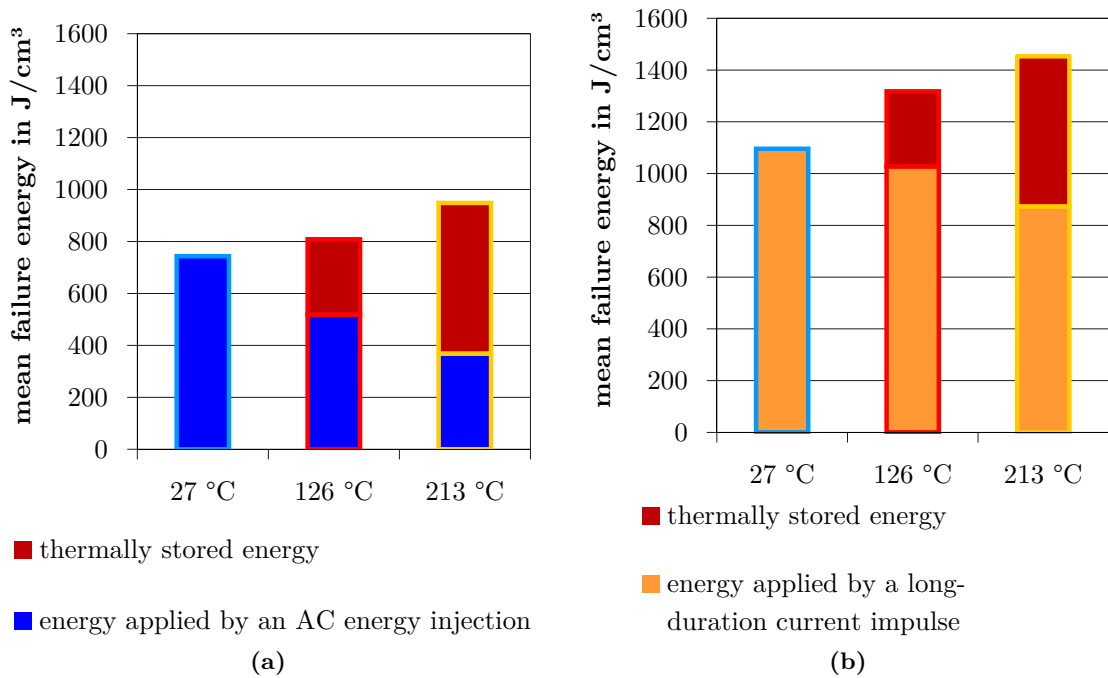
Figure 5.21: Mean failure energy plus the thermally stored energy for: (a) AC energy injections and (b) energy injections with long-duration current impulses.

the current distribution is relevant due to the microstructure of the MOV whereas the temperature dependence of the *V-I* characteristic only plays a minor part.

5.3 Double Impulse Energy Handling Capability of MOVs

During operation, surge arresters can be stressed with multiple energy injections (see chapter 2.3) in time intervals of < 1 ms (see for example [Cig13a] and [Cig13b]), for example due to stresses caused by lightning re-strike or re-strike of circuit breakers. Also in standard testing, such as according to [IEEEC62.11-2012], [IEC60099-4] and [IEC-37/416/FDIS], long-duration current impulses are injected in time intervals of less than 60 s. Despite the high practical relevance, publications on multiple impulse stresses are mainly limited to stresses with double-exponential discharge currents that are especially relevant for surge arresters used for the medium-voltage level (see for example [Dar97], [Den98] and [Kle04]). These stresses are characterized by high current densities and high current rise times but relatively low energy contents. Long-duration current impulses with high energy content are of greater importance for MOVs that are used for the high-voltage level. In order to differentiate multiple impulse energy injections from single impulse energy injections with long-duration current impulses, the following investigation is carried out.

For this investigation, the long-duration current impulse generator of chapter 4.3 is split into two parallel generators. Each of these can independently generate a long-duration current impulse with a virtual duration of 1.9 ms. The schematic diagram of this set-up is shown in figure A.4.

An example of a double impulse of two long-duration current impulses at an interval of about 80 ms thus generated is depicted in *figure 5.22*. Here, the MOV fails mechanically during the second energy injection, which results in a voltage collapse and nearly a doubling of the current[115].

In order to investigate double impulse energy handling capability, MOVs are stressed with two long-duration current impulses with a duration of 1.9 ms each and at an interval between the triggering[116] of 80 ms or 3 s. Since it is generally unknown whether the double stresses have a greater influence on the *V-I* characteristics of the stressed MOVs than a single stress, the first of the test series introduced in the following is carried out applying

---

[115] The current does not die away after the destruction of the MOV since the second long-duration current impulse is triggered through a semiconductor switch consisting of thyristors. The semiconductor switch prevents the polarity reversal of the current.

[116] Intervals exceeding 3 s were not investigated so as to limit the influence of the heat emission behavior of the MOV towards its surroundings and the test set-up.
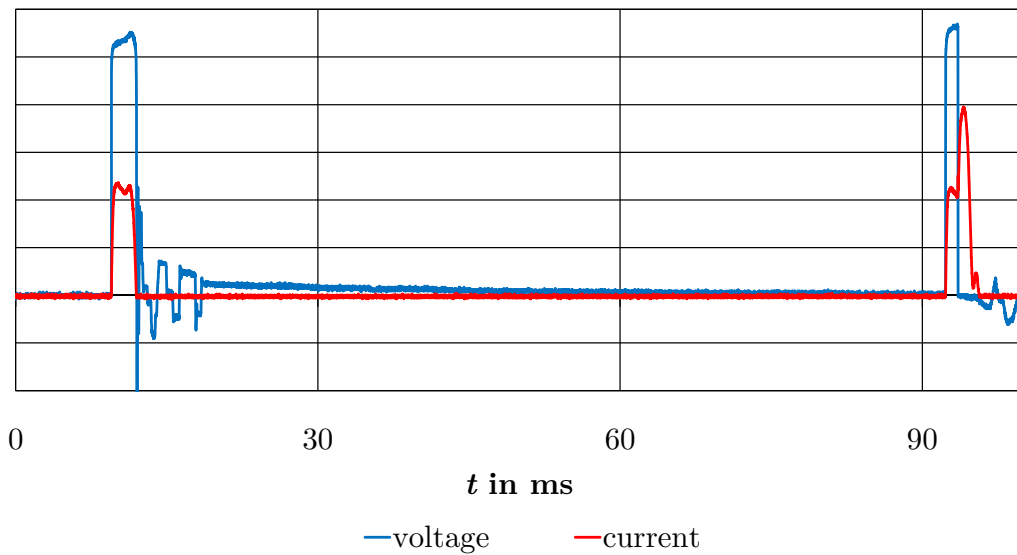
Figure 5.22: Oscillogram of current and voltage (each anonymized) of an MOV during a destructive stress using a double impulse consisting of two long-duration current impulses at an interval of about 80 ms.

the "complex failure criterion" (as shown in figure 5.1). Here, MOVs of "size 2" of one production lot are stressed. For the investigations up to mechanical failure of the MOVs, MOVs of "size 2" of another production lot are used.

The results of the investigation of the double impulse energy handling capability as compared to the single impulse energy handling capability (both when applying the "complex failure criterion") are shown[117] in *table 5.2*. The mean current density of the individual energy injections has the same value ($70 \, \text{A/cm}^2$) for each of the double impulses. With $75 \, \text{A/cm}^2$, the value of the current density of the single impulse with a virtual duration of $3.9 \, \text{ms}$ is a little higher than that of the double impulse stresses. With $131 \, \text{A/cm}^2$ however, the mean current density of the long-duration current impulse with a virtual duration of $1.9 \, \text{ms}$ is of a value almost twice as high because here a little less than half the virtual duration is used to inject the energy. The sum of the first and second energy injection is given for the mean failure energy of the double impulse stresses. It draws on the mean failure energy of the long-duration current impulse with a virtual duration of $3.9 \, \text{ms}$. For the double impulses, this mean failure energy differs only slightly from that of the single impulse energy injections with a virtual duration of $1.9 \, \text{ms}$. Taking the coefficients of variation[118] into consideration, the difference regarding an energy injection with a virtual duration of

---

[117] The results are documented and evaluated in the research paper by [Gie11], too.

[118] The coefficient of variation is a statistical parameter that is defined as standard deviation divided by the mean value (see for example [Leh85]).

Table 5.2: Overview of the double impulse energy handling capability of MOVs using long-duration current impulses compared to the single impulse energy handling capability. For the investigations, the "complex failure criterion" (as shown in figure 5.1) has been applied.

virtual duration /time interval	double impulse		single impulse	
	1.9 ms/3 s	1.9 ms/80 ms	3.9 ms/-	1.9 ms/-
mean current density in A/cm^2	70	70	75	131
mean (sum of) failure energy in p.u.	0.95	0.95	1.00[a]	0.94
Coefficient of variation	0.21	0.15	0.17	0.11

[a] reference value

Table 5.3: Overview of the double impulse energy handling capability of MOVs using long-duration current impulses compared to the single impulse energy handling capability. For the investigations, the MOVs were stressed up to mechanical failure.

virtual duration /time interval	double impulse		single impulse	
	1.9 ms/3 s	1.9 ms/80 ms	3.9 ms/-	1.9 ms/-
mean current density in A/cm^2	106	111	111	233
mean (sum of) failure energy in p.u.	1.04	1.02	1.00[a]	1.02
Coefficient of variation	0.09	0.12	0.07	0.10

[a] reference value

3.9 ms is small, too. In this investigation, no difference between double and single impulse stresses (as shown in figure 5.8) can be observed for the same production lot when looking at the failure mechanisms.

As an interim result, it can be stated that the differences that could be observed between the failure energy of single and multiple impulse stresses are so little that they could not be rendered visible at a coefficient of variation from 0.11 to 0.21. Since the double impulse stresses lead to similar failure symptoms as single impulses do, the application of the "complex failure criterion" does not seem to generate any additional information. In order to verify the results of the investigation for a second production lot (which shows a higher failure energy) as well as to reduce the coefficient of variation, the test series is repeated for another production lot without applying the "complex failure criterion", but instead by stressing the MOVs up to mechanical failure. The results of this investigation are documented[119] in *table 5.3*.

---

[119] The results are also shown in [Tuc13a].

In this test series, too, the mean impressed current of the double impulses with $106\,\text{A/cm}^2$ to $111\,\text{A/cm}^2$ lies within the same range as that of the single impulse stresses with $111\,\text{A/cm}^2$ for a long-duration current impulse with a virtual duration of $3.9\,\text{ms}$. However, the mean current density of the single impulse stresses at a virtual duration of $1.9\,\text{ms}$ is again twice as high, amounting to $233\,\text{A/cm}^2$. Taking the coefficient of variation of 0.07 to 0.12 (which is reduced a little due to the changed failure criterion) into consideration, the mean (sums of) failure energies differ only marginally. Also, in this investigation, the failure symptoms of those MOVs that were stressed with different time intervals do not differ significantly. Thus, the second investigation confirms the first investigation in this section.

It can be concluded from both investigations that, within the observed range, the energy handling capability for long-duration current impulses does not vary significantly for single and double impulse stresses for triggering intervals of up to $3\,\text{s}$. The results of the investigations suggest that the heat distribution inside the MOV - caused by an uneven current distribution after a first long-duration current impulse stress (with the considered current density) - is not improved within a time interval of $3\,\text{s}$. The reason for this could either be that the time interval is too short or that the heat distribution is not so distinct as to have a significant influence. The findings of chapter 5.2.3 indicate that the uneven heat distribution after a long-duration current impulse pre-stress within the respective range of the current density is only slightly marked and thus the difference in energy handling capability between double and single impulse stresses within the same range of the current density is very little.

Consequently, the individual energy injections must be added for investigations on the energy handling capability for multiple impulses with short time intervals within the observed range of the current density. It can be assumed that this approach is valid for any time interval between the stresses as long as the MOV is not able to dissipate a considerable amount of heat[120]. In the "single impulse withstand rating test" in [IEEEC62.11-2012] and in the "test to verify the repetitive charge transfer rating" in [IEC-37/416/FDIS][121], the MOVs are tested by two successive impulses with a time interval of $50\,\text{s}$ to $60\,\text{s}$. The results described here indicate that, dependent on how much heat the specimen fixtures[122] dissipate from the tested MOVs, the MOVs in this testing according to the standard are exposed to a stress that is within the range of two individual energy injections up to a

---

[120] At which point of time this is the case depends less on the MOV but rather on the design of the specimen fixture or the surge arrester in operation. For this reason, the exact point of time cannot be investigated further in this general consideration.

[121] In [IEC60099-4], the impulse handling capability is tested with 18 energy injections split into six groups with three impulses each that are carried out at an interval of $50\,\text{s}$ to $60\,\text{s}$. The MOVs are cooled down to ambient temperature between the stresses.

[122] The specimen fixture is not specified further within the mentioned standards.

single energy injection with twice the specified energy content. Recommendations on the further development of the standard are introduced in chapter 6.2.

5.4 Energy Handling Capability of MOVs Concerning Repetitive Energy Injections

After outlining the single impulse energy handling capability and showing the differences compared to the multiple impulse energy handling capability with the help of investigations on the double impulse energy handling capability, the focus in this section is on investigations of the energy handling capability of MOVs concerning repetitive energy injections. Repetitive stresses are repeated stresses where the test specimens cool down to ambient temperature between each stress. The properties of energy injections that cause a fatigue or a degradation of MOVs at repetitive stresses are to be defined in this section.

The variances of repetitive stresses are big if the different kinds, interdependencies, amount of stresses, heights, polarities (polarity reversal) of the current density as well as different exit measurements, which might influence each other or can also be destructive sometimes, are taken into consideration. Since the investigation of repetitive stresses (especially for high numbers of stresses) is very complex, only lower numbers of specimens and less production lots[123] compared to the testing of the single impulse energy handling capability can be investigated. This limits i.a. the evaluation possibilities of the failure symptoms of the stressed MOVs.

In the following, the behavior of MOVs at repetitive stresses with the same properties (type of stress, current density, polarity etc.) is fundamentally investigated with up to 100 stresses. Afterwards, individual parameters are modified in order to determine their influence. For the characterization of the fatigue behavior, the "characteristic voltage" is determined (as for the single impulse energy handling capability) within the pre-breakdown region of the *V-I* characteristic and, in some cases, the residual voltage within the breakdown region of the *V-I* characteristic of the pre-stressed MOVs. Additionally, the single impulse energy handling capability is evaluated by applying stresses up to mechanical failure subsequent to the repetitive stresses. All investigations introduced here (with the exception of the investigations in chapter 5.4.4 and 5.5) are carried out for MOVs of "size 1".

---

[123] The number of specimens used and the number of production lots are pointed out in the respective sections.

5.4.1 Repetitive Impulse Energy Handling Capability Concerning AC Energy Injections

Repetitive AC energy injections can occur particularly in surge arresters for the protection of serial capacitors (see chapter 2.1). However, surge arresters of the UHV level are also increasingly considerably stressed with temporary overvoltages and thus with AC energy injections (see for example [Hin12]). The reason for this is that, in this field of application, extremely low protection levels are used that shift the whole *V-I* characteristic towards higher leakage currents (see for example [Hin12]). The aim of the investigation[124] introduced in this section is to increase the knowledge of the stress handling capability of MOVs concerning AC energy injections.

For the investigation of the stress handling capability, ten MOVs per production lot of three different production lots[125] (labelled "I", "II" and "III") are stressed with 100 AC energy injections each. The flowchart of the investigation is depicted in *figure 5.23*. From this, it can be seen that, at the start, all MOVs undergo an initial measurement where the "characteristic voltage" is determined at a current density peak value of $0.12\,\mathrm{mA/cm^2}$. Since the lightning current impulses used for the measurement of the residual voltage show relatively high current rise times and current peak values compared to the AC energy injections used for the pre-stresses, a measurement of the residual voltage could change the MOV to a higher degree than the applied pre-stresses. For this reason, no measurement of the residual voltage for the initial and exit measurement is carried out in this measurement series.

Following the initial measurement, a pre-stress with an AC energy injection at a power frequency of $50\,\mathrm{Hz}$ at a current density of $3.5\,\mathrm{A/cm^2}$ is carried out. The duration of the energy injection is chosen so that the injected energy of the pre-stress amounts to about $80\,\%$ of the mean single impulse energy handling capability[126] of the respective MOVs (see chapter 5.1). This leads to energy injections of the pre-stress of about $600\,\mathrm{J/cm^3}$ to $700\,\mathrm{J/cm^3}$ that are applied with AC energy injections with a duration of $200\,\mathrm{ms}$ to $300\,\mathrm{ms}$. After the pre-stress, the MOVs are cooled down to ambient temperature by forced cooling within about $15\,\mathrm{min}$. The cool-down time is relatively long compared to the heating-up time by the energy injection. Thus, it can be presumed that the mechanical tensions inside

---

[124] The results of this investigation are also described in [Tuc13a].

[125] The results of one production lot are also documented and evaluated in the research paper [Gol09].

[126] $80\,\%$of the mean single impulse energy handling capability are used because further evaluations of the results of chapter 5.1 show that, for this amount, the failure probability at a single energy injection lies below $0.01\,\%$ for the whole production lot.
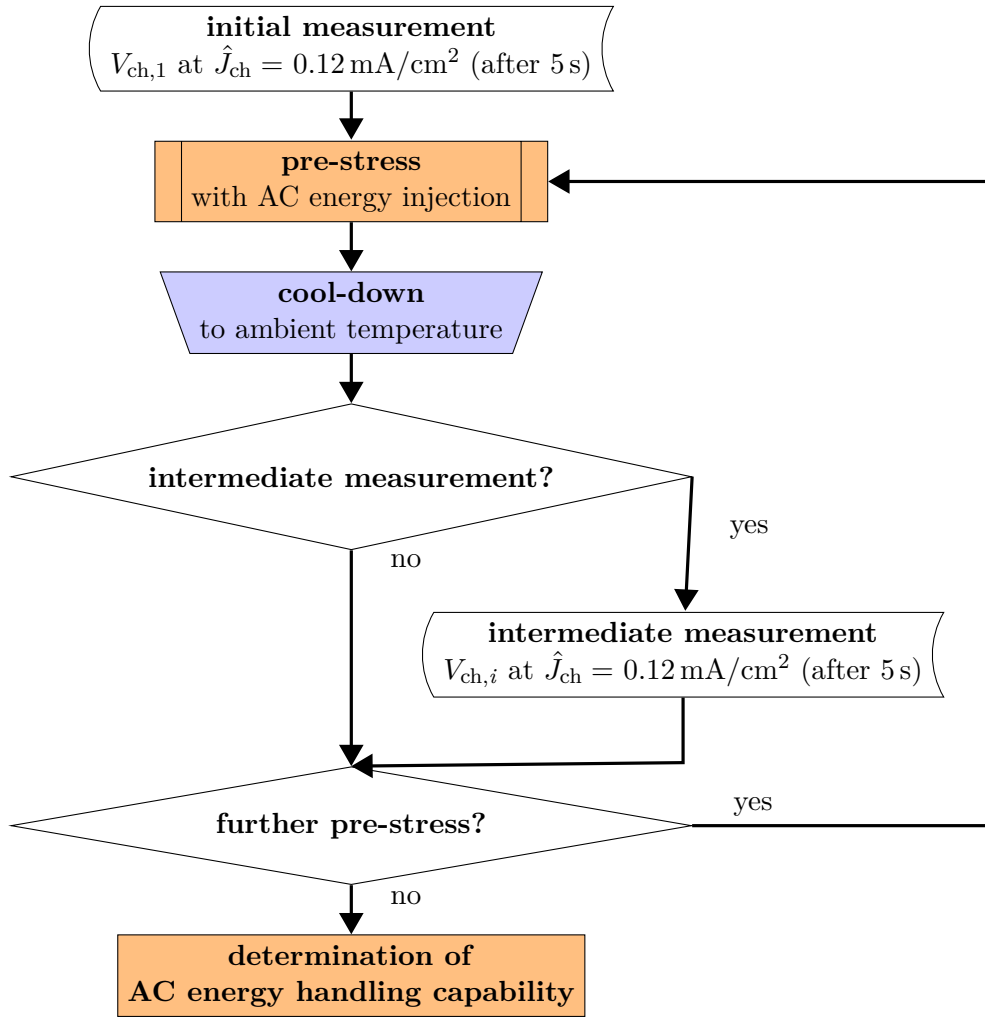
Figure 5.23: Flowchart of repetitive stresses with AC energy injections (according to [Tuc13a])

the MOV caused by the cool-down process are negligible in comparison to those caused by the heating-up process.

After every fifth pre-stress[127], the change of the "characteristic voltage" due to the pre-stresses is determined with the help of an intermediate measurement. Subsequently, the next pre-stress is applied.

After 100 pre-stresses, the energy handling capability is determined for MOVs that show no mechanical macroscopic damages after these stresses. It is determined with an AC energy injection with a current density of $3.5\,\text{A/cm}^2$. In doing so, the MOVs are stressed up to

---

[127] An intermediate measurement is only carried out after every fifth pre-stress because the gain of knowledge of carrying out an intermediate measurement after each pre-stress cannot justify the effort.

mechanical failure and the determined energy injection is compared to the energy handling capability of brand-new MOVs. An AC energy injection with a current density of $3.5 \, \mathrm{A/cm^2}$ is used because, according to the investigations in chapter 5.1 (see figure 5.5), it can be rated as being especially sensitive. Moreover, for low current densities, the single impulse energy handling capability is relatively close to the nominal energy handling capability of standard surge arresters. This is why changes in the energy handling capability within this range of the current density are rated as being particularly crucial.

The mean value and the standard deviation of the change of "characteristic voltage" due to repetitive AC energy injections at an energy injection that amounts to 80 % of the mean single impulse energy handling capability is shown in *figure 5.24* for the MOVs of the three investigated production lots. For all three investigated production lots, the "characteristic voltage" increases as a consequence of the pre-stresses, meaning that a higher voltage within the pre-breakdown region of the *V-I* characteristic is necessary so that the MOVs carry the same current density. This is an improvement of the *V-I* characteristic in terms of thermal stability of a surge arrester. This increase of "characteristic voltage" seems to approach a limiting value after a certain amount of stresses (depending on the production lot). After 100 pre-stresses (depending on the production lot), this limiting value seems to be in the range of 1 % to 4 %. Even though it has not been proven yet, it can be assumed that, due to the repetitive AC energy injections or the heat thus generated, the changes of the *V-I* characteristic of the MOVs that were caused by the routine tests by the manufacturers are reduced. Here, the degradation in the form of oxygen migrations that was caused by high current peak values and high current rise times (for example by the measurement of the residual voltage) is reversed by diffusion processes (see [Den98] and [Stu90]). The latter process is supported by the increased temperature resulting from an energy injection (see also chapter 5.5.2).

None of the ten MOVs of production lot "I" fails during the 100 AC energy pre-stresses. On the other hand, three MOVs out of ten of production lot "II" (during pre-stresses 4, 45 and 50)[128] and one MOV out of ten of production lot "III" (during pre-stress 40) fail. None of the MOVs that failed showed peculiarities such as significant changes of the "characteristic voltage" or the like before failing. However, it must be added that also none of the MOVs failed in a pre-stress directly after an intermediate measurement.

Table 5.4 shows the single impulse energy handling capability after 100 pre-stresses (of those MOVs that withstood the pre-stressing) referred to the single impulse energy handling capability of brand-new MOVs (see chapter 5.1) and tested with an AC energy injection at a current density of $3.5 \, \mathrm{A/cm^2}$. The mean failure energy is about 10 % to 20 % higher than

---

[128] One MOV had to be removed during the test series due to inappropriate handling.
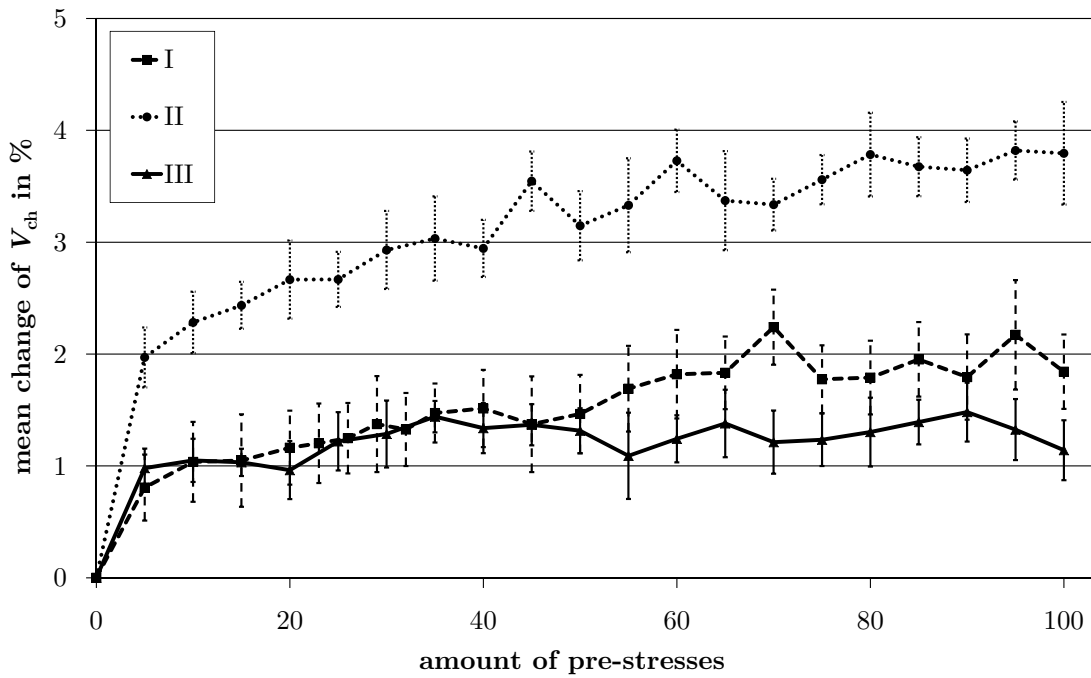
Figure 5.24: Changes of "characteristic voltage" due to repetitive AC energy injections (according to [Tuc13a]).

that of brand-new MOVs of the same production lot, the coefficient of variation ranging from 0.014 to 0.038. The evaluation of the failure symptoms of the stressed MOVs show no significant differences compared with the failure symptoms after single impulse stresses.

It cannot be assumed that the pre-stresses actually increased the energy handling capability of the stressed MOVs. Rather it can be presumed that the supposed increase can be attributed to the failing of the MOVs with lower energy handling capability during the pre-stresses. Such MOVs lower the determined mean energy handling capability during the investigations on the single impulses in chapter 5.1. However, comparable MOVs fail during pre-stresses with AC energy injections, which is why they do not reduce the mean

Table 5.4: AC energy handling capability of MOVs after 100 AC pre-stresses compared to the single impulse energy handling capability of brand-new MOVs of the same current density (according to [Tuc13a]).

production lot	"I"	"II"	"III"
amount of tested MOVs	10	6	9
mean failure energy in p.u.	1.1	1.1	1.2
coefficient of variation	0.038	0.014	0.029

failure energy of the pre-stressed MOVs. Doubtlessly it can be said that the investigated AC energy injections with energy contents of about 80 % of the mean single impulse energy handling capability do not affect the energy handling capability of the MOVs. Obviously, the low current rise time and current density of the pre-stresses damage the MOVs only very little so that the handling capability concerning those repetitive stresses comes very close to the single impulse energy handling capability.

5.4.2 Repetitive Impulse Energy Handling Capability Concerning Long-Duration Current Impulses

Energy injections with repetitive long-duration current impulses are even of a higher relevance for manufacturers and operators of surge arresters than repetitive AC energy injections. Long-duration current impulses simulate line discharges that can lead to high energy-related stressing of surge arresters in high-voltage grids (see for example [IEC60099-5]). For this reason, they constitute a standard stress for MOVs in surge arresters of the high-voltage level and thus are used in [IEC60099-4] (respectively [IEC-37/416/FDIS] and [IEEEC62.11-2012]) in order to test the energy handling capability of MOVs. Moreover, routine tests at the end of the manufacturing process are often carried out by applying long-duration current impulses.

Regarding the long-duration current impulses normally used, current rise time and current peak value usually are higher whereas the duration of the energy injection is lower then that for the AC energy injections used in chapter 5.4.1. In addition, the stress caused by a long-duration current impulse is monopolar, which might influence the distribution of charge carriers inside the MOV (see chapter 2.2). In order to determine the energy handling capability of MOVs concerning repetitive long-duration current impulses, the following investigations are carried out.

In a pre-investigation, one MOV of each of the five production lots was exposed to repetitive long-duration current impulse pre-stresses at an energy level of 50 % of the mean failure energy determined in chapter 5.1 (applying the "complex failure criterion"). Depending on the production lot, this led to energy injections with a pre-stress of about $450 \, \text{J/cm}^3$ to $550 \, \text{J/cm}^3$. During this repetitive pre-stress, four of the five investigated MOVs failed mechanically before reaching the 20th pre-stress. Obviously, the energy level that can be applied using repetitive long-duration current impulses is lower than for repetitive AC energy injections.

However, in another pre-investigation, in four out of five production lots, one MOV could be found that withstood 100 repetitive long-duration current impulses[129] at an energy level of $300 \, \text{J/cm}^3$. It can be assumed that the limit of the repetitive long-duration current impulse handling capability lies within this energy range. In order to determine the energy level of various production lots where none of the investigated MOVs fails mechanically during 20 pre-stresses[130], a testing program was developed in cooperation with the Cigré working group A3.25 and carried out by the author of this thesis. It is described in the following.

Within this testing program, 20 MOVs each out of three production lots (labelled "α", "β" and "γ"), are pre-stressed with 20 long-duration current impulses of one energy level. If there is at least one mechanical failure during the pre-stresses, the test is repeated for 20 other brand-new MOVs at an energy level $50 \, \text{J/cm}^3$ lower than the energy level tested before. This process is carried out for the MOVs of each production lot until an energy level is reached where 20 MOVs do not fail mechanically during the pre-stress of 20 long-duration current impulses.

The flowchart of each single measurement series where 20 MOVs are pre-stressed with 20 long-duration current impulses is shown in *figure 5.25*. In order to sort out MOVs with an especially low energy handling capability, all investigated MOVs are pre-stressed in advance with an AC energy injection with a current density of $3.5 \, \text{A/cm}^2$ at an energy level of about $80\,\%$ of the mean single impulse failure energy[131].

For 20 MOVs that withstand this pre-stress, an initial measurement is carried out during which the "characteristic voltage" is determined at a peak value of the current density of $0.12 \, \text{mA/cm}^2$. Subsequently, the 20 pre-stresses with a long-duration current impulse with a virtual duration of $1.9 \, \text{ms}$ are carried out. The energy level is regulated by the current density of the energy injection, the current densities of the pre-stresses being adjusted to about $25 \, \text{A/cm}^2$ to $60 \, \text{A/cm}^2$. After each pre-stress, die MOVs are cooled down to ambient temperature.

After 20 pre-stresses, an exit measurement is carried out during which the "characteristic voltage" again is measured at a peak value of the current density of $0.12 \, \text{mA/cm}^2$. The "characteristic voltage" is not determined after each energy injection because the gain of knowledge has turned out to be low in the pre-investigations.

---

[129] The "characteristic voltage" of the pre-stressed MOVs increased by about $1\,\%$ to $4\,\%$ during the pre-stresses.

[130] This amount of 20 pre-stresses is particularly interesting due to the energy tests according to [IEEEC62.11-2012], [IEC60099-4] as well as [IEC-37/416/FDIS].

[131] It can be concluded from the investigations in chapter 5.4.1 that this stress does not lead to any pre-damage inside the MOV.
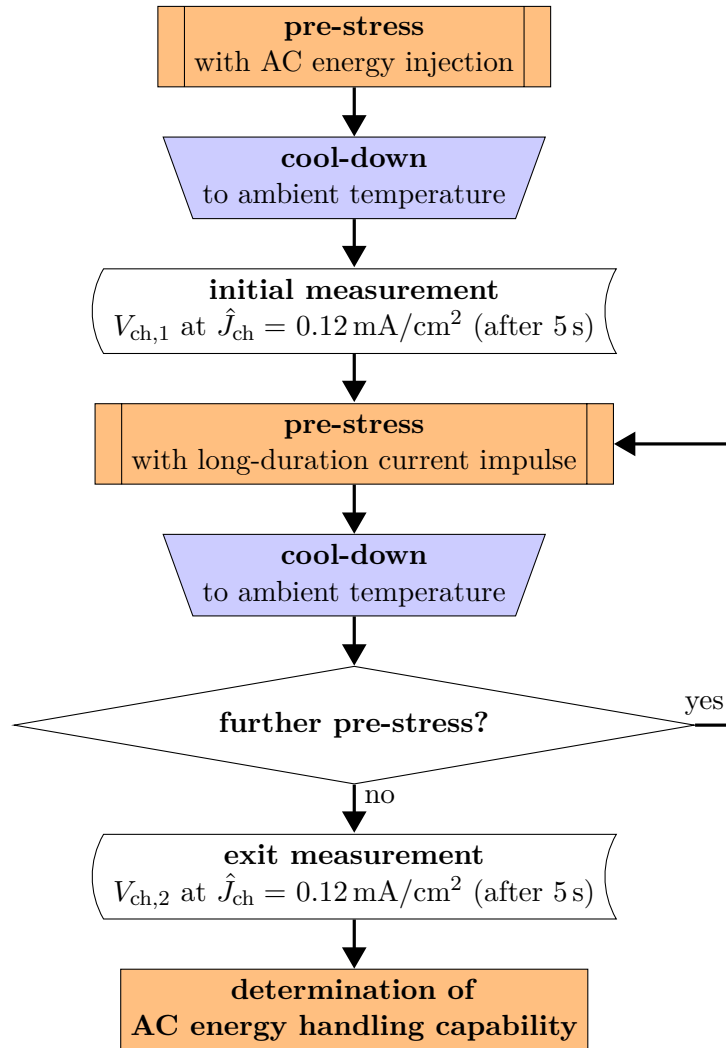
Figure 5.25: Flow chart of repetitive stresses with long-duration current impulses (according to [Tuc13a]).

At the end of each test series, the single impulse energy handling capability of those MOVs that withstood the pre-stresses without being mechanically damaged is determined by a stress with an AC energy injection with a current density of $3.5 \, \mathrm{A/cm^2}$. The same energy injection is chosen as described in chapter 5.4.1 and not for example a destructive long-duration current impulse so that the results can be compared directly with those of the repetitive AC stresses.

The highest energy level of the pre-stress where none of the MOVs fail during the investigations due to pre-stresses as well as the energy level where the first MOVs fail is depicted in *table 5.5*. Since only one of the MOVs of production lot "α" failed at an energy level of

Table 5.5: Energy level and MOV failures during 20 pre-stresses of 20 MOVs with repetitive long-duration current impulses (according to [Tuc13a]).

production lot	"α"		"β"		"γ"	
energy level in J/cm^3	150	200	250	300	300	350
amount of failures (out of 20 MOVs)	0	1	0	2	0	8
number of the impulse during which the MOVs failed	-	5	-	3, 6	-	1, 1, 3, 4, 4, 4, 19, 20

200 J/cm^3, the low energy level of this production lot should not be overestimated. The other energy levels, lying between 250 J/cm^3 and 300 J/cm^3, are at around 1/3 to 1/2 of the energy that can be applied during pre-stresses with repetitive AC energy injections (see chapter 5.4.1). This means they are very close to or partly lower than the typical nominal energy handling capability[132] of standard surge arresters. However, all in all, it can be noted that the energy that can be applied during repetitive long-duration current impulses lies clearly below the mean single impulse energy handling capability. According to chapter 5.1, this mean single impulse energy handling capability lies between about 800 J/cm^3 and 1200 J/cm^3 when applying the same impulse duration but higher current densities.

In *table 5.6*, the change of the "characteristic voltage" and of the single impulse energy handling capability is given for the energy level of the MOVs of each of those investigated production lots where none of the 20 MOVs failed during the 20 pre-stresses. The "characteristic voltage" only increases marginally within the range of 0.5 % to 2.2 % due to the pre-stresses. However, since the MOVs investigated here differ from those investigated in chapter 5.4.1, no direct comparison can be drawn. Since "characteristic voltage" also rises during repetitive stresses with long-duration current impulses, neither is the thermal stability of standard surge arresters threatened by this type of stress. Hence, exposing the MOVs to repetitive long-duration current impulses prior to the testing of the thermal stability as suggested by [IEEEC62.11-2012] seems to be inadvisable.

Those MOVs that withstood 20 pre-stresses are stressed with an AC energy injection with a current density of 3.5 A/cm^2 up to mechanical failure at the end of the investigation. The failure symptoms of these MOVs resemble those of brand-new MOVs that are stressed up to mechanical failure by applying an AC energy injection of the same current density. The

---

[132] According to [Hin12], the nominal energy handling capability usually is within the range of 200 J/cm^3 to 300 J/cm^3.

Table 5.6: Change of the "characteristic voltage" and the mean single impulse energy handling capability due to 20 pre-stresses with repetitive long-duration current impulses of the mentioned energy level (according to [Tuc13a]).

production lot	"α"	"β"	"γ"
energy level of the pre-stress without failing of the MOV in J/cm^2	150	250	300
rise of the "characteristic voltage" due to the pre-stresses in %	0.5	1.3	2.2
mean single impulse energy handling capability in p.u.	1.09	1.07	1.05
coefficient of variation	0.078	0.032	0.044

mean failure energy of the MOVs that were stressed by 20 long-duration current impulses is compared to that of brand-new MOVs in table 5.6. Just as it is the case for repetitive AC energy injections, it rises slightly for repetitive long-duration current impulses. Here, however, the MOVs of those test series that showed no failures during the pre-stresses with long-duration current impulses are investigated. On the other hand, those MOVs with a low energy handling capability were sorted out by a pre-stress with an AC energy injection. For this reason, also this case, the rise in mean failure energy can be attributed to missing "outliers" with lower energy handling capability. Considering the coefficient of the variation, however, this rise is very low. Regarding the MOVs of production lot "γ", one MOV failed at the 19th and one at the 20th pre-stress during the pre-stresses at an energy level of $350\,\text{J/cm}^3$. This could indicate that during this kind of pre-stress, a pre-damage of the MOVs takes place, which, on the other hand, is not supported when considering the determination of the single impulse energy handling capability (as described above). Neither does the evaluation of the failure symptoms suggest a pre-damage. Thus, it can be stated that no symptoms of fatigue can be detected for the energy levels (of the respective production lots) mentioned in table 5.6 for repetitive long-duration current impulses. Higher stresses seem to fatigue the material, which however cannot be classified with this investigation[133].

As a result of the investigation, it can be concluded that, in contrast to AC energy injections, the energy that can be applied repetitively with long-duration current impulse stresses is significantly lower than the single impulse energy handling capability. One reason for this could be the distinctly higher current peak value, the higher current rise time or

---

[133] The evaluation of the AC energy injections of those MOVs that were pre-stressed with energy levels that led to primary failures (the higher energy level of those depicted in table 5.5), also does not show a reduction of the mean energy handling capability or noticeable features in the failure symptoms.

the significantly shorter duration of the energy injection, which might lead to mechanical tensions and thus to a progressing crack formation inside the MOV.

5.4.3 Comparison of the Repetitive Impulse Energy Handling Capability Concerning Different Types of Impulses of the Same Energy Density

The investigations of repetitive impulse energy handling capability when applying AC energy injections and long-duration current impulses introduced above show that the repetitive impulse energy injection bears no relation to the single impulse handling capability but is dependent on the kind of impulse or the current density / current rise time of the energy injection. In the following, the influence of the energy injection of the repetitive stresses is to be investigated comparing different types of impulses[134]. The aim here is to further narrow down the fatigue behavior and the parameters that lead to fatigue.

The types of stresses analyzed here are, like in the previous investigations, AC energy injections, long-duration current impulses with a virtual duration of $1.9\,\text{ms}$ and, additionally, double-exponential discharge currents of the $90/200\,\text{μs}$ type. On the basis of the results of the investigation with repetitive long-duration current impulses, the following energy stress levels are determined: $200\,\text{J/cm}^3$, $300\,\text{J/cm}^3$, and $400\,\text{J/cm}^3$. Furthermore, the duration of the energy injection for the different energy levels is kept constant for all types of impulses; solely the current density (and thus the voltage stress) is varied. The amount of 20 comparable specimens is maintained due to statistical validity, the amount of investigated production lots however is limited to two (labelled "1" and "2"). The previous investigations show differences for MOVs of different production lots. However, the gain of information does not seem to justify the additional effort.

The flowchart of the investigation that was carried out for 20 MOVs per energy level, type of stress and production lot is shown in *figure 5.26*. First of all, an initial measurement is carried out for each MOV, where the residual voltage[135] at a lightning current impulse with a current peak value of $10\,\text{kA}$ and a "characteristic voltage" at a peak value of the current density of $0.07\,\text{mA/cm}^2$ is determined. The reduction of the current density has practical reasons and, additionally, it reduces the influence of the determination of the

---

[134] Since the current density is linked to the energy injection via the current waveform of the applied impulse, the influence of the waveform cannot be separated from the current density / current rise time of the energy injection.

[135] In the initial and exit measurement, a measurement of the residual voltage is carried out because changes in residual voltage are of big importance for the protection characteristics of surge arresters. In order to limit the stress caused by the residual voltage measurement, it is not repeated for the intermediate measurements.
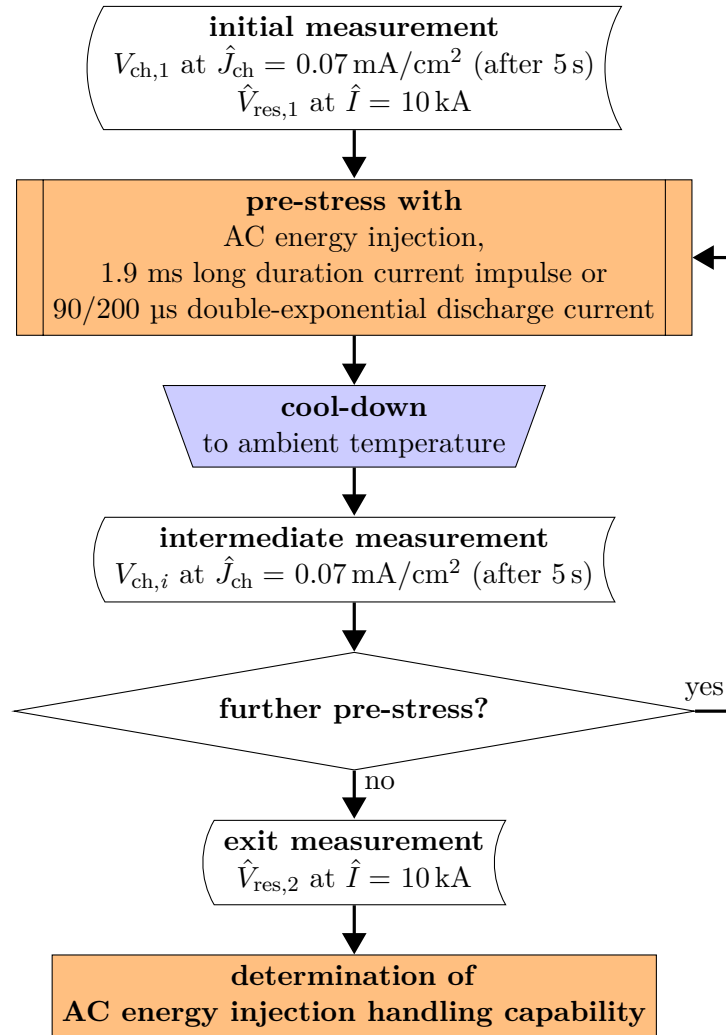
Figure 5.26: Flowchart of the repetitive stresses with AC energy injections, long-duration current impulses and double-exponential discharge currents with the same energy density.

"characteristic voltage" (carried out after each stress in this investigation) on the charge distribution inside the MOV.

The subsequent pre-stress with an AC energy injection (with a duration of eight half-waves independent of the chosen energy level), a long-duration current impulse with a virtual duration of 1.9 ms or a double-exponential discharge current of the 90/200 µs type are carried out at an energy level[136] of $200\,\mathrm{J/cm^3}$, $300\,\mathrm{J/cm^3}$ or $400\,\mathrm{J/cm^3}$. For the energy level of $300\,\mathrm{J/cm^3}$, this results in an energy density of about $5\,\mathrm{A/cm^2}$ for AC energy injections, about $50\,\mathrm{A/cm^2}$ for long-duration current impulses and about $550\,\mathrm{A/cm^2}$ for

---

[136] The pre-stresses with long-duration current impulses at an energy density of $200\,\mathrm{J/cm^3}$ and, for production lot "2", the AC energy injections at $200\,\mathrm{J/cm^3}$ and $300\,\mathrm{J/cm^3}$ are not carried out.

double-exponential discharge currents of the 90/200 µs type. For this energy level, the transferred charge was about 3.8 C for AC energy injections, about 3.5 C for the long-duration current impulses and about 2.8 C for double-exponential discharge currents of the 90/200 µs type. The energy level is determined for all types of energy injections by variation of the current density of the stress (and thus also by variation of the voltage stress), not its duration.

After each pre-stress, the specimen is cooled down to ambient temperature within about 15 min by forced cooling. Subsequently, an intermediate measurement is carried out where the "characteristic voltage" is determined. The "characteristic voltage" is determined after each energy injection in order to further narrow down the failure mechanism of a failure during the pre-stresses. The contact electrodes are replaced after each pre-stress. It could be demonstrated that this replacement has only little influence on the metallization of the MOVs and does not have an impact on the results of the investigation.

After 20 pre-stresses, an exit-measurement is carried out for those MOVs that mechanically withstood the pre-stresses. Here, the residual voltage during a lightning discharge current with a current peak value of 10 kA is determined and, subsequently, the single impulse energy handling capability during an AC energy injection up to mechanical failure with an energy density of $3.5\,\mathrm{A/cm^2}$.

Each test series for one energy level and one kind of stress of one production lot is begun with 20 MOVs and the amount of failures as well as the impulse number of any occurring failure is documented. In *figure 5.27*, an overview of how many MOVs of the different measurement series withstood how many pre-stresses is given for the MOVs of production lots "1" (a) and "2" (b). For the MOVs of production lot "2", the pre-stresses with AC energy injections at the energy leveles of $200\,\mathrm{J/cm^3}$ and $300\,\mathrm{J/cm^3}$ are not carried out because no failure did occur at an energy level of $400\,\mathrm{J/cm^3}$, thus no failures are expected for lower energy levels.

For the MOVs of production lot "1" it can be observed that four, respectively three, MOVs fail already at the first pre-stress when pre-stressed with AC energy injections at an energy level of $300\,\mathrm{J/cm^3}$ and $400\,\mathrm{J/cm^3}$, whereas only one MOV in total fails at the eighth pre-stress at $200\,\mathrm{J/cm^3}$. Moreover, additional MOVs fail when pre-stressed with AC energy injections at an energy level of $400\,\mathrm{J/cm^3}$, with the result that, at this energy level, only thirteen MOVs withstand the 20 pre-stresses.

For the pre-stresses with long-duration current impulses with a virtual duration of 1.9 ms it can be observed that, at an energy level of $300\,\mathrm{J/cm^3}$, only two MOVs fail (both at
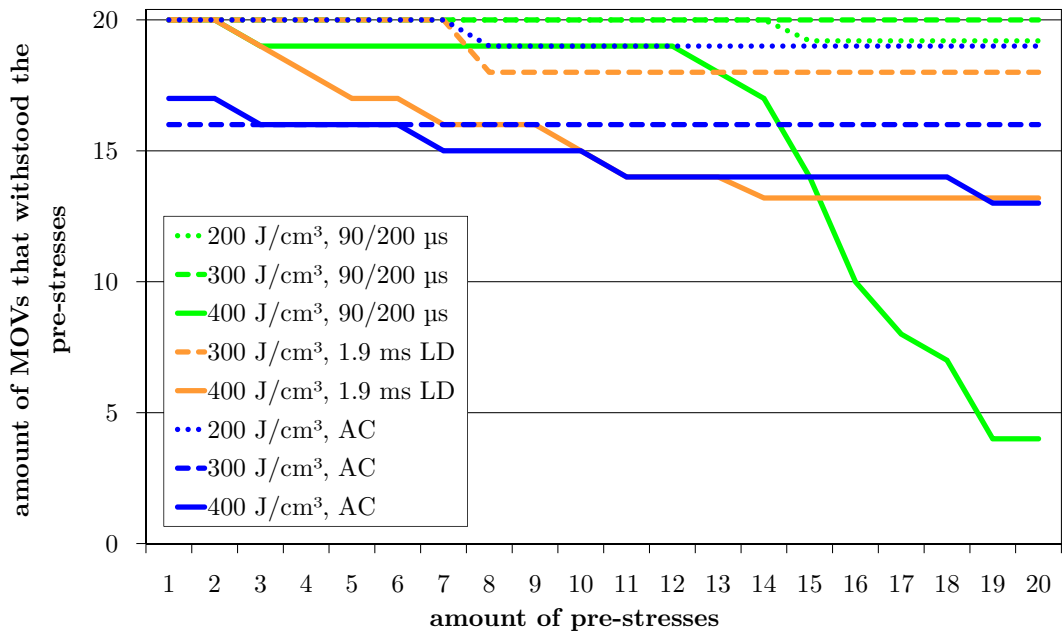
(a)
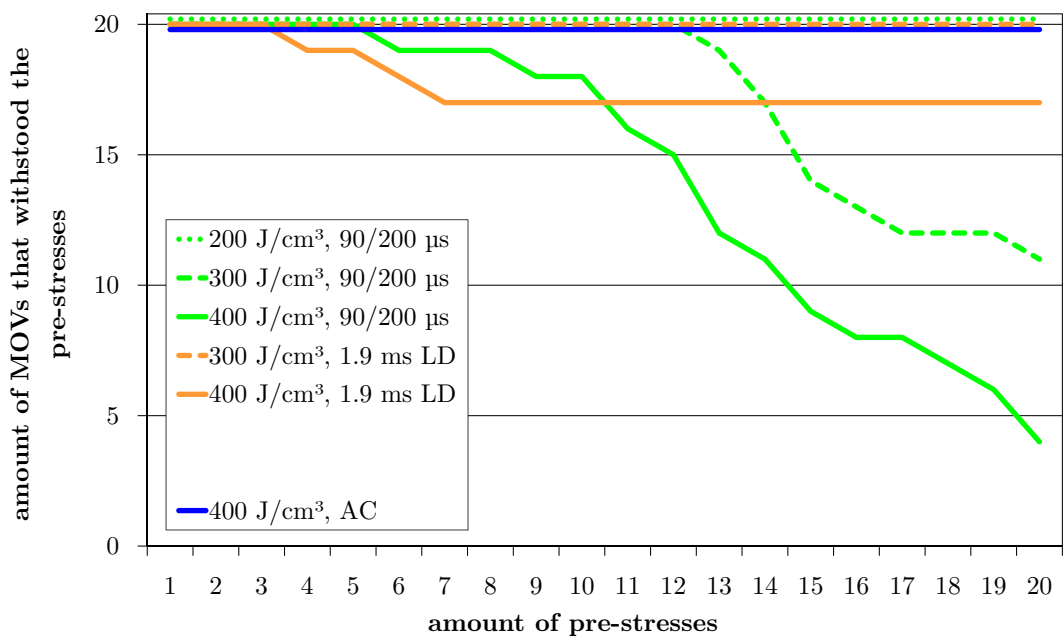
(b)

Figure 5.27: Amount of MOVs (out of 20) that withstood the pre-stresses with the double-exponential discharge current of the 90/200 µs type, the long-duration current impulses ("LD") with a virtual duration of 1.9 ms or the AC energy injections ("AC"). (a) production lot "1", (b) production lot "2".

the eighth pre-stress) whereas, at an energy level of $400\,\text{J/cm}^3$, continuous failures can be observed the amount of which decreases towards the end of the test series.

For the pre-stresses with the double-exponential discharge current of the $90/200\,\mu\text{s}$ type, a failure at the 15th pre-stress occurs at the energy level of $200\,\text{J/cm}^3$. Regarding the energy level of $300\,\text{J/cm}^3$, there is no failure. However, at an energy level of $400\,\text{J/cm}^3$, a great many MOVs fail after the 12th pre-stress, leaving only four MOVs that withstand 20 pre-stresses.

The results for the MOVs of production lot "2" confirm the results of the investigations of production lot "1". Yet, they show some particularities. For MOVs of production lot "2", there are no failures for AC energy injections with $400\,\text{J/cm}^3$, particularly not during the first pre-stress. During the pre-stresses with long-duration current impulses, less MOVs fail compared to production lot "1". The pre-stresses at an energy level of $400\,\text{J/cm}^3$ lead to three failures between the fourth and seventh pre-stress. Also for the MOVs of production lot "2", the pre-stress with the double-exponential discharge current of the $90/200\,\mu\text{s}$ type is the kind of stress that leads to the highest amount of failures. Here, however, a marked rise in failures can already be observed at an energy level of $300\,\text{J/cm}^3$ starting with the 13th pre-stress. This tendency is even intensified by increasing the energy level to $400\,\text{J/cm}^3$.

The change of the "characteristic voltage" during the pre-stresses is depicted in **figure 5.28** for the MOVs of production lot "1" for the different kinds of stresses at an energy level of $400\,\text{J/cm}^3$. Each line represents a pre-stressed MOV. The last value of the "characteristic voltage" before a failure is marked red. It is noticeable that, in contrast to the AC energy injections, for the stresses with the double- exponential discharge current and the long-duration current impulse, a marked decrease of the "characteristic voltage" can often be observed immediately before a failure. This behavior of a distinctly decreasing "characteristic voltage" before a failure can also be observed for MOVs of production lot "2" that were stressed with double- exponential discharge currents. Moreover, the MOVs of both production lots show "black spots" on the metallization before failing during the pre-stresses with double- exponential discharge currents and long-duration current impulses. These "black spots" as well as the reduction of "characteristic voltage" suggest the beginning of the forming of melting channels inside the MOV, which might perhaps lead to a puncture through the MOV during the pre-stresses.

The mean change of the "characteristic voltages" and the residual voltage after 20 pre-stresses of the MOVs that withstood these pre-stresses is depicted in *table 5.7* for both production lots. For the evaluation of these parameters it has to be noted that the coefficient

(a)

(b)

(c)
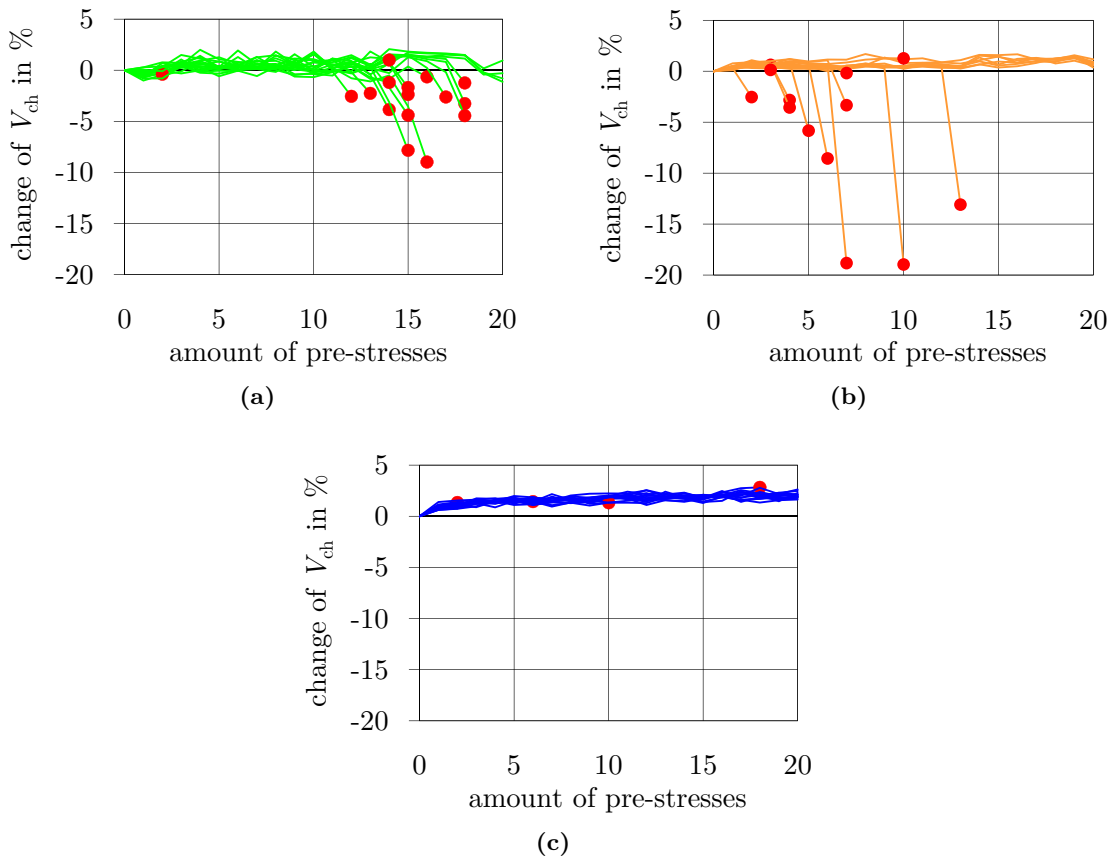
Figure 5.28: The change of the "characteristic voltage" V_{ch} of MOVs of production lot "1" resulting from the pre-stresses at an energy level of $400 \, \text{J/cm}^3$ for (a) double- exponential discharge current of the $90/200 \, \mu\text{s}$ type, (b) long-duration current impulse with a virtual duration of $1.9 \, \text{ms}$ and (c) AC energy injections.

of variation of the mean values lies within the range of 0.01 and 0.02. Thus the deviation between the different stresses is mostly lower than a standard deviation.

The "characteristic voltage" changes only little (as in the previous investigations) due to the pre-stresses. Moreover, the change has a positive sign (with one exception), which leads to a lower power loss at constantly applied voltage. A rise of the "characteristic voltage" can probably be attributed to a recovery (caused by diffusion processes, which are supported by the rise in temperature) of the degradation resulting from the routine test. It can be stated that the thermal stability of standard surge arresters is not threatened by the repetitive stresses investigated here. The only negative value was measured at a pre-stress with double-exponential discharge currents at an energy level of $400 \, \text{J/cm}^3$ for MOVs of production lot "1" and can be attributed to statistical dispersion of the measurement, as is

Table 5.7: Mean change of "characteristic voltage" and residual voltage during repetitive pre-stresses with the double-exponential discharge current of the 90/200 µs type ("DEDC"), the long-duration current impulse with a virtual duration of 1.9 ms ("LD") or an AC energy injection ("AC").

type of stress	energy level in J/cm^3	production lot "1"		production lot "2"	
		change of V_{ch} in %	change of $\hat{V}_{res}$ in %	change of V_{ch} in %	change of $\hat{V}_{res}$ in %
pre-stress with 90/200 µs "DEDC"	200	1.3	0.5	1.5	1.5
	300	0.6	0.7	1.4	1.2
	400	-0.3	-0.1	0.3	0.7
pre-stress with 1.9 ms "LD"	300	1.1	1.9	1.1	0.6
	400	0.8	0.8	1.5	0.4
pre-stress with "AC"	200	2.3	-1.5	not carried out	
	300	2.4	-0.1	not carried out	
	400	2.1	0.6	3.5	2.8

illustrated in figure 5.28 (a) (the figure showing exactly this measurement series).

If the mean changes of the "characteristic voltages" for the different pre-stresses are compared, it is apparent that the pre-stresses with double-exponential discharge currents and long-duration current impulses lead to a mean change that is 1 % to 2 % lower than for pre-stresses with AC voltages. One explanation for this could be that the *V-I* characteristic is changed within the pre-breakdown region during the routine test after the production process. A change within the pre-breakdown region due to impulse current stress is characterized (see for example [Kle04]) by a current asymmetry during the measurement of the "characteristic voltage", as is the case in this investigation, too. According to [Kle04], this current asymmetry is only changed marginally by impulse current stresses of the same parameters, especially of the same polarity. An evaluation of the current waveforms of the "characteristic voltage" after pre-stresses with double-exponential discharge currents of the 90/200 µs type shows that the current asymmetry is changed only insignificantly by these pre-stresses. Thus, it can be assumed that the charge carrier distribution is not changed any further by this kind of stress and that, consequently, no further change of the "characteristic voltage" occurs. In contrast, the current asymmetry decreases slightly after AC energy injections, which suggests that the predominant direction due to the charge carrier distribution along the grain boundary is partly reversed by the pre-stresses with alternating polarity. This could be the reason for the "characteristic voltage" to rise stronger concerning this type of stress.

The evaluation of the mean changes of the residual voltage shows that it is influenced only marginally by the pre-stresses, which was to be expected on the basis of the results concerning the single impulse energy handling capability in chapter 5.1 (where changes in residual voltage are detected only very rarely).

The failure symptoms of the stressed MOVs show no particularities after pre-stresses with AC energy injections. At higher current densities of the pre-stress (at higher energy levels of the pre-stress much more often than at lower energy levels), residues of local thermal overloads (commencing melting channels) can be detected on the front surfaces of the MOVs. The amount of meltings increases with rising energy level. However, there seems to be no system as to how they are distributed on the front surface. If the meltings occur during the pre-stresses, their amount and size rises with increasing amount of pre-stresses, until, in some circumstances, the MOV fails mechanically (puncture that leads to a cracking of the MOV) during one of the subsequent pre-stresses. If meltings can be identified on the front surfaces before the final destructive stress with an AC energy injection, the biggest of them seems to trigger the failure during this destructive stress[137]. For those MOVs that seemingly show no meltings on the front surfaces after the pre-stresses, it is noticeable that the failure channel always occurs close to the edge at a destructive AC energy injection after pre-stresses with AC energy injections (no difference compared to the failure symptom of brand-new MOVs), whereas the failure channel spreads unsystematically on the front surface after pre-stresses at higher current densities. All in all, the evaluation of the failure symptoms suggests a pre-damage of the MOVs by energy injections at higher current densities where higher energy levels of the pre-stresses seem to lead to worse pre-damages.

At the end of the investigation, the single impulse energy handling capability is determined with an AC energy injection for those MOVs of both production lots that withstood the pre-stresses[138]. The evaluation of the single impulse energy handling capability after 20 pre-stresses is depicted in *figure 5.29* for the MOVs of both production lots, each mark representing one investigated MOV. The failure energies are scaled to those of brand-new MOVs of the respective production lot at the same stress. It can be seen from the diagrams that the failure energies marked green after the pre-stresses with the double-exponential discharge currents of the $90/200\,\mu s$ type spread very intensely and drop with increasing energy level. On the other hand, the failure energies after AC energy pre-stresses (marked blue) spread much less (except for the outliers of the MOVs of production lot "1" at an energy level of $200\,J/cm^3$) and lie within the range of failure energies of brand-new MOVs. The failure energies after pre-stresses with long-duration current impulses show an

---

[137] A more precise statistical evaluation is not possible since the amount of investigated MOVs is too small.
[138] Two MOVs per test series of production lot "1" were not destructed but kept for further material analysis.

inhomogeneous behavior. The MOVs of production lot "2" spread only very little and are within the range of brand-new MOVs, whereas, concerning the failure energies of the MOVs of production lot "1", there are several outliers with very low energy handling capability.

During the pre-stresses of the MOVs of production lot "1" with AC energy injections, three to four MOVs per energy level fail at the first pre-stresses at the energy levels $300\,\mathrm{J/cm^3}$ and $400\,\mathrm{J/cm^3}$. On the other hand, for the energy level $200\,\mathrm{J/cm^3}$, none of the MOVs failed during the first pre-stresses. However, it can be seen in figure 5.29 that five MOVs that withstood the pre-stress show a lower energy handling capability than the other MOVs[139]. This suggests the assumption that approximately $20\,\%$ of the MOVs of the investigated production lot "1" have a lower single impulse energy handling capability. These MOVs seem to fail mechanically during the pre-stress at the energy levels of $300\,\mathrm{J/cm^3}$ and $400\,\mathrm{J/cm^3}$ whereas they withstand the pre-stresses at $200\,\mathrm{J/cm^3}$. The investigated production lot "2" on the other hand does not seem to contain equivalent outliers with lower AC energy handling capability.

Concerning the pre-stresses of the MOVs of production lot "1" with long-duration current impulses, MOVs fail during the first pre-stresses only at the energy level of $400\,\mathrm{J/cm^3}$. During the pre-stresses with double-exponential discharge currents, only one MOV fails at an energy level of $400\,\mathrm{J/cm^3}$ and none during the first pre-stresses at the other energy levels. It can be concluded that, since the groups of MOVs of production lot "1" that were stressed with long-duration current impulses or double-exponential discharge currents probably contain the same amount of MOVs with low AC energy handling capability, these MOVs are not destroyed mechanically by the pre-stresses with long-duration current impulses and double-exponential discharge currents. It can be assumed that the MOVs with a lower AC energy handling capability contain defects or inhomogeneities[140], which obviously lead to a reduction of the AC energy handling capability. On the other hand, these defects or inhomogeneities apparently have no or only little effect on the impulse handling capability for quicker energy injections with higher current densities.

It can be summarized that, evidently, AC energy injections – in contrast to long-duration current impulses and double-exponential discharge currents – fatigue the MOVs less strongly and that MOVs with defects can probably be better detected by means of AC energy injections (by a mechanical failure). For this reason, the hypothesis is developed that AC

---

[139] A correlation between the failure symptoms of the destructive AC energy injections and the energy handling capability of the MOVs cannot be identified.

[140] An investigation of the failure channels of MOVs with low AC energy handling capability by means of a scanning electron microscope does not lead to definite results concerning the failure cause. Only for one MOV a higher bismuth concentration (compared to the remainder of the ceramic) could be detected at one spot of the failure channel. It is possible that that the electric arc in consequence of the failure changes the defect too intensely so that the failure cause cannot be determined anymore afterwards.

(a)

(b)
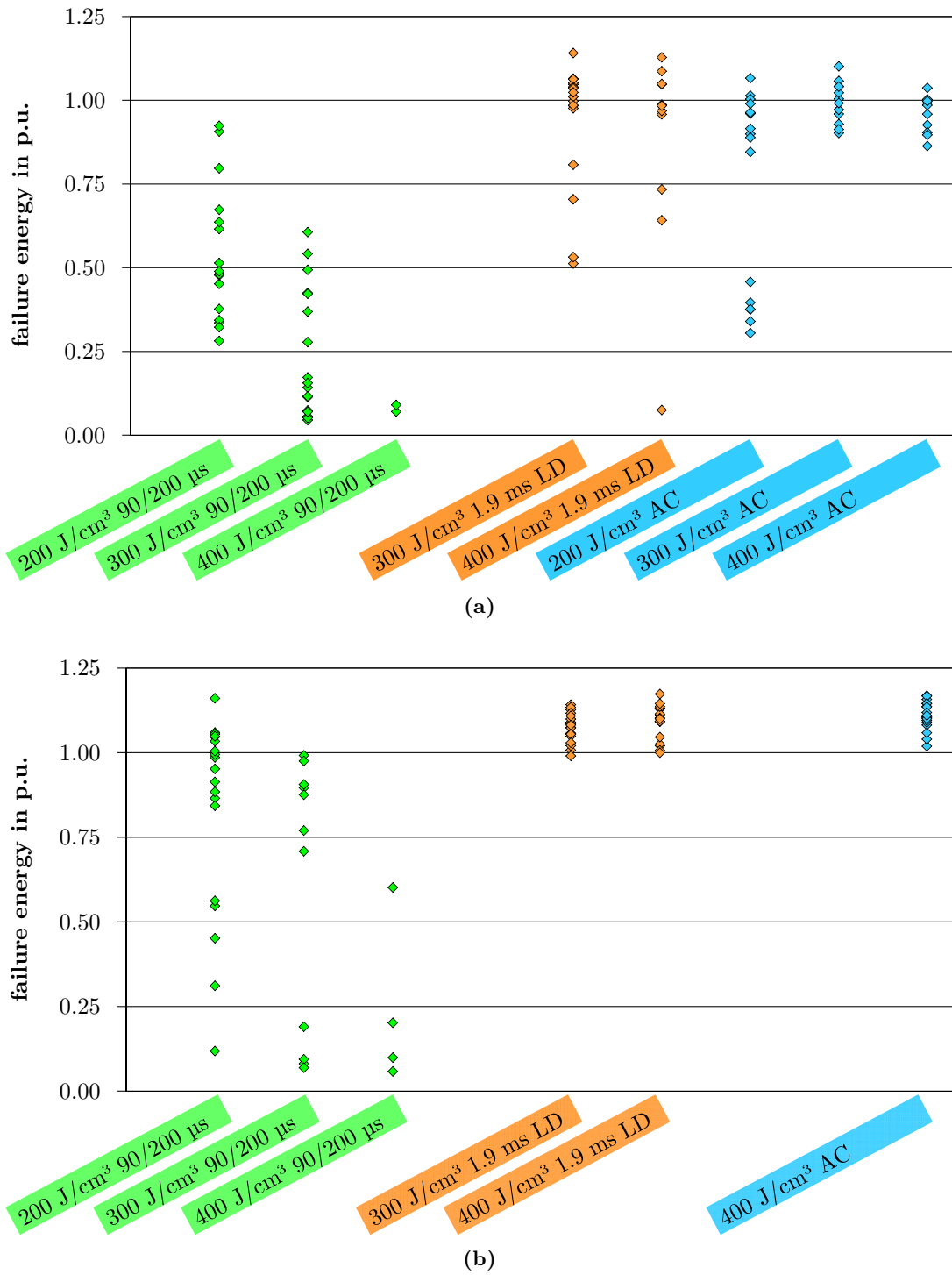
Figure 5.29: Single impulse energy handling capability (AC energy injection) during stressing of those MOVs that withstood 20 pre-stresses of the different kinds and energy levels. Each mark describes the failure energy of an MOV. (a) production lot "1" and (b) production lot "2".

energy injections are more suitable for a routine test (after the manufacturing process) than shorter energy injections such as long-duration current impulses, which are commonly used currently. Possibly, concerning energy injections with lower energy density and longer stress duration (see [Bar96b] and [Bar01]), there is a higher concentration of the current flow towards current paths with defects due to the more inhomogeneous current distribution than this is the case for quicker energy injections with a higher current density. A direct comparison of two routine test procedures is introduced in chapter 5.4.4.

Comparison of the Failure Energies of AC Energy Injections with Long-Duration Current Impulses after Repetitive Stresses

In the investigations described so far, the single impulse energy handling capability of MOVs that withstood repetitive stresses had always been determined by AC energy injections. Since different stresses (stress durations or current densities) can be critical for different failure mechanisms, in this section, the single impulse energy handling capability for an AC energy injection is compared to that for a long-duration current impulse for MOVs that were stressed repetitively.

To this end, the investigations concerning repetitive energy handling capability in chapter 5.4.3 are repeated for MOVs of production lot "1". The types of stresses used for this are AC energy injections or energy injections with double-exponential discharge currents of the $90/200\,\mu\text{s}$ type at an energy level of $300\,\text{J/cm}^3$. Those are chosen because they are the two extremes of the pre-stresses regarding current density and stress duration. The energy level of $300\,\text{J/cm}^3$ is used due to the fact that, at a higher energy level of the double-exponential discharge current, only very little test specimens withstand the pre-stresses and that, at a lower energy level, potential pre-damages are probably less strongly marked. The process of the investigation is similar to that shown in figure 5.26. The only difference is that the single impulse energy handling capability is not determined with an AC energy injection, but with a long-duration current impulse with a prospective peak value[141] of $1.9\,\text{ms}$ and a current density of about $180\,\text{A/cm}^2$. Since the amount of available test specimens is limited and the investigations regarding the comparability have to be carried out for the same production lot, the amount of investigated MOVs per type of stress is reduced to ten.

The failures during the pre-stresses do not show any significant differences compared to those depicted in figure 5.27. The changes in "characteristic voltage" and residual

---

[141] The MOVs are stressed up to mechanical failure, thus the actual stress duration is determined by the energy handling capability of the respective specimen and is therefore shorter than $1.9\,\text{ms}$.
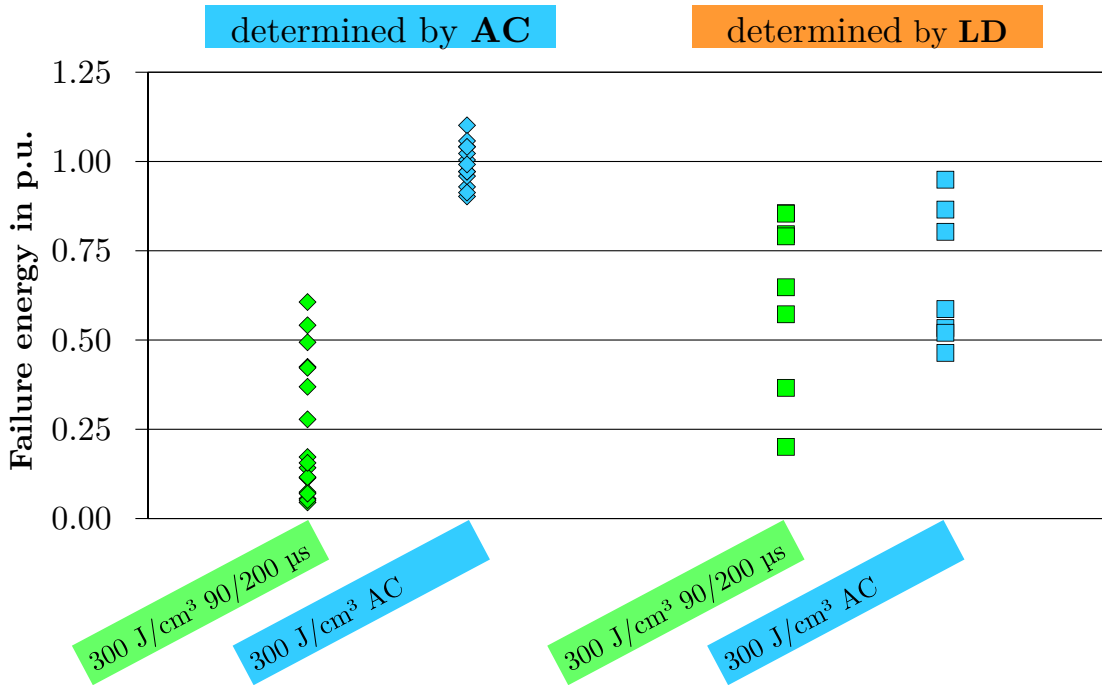
Figure 5.30: Single impulse energy handling capability of the MOVs of production lot "1" when stressed with an AC energy injection ("AC") or a long-duration current impulse ("LD") up to mechanical failure after repetitive stresses.

voltage also do not differ from the changes introduced in chapter 5.4.3. Neither is there any significant difference between the failure symptoms resulting from the final determination of the single impulse energy handling capability after 20 pre-stresses and those after stressing brand-new MOVs. Just as it is the case for destructive AC energy injections, no correlation between failure symptom and energy handling capability of the MOVs can be detected for a stressing with a destructive long-duration current impulse.

In *figure 5.30*, the results of the final determination of the single impulse energy handling capability with a mechanically destructive long-duration current impulse are compared to the results of the investigations of the previous chapter, where a mechanically destructive AC energy injection was used. The failure energy of each single MOV is scaled to the mean failure energy at the same stress.

For the pre-stresses with double-exponential discharge currents of the 90/200 µs type at an energy level of 300 J/cm^3, the same behavior can be observed for both failure types. The failure energies for stresses up to mechanical failure with a long-duration current impulse also spread within a very broad range. However, here the absolute values of the failure energies lie above typical nominal energies of surge arresters in standard applications because the

reference value, the mean single impulse energy handling capability of brand-new MOVs, is about 25 % higher for this failure type compared to AC energy injections.

The failure energies that are determined with long-duration current impulses after pre-stresses with AC energy injections disperse much more than might have been expected after the previous investigations (especially after that shown in figure 5.5). According to the results of the investigation introduced here, it could be assumed that the pre-stresses with AC energy injections cause pre-damages inside the MOV that affect the failure energy for stresses with long-duration current impulses but not the failure energy for stresses with AC energy injections. So far, however, there is no model concept for this behavior. Nonetheless, one result is that the failure energies for this type of stress lie significantly above the typical nominal energy of surge arresters in standard applications and thus the worst case scenario is tested by the determination of the failure energy by means of an AC energy injection.

Repetitive Impulse Energy Handling Capability Concerning Energy Injections with Alternating Polarities

In the investigations described above, fundamental differences concerning the fatigue behavior occurred between AC energy injections and impulse energy injections with long-duration current impulses or double-exponential discharge currents. In addition to differences concerning current density and waveform, these types of stresses also differ in the polarity of the stresses. While the impulse stresses put a monopolar stress on the MOVs (at repetitive energy injections, the MOVs are always stressed with the same polarity), an AC energy injection is a bipolar stress. In order to determine the influence of the polarity, the following investigation is carried out. Here, the repetitive impulse stresses are carried out with alternating polarity and compared to the monopolar stresses already described above.

The process of the investigation is similar to that shown in figure 5.26 with the exception that consecutive pre-stresses have a reverse polarity since the test specimens are assembled in reverse order inside the test fixture. This is called "alternating" in the following. The handling of the MOVs is equal for both investigations. The monopolarly stressed specimens were also removed from the test fixture after each energy injection to let them cool down.

Figure 5.31 shows how many of the MOVs withstood the given amount of pre-stresses with monopolar or alternating polarity. Since the monopolar stresses were carried out for 20 MOVs per test series, whereas (due to the shortage of test specimens) only ten specimens

per test series could be used for the alternating stresses, the percentage of MOVs that withstood the stresses is depicted.

It can be seen that the MOVs of production lot "1" fail earlier when applying alternating pre-stresses with repetitive long-duration current impulses at an energy level of $400\,\mathrm{J/cm^3}$ than when applying monopolar pre-stresses. None of the ten MOVs pre-stressed alternatingly and repetitively withstands more than ten stresses, whereas 13 of the 20 MOVs that were pre-stressed monopolarly withstand 20 stresses.

The investigations for the MOVs of production lot "2" confirm this result. At an energy level of $400\,\mathrm{J/cm^3}$, these MOVs also withstand monopolar long-duration current impulses much better than alternating long-duration current impulses. For pre-stresses with double-exponential discharge currents at an energy level of $300\,\mathrm{J/cm^3}$, however, a significant difference could not be determined anymore.

The failure energies (determined by a mechanically destructive AC energy injection) of the MOVs of production lot "2" that withstood the pre-stresses with monopolar or alternating polarity are depicted in *figure 5.32* (referring to the failure energy of brand-new MOVs). It must be pointed out again that only ten MOVs per energy level and type of energy injection were stressed with alternating polarity. Thus, the failure energies of MOVs can only be determined accordingly. The failure energies of the MOVs show a similar behavior, too, if the low sample size is taken into consideration. The failure symptoms of those MOVs stressed with alternating polarity are similar to those stressed with monopolar polarity. Hence, the result ist that, all in all, no clear tendency can be observed as to which polarity variant leads to the higher fatigue.

The results gained so far suggest that the lower fatigue behavior observed for AC energy injections in chapter 5.4.3 is not caused by the change of polarity of this kind of energy injection[142]. It rather seems that, concerning the long-duration current impulses, repetitive pre-stresses with alternating polarity lead to a stronger fatigue of the MOVs. On the basis of the investigations carried out so far, it cannot be fully determined whether repetitive stresses with alternating polarity lead to a stronger fatigue concerning stresses with double-exponential discharge currents with the investigated parameters.

From the results of chapter 5.4.3, it can be said that MOVs are obviously more heavily pre-damaged by energy injections with higher current density and shorter duration of the stress than by energy injections of lower current density and longer duration of the stress. At the same time, the pre-damage has an effect on the failure rate during repetitive

---

[142] However, it cannot be ruled out that the current density of the pre-stresses has an impact on the fatigue behavior and therefore on the observed effects.
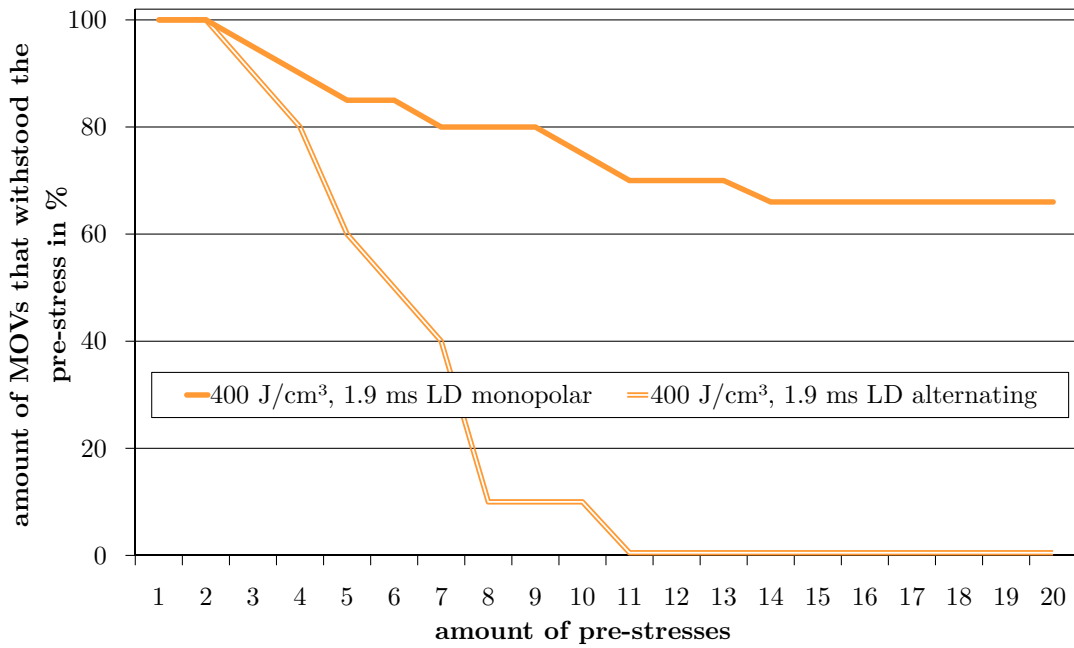
(a)
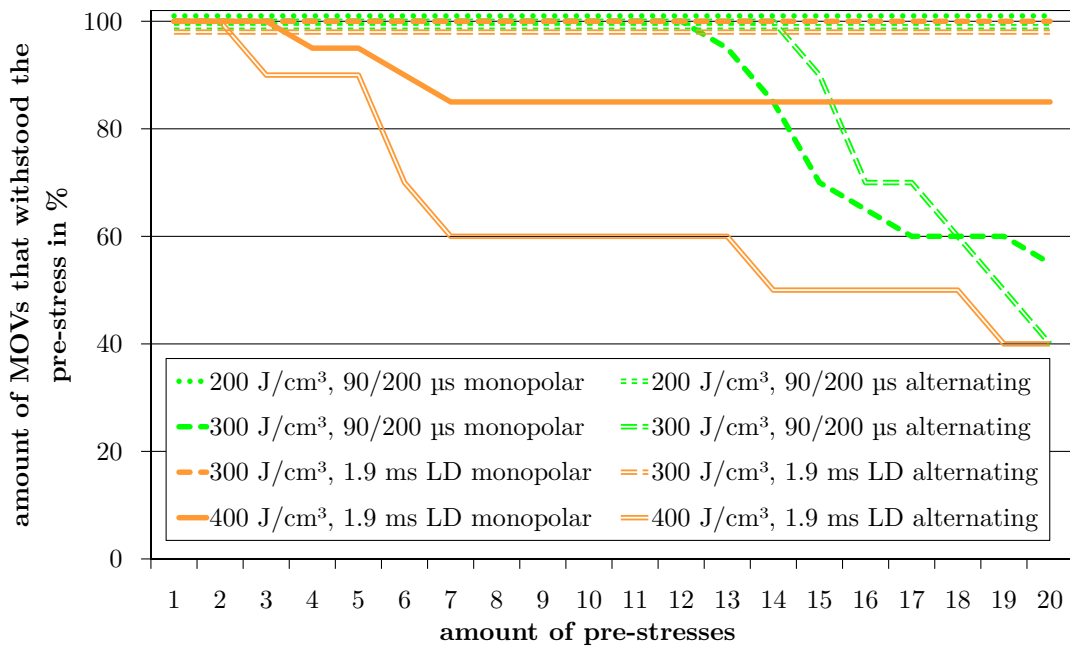
(b)

Figure 5.31: Percentage of the MOVs that withstand the monopolar or alternating pre-stresses with the double-exponential discharge current of the 90/200 µs type or the long-duration current impulse ("LD") with a virtual duration of 1.9 ms. (a) production lot "1", (b) production lot "2".
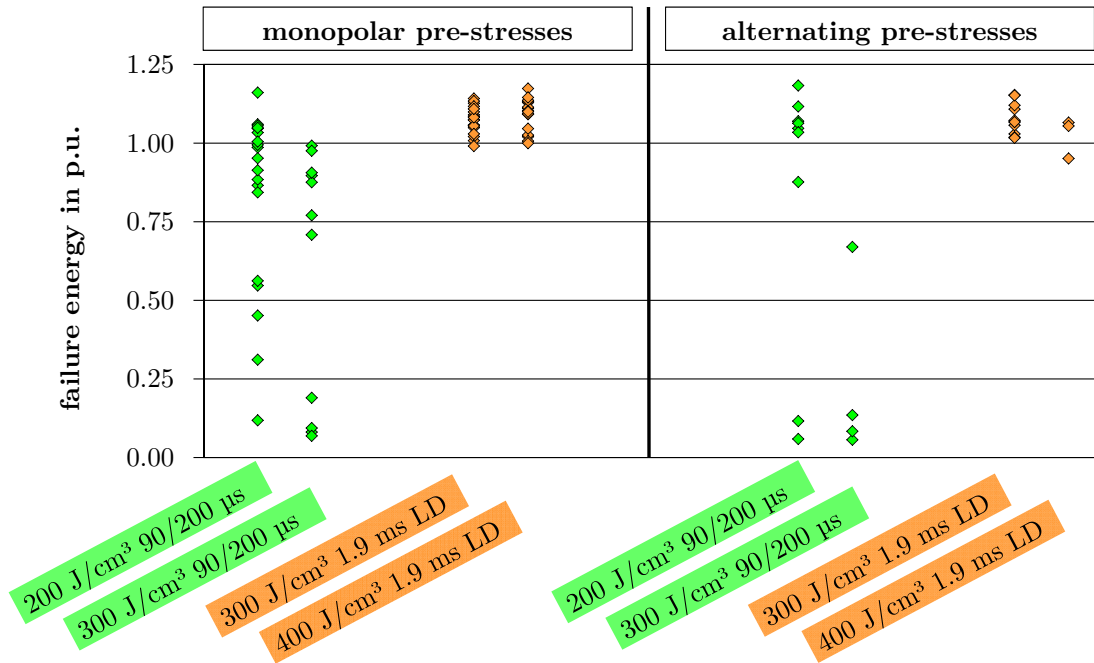
Figure 5.32: Single impulse energy handling capability of the MOVs of production lot "2" when stressed with an AC energy injection up to mechanical failure, after repetitive pre-stresses of monopolar or alternating polarity with double-exponential discharge currents of the 90/200 µs type or long-duration current impulses ("LD") with a virtual duration of 1.9 ms. The failure energy is depicted referring to that of brand-new MOVs.

pre-stresses and on the single impulse energy handling capability during destructive AC energy injections. A difference between repetitive pre-stresses with alternating or monopolar polarity can only be observed for the investigated long-duration current impulses; the investigations concerning double-exponential discharge currents do not lead to a clear result. Regarding the long-duration current impulses, the pre-stresses with alternating polarity seem to lead to a stronger fatigue and thus to a heavier pre-damage of the MOVs. Moreover, it becomes apparent that MOVs with a low single impulse energy handling capability can be detected by repetitive AC energy injections through mechanical failure. For this reason (and also taking its low pre-damage behavior into consideration), this type of stress seems to be particularly suitable for routine tests after manufacturing processes.

The marked differences between different kinds of stresses (current density or duration of the energy injection) at the same energy level regarding fatigue behavior clearly show that the choice of the types of stresses in order to determine the impulse energy handling capability has to be limited, as has been done in [IEC-37/416/FDIS]. Additionally, it seems to be sensible that the type of stress used to determine the impulse energy handling

capability complies with the stresses expected during operation (for example concerning line arresters).

5.4.4 Comparison of Two Routine Test Procedures

All of the investigations introduced so far were carried out for MOVs that had undergone a routine test by the manufacturer. The impact these stresses during routine tests have on the MOVs is unknown and the amount of failures during the routine tests (outliers) usually a company secret. The aim of the investigation introduced in the following is the direct comparison of a routine test with long-duration current impulses, which has been carried out up to now, with a routine test procedure where MOVs that have not yet undergone any routine test are stressed with an AC energy injection. Thus, knowledge is to be gained about which routine test separates out MOVs with defects most selectively and at the same time pre-damages the MOVs as little as possible.

For this purpose, a manufacturer was found who would provide a production lot that consists of 2133 MOVs of a much bigger diameter[143] than those of "size 1" mentioned above. About half of those MOVs were tested routinely inside the factory with long-duration current impulses within the current density range of $15\,\mathrm{A/cm^2}$. The other half was tested by the TU Darmstadt with an AC energy injection with a current density of about $1.5\,\mathrm{A/cm^2}$ and at the same energy level (above the typical nominal energies of standard surge arresters).

Out of the 1129 MOVs that are tested with long-duration current impulses, five MOVs fail mechanically during the routine test. Out of the 1004 MOVs that are tested with an AC energy injection, five MOVs fail mechanically, too. Likewise, there are no differences concerning the energy handling capability when the single impulse energy handling capability is determined for a group of 100 tested MOVs per procedure with an AC energy injection at a current density of $1.5\,\mathrm{A/cm^2}$.

The MOVs that failed during the routine test show different failure symptoms. The MOVs that failed during long-duration current impulses fail due to a puncture close to the edge, whereas for those MOVs that failed during destructive AC energy injections, the puncture channel spreads across the front surface. The comparison of the failure symptoms of the

---

[143] The reason why MOVs with a bigger diameter were used is that, according to the results of chapter 5.1 (see figure 5.10), they are more likely to contain inhomogeneities. Moreover, this type of MOV is used for the protection of series compensation systems and thus is stressed with AC energy injections while being operated.

destructive AC energy injections after the two routine test procedures does not show any difference between the MOVs that were pre-stressed differently.

The investigated production lot contains only a very small number of MOVs that fail during the respective routine test with a low energy handling capability. Additionally, it is unknown whether equivalent MOVs are detected as outliers by the different routine test procedures or whether about $0.5\,\%$ outliers would be detected, too, if the MOVs that had already been tested were each tested again with the respective other of the two procedures. Moreover, it is not known whether there are additional outliers (such as those shown in figure 5.4) in either group of MOVs.

Finally, it can be concluded that in this investigation, which is limited but has been carried out on such a large scale for the first time, no differences concerning selectivity and pre-damage were found between the two routine test procedures with long-duration current impulses or an AC energy injection. Thus, no final recommendation can be given as to which routine test procedure should be carried out under which conditions. Due to the results of the investigation of chapter 5.4.3, however, within the considered current density range, the routine test procedure with AC energy injections still seems to be an alternative. Furthermore, a routine test with AC energy injections is more efficient regarding the amount of time and energy needed for the test. Therefore, this routine test is interesting for the manufacturers of MOVs and should be further investigated[144].

5.5 Energy Handling Capability of Pre-Stressed MOVs

With the help of the investigations introduced in chapter 5.4.3, the repetitive impulse energy handling capability with repetitive pre-stresses of the same type can be narrowed down. So far, the correlation between different consecutive energetic stresses has only been marginally considered. The aim of the following investigations is to narrow down the correlations between different stresses.

Concerning correlations between consecutive energy injections, the impact of temperature has already been discussed in chapter 5.2 and the impact of mechanical pre-stresses in chapter 5.4. The influence of charge carrier shifts due to an energy injection, which lead, for example, to a change of the *V-I* characteristic, has not yet been considered. As is already known from previous investigations (see for example [Dar94], [Den98], [Kle04]

---

[144] It has to be observed that a transformer of the required size (up to $10\,\text{kV}$ test voltage and about $450\,\text{kVA}$ apparent power) that has been stressed single-phase non-linearly must often not be operated in existing grids.

and [Rei08]), double-exponential discharge currents with high current density and high current rise time lead to changes of the *V-I* characteristic within the pre-breakdown region. Whether these changes also have an impact on the energy handling capability, whether and how these changes reverse during operation with AC voltage at an increased temperature is determined in the investigations of the following section. In the final section, the energy handling capability of MOVs from surge arresters that were being operated in the electric power system over longer periods of time (and thus were exposed to realistic stresses) is compared to that of brand-new MOVs.

5.5.1 Impact of the Degradation of the *V-I* Characteristic on the Impulse Energy Handling Capability

In the investigations of [Rei08], the main reason that causes the MOVs of "size 2" (which were stressed with double-exponential discharge currents of the $4/10\,\mu s$ type) to fail is that the change of the "characteristic voltage" amounts to more than $5\,\%$. This limiting value was defined because, according to [Rei08], it was assumed that a change of the "characteristic voltage" above $5\,\%$ leads to a "permanent change in the ZnO material". In the following investigation, it is to be determined whether changes of the "characteristic voltage" can be reversed respectively whether these changes are a measure for mechanical pre-damage.

For these investigations, MOVs of "size 2" of three production lots are used that showed significant changes of the "characteristic voltage" during the investigations of [Rei08] (see figure 5.9). The flowchart of the investigation is shown in *figure 5.33*. Firstly, all MOVs undergo an initial measurement where the "characteristic voltage" is determined at a peak value of the current density of $0.12\,\text{mA/cm}^2$ (like in [Rei08]). After this, the MOVs are stressed with a double-exponential discharge current of the $4/10\,\mu s$ type. For the MOVs of each production lot, three current densities are defined individually, the highest current density thus chosen that none of the MOVs fail during the pre-stresses.

After the pre-stress, the MOVs are cooled down to ambient temperature within about $15\,\text{min}$ by forced cooling. Subsequently, the exit measurement is carried out during which the "characteristic voltage" is determined again.

At the end of the investigation, the energy handling capability is determined by means of a long-duration current impulse with a virtual duration of about $3.9\,\text{ms}$, stressing the MOVs up to mechanical failure. As this long-duration current impulse is a monopolar stress with a relatively low current density of about $60\,\text{A/cm}^2$, it helps to detect any polarity-dependent

initial measurement
$V_{\mathrm{ch},1}$ at $\hat{J}_{\mathrm{ch}} = 0.12\,\mathrm{mA/cm^2}$ (after $5\,\mathrm{s}$)

pre-stress with
double-exponential discharge current of the $4/10\,\mathrm{\mu s}$ type

cool-down
to ambient temperature

exit measurement
$V_{\mathrm{ch},2}$ at $\hat{J}_{\mathrm{ch}} = 0.12\,\mathrm{mA/cm^2}$ (after $5\,\mathrm{s}$)

determination of the energy handling capability
with a $3.9\,\mathrm{ms}$ long-duration current impulse
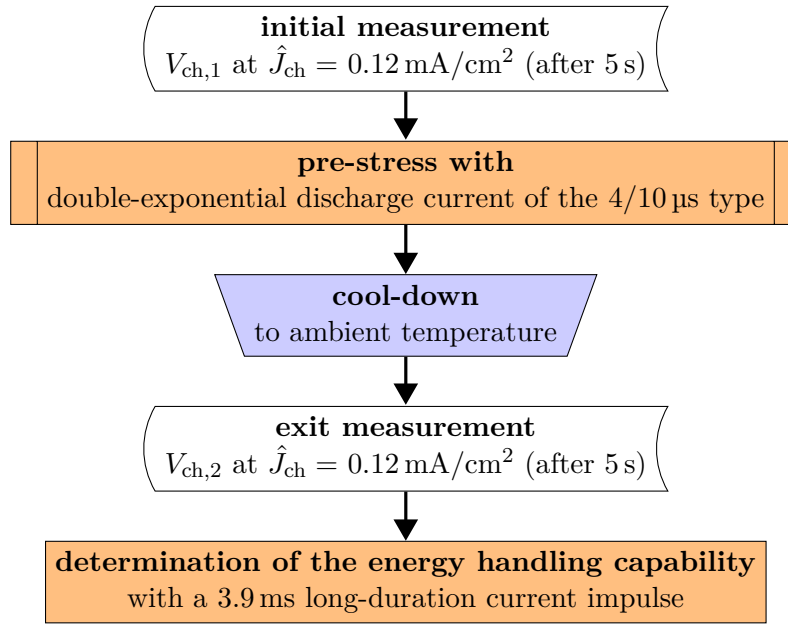
Figure 5.33: Flowchart for the determination of the failure energy after pre-stresses with double-exponential discharge currents of the $4/10\,\mathrm{\mu s}$ type.

effects. The energy handling capability is determined for ten MOVs per production lot and current density level of the pre-stress with a long-duration current impulse of the same polarity as the pre-stress and for ten other MOVs with reverse polarity.

As depicted in chapter 5.1, figure 5.9, the MOVs of different production lots show significant differences concerning the changes of the "characteristic voltage" for the same amperage of the pre-stress. Moreover, since the failure limit during the pre-stress (referred to the amperage of the pre-stress) varies between MOVs of the different production lots, the changes of the "characteristic voltage" generated for this investigation show distinct differences between the production lots. The results of the determination of the energy handling capability depending on the change of the "characteristic voltage" due to the pre-stress are depicted in *figure 5.34*. The mean failure energies are scaled to those of brand-new MOVs, the standard deviation of brand-new MOVs being plotted at a change of V_{ch} of "$0\,\%$". Failure energies, for which the destructive long-duration current impulse has the same polarity as the previous pre-stress, are marked with "equal polarity", those with reverse polarity accordingly with "reverse polarity".

For the MOVs of the production lots with the investigation results shown in the diagrams of figures 5.34 (a)and (c), there is no significant reduction of the energy handling capability. This holds true even for pre-stresses that lead to a change of the "characteristic voltage" within the range of $20\,\%$. Concerning the MOVs of the production lot the investigation
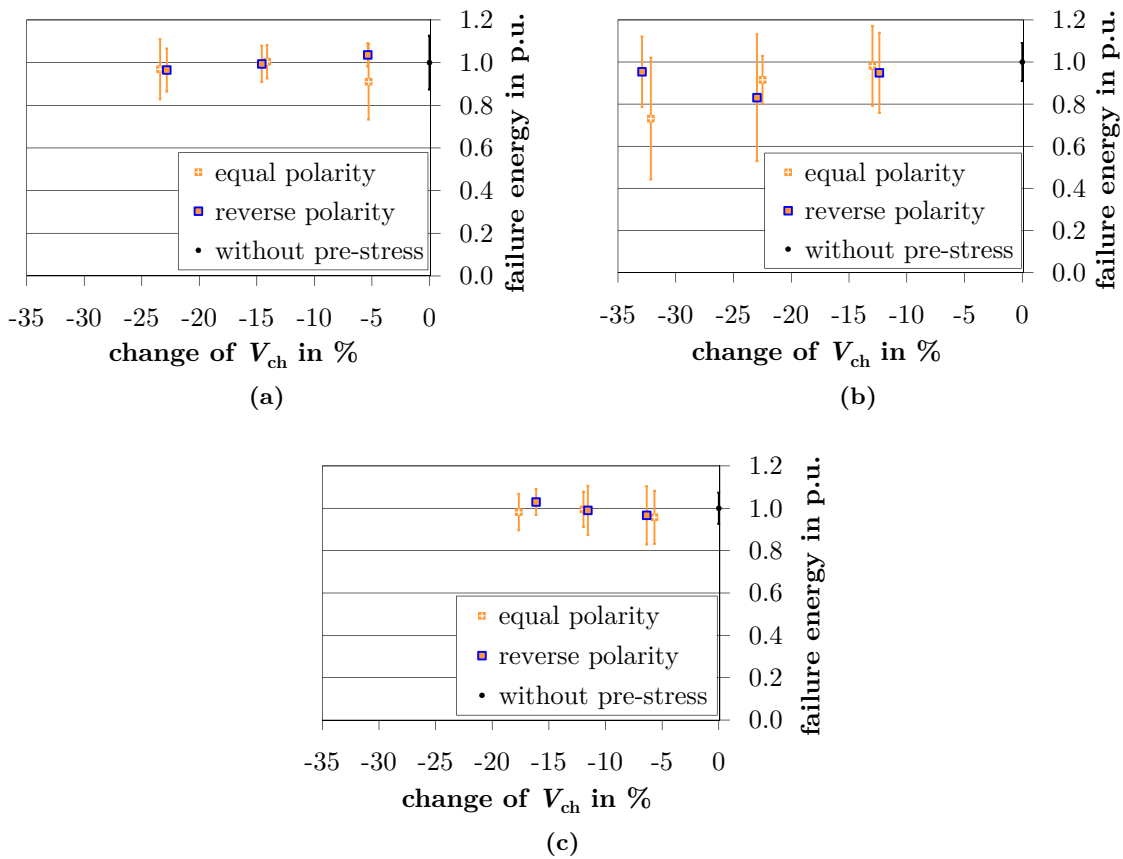
Figure 5.34: Failure energy (determined with long-duration current impulses with a virtual duration of 3.9 ms) for pre-stresses with double-exponential discharge currents of the 4/10 μs type that lead to a significant change of the "characteristic voltage" V_{ch} for the MOVs of three different production lots (a), (b) and (c). The failure energies depicted here are referred to the failure energies of the respective brand-new MOVs ("without pre-stress").

results of which are depicted in figure 5.34 (b), there is an unspecific behavior. Two measurement series, the change of the "characteristic voltage" of which was about 32 % or about 23 % in consequence of the pre-stress, show a mean failure energy that is about 27 % or 17 % lower than that of new MOVs of this production lot. However, it must be observed that these reductions are lower than the respective coefficients of variation and that the latter are comparatively high concerning the mentioned measurement series. The reason for this is that, for each of these measurement series, one MOV had a particularly low energy handling capability after the pre-stress, which has a strong influence on mean value and standard deviation considering the group size of ten test specimens. Additionally, the evaluation of the failure symptoms after the destructive energy injection does not suggest

a difference between the MOVs that were pre-stressed varyingly strong.

In another investigation, the MOVs of one production lot are pre-stressed with double-exponential discharge currents of the $4/10\,\mu s$ type, which lead to significant changes of the "characteristic voltage" and, subsequently, the energy handling capability is determined during a stress with an AC energy injection at a current density of $3.5\,\text{A/cm}^2$. The pre-stress causes an asymmetric current in the course of the energy injection, the asymmetry staying rather constant. The polarity of the half-wave during which the MOVs fail is equally distributed independent of the intensity of the pre-stress. Thus, the pre-stress does not seem to influence the failure behavior. It applies to this investigation, too, that there is no significant reduction of the energy handling capability due to a pre-stress with a double-exponential discharge current of the $4/10\,\mu s$ type.

It can be said, that even when pre-stresses with double-exponential discharge currents of the $4/10\,\mu s$ type that lead to changes of the "characteristic voltage" within a range of $20\,\%$ to $35\,\%$ are carried out, a reduced energy handling capability can only be observed for individual MOVs. Thus, a reduced "characteristic voltage" does not necessarily indicate pre-damages that have an impact on the single impulse energy handling capability during an energy injection of the investigated kinds. However, if the reduction of the "characteristic voltage" is of such intensity as could be observed here, this has an impact on the thermal energy handling capability. This must be taken into consideration when determining continuous operating and rated voltage (see [IEC60099-4]). Nevertheless, this problem apparently can be solved as MOVs that are identical in construction to those investigated here are being operated successfully in surge arresters of the medium-voltage level and that the operating duty tests according to [IEC60099-4] and [IEEEC62.11-2012] are passed with these MOVs.

Monitoring systems for standard surge arresters often evaluate the leakage current during operation (see for example [Hei01]). The assumption that the resistive component of the leakage current is a measure for the degradation of MOVs inside surge arresters will not be challenged at this point. However, the investigations introduced above show that the leakage current does not necessarily have to be a measure for the single impulse energy handling capability. Thus, evaluating the condition of the single impulse energy handling capability by means of "characteristic voltage" (meaning the change of the *V-I* characteristic within the leakage current range) does not seem to be possible.

5.5.2 Reversal of the Changes of the *V-I* Characteristic during Operation at Applied Continuous Operating Voltage

As shown in the previous section, the MOVs that are pre-stressed with double-exponential discharge currents of the 4/10 μs type in some circumstances might not display a change in single impulse energy handling capability although there is a significant change of the *V-I* characteristic within the pre-breakdown region. For this reason, it can be assumed that changes of the *V-I* characteristic within the pre-breakdown region after these pre-stresses are solely attributed to charge carrier migration and not to mechanical defects, such as beginning melting channels. If this is true, it should be possible to reverse the change of the *V-I* characteristic because charge carrier migration, in contrast to mechanical defects, is a reversible change in material. The aim of the following investigation is to find out whether these changes are indeed reversible and, if this applies, to narrow down the parameters for the reversal.

As is known from previous investigations such as [Den98] and [Kle04], changes of the *V-I* characteristic within the pre-breakdown region might in some circumstances be reversed if the MOVs are stored at an increased temperature and at applied voltage (in the range of the continuous operating voltage). In each of these investigations, however, the influence of voltage was rated differently and no such extreme changes of the *V-I* characteristic were analyzed as in the following section.

The flowchart of the investigation is shown in *figure 5.35*. MOVs of "size 2" are investigated, which all undergo an initial measurement in the first place, where the "characteristic voltage" is determined at a peak value of the current density of $\hat{J}_{\mathrm{ch}} = 0.12 \, \mathrm{mA/cm^2}$. Subsequently, a pre-stress is carried out with a double-exponential discharge current of the 4/10 μs type at a current density that might occur in an operating duty test according to [IEC60099-4] and that leads to a change of the "characteristic voltage" of the MOVs in the range of 12.5 %. This is checked in an intermediate measurement after cooling the MOVs down to ambient temperature.

In order to reverse the degradation, the MOVs are stored/ operated at increased temperature respectively at a voltage in the range of the continuous operating voltage over a 1000 h to 1200 h period. The continuous operating voltage is not a fixed value bearing a relation to a feature of the MOV, but a design value of surge arresters. For this reason, manufacturers can choose the value freely and they can also decide to use the same MOV in different surge arresters. Regarding the choice of continuous operating voltage, manufacturer's information was considered. For non-stressed MOVs at ambient temperature, the voltage applied here

initial measurement
$V_{ch,1}$ at $\hat{J}_{ch} = 0.12\,\text{mA/cm}^2$ (after 5 s)

pre-stress with
double-exponential discharge current of the $4/10\,\mu\text{s}$ type

cool-down
to ambient temperature

intermediate measurement
$V_{ch,2}$ at $\hat{J}_{ch} = 0.12\,\text{mA/cm}^2$ (after 5 s)

storage at increased temperature,
operation at continuous operating voltage

intermediate measurement?
yes   no

cool-down
to ambient temperature

intermediate measurement
$V_{ch,i}$ at $\hat{J}_{ch} = 0.12\,\text{mA/cm}^2$ (after 5 s)

exit measurement?
yes   no

determination of the energy handling capability
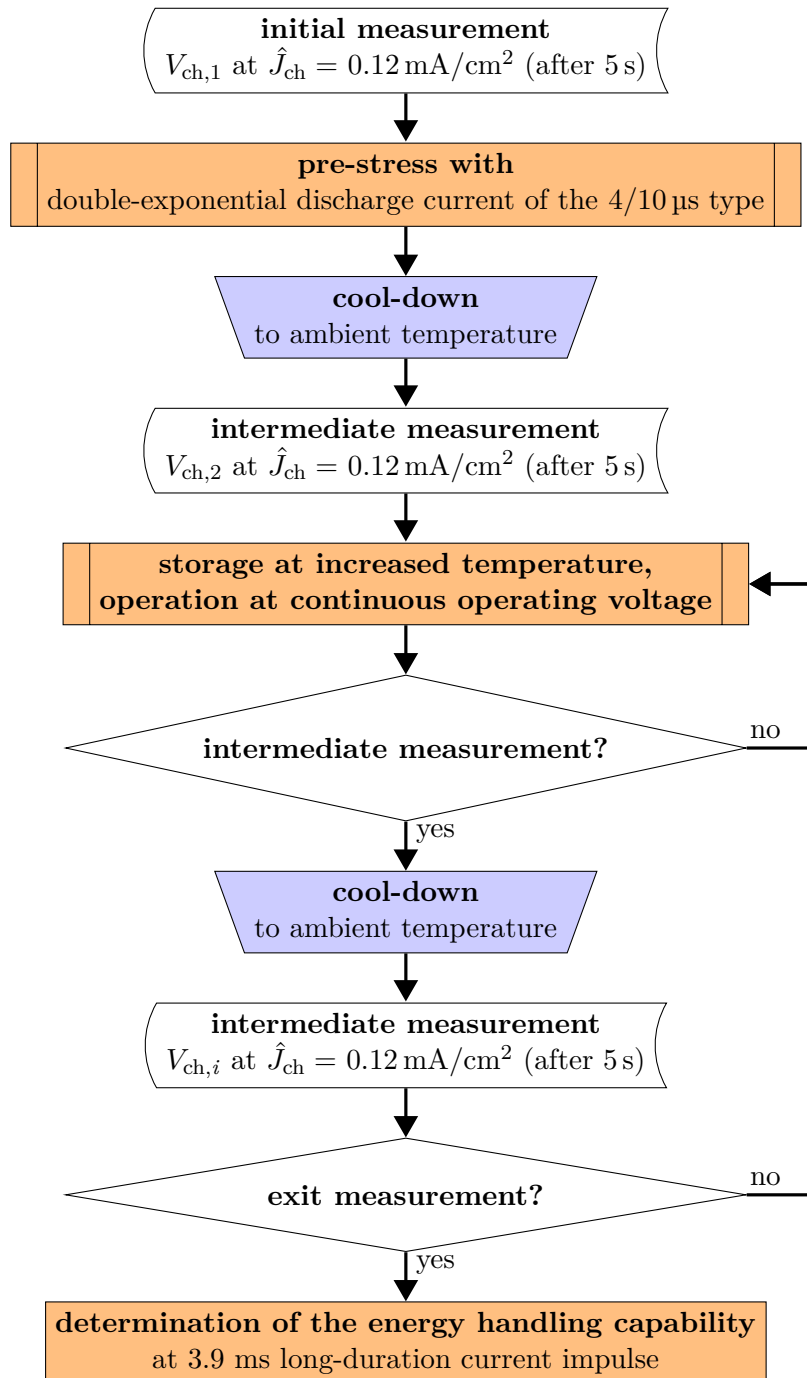at 3.9 ms long-duration current impulse

Figure 5.35: Flowchart for the determination of the reversal of changes of the "characteristic voltage" in consequence of pre-stresses with double-exponential discharge currents of the $4/10\,\mu\text{s}$ type.

leads to a resistive component significantly (by factors) lower than the capacitive component of the current.

The temperature level used is 30 °C respectively 115 °C in order to get an indication of how the test specimens behave within the range of ambient temperature and within the temperature range that is prescribed in the accelerated aging test according to [IEC60099-4] and [IEEEC62.11-2012] . According to [IEC60099-4], storage at a temperature of 115 °C for 1000 h can simulate an operating time of at least 110 years at a maximum temperature of 40 °C. This projection, however, implies the applicability of the Arrhenius law, which is highly controversial[145] in IEC itself. Since no reliable acceleration factor could be identified so far, this projection of the operating time can only serve as a reference point.

Due to the fact that, depending on the converted power loss, the temperature of those MOVs that are stressed with voltage is higher than the air temperature inside the temperature chamber, only one MOV per temperature chamber is operated at voltage. The temperature of the MOV itself is monitored and kept constant within a range of ±0.2 K (without taking the measuring uncertainty of the temperature measurement system into consideration) around the target value.

In *figure 5.36*, an example of the reversal of the "characteristic voltage" is given for four MOVs, the change being referred to the value of the pre-stress with a double-exponential discharge current of the 4/10 µs type. The time range depicted here shows the duration of the stress at increased temperature / continuous operating voltage. One MOV each is operated at a temperature of 115 °C respectively 30 °C as well as without respectively with a voltage within the range of continuous operating voltage. Every 220 h, the "characteristic voltage" is determined. To this end, the MOVs are cooled down to ambient temperature. In order to check whether the intermediate measurements have an impact on the reversal behavior, a comparative investigation without intermediate measurement is carried out. Here, no noticeable difference concerning the reversal behavior could be detected.

In another pre-investigation, MOVs that were not pre-stressed with a double-exponential discharge current of the 4/10 µs type are operated for 1000 h at a voltage within the range of continuous operating voltage at 30 °C respectively 115 °C. Due to the "aging", those MOVs show a change of the "characteristic voltage" in the range of 1 % to 2 %, the asymmetry of the current waveform decreasing at applied "characteristic voltage" in the course of the "aging".

---

[145] For example, it is discussed in [Cig13a] that the power loss behavior of long-term stable MOVs does not follow the Arrhenius law.
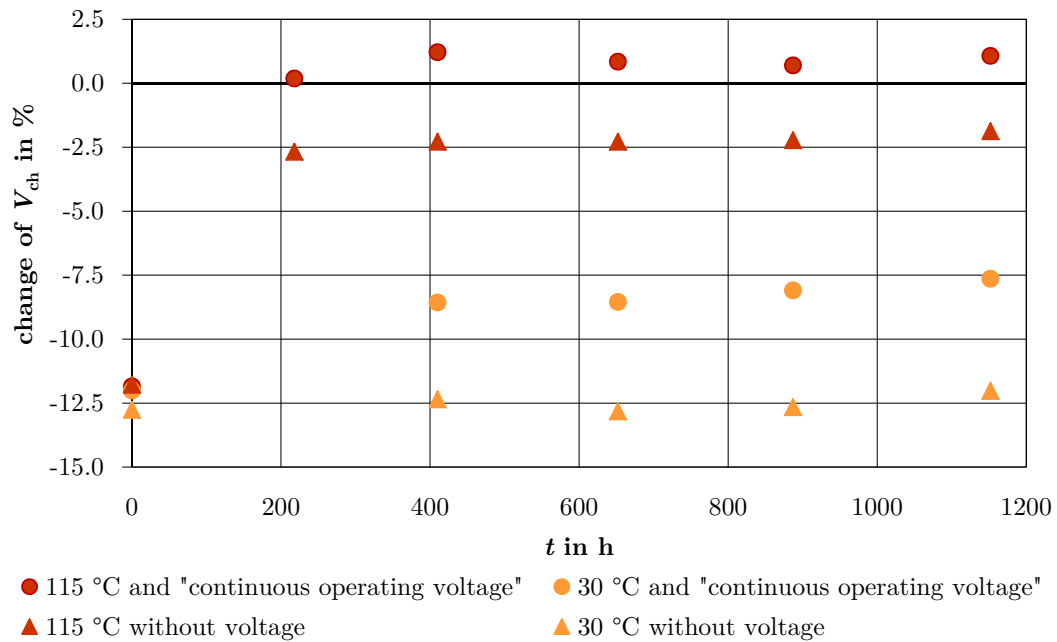
Figure 5.36: Reversal of the "characteristic voltage" when stored at increased temperature and operation at a voltage in the range of continuous operating voltage. The change of the "characteristic voltage" is referred to that of the unstressed state of the respective MOV.

The change of the "characteristic voltage" shown in figure 5.36 for point "0 h" represents the change resulting from the energetic pre-stress. The MOV that is stored without applied voltage at a temperature of 30 °C shows only a very low reversal of the "characteristic voltage" in the course of the storage. However, the MOV that is operated at the same temperature at a voltage in the range of continuous operating voltage displays a much more significant reversal in the course of the stresses. On the other hand, it has to be considered that the most distinct change occurs within the first 400 h.

Those MOVs that were stored at 115 °C show a much more significant reversal of the "characteristic voltage", the biggest reduction in this case taking place during the first 200 h, too. During operation at voltage, the reversal is bigger than without voltage. However, the difference is less significant than for those MOVs stored / operated at 30 °C. For the MOV that is operated at a temperature of 115 °C, the change of the "characteristic voltage" reaches positive values after only 200 h compared to the "characteristic voltage" before the pre-stress with a double-exponential discharge current of the 4/10 μs type. This means that, from this point in time, the "characteristic voltage" is higher than it was before the pre-stress, which can be explained by the reversal of the changes of the *V-I* characteristic that were impressed by the routine test (as has already been discussed in the previous chapters).

After the storing / "aging", the single impulse energy handling capability is determined with a long-duration current impulse with a virtual duration of 3.9 ms up to mechanical failure. Due to the small number of tested MOVs that were equally stressed, however, there is no clear result.

The results introduced here[146] confirm the assumption that changes of the *V-I* characteristic of MOVs caused by routine tests (for example measurement of the residual voltage with a lightning current impulse) or other pre-stresses with high current peak values or current rise times can only be reversed to a very low degree by storing the MOVs without voltage at ambient temperature. Storage at higher temperatures and / or applied voltage accelerate the process, the values chosen for the temperature having a much bigger impact than those for the applied voltage. According to [Den98], this can be thus explained: the process of reversal / recovery is attributed to a diffusion process that is accelerated more strongly by higher temperatures than by the applied voltage. According to this, the oxygen ions that migrated from the grain into the grain boundary during an impulse stress[147] migrate into the opposite direction during the recovery phase until the initial balance is established again. Here, the temperature-dependent oxygen ion conductivity of the Bi_2O_3 (see [Stu90]) is of the biggest importance.

The changes of the *V-I* characteristic within the pre-breakdown region that were caused by pre-stresses with double-exponential discharge currents of the 4/10 μs type (with the chosen values) obviously are reversible and do not reduce the single impulse energy handling capability (see chapter 5.5.1). In the reversal process, the duration of the reversal depends heavily on the temperature of the MOVs and the applied voltage during the recovery process. It should be noted that the cooling process for surge arresters in electric power systems after an energy injection takes longer than during the investigations described above that were carried out in a laboratory. For one thing, this is because the surge arresters are usually still operated at system voltage during the cooling process and thus electric power loss is converted inside them that is bigger than in an unstressed state due to the increased temperature of the surge arrester. Additionally, the housing of the surge arrester has a thermally insulating function, which slows down the cooling process. Thus, it can be assumed that, due to the cooling process taking longer concerning a surge arrester in the power system, the reversal of the *V-I* characteristic within the pre-breakdown region is higher for these surge arresters than for those tested under laboratory conditions, too.

It can be assumed that the stress investigated here is an extreme stress and that surge

---

[146] The tendency of these investigations could be confirmed in further investigations where the values were varied.

[147] This effect is described in chapter 2.2 under the heading "hot electrons".

arresters inside electric power systems most likely are not stressed with such high current peak values (see [Cig13b]). Consequently, surge arresters in electric power systems probably are not operated with such significant changes of the *V-I* characteristic (as investigated here).

5.5.3 Energy Handling Capability of MOVs Aged During Operation

In the previous investigations, the impacts of energy injections on MOVs and particularly on the single impulse energy handling capability have been investigated. However, since stresses concerning surge arresters in electric power systems are mostly only fragmentarily documented, it is hard to assess the practical relevance of the investigations described above if there are no additional considerations concerning this matter. In this section, MOVs used in surge arresters are investigated, which have been operated for several years and thus were subjected to real stresses. The aim of this investigation is to gain knowledge of whether the single impulse energy handling capability is reduced by the stresses occurring during operating time.

The actual stresses that occurred during the operating time of a surge arrester cannot be easily traced back afterwards. Only very few of the available monitoring systems for surge arresters evaluate energy injections or they are documented inconsistently. Moreover, the procedure concerning the evaluation of monitoring systems is different for the different transmission system operators. For this reason, energetic stresses due to overvoltages of the investigated surge arresters (that were equipped with, for example, monitoring spark gaps) can only be given with a great uncertainty. The only thing that can be presumed is that the surge arresters were stressed with system voltage during the operating time.

For the investigation, MOVs of surge arresters of the extra-high-voltage level (240 kV respectively 380 kV) with a one-column active part are provided by three different manufacturers. Each of the respective transmission system operators has also provided information on operating time, removal from service, site of the surge arresters, as well as, often, monitoring systems. The investigated surge arresters are labelled "SA1" to "SA9" in the following. Here, concerning "SA1" to "SA5" and "SA8", the three identically constructed surge arresters of one three-phase-system are each subsumed under one label. All of the 22 surge arresters that were investigated were inconspicuous during operation without exceptions; none of the surge arresters was removed from operation due to conspicuities (not even surge arrester "SA7").

Table 5.8: History of the investigated surge arresters according to the information provided by the respective transmission system operator.

	SA1	SA2	SA3	SA4	SA5	SA6	SA7	SA8	SA9
amount	3	3	3	3	3	1	1	3	2
year of manufacture	1988	1992	1994	1994	1997	1997	1997	1997	1998
years of operation	1^a	19	17	15	13	12	6	9	12
stress^b	none	none	unknown	1-2	unknown	unknown	1^c	none	none

---

[a] Due to the year of manufacture and the date of removal from service, it must be assumed that this surge arrester was being operated for much longer than one year.

[b] The actual stress is unknown. It can be presumed that the surge arresters were stressed more often than is given in the table above.

[c] The stress led to an undiscovered mechanical failure of individual MOVs of the surge arrester.

The information that was provided concerning the history of the investigated surge arresters is depicted in *table 5.8*. It can be seen that the majority of the investigated surge arresters was produced in the 1990s and that they were operated six to 19 years until they were removed from service according to the respective transmission system operator[148]. The information on previous stresses gained with the help of the monitoring systems are shown in the last row of the table. They entail a big uncertainty as can be taken from the previous section on monitoring systems. It is very unlikely that the surge arresters were only exposed to so few stresses during so many years of operation. The surge arrester labelled "SA7" contained individual MOVs that had failed and where the failure symptoms hint at an electrical overload.

In order to determine the single impulse energy handling capability of the MOVs inside the surge arresters and to compare it to that of brand-new MOVs, the investigation introduced in chapter 5.1 is carried out. Accordingly, the flow chart is to be found in figure 5.1. The amount of MOVs inside the surge arresters is different for the surge arresters "SA1" to "SA9" (depending on the rated voltage of the surge arresters and the *V-I* characteristic of the MOVs inside them). Out of most of the surge arrester sets, about 100 MOVs each can be used for the investigations. However, due to the test facility, not all types of MOVs can be stressed with all waveforms up to the limit of their energy handling capability. Hence, not all stresses mentioned in chapter 5.1 are carried out but only AC energy injections with a peak value of the current density[149] of about $3.5\,\text{A/cm}^2$ and long-duration current impulses

---

[148] Older surge arresters could not be provided.

[149] The single impulse energy handling capability of the MOVs of the surge arresters "SA4" is also determined by an AC energy injection with a peak value of the current density of about $0.35\,\text{A/cm}^2$.
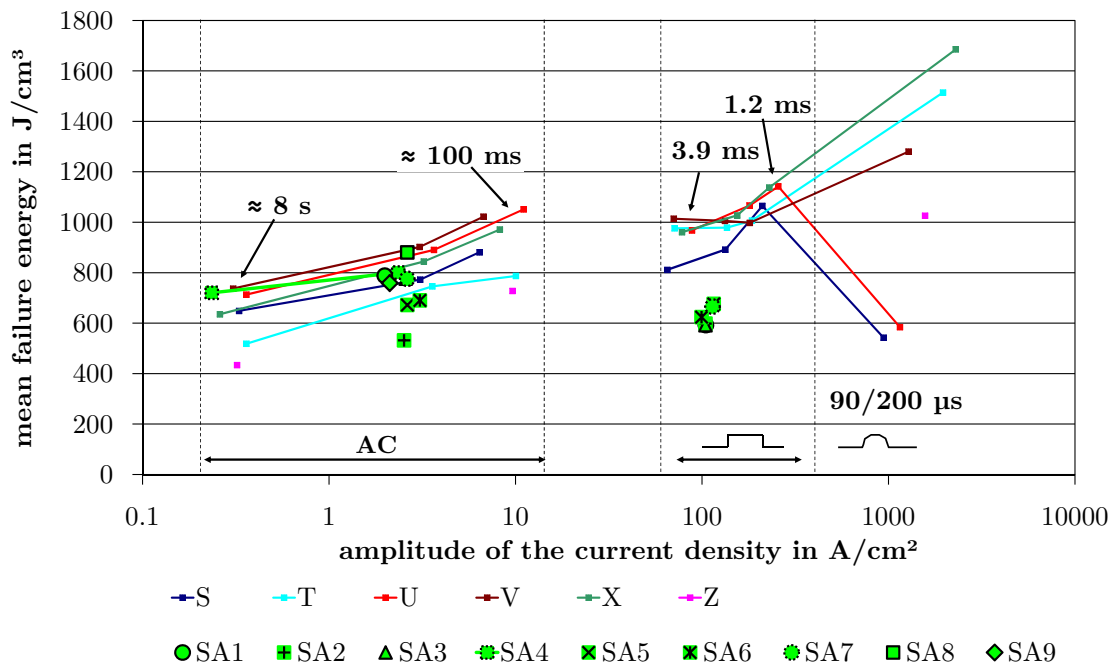
Figure 5.37: Mean single impulse energy handling capability of the investigated surge arresters compared to the mean energy handling capability of brand-new MOVs of "size 1" (see chapter 5.1).

with a virtual duration of 1.9 ms. In doing so, just as this was the case in chapter 5.1, the "complex failure criterion" is applied for the long-duration current impulses, whereas the MOVs are stressed up to mechanical failure regarding the AC energy injections. For the AC energy injections, 50 MOVs are stressed per current density of each surge arrester set, whereas, regarding the long-duration current impulses, 40 MOVs are stressed.

The mean single impulse energy handling capability of MOVs from the described surge arresters compared to that of brand-new MOVs of "size 1" is depicted in *figure 5.37*. There is no information given as to how high the mean single impulse energy handling capability of those MOVs taken out of the surge arresters was when they were brand-new. In chapter 5.1 (see figure 5.2), the single impulse energy handling capability of production lots "S" to "Z" was discussed in comparison to the investigation results presented in [Rin97]. Here, it was assumed that the single impulse energy handling capability of the MOVs that were manufactured in the 1990s (see [Rin97]) was probably a little lower than that of production lots "S" to "Z". However, since it lies within the same range in both cases, the single impulse energy handling capability of production lots "S" to "Z" in figure 5.37 is used as reference point for that of the MOVs that were taken from the surge arresters.

It can be seen that the mean single impulse energy handling capability concerning the AC energy injections basically lies within the spread of the brand-new MOVs investigated before. Merely the MOVs of the surge arresters "SA2" display a lower energy handling capability. They show a similar behavior to that depicted in figure 5.5: the MOVs fail at two different energy levels that are clearly distinguishable, about $350\,\text{J/cm}^3$ and about $700\,\text{J/cm}^3$. Also in this case it can be assumed that the reason for this could be inhomogeneities that lead to a current path concentration at this current density. Here, the evaluation of the failure symptoms does not display any conspicuities and especially no correlation between the energy handling capability and the failure symptom either.

In additional investigations, no significant conspicuity can be detected between the MOVs of different construction units of the surge arrester concerning the single impulse energy handling capability for stresses with the AC energy injections described above. For this type of stress, differences regarding the energy handling capability of MOVs of different surge arresters of one set can neither be measured.

Concerning the stresses with long-duration current impulses, the MOVs of those six surge arresters where this type of stress was applied show a significantly lower single impulse energy handling capability than brand-new MOVs, which, however, is still way above the typical nominal energy handling capability of standard surge arresters. Here, the reduction of the "characteristic voltage" is by far the most dominant failure cause. As can be seen from figure 5.3, for the brand-new MOVs this is the case much more rarely. Presumably, the stressing with system voltage during operation inside the power system has reversed the changes of the *V-I* characteristic that resulted from the routine tests carried out for these MOVs. As is known (see for example [Den98] and [Kle04]), the first impulse causes the biggest change of the *V-I* characteristic if consecutive impulse stresses are applied. For this reason, the energy injections applied to the brand-new MOVs that still contain charge carrier shifts in consequence of the routine test cause a lower reduction of the "characteristic voltage" than when applied to the MOVs of surge arresters "SA1" to "SA9".

Those surge arresters that had been exposed to energetic stresses during operation according to the monitoring systems did not display any conspicuities with regard to the single impulse energy handling capability. Even the MOVs without optically noticeable failure symptoms that were taken from surge arrester "SA7" (that contained mechanically failed MOVs) show the same behavior concerning the single impulse energy handling capability as those of the other surge arresters.

The amount of investigated surge arresters can certainly not be considered a representative sample and there is too little information on the energetic pre-stresses of the surge arresters.

However, it can be said that even at a stress[150] that leads to a mechanical failure of individual MOVs in a surge arrester, no reduction of the single impulse energy handling capability at AC energy injections within the investigated range can be detected. For the range that is investigated with long-duration current impulses, a clear reduction of the single impulse energy handling capability can be observed indeed. However, this can be attributed to changes of the "characteristic voltage". Within this range, too, the failure criterion and the height of the mean failure energies point to the fact that a safe operation of these surge arresters has never been disputable.

Only surge arrester "SA7", which had obviously been exposed to a high energetic stress during operation and, as a result, supposedly contained individual MOVs that had failed mechanically, was limited in its functionality due to the failed MOVs. Nonetheless, it is remarkable that this surge arrester was inconspicuous inside the power system despite the failure of a little less than 10 % of the built-in MOVs. Due to its limitations concerning functionality and thus that the failure cause could not be narrowed down, it should be investigated whether other similar cases can be found inside electric power systems.

---

[150] Type of the energy injection, current density, waveform etc. could not be reconstructed.

6 Summary

Structure and conduction mechanism of MOVs have been extensively investigated even though not all effect mechanisms of the used additives etc. are known in every detail. Additionally, the single impulse energy handling capability has been experimentally determined and verified with simulations for wide current ranges in previous investigations. According to these investigations, the single impulse energy handling capability increases with rising current density of the stress within the breakdown region of the V-I characteristic until, if very high current densities are applied, the breakdown / flashover behavior of the coating limits the stress handling capability. Concerning stresses with double-exponential discharge currents, alongside mechanical aspects, changes of the V-I characteristic of the stressed MOVs have been noticed to an increasing extent.

The multiple stresses that have been investigated so far were limited mainly to multiple double-exponential discharge currents at high current densities and high current rise times. Here, alongside the changes of the V-I characteristic already mentioned, an increasing amount of breakdowns through the coating of the MOV could be observed at increased stressing of the MOVs.

In the investigations introduced in this thesis, it could be shown that there is a positive temperature coefficient of the resistance at high current densities, meaning the V-I characteristic of MOVs shifts towards higher voltages at a higher temperature and the same current density. It was also possible to develop a physical model for this behavior. The shift of the V-I characteristic is marked only weakly, not constant at different temperatures and, additionally, it is different for the two MOV ceramics investigated here.

The temperature dependency of the V-I characteristic only has a small impact on the energy handling capability of MOVs at energetic stresses. When several MOVs, the different V-I characteristics of which led to current densities of the stress that differed by about a third, were stressed parallel, only a relatively low assimilation of the current densities during the stress with long-duration current impulses could be observed.

The investigation of the energy handling capability of pre-heated MOVs displays differences concerning the energy that can be applied electrically at different initial temperatures. However, within the investigated current density range, no impact of the temperature dependency of the *V-I* characteristic on the energy handling capability could be detected. Obviously, the current distribution depending on the microstructure of the MOV is crucial for the single impulse energy handling capability whereas the temperature dependency of the *V-I* characteristic only plays a secondary role.

The energy handling capability concerning double-impulse stresses was investigated within the time span of single impulse stresses and repetitive stresses with an interval between the stresses of up to 3 s. In doing so, the same energy handling capability was detected for single impulse stresses as well as for double impulse stresses with the time intervals mentioned above at the investigated current density. Hence, it can be assumed that the heat distribution inside the MOV cannot be improved considerably concerning double impulse stresses within the time intervals between the impulses. For this reason, the stresses of energy injections that occur in quick succession (up to time intervals where a considerable amount of heat is dissipated from the MOV to its surroundings) must be added up in order to determine the equivalent overall stress for the MOV. This has been known with regard to the impact on the thermal stability of surge arresters, but, so far, not for the single impulse energy handling capability.

The focus of the investigations introduced here is on repetitive energy injections where the MOVs are cooled down to ambient temperature between the energy injections. Here, it could be demonstrated that there is no clear relation between repetitive and single impulse energy handling capability. During the investigation, MOVs of three different production lots (of different manufacturers or different types) were stressed with 100 repetitive AC energy injections at a peak value of the current density of $3.5\,\mathrm{A/cm^2}$. This range of the current density was used because it can occur for example in surge arresters for the protection of capacitors inside series compensation systems for this type of stress. During the pre-stresses, individual MOVs of two of the three investigated production lots failed. However, in the exit measurement, the pre-stressed MOVs did not display any pre-damages that would influence the energy handling capability. Thus, it can be presumed that, if anything, AC energy injections at the mentioned current density fatigue MOVs only to a small degree (individual failures during the pre-stresses can probably be attributed to defects inside the MOVs).

Concerning repetitive long-duration current impulses with a higher current density and a lower duration of the energy injection, it could be observed that the percentage difference between the single and the repetitive energy handling capability of the MOVs is bigger

than for the AC energy injections mentioned before. In contrast, the energy levels at which individual MOVs of one group of for example ten MOVs fail during repetitive stresses lies within a similar range for both types of energy injections / current densities.

For this reason, a systematic investigation of the energy handling capability of MOVs was exemplarily carried out by applying AC energy injections with a duration of about $80\,\text{ms}$, long-duration current impulses with a virtual duration of $1.9\,\text{ms}$ and double-exponential discharge currents of the $90/200\,\upmu\text{s}$ type. In doing so, the energy level was varied within the same range of $200\,\text{J/cm}^3$ to $400\,\text{J/cm}^3$ for all types of energy injections. It became apparent that shorter stresses at higher current densities pre-damage the MOVs to a larger extent than the AC energy injections. This can be taken from the failure rate during the pre-stresses and the single impulse energy handling capability after 20 pre-stresses. Obviously, the degree of the current distribution inside the MOV is of minor relevance concerning these repetitive stresses. Whether mechanical tensions, which occur at shorter energy injections, lead to mechanical pre-damage inside the MOVs could not be proven.

Furthermore, the evaluation of the failure rates and the single impulse energy handling capability after repetitive pre-stresses indicate that stresses with a lower energy density are more suitable for the detection of MOVs with a low single impulse energy handling capability, so-called outliers, than stresses with a high current density. For outliers, the AC energy injections applied here probably already lead to failures at smaller amounts of impulses (often even at the first one). In addition, they seem to pre-damage the MOVs to a lesser extent than energy injections at higher current densities and the same energy level. It is assumed that one reason for the selective failure behavior is the more favorable ratio of current path concentration and heat equalization inside the MOV during the energy injection at the applied current density. This is supported by the analysis of the spread of the single impulse energy handling capability of MOVs of one production lot, some of which display a considerably lower energy handling capability. These MOVs were stressed with different current densities. Here, the most distinct differences regarding the energy handling capability can be detected at a current density of about $3.5\,\text{A/cm}^2$.

For this reason, the stress mentioned above seems to be particularly promising for routine tests. However, in a direct comparison of a conventional routine test procedure with long-duration current impulses and with AC energy injections of the same energy level, no significant difference between the two procedures with regard to selectivity could be detected. This was due to the small amount of MOVs with low energy handling capability. Thus, the final evidence for the advantage of a routine test procedure with AC energy injections has yet to be provided.

Apart from mechanical pre-damages, pre-stresses, particularly those with high current densities and high current rise times, can cause changes of the *V-I* characteristic within the pre-breakdown region. In previous investigations, a correlation between the current peak value of a pre-stress with a double-exponential discharge current of the 4/10 μs type and the change of the "characteristic voltage" (comparable to the reference voltage) caused by this pre-stress was detected. However, further investigations introduced here do not suggest a correlation between the change of the *V-I* characteristic and the single impulse energy handling capability. Obviously, the migration of oxygen ions resulting from discharge current stresses at a high current density and high current rise time (which is known from the technical literature) does not cause a reduction of the energy handling capability. In other words, the investigated pre-stresses do not cause pre-damages that would contribute to a reduction of the energy handling capability.

Those changes of the *V-I* characteristic that are caused by double-exponential discharge currents of the 4/10 μs type might in some circumstances be reversed by storing the MOVs at increased temperature and at AC voltage at power frequency. It became apparent during the investigations that, at the chosen values (which are of high relevance in power systems), temperature probably has a bigger impact than voltage, which is in accordance with findings that were previously published.

Exemplarily, the single impulse energy handling capability of MOVs that had been taken from surge arresters of the high-voltage level were investigated after they had been operated in real electric power systems for years. Compared to brand-new MOVs, these MOVs do not display any considerable differences concerning the energy handling capability when stressed with AC energy injections within the investigated range of current density. When stressed with long-duration current impulses, they already show changes of the *V-I* characteristic at lower energy levels. However, this is not to be considered crucial due to the previously mentioned investigation results. MOVs that had been taken from surge arresters that were exposed to distinct energetic stresses during operation showed an inconspicuous behavior concerning the single impulse energy handling capability, too.

6.1 Consequences for the Operation of Surge Arresters

Multiple impulse stresses with long time intervals between the stresses seem to be uncritical for surge arresters in standard applications at the specified nominal energies commonly used today. The energy injections that lead to symptoms of fatigue and were identified in the investigations introduced above lie almost exclusively higher and only rarely lower

than typically used specified nominal energies. Since the energy levels from which a fatigue of the MOVs can be assumed to start are only a little above the commonly specified energy handling capability, a lifting of this specified energy handling capability does not seem to be possible. In special applications of surge arresters, such as when used as line arresters or in series compensation systems, special stresses can occur, which is why these have to be taken into consideration separately.

Line arresters are possibly increasingly exposed to energy injections with high current rise times and current peak values. In the investigations introduced above, this kind of energy injection has already led to symptoms of fatigue at lower energy levels. This should be considered when designing and operating line arresters.

Surge arresters for the protection of capacitors in series compensation systems are mostly exposed to stresses with AC energy injections. According to the introduced investigations, these stresses with low current peak values and low current rise times either seem to fatigue MOVs to a lesser extent or not at all. Thus, for these surge arresters, it would be possible to specify higher energy densities inside the MOVs. However, it has to be observed that, at low current densities, inhomogeneities inside the MOVs have a particularly big impact on the current distribution inside the MOV during stresses and therefore reduce the energy handling capability. Hence, with regard to these stresses, outliers with a low energy handling capability affect the overall energy handling capability to a much higher degree. In other words, a lifting of the specified nominal energy can lead to a higher failure risk despite the lower fatigue risk because it is more likely that the limit of the single impulse energy handling capability of individual MOVs is reached. Since the latter depends on the particular manufacturer respectively the production lot, a general statement cannot be made here.

During the application in series compensation systems, the spatial extension of surge arrester banks can cause temperature changes between columns of MOVs. Within the range of the investigated current densities, these changes only lead to small changes concerning the current distribution between the columns. Thus, with regard to the current distribution within the investigated range, temperature changes do not have to be considered any further.

For surge arresters used in medium-voltage grids, significant changes of the V-I characteristic within the pre-breakdown region at stresses with double-exponential discharge currents with high current densities and high current rise times were observed in the previous investigations. It can be assumed that surge arresters in power systems are not exposed to such significant changes. Moreover, it could be verified in the investigations introduced

here that such changes can be reversed during operation and that these changes do not necessarily influence the single impulse energy handling capability.

This result also has an effect on the determination of pre-damages inside surge arresters for example by means of monitoring systems. It does not seem to be possible in all cases to unambiguously determine a pre-damage of MOVs that leads to a reduction of the single impulse energy handling capability on the basis of a change of the *V-I* characteristic within the pre-breakdown region[151].

From the finally introduced investigation on the single impulse energy handling capability of MOVs which were taken out of surge arresters that had been operated in power systems, it can be concluded that their energy handling capability had not been reduced by the stresses that occurred during operation. Thus, a replacement of surge arresters after a certain amount of years of operation simply out of concern about their energetic stress handling capability does not seem to be necessary[152]. However, the surge arrester that was identified as contained failed MOVs indicated that, in some circumstances, it is not easy to determine from the outward appearance whether the MOVs are intact or not.

6.2 Recommendations for International Standardization

The international standards for surge arresters of the medium- and high-voltage level in IEC and IEEE have developed a lot in recent years also with regard to the verification of the impulse energy handling capability. If the general validity of the investigation results introduced in this thesis is verified, it is suggested that the following recommendations are taken into consideration when [IEC-37/416/FDIS] (respectively IEC 60099-4, which would then be up-to-date) and [IEEEC62.11-2012] are revised again. These recommendations are to be seen from a scientific point of view.

Concerning the "test to verify the repetitive charge transfer rating" in [IEC-37/416/FDIS], for NGLA and surge arresters of the medium-voltage level, a choice of the type of stress for a very wide time range of the stress is provided. This does not seem to be expedient because, according to the investigations introduced here, short stresses (with the same energy content) fatigue MOVs much more than longer stresses with lower current density. If the investigations are confirmed also for the same charge transport of the stresses (which

---

[151] On the other hand, the impacts changes of the *V-I* characteristic have on thermal energy handling capability are indisputable.

[152] Other negative impacts such as, for example, leaks inside the housings were not investigated here.

can be assumed), this option should be reconsidered. In doing so, due to the application, it seems to be sensible to limit the choice to shorter energy injections.

The results of the "test to verify the repetitive charge transfer rating" in [IEC-37/416/FDIS] and the "single impulse withstand rating test" in [IEEEC62.11-2012] are influenced by the test fixtures used. In both standards, the series of stresses consists of ten groups with two impulses each with a time interval between the impulses of 50 s to 60 s, the test specimens being cooled down to ambient temperature between the groups. The test fixture has a significant impact on the temperature of the MOVs prior to the beginning of the second impulse of a group. However, a standardization of the test fixture that is reasonable is very difficult to achieve. Due to the fact that the temperature prior to the second impulse influences the energy handling capability during the second energy injection, it is more expedient to cool down the specimens to ambient temperature after each energy injection. Since this method increases the test duration, a comment in the standard would be useful that clarifies that an initial temperature of the specimens above ambient temperature when the second energy injection is applied represents the more critical case. When taken into consideration, this comment would lead to a reduction of the cool-down time. Overall, the cooling down of the test specimens to ambient temperature reduces the influence of the text fixture and thus helped to render the test results more repeatable.

Moreover, the validity of the exit measurement of the tests concerning the repetitive stress handling capability mentioned above in [IEC-37/416/FDIS] as well as in [IEEEC62.11-2012] has to be reconsidered. It becomes clear from the investigations introduced above that a change of the reference voltage is not a sure sign for mechanical pre-damage. Furthermore, it is known that thermal stability is in some circumstances dependent on additional factors. In the investigations introduced here, it could not yet be entirely verified whether the non-standardized routine test after the manufacturing process has an impact on the change of the reference voltage due to the applied energy injections. It can be assumed that the *V-I* characteristic of MOVs that were exposed to a routine test with an energy injection with a high current peak value and a high current rise time changes to a lesser extent than in a routine test that leads to a lower charge carrier migration. Thus, it is possible that a change of reference voltage depends on the type of routine test but has only a minor influence on the operation of the MOVs.

In the exit measurement of the "test to verify the repetitive charge transfer rating" in [IEC-37/416/FDIS], the testing at a double-exponential discharge current of the 8/20 μs type is prescribed. The investigations introduced here suggest that, with this type of energy injection, pre-damages of MOVs cannot in all cases be identified. This stress should be complemented with a testing of the single impulse energy handling capability with an

energy injection that can be regarded as particularly critical in order to increase the validity of the test. According to the introduced investigations, an AC energy injection with a current density of $< 10\,\text{A/cm}^2$ seems to be especially sensitive for defects and pre-damages inside the MOV. It is possible that an energy injection only up to the nominal energy handling capability suffices as evidence, which would reduce the strains on the test facility. Moreover, it has yet to be clarified to which extent the current density would have to be limited and whether the testing equipment of the manufacturers can be used for the "Power-frequency voltage-versus-time test" of [IEC-37/416/FDIS] for this investigation. The latter would considerably enhance the acceptance of such a test.

The conditioning of the MOVs in the beginning of the "switching surge energy rating test" of [IEEEC62.11-2012] with 18 long-duration current impulses seems to be unrewarding because it does not affect the V-I characteristic negatively within the pre-breakdown region according to the investigations introduced above. For this reason, it might be possible to omit this conditioning as it is the case in [IEC-37/416/FDIS] for non-gapped surge arresters.

According to the investigations introduced here, the power loss behavior of the "test to verify long-term stability under continuous operating voltage" according to [IEC-37/416/FDIS] and the "accelerated aging test of varistors" according to [IEEEC62.11-2012] is influenced by changes of the V-I characteristic resulting from the non-standardized routine test. Since the power loss behavior is influenced during the first hours at the temperatures and common voltages used in these standards, the routine test has an impact on the reference value of the criterion for passing this test. The reference value should be placed in a time interval of the aging test that is not influenced by the applied routine test. In the investigations described above, the resolution of the range of the first 200 h of the aging test is too low to give a more precise recommendation.

If this recommendation is not implemented, the time for the reference value in the standard [IEEEC62.11-2012] should be narrowed down more exactly than the time span "after 2 h to 5 h" given so far. Due to the dynamics of the power loss behavior in the first hours, which can be strong in some circumstances, in [IEC-37/416/FDIS], the reference value is narrowed down to 15 min before resp. after 3 h. This should be easily achievable with the measurement technology available today and thus transferred into [IEEEC62.11-2012].

Due to the investigations on the regeneration of degradations inside the MOVs mentioned above, it seems to be sensible to limit the maximum pre-heating time after the conditioning in the "thermal recovery test" according to [IEC-37/416/FDIS]. So far, [IEEEC62.11-2012] lacks such a guideline and should be amended.

6.3 Perspectives for Future Research

By carrying out the above mentioned investigations, a lot of questions could be answered and tendencies could be pointed out. A few questions, however, could not be answered in detail due to the limited resources. For this reason, the author of this thesis is of the opinion that it would be promising to carry out further investigations on the following issues:

In this thesis, the temperature dependency of the *V-I* characteristic was investigated for two different MOV ceramics within a limited temperature and current density range. It remains unresolved which factors influence the temperature dependency within the breakdown region. It would be interesting to find out whether a correlation exists between the temperature dependency of the *V-I* characteristic and the single impulse energy handling capability of different MOV ceramics.

Moreover, it is yet unresolved which criteria lead to a reduced single impulse energy handling capability of individual brand-new MOVs of a production lot. As soon as this can be narrowed down, one would have to investigate which test procedures respectively types of stresses could identify such MOVs with low effort and at the same time keep the pre-damages of the other MOVs as low as possible. This could be of relevance for routine tests of MOVs after the manufacturing process.

For the operators of surge arresters, on the other hand, it is important to identify pre-damages, ideally during operation. The investigations introduced above show that significant changes of the *V-I* characteristic are no sure sign for practice-oriented pre-damages of MOVs. The question remains to be answered which type of commercially applicable procedure would make it possible to identify these.

In the investigations carried out so far, different ranges of current density were tested with different types of impulses. It is still to be examined at which ratio of the current peak values the single impulse energy handling capability of an AC energy injection is equivalent to that of, for example, a DC energy injection.

In this context, the question of polarity effects of repetitive stresses has been analyzed insufficiently so far, too. The investigations on repetitive stresses of alternating polarity introduced here show differences regarding the pre-damage behavior. These investigations should be expanded with regard to other current density ranges and types of stresses. The results gained from this could be of help when figuring out whether a certain series of polarities should be prescribed or precluded in standardization.

Resulting from this, there is the question of the correlation between different stresses. So far, it has not been analyzed systematically whether there are certain combinations of energetic stresses that lead to a particularly low energy handling capability of MOVs. It is conceivable that special pre-stresses cause for example mechanical pre-damages that have a very big impact on the energy handling capability at certain stresses.

It could also be demonstrated that, in some circumstances, changes of the V-I characteristic are reversible. It remains to be investigated whether this type of change of the V-I characteristic is of practical relevance and whether a procedure for an accelerated reversal could increase the operating safety of surge arresters.

Appendix

A Additional Information Concerning the Test Facilities Used

In this chapter, additional information concerning the test facilities used is given that exceeds the information necessary to understand the investigations described above. To that end, the measuring equipment is introduced and a deeper insight into the test facilities is given in the following sections.

A.1 AC Energy Injection Test Set-Up

Figure A.1 presents an overview of the test facility. Here, the primary and secondary circuit breakers, the testing transformer as well as the control cabin[153] are depicted. The power unit of the test set-up (including control and protection) was installed by HIGHVOLT. For the most part, it consists of the single-phase Thoma type regulator, the technical specifications of which are given in *table A.1*.

Table A.1: Technical specifications of the single-phase Thoma type regulator inside the wiring used for the investigations.

label	
manufacturer:	HTT (Hochspannungstechnik und Transformatorbau)
rated power:	450 kVA
rated frequency:	50 Hz
rated voltage:	0 kV to 10 kV (continuously adjustable)
rated current:	45 A

The equivalent circuit diagram can be taken from figure 4.2. The voltage drop across the test specimen is measured with an ohmic voltage divider with a high voltage resistor of

---

[153] Seen from the observer, the specimen fixture is arranged in front of the secondary circuit breaker.
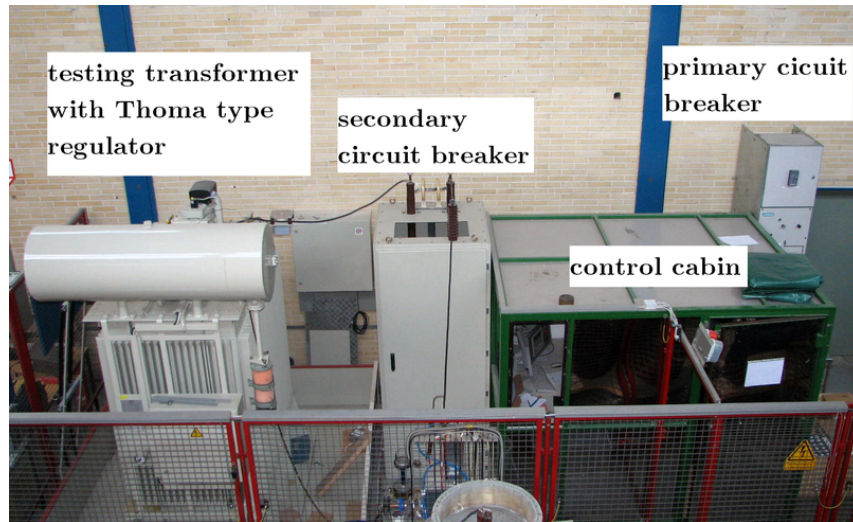
Figure A.1: Overall presentation of the AC energy injection test set-up [Rei08].

$50\,\mathrm{M\Omega}$ and an intermediate voltage resistor of $3.3\,\mathrm{k\Omega}$[154]. Depending on the current peak value of the energy injection, the current flowing through the specimen is measured by two different current transducers. The technical specifications of these current transducers are given in *table A.2* respectively *table A.3*. In order to achieve a galvanic isolation between test set-up and PC data acquisition card, the transformed voltage and the transformed current are transferred by an optical transmission system[155] (the technical specifications of which are depicted in *table A.4*). The measurement data is recorded by a PC data acquisition card with the technical specifications mentioned in *table A.5* and evaluated and documented by a LabVIEW program. With this program, beginning and end of the energy injection are detected by evaluation of the current and voltage waveform and the energy injection for this time span is calculated.

The inductive voltage drop across the test specimen is not compensated inside this test set-up due to the current rise time of the AC energy injections being comparatively low. One example of an unfiltered voltage and current waveform during the stressing of a metal test specimen[156] with the geometric dimensions of MOVs that are typically used for the high-voltage level is given in *figure A.2*. It can be observed that the voltage signal lies within the same range for the entire test duration and particularly during the current flow. This is why a compensation is not required.

---

[154] The transmission ratio (including FOC transmission etc.) was set to 15779:1 with the help of a reference measurement where the measurement system was calibrated to the voltage range used.

[155] The zero point and the amplification of the transmission system are adjustable.

[156] This refers to the test fixture introduced for the tests in chapter 5.2.3 at a temperature inside the test chamber of about $210\,^{\circ}\mathrm{C}$ because this test chamber is the worst case concerning ohmic and inductive voltage drops.

Table A.2: Technical specifications of the Hall effect current transducer used for AC energy injections with current peak values of $< 15\,\mathrm{A}$ in the AC energy injection test set-up.

label	
manufacturer:	LEM (Liaisons Electroniques-Mécaniques)
type:	PCM 10-P
current measurement range:	$0\,\mathrm{A}$ to $\pm 20\,\mathrm{A}$
accuracy:	$\pm 1\,\%$
linearity ($0\,\mathrm{A}$ to $\pm 20\,\mathrm{A}$):	$\pm 0.2\,\%$
max. temperature drift:	$\pm 0.03\,\mathrm{mA/K}$
frequency range ($-3\,\mathrm{dB}$):	$0\,\mathrm{kHz}$ to $1\,\mathrm{kHz}$
ambient temperature:	$-25\,\mathrm{°C}$ to $55\,\mathrm{°C}$

Table A.3: Technical specifications of the Hall effect current transducer used for AC energy injections with current peak values of $\geq 15\,\mathrm{A}$ in the AC energy injection test set-up.

label	
manufacturer:	LEM (Liaisons Electroniques-Mécaniques)
typ:	LF 1005-S
current measurement range:	$0\,\mathrm{A}$ to $\pm 1500\,\mathrm{A}$
accuracy:	$\pm 0.4\,\%$
linearity:	$< 0.1\,\%$
max. temperature drift:	$\pm 0.5\,\mathrm{mA}$
frequency range ($-1\,\mathrm{dB}$):	$0\,\mathrm{kHz}$ to $150\,\mathrm{kHz}$
ambient temperature:	$-10\,\mathrm{°C}$ to $85\,\mathrm{°C}$

Table A.4: Technical specifications of the optical transmission system used in the AC energy injection test set-up.

label	
manufacturer:	Nicolet Instrument Technologies
type:	ISOBE 3000
frequency range ($-3\,\mathrm{dB}$):	$0\,\mathrm{MHz}$ to $15\,\mathrm{MHz}$
input impedance:	$1\,\mathrm{M\Omega}$, $30\,\mathrm{pF}$
DC drift:	$< 2.5\,\mathrm{mV/K}$
accuracy of the DC amplification:	$\pm 3\,\%$ at $23\,\mathrm{°C}$ ($\pm 5\,\mathrm{°C}$)

Table A.5: Technical specifications of the PC data acquisition card used in the AC energy injection test set-up, in the reference voltage test set-up and in the aging test set-up.

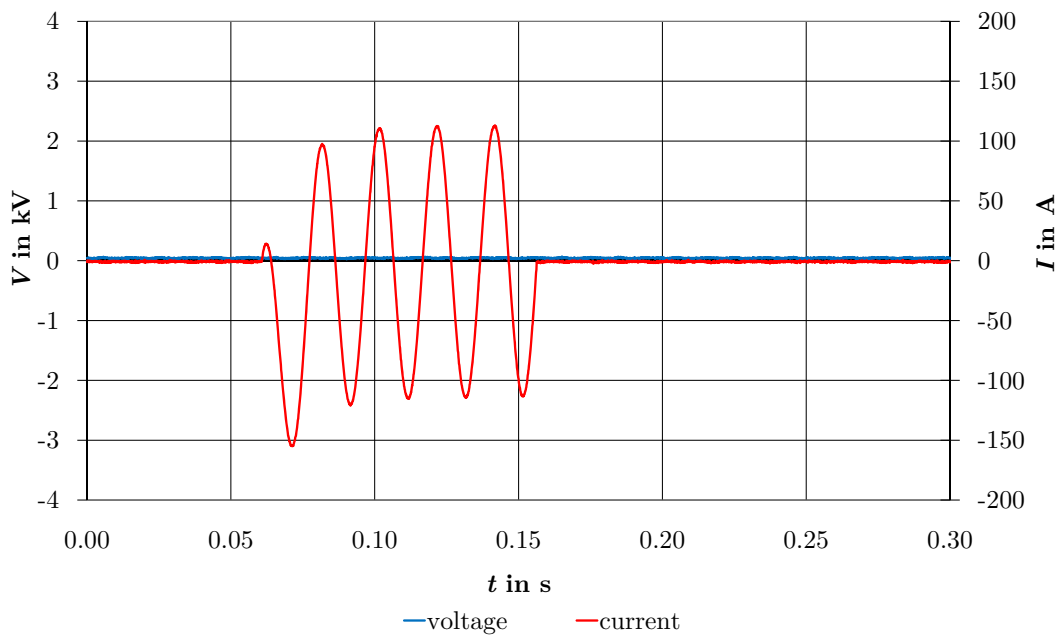| label	
manufacturer:	NI (National Instruments)
type:	PCI NI 6221
ADC resolution:	16 bit
max. sampling rate:	250 kS/s
max. input voltage:	$\pm 10\,\mathrm{V}$
max. output voltage:	$\pm 10\,\mathrm{V}$
max. output current:	$\pm 5\,\mathrm{mA}$
input impedance:	$> 10\,\mathrm{G\Omega},\ 100\,\mathrm{pF}$
output impedance:	$\pm 0.2\,\Omega$
absolute accuracy (at V_{max}):	$3.1\,\mathrm{mV}$

Figure A.2: Oscillogram of voltage and current applied to a metal test specimen in the AC energy injection test set-up.

A.2 Long-Duration Current Impulse Generator

In *figure A.3*, the long-duration current impulse generator is depicted at a very early stage of the setting up with ten stages. During the investigations of [Rei08], the generator was designed and set up with 20 stages and was extended to 34 stages for the investigations introduced in this thesis. The charging unit used here is also put to use for the double-exponential discharge current generator and is revised during the course of the investigations. The equivalent circuit diagram of the generator can be seen from figure 4.4. Each stage consists of a capacitor with a capacity of $10\,\mu F$ with a nominal voltage of at least $40\,kV$ and an inductance the technical specifications of which can be found in *table A.6*. By combining the individual coil sections inside the different stages of the long-duration current impulse generator, long-duration current impulses of different virtual durations can be generated.

Figure A.3: The long-duration current impulse generator during the setting up with ten stages.

Table A.6: Technical specifications of the individual sections of one inductance of a stage inside the long-duration current impulse generator in figure A.3 (the sections of the inductance are numbered bottom-up).

Coil section	L	R
1 and 2	$300\,\mu H$	$125\,m\Omega$
3	$1430\,\mu H$	$349\,m\Omega$
4	$250\,\mu H$	$107\,m\Omega$
5	$500\,\mu H$	$186\,m\Omega$

Depending on the expected current peak value, the current flowing through the specimen is measured with one of the current transducers depicted in *table A.7*. The universal voltage divider with the technical specifications given in *table A.8* is used to determine the voltage drop across the specimen. The measurement data is gathered by an oscilloscope the technical specifications of which can be seen from *table A.9*. The data recorded by the oscilloscope is read by a PC and evaluated and documented on by a LabVIEW program on this PC. In order to protect the equipment, especially concerning the quick double-exponential discharge currents of the $90/200\,\mu s$ type that are also produced by this generator, a galvanic isolation is applied between oscilloscope and PC.

The long-duration current impulse generator is also used to generate the double impulses (see chapter 5.3) that consist of two long-duration current impulses. To this end, the long-duration current impulse generator is split into two generators that can be triggered independently. The equivalent circuit diagram of this set-up[157] can be seen from *figure A.4*. In order to prevent a self-triggering of the second half of the generator due to voltage fluctuation caused by the first energy injection (an example of such an energy injection is given in figure 5.22), only the first energy injection is triggered by a spark gap; the second, on the other hand, by means of a semiconductor switch[158].

In this test set-up, too, the inductive voltage drop across the specimen is not compensated. In *figure A.5*, the unfiltered voltage and current characteristic during the stressing of the metal specimen[159] with the geometric dimensions of an MOV of "size 1" (as is used for the high-voltage level) is depicted. This long-duration current impulse with a virtual duration of about $1.9\,ms$ was produced with the long-duration current impulse generator that had been extended to 34 stages. It can be seen that the voltage is not influenced by the current characteristic. This is the reason why a compensation of the voltage is not required[160].

---

[157] At the time at which the investigations regarding the double impulse energy handling capability were carried out, the generator consisted of two times ten stages. At the time of completion of this thesis, it consists of two times 17 stages.

[158] Such a semiconductor switch is not commercially available and was designed and built by Thomas Wietoska, Dr.-Ing. (employee at the High Voltage Laboratories of the TU Darmstadt) for this application.

[159] The test fixture used here is the one introduced for the tests in chapter 5.2.3 with a temperature of about 130 °C inside the test chamber as this is the worst case regarding the ohmic and inductive voltage drop.

[160] The zero shift of current and voltage at the end of the energy injection are of no relevance for the calculation of the energy injection.

Table A.7: Technical specifications of the three Rogowski coils used inside the long-duration current impulse generator depending on the expected current level.

label			
manufacturer:	Power Electronic Measurments		
upper cutoff frequency:	16 MHz		
accuracy:	$\pm 1\%$		
type:	CWT30	CWT150	CWT600
max. current peak value:	6 kA	30 kA	120 kA
sensitivity:	1 mV/A	0.2 mV/A	0.05 mV/A
lower cutoff frequency:	0.9 Hz	0.3 Hz	0.1 Hz

Table A.8: Technical specifications of the voltage divider used inside the long-duration current impulse generator for the investigations.

label	
manufacturer:	HILO-TEST
type:	HVT 40 RCR
max. AC voltage:	30 kV
max. impulse voltage:	100 kV
transmission ratio:	2500:1
accuracy:	$\pm 1\%$
HV resistor	150 MΩ
HV capacitor:	50 pF
bandwidth:	20 MHz

Table A.9: Technical specifications of the oscilloscope used inside the long-duration current impulse generator and inside the double-exponential discharge current generator.

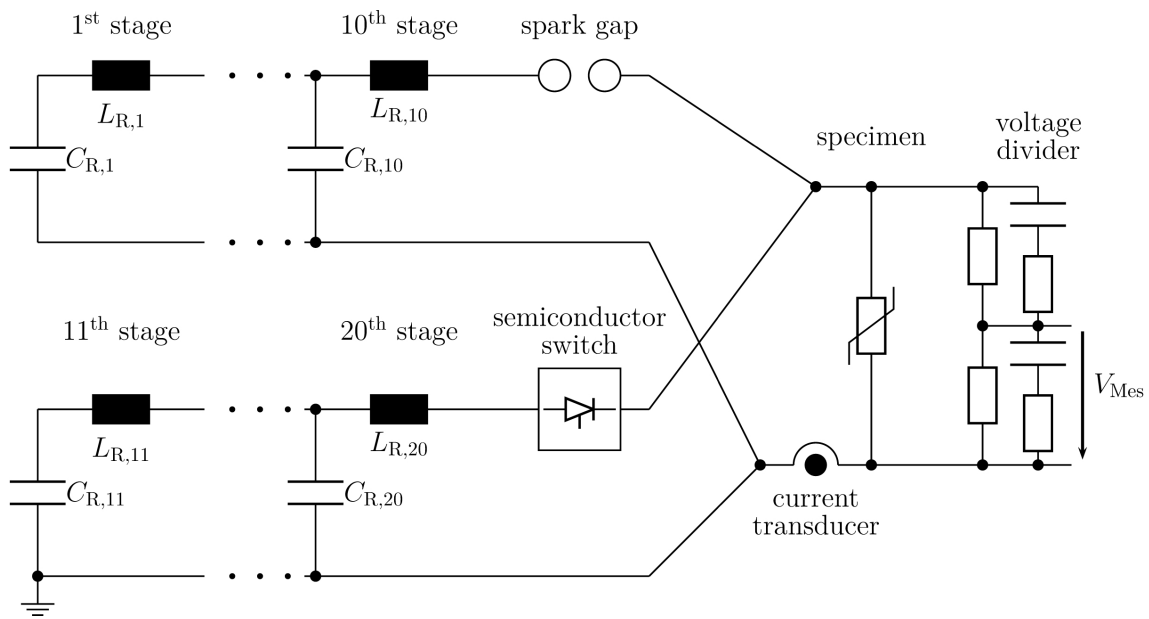| label	
manufacturer:	Tektronix
type:	TDS3034
bandwidth:	300 MHz
max. sampling rate per channel:	2.5 GS/s
max. record length:	10000 points
vertical resolution:	9 bit
vertical accuracy:	$\pm 2\%$
max. input voltage:	150 V$_{\mathrm{RMS}}$
input impedance:	1 MΩ, 13 pF or 50 Ω

Figure A.4: Equivalent circuit diagram of the long-duration current impulse generator for the generating of double impulses. V_{Mes} is the voltage that is transmitted to the oscilloscope.
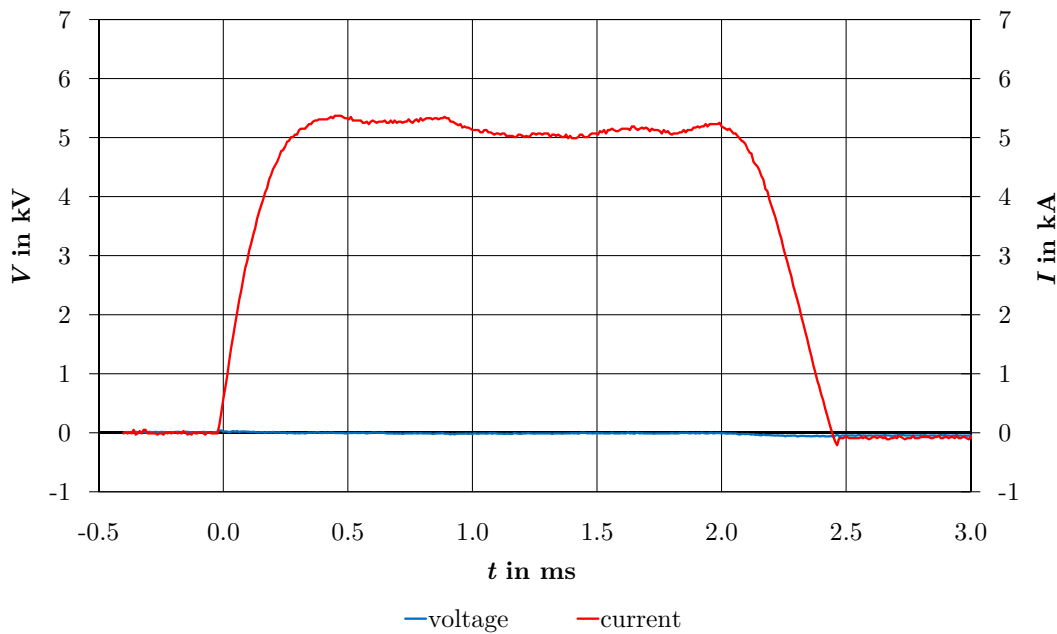

Figure A.5: Oscillogram of voltage and current along a metal test specimen stressed by the long-duration current impulse generator.

A.3 Double-Exponential Discharge Current Generator

The double-exponential discharge current generator, the equivalent circuit diagram of which can be seen in figure 4.7, was installed by the HIGHVOLT company including control and charging unit (in the original condition). The impulse generator (as shown in *figure A.6*) consists of up to eight parallel sections, with a 2-µF-capacitor as well as an inductance-resistor combination[161] each (the parameters of which can be seen from *table A.10*).
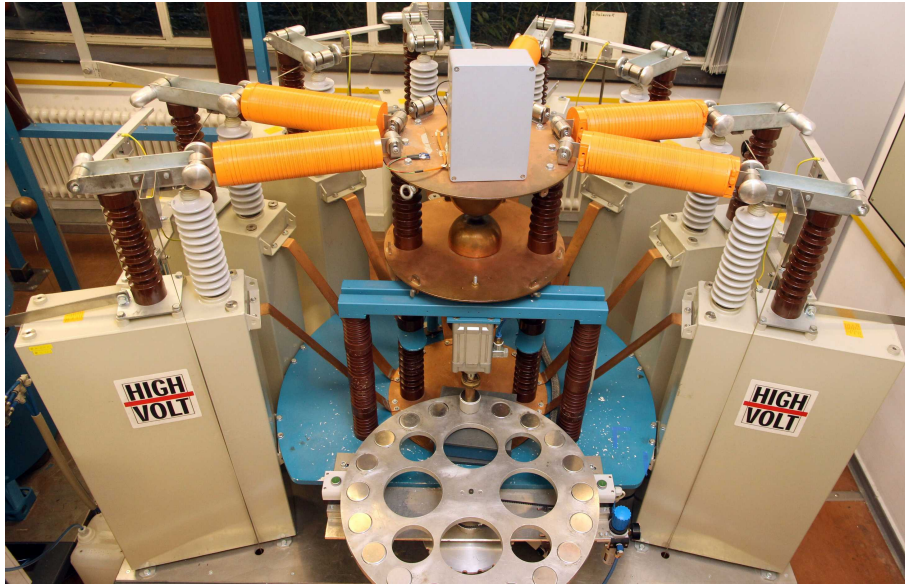

Figure A.6: The double-exponential discharge current generator when configured in order to test the residual voltage with a lightning current impulse of the 8/20 µs type.

Table A.10: Parameters of the inductance-resistor combination used inside the double-exponential discharge current generator for the different types of impulses.

label	waveform	amount	L	R
steep current impulse	1/<20 µs	5	0.3 µH	10 Ω
high-current impulse	4/10 µs	8	1.44 µH	≈ 0 Ω
lightning current impulse	8/20 µs	5	32 µH	1.3 Ω
switching current impulse	30/60 µs	2	380 µH	2.1 Ω

Depending on the expected current peak value, the current flowing through the specimen is measured by means of the current transducer shown in *table A.11* or the one shown in

---

[161] The inductance-resistor combinations from [Rei08] were not used for the high-current energy injections. Instead, new ones were designed and manufactured that allow for a quicker modification of the generator.

table A.12; the voltage is measured with the help of the voltage divider [162] from *table A.13*. The measurement data is recorded by the oscilloscope already mentioned (see table A.9), transmitted to a PC via radio connection (in order to protect the equipment) and evaluated and documented by a LabVIEW program. The voltage peak value is located by determining the maximum that is averaged over 4 % of the record length, while the current peak value is only averaged over 2 % (due to the higher gradient).

In this test set-up, the inductive voltage drop across the MOV must be compensated. The procedure of compensation with an inductance inside the measurement path through which the magnetic field of the main current path flows is documented in detail in [Rei08]. As shown in the equivalent circuit diagram in *figure A.7*, the voltage that is induced by the magnetic field of the main current path, V_{IND}, is mostly compensated by the voltage inside the compensation coil (with negative polarity,) V_{COMP}, that is induced by the magnetic field of the main current path, too. The compensation of the inductive voltage drop thus gained is independent of the amperage of the main current path. *Figure A.8* shows the unfiltered oscillogram of a voltage and current waveform when stressing a metal test specimen[163] with a high-current impulse of the 4/10 μs type and a current peak value of about 100 kA in the compensated test set-up in comparison to the voltage waveform of an equivalently stressed MOV. It can be observed that, concerning the compensated voltage signal, there is only a very small inductive share left.

According to [IEC60099-4], no further compensation of the voltage is necessary if the inductive share of the voltage when stressing a metal test specimen is < 2 % of the voltage peak value of the object that is to be tested. This limiting value has also been applied here as the measuring error thus generated is smaller than the measuring uncertainty of the overall system. Regarding the stressing of the specimens with high-current impulses of the 4/10 μs type and at current peak values in the range of 100 kA used in chapter 5, a further compensation is unnecessary because the voltage peak value is clearly above 15 kV.

---

[162] In order to monitor the deviations of the measurement system, a measurement of the residual voltage is carried out for a "calibration MOV" before each measurement series. Additionally, this measurement is carried out each year for another MOV.

[163] With the same geometric dimension as that of an MOV used for the high-voltage level.

Table A.11: Technical specifications of the current transducer for measurements with current peak values $< 120\,\text{kA}$ used inside the double-exponential discharge current generator.

label	
manufacturer:	Stangenes Industries
type:	3.5-0.005
sensitivity:	$0.005\,\text{V/A}$
accuracy:	$\pm 0.02\,\%$

Table A.12: Technical specifications of the Rogowski coil for measurements with current peak values $\geq 120\,\text{kA}$ used inside the double-exponential discharge current generator.

label	
manufacturer:	PEM (Power Electronic Measurments)
type:	CWT1500
max. current peak value:	$300\,\text{kA}$
sensitivity:	$0.02\,\text{mV/A}$
lower cutoff frequency:	$0.03\,\text{Hz}$
upper cutoff frequency:	$16\,\text{MHz}$
accuracy:	$\pm 1\,\%$

Table A.13: Technical specifications of the voltage divider used inside the double-exponential discharge current generator.

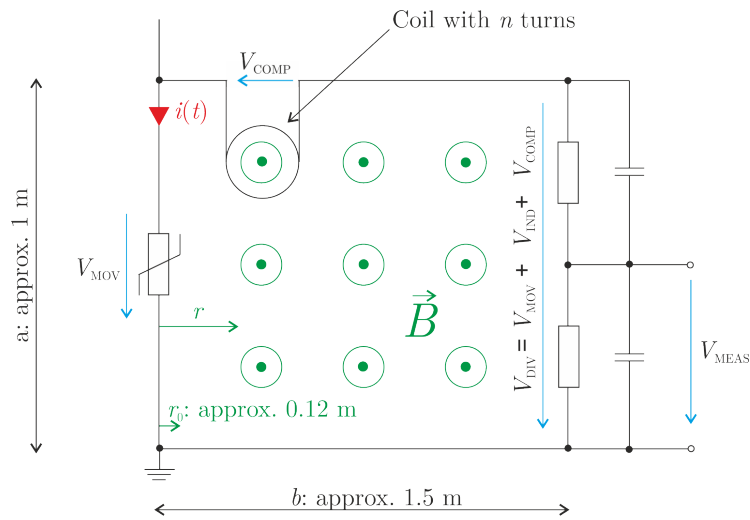| label	
manufacturer:	HIGHVOLT
type:	MCR 0.5/200-100/4C
nominal lightning impulse voltage:	$200\,\text{kV}$
scale factor:	226
measuring uncertainty voltage:	$3\,\%$
measuring uncertainty time:	$10\,\%$

Figure A.7: Equivalent circuit diagram for the compensation inside the double-exponential discharge current generator (according to [Rei08]). The voltage V_{IND} induced by the magnetic field of the main current path is compensated for the voltage of the compensation coil (with negative polarity) V_{COMP}.
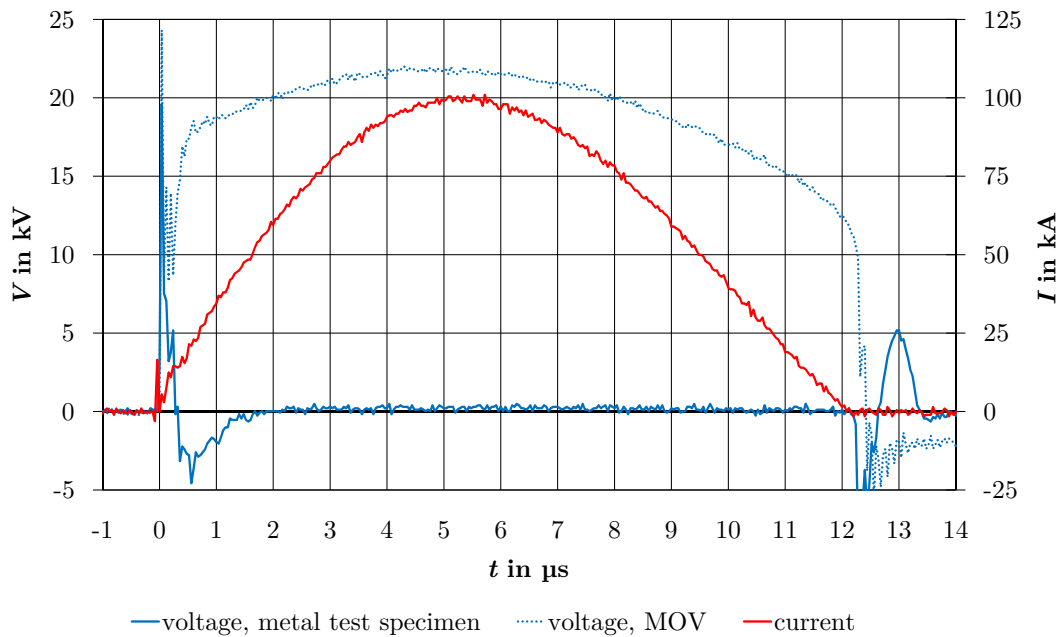

Figure A.8: Oscillogram of voltage and current of a high-current impulse of the $4/10\,\mu\mathrm{s}$ type through a metal test specimen in comparison to a voltage waveform of an equivalently stressed MOV. The high-current impulses are produced by the double-exponential discharge current generator.

A.4 Reference Voltage Test Set-Up

The reference voltage test set-up as shown in *figure A.9* was developed largely[164] during the investigations of [Rei08]. As can be taken from the equivalent circuit diagram in figure 4.11, the voltage waveform is generated by a PC data acquisition card (the technical specifications of which are given in table A.5). This voltage waveform is amplified by a linear amplifier with a maximum output power of about 300 VA and stepped up by a high-voltage transformer. The current flowing through the specimen is measured with the help of a shunt with 495 Ω and the voltage drop across the specimen by means of an ohmic voltage divider[165] with a high voltage resistor with 50 MΩ and an intermediate voltage resistor with 25 kΩ. The measurement data is gathered by a PC data acquisition card (the technical specifications of which are given in table A.5) and evaluated and documented by a LabVIEW program. As can be seen from the previous sections, a compensation of the inductive voltage drop is not necessary and thus is not carried out.

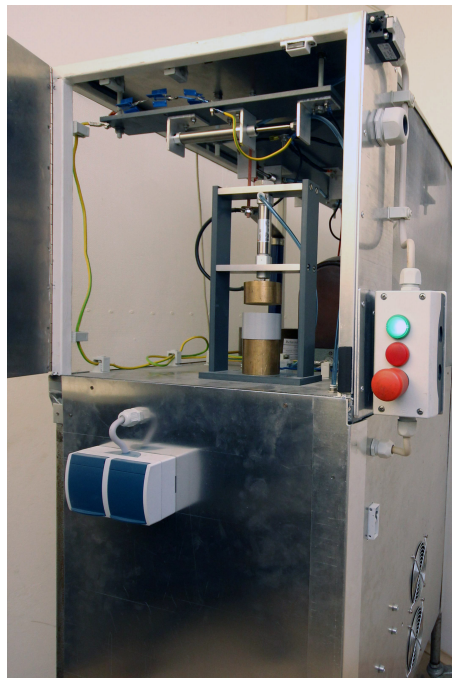**Figure A.9:** The reference voltage test set-up used for the testing of the characteristic voltage.

---

[164] Contrary to the investigations in [Rei08], a pneumatic test fixture is used here for the clamping of the test specimen.

[165] The transmission ratio of the ohmic voltage divider has been set to 1990:1 with the help of a comparative measurement with a measuring system that was calibrated within this voltage range.

A.5 Aging Test Set-Up

The aging test set-up has been developed and installed in the course of the investigations introduced here. The equivalent circuit diagram resembles that of the reference voltage test set-up, except that, in the aging test set-up, up to 15 specimens can be tested simultaneously. A total view of the set-up is given in *figure A.10.* For the tests, three temperature chambers of the "FED 115" type are provided by the "BINDER" company and controlled by a LabVIEW program. For the temperature measurement, an optical measurement system is used. The technical specifications of the evaluation unit of this system are given in *tableA.14* and those of the temperature sensors used in table A.15. The output signal generated by the evaluation unit is recorded by a PC data acquisition card, the technical specifications of which can be found in table A.5.

Figure A.10: Total view of the aging test set-up.

For the voltage stress, the voltage waveform is generated by the PC data acquisition card mentioned above, amplified by a power amplifier (by the company "the t.amp", type "D3400" with a maximum output power of 2 kW) and stepped up by a high-voltage transformer. The current flowing through each individual specimen is measured with the help of one shunt

Table A.14: Technical specifications of the temperature measurement system used inside the aging test set-up.

label	
manufacturer:	FISO Technologies
type:	TMI 4
accuracy:	0.025 % of the maximum value
resolution:	0.01 % of the maximum value
sampling rate:	20 Hz
switching time between two channels:	150 ms
output voltage:	±5 V

Table A.15: Technical specifications of the temperature sensor used inside the aging test set-up.

label	
manufacturer:	FISO Technologies
type:	FOT-L-SD
measurement range:	$-40\,°C$ to $300\,°C$
accuracy:	$0.1\,°C$
resolution:	$0.1\,°C$
response time:	$\leq 1.5\,s$

each with about $1\,k\Omega$. These shunts were installed outside of the temperature chambers. The voltage drop across all specimens is measured by means of a central voltage divider[166] with a high voltage resistor with $150\,M\Omega$ and an intermediate voltage resistor with $9.93\,k\Omega$. The measurement data is gathered by the PC data acquisition card mentioned above and evaluated and documented by a LabVIEW program. High voltage generation, safety circuit, PC and temperature measurement system are supplied via an uninterrupted power supply (UPS), which ensures further operation during interruptions of the supply voltage of $< 1\,h$.

As described in the previous sections, a compensation of the inductive voltage drop across the specimens is unnecessary and thus is not carried out.

---

[166] The transmission ratio of the voltage divider has been set to 15000:1 with the help of a comparative measurement with a measuring system that was calibrated within this voltage range.

B Statistical Basis

In this chapter[167], an overview of the mathematical principles that are necessary for the evaluation of the investigations described in chapter 5 is given. It is assumed that the reader is familiar with the basic concepts of statistics. For this reason, the distribution functions used for similar issues are only briefly described. After this, this chapter goes into detail about the estimation procedures necessary for the calculation of the mean failure energies carried out later on. In the end of this chapter, a description of the determination of the confidence interval with the help of the classical estimation method as well as with the maximum likelihood method is given.

B.1 Density and Distribution Functions

(see [Hau84] and [Har95])

With the help of density functions, continuous random processes can be described. Density functions can be adjusted to specific problems by choosing density-specific parameters (for example in the case of the normal distribution μ and σ). The different progressions can be reproduced with different density functions.

B.1.1 Normal Distribution

The most commonly used distribution is, according to [Har95], the normal distribution. As a function of the expected value μ and the standard deviation σ, the density function is:

$$f_{\mathrm{N}}(t) = \frac{1}{\sigma \cdot \sqrt{2\pi}} \cdot \mathrm{e}^{-\frac{1}{2}\left(\frac{t-\mu}{\sigma}\right)^2} \tag{B.1}$$

---

[167] This chapter has been taken to a great extent from the diploma thesis of the author.

The distribution function is:

$$F_{\mathrm{N}}(x) = \frac{1}{\sigma\sqrt{2\pi}} \cdot \int_{-\infty}^{x} \mathrm{e}^{-\frac{1}{2}\left(\frac{t-\mu}{\sigma}\right)^2} \mathrm{d}t \tag{B.2}$$

The normal distribution is symmetrical to its expected value and is often used in mathematics as it offers the possibility to assume a normal distribution of the sum of a finite number of independent and normally distributed random variables by applying the central limit theorem.

Moreover, the normal distribution is very highly developed in mathematics and there is a high number of robust estimators[168].

B.1.2 Log-Normal Distribution

If the logarithm of a random variable is normally distributed, this random variable is labelled "log-normally distributed". A log-normal distribution is a continuous right-skewed distribution. The density of the distribution is:

$$f_{\mathrm{l}}(t) = \begin{cases} \frac{1}{\sqrt{2\pi}\sigma t} \cdot \mathrm{e}^{-\frac{(\ln(t)-\mu)^2}{2\sigma^2}} & t > 0 \\ 0 & t \leq 0 \end{cases} \tag{B.3}$$

The distribution function is:

$$F_{\mathrm{l}}(x) = \frac{1}{\sqrt{2\pi}\sigma} \int_{0}^{x} \frac{1}{t} \mathrm{e}^{-\frac{(\ln(t)-\mu)^2}{2\sigma^2}} \mathrm{d}t \tag{B.4}$$

B.1.3 Double Exponential Distribution

The double exponential distribution is a symmetric continuous function and has the shape of two exponential distributions put together. It is often called Laplace distribution (named after Pierre-Simon Leplace). Its density function is defined by:

$$f_{\mathrm{d}}(t) = \frac{1}{2\sigma} \mathrm{e}^{-\frac{|t-\mu|}{\sigma}} \tag{B.5}$$

with $t, \mu \in \mathbb{R}$, $\sigma \in \mathbb{R}^+$

---

[168] Robust estimators are estimators that are insensitive to deviations from the distribution.

The distribution function is:

$$F_{\mathrm{d}}(x) = \begin{cases} \frac{1}{2}\mathrm{e}^{-\frac{\mu-x}{\sigma}} & x \leq \mu \\ 1 - \frac{1}{2}\mathrm{e}^{-\frac{x-\mu}{\sigma}} & x > \mu \end{cases} \tag{B.6}$$

B.1.4 Weibull distribution

The Weibull distribution is widely used for the description of durability and quality distributions. The two-parameter density function is defined by:

$$f_{\mathrm{w}2}(t) = \alpha\beta \cdot t^{\beta-1} \cdot \mathrm{e}^{-\alpha t^{\beta}} \tag{B.7}$$

with $\alpha > 0$, $\beta > 0$ and $t > 0$.

Correspondingly, the two-parameter distribution function is constituted by:

$$F_{\mathrm{w}2}(t) = 1 - \mathrm{e}^{-\alpha t^{\beta}} \tag{B.8}$$

with $\alpha > 0$, $\beta > 0$ and $t > 0$.

It can be seen that, if α and β are known, the distribution function of the two-parameter Weibull distribution can be calculated easier than for example for the normal distribution.

A special case of the Weibull distribution is the exponential distribution. It results from *equation B.7* and *equation B.8* for $\beta = 1$.

Along with the two-parameter Weibull distribution, the three-parameter Weibull distribution is used. The distinction between the two is that the distribution function of the latter has a defined starting point t_0 that describes a value below which the criterion (for example a flashover) cannot occur.

The three-parameter density function is:

$$f_{\mathrm{w}3}(t) = \begin{cases} \alpha\beta \cdot (t-t_0)^{\beta-1} \cdot \mathrm{e}^{-\alpha(t-t_0)^{\beta}} & t > t_0 \\ 0 & t \leq t_0 \end{cases} \tag{B.9}$$

with $\alpha > 0$, $\beta > 0$ and $t > 0$.

The distribution function is defined by:

$$F_{\mathrm{w3}}(t) = \begin{cases} 1 - \mathrm{e}^{-\alpha(t-t_0)^\beta} & t > t_0 \\ 0 & t \leq t_0 \end{cases} \tag{B.10}$$

with $\alpha > 0$, $\beta > 0$ and $t > 0$.

B.2 Maximum Likelihood Estimator

(see [Fin02] and [Car90])

The maximum likelihood estimator is used to estimate the unknown parameters of a distribution (for the normal distribution μ and σ) based on a sample for a known (or assumed) distribution. According to [Car90], the relevance of this method increases with the spreading of personal computers as this method is, to some extent, very CPU-intensive. In this chapter, basic ideas and equations are introduced.

The basic idea of the maximum likelihood method is to generate a function from the measurement data gathered based on which the likeliest pair of values of expected value and standard deviation of the distribution can be determined. Thus, θ_1 and θ_2 of the maximum of the maximum likelihood function are most likely the expected value and the standard deviation of the basic distribution of the investigated sample.

The described maximum likelihood function for a density function $f_\theta(x)$ (for example one from chapter B.1) for a measurement series $x_1, ..., x_n$ is:

$$L(\theta_1, \theta_2, x_1, ..., x_n) = f_\theta(x_1) \cdot ... \cdot f_\theta(x_n) \tag{B.11}$$

The maximum of this function is achieved by zeroing of the first derivative of the maximum likelihood function with respect to one of the parameters wanted (the second derivative must be positive for the same position).

According to [Wil62], it is not only possible to calculate the likeliest pair of values $\hat{\theta}_1$ and $\hat{\theta}_2$ (the pair belonging to the distribution function due to the measurement values) with the help of the maximum likelihood function, but also to indicate confidence regions. In *figure B.1*, a maximum likelihood function scaled to its maximum is plotted above the expected value as well as the standard deviation. It holds true for all $L/L_{\max} \geq K(r; C)$ that the related distributions are inside the confidence region C. In descriptive terms it

means that if the graph is intersected at the height $K(r; C)$, with a certainty C the pair of values θ_1 and θ_2 of the wanted distribution lies inside the intersected surface.
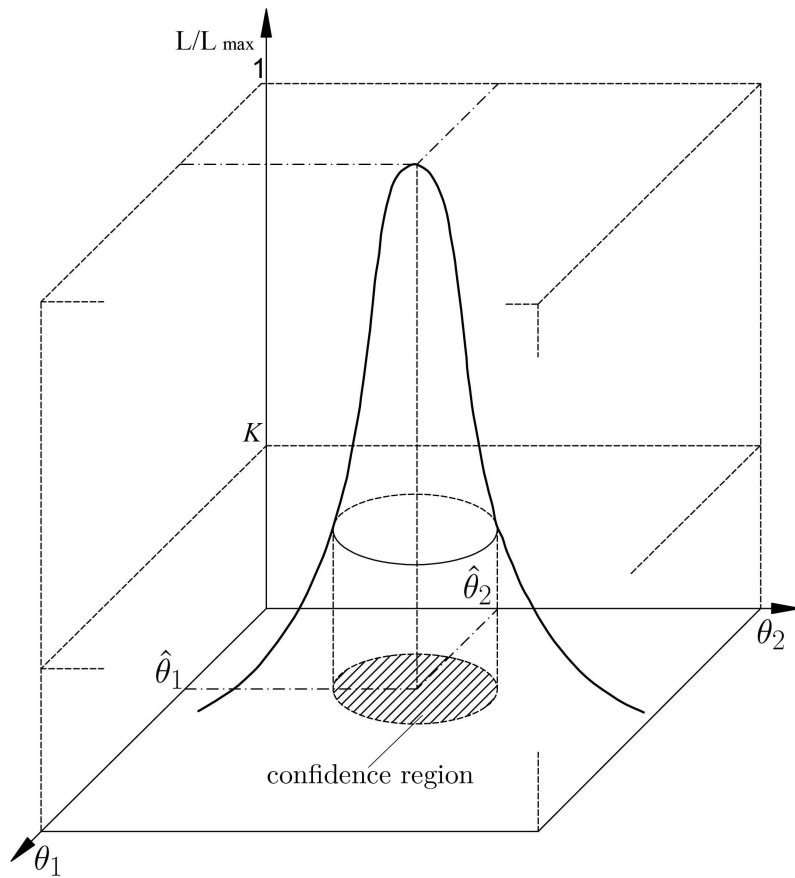

Figure B.1: Example of a maximum likelihood function scaled to $L_{\max}$above θ_1 and θ_2 (see [Car90])

K can be calculated with the help of the χ^2 distribution. The most important values for the degree of freedom r (number of unknown parameters) and the confidence region C can be seen from *table B.1*.

If, for example, one wants to find the combinations of θ_1 and θ_2 that belong to the distribution searched for with a certainty of 95 %, the maximum likelihood function is intersected at the height of $K(2; 0.95) = 0.05$. The parameters wanted are all inside the θ_1 and θ_2 that lie inside the intersected surface.

By means of the collected points θ_1 and θ_2, confidence limits can be drawn onto a normal probability plot. It is shown in *figure B.2* how the confidence region of a distribution function can be drawn into a graph with the extremes taken from *figure B.3*. The distribution function M is the point estimation with $\hat{\theta}_1$ and $\hat{\theta}_2$. The dashed lines indicate the lower as

Table B.1: Constant K for point estimations [Car90]

degree of freedom	K values for confidence regions		
r	$C = 0.90$	$C = 0.95$	$C = 0.99$
1	0.258	0.147	0.0363
2	0.100	0.050	0.0100
3	0.044	0.020	0.0034

well as the upper limit of the confidence region of the distribution. The distributions *A–D* are the distribution functions that result from the extremes *A–D* (figure B.3).

For the statistical evaluations of the investigations introduced in chapter 5.1, two different approaches must be distinguished due to the execution of the measurements. One is the "Progressive Stress Method" (PSM), the other one is the "Multiple Level Method" (MLM). With the help of the PSM, investigations are evaluated where each specimen is tested up to the occurrence of the event (mechanical failure of the specimen). The MLM is used for the evaluation of those investigations where groups of specimens are exposed to the same stress and where it is observed how high the failure rate of the groups is.

For the investigations carried out in chapter 5.1, the difference between the different distribution functions is very low. This is, above all, due to the low number of investigated units. In his investigations of the energy handling capability of MOVs, [Rin97] has also noticed that the difference between the different distributions (he used the normal, the Gumbel and the Weibull distribution) is only very low and thus, for reasons of simplification, settled for the normal distribution. In this thesis, a comparable amount of test specimens is used and the normal distribution is chosen to evaluate the single impulse energy handling capability, too. For this reason, the maximum likelihood estimator for a normal distribution is introduced in the following.

B.3 Multiple Level Method

Concerning the MLM, the failure probability is to be described by a binomial distribution according to [Car90]. The maximum likelihood function for n groups of specimens where one class j was exposed to a stress E_j and contained m_j specimens, k_j of which failed and thus $w_j = m_j - k_j$ withstood the stress E_j, is:

$$L_{\mathrm{MLM}}(\theta_1, \theta_2) = \prod_{j=1}^{n} \binom{m_j}{k_j} (F_{\mathrm{N}}(E_j))^{k_j} \cdot (1 - F_{\mathrm{N}}(E_j))^{w_j} \tag{B.12}$$
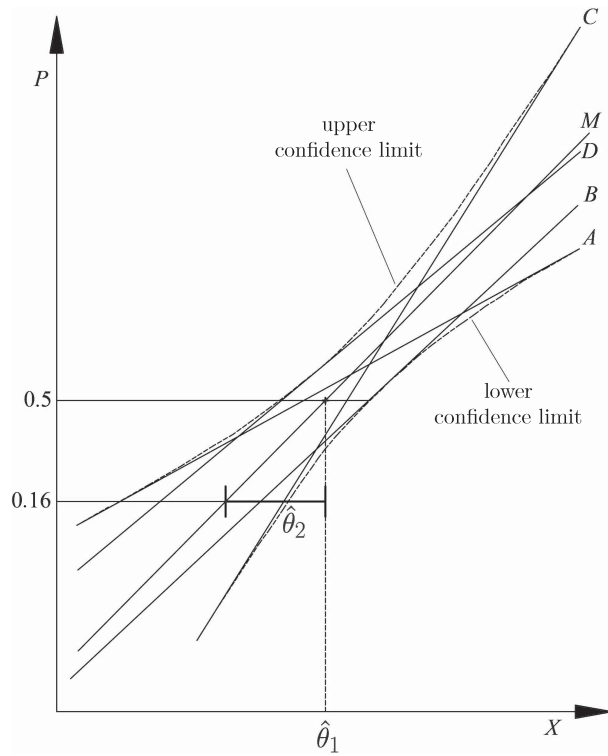
Figure B.2: Confidence region of a distribution function. The distributions *A–D* describe the distributions towards the extremes in figure B.3. The distribution function *M* is the likeliest distribution with the expected value $\hat{\theta}_1$ and the standard deviation $\hat{\theta}_2$ (see [Car90]).
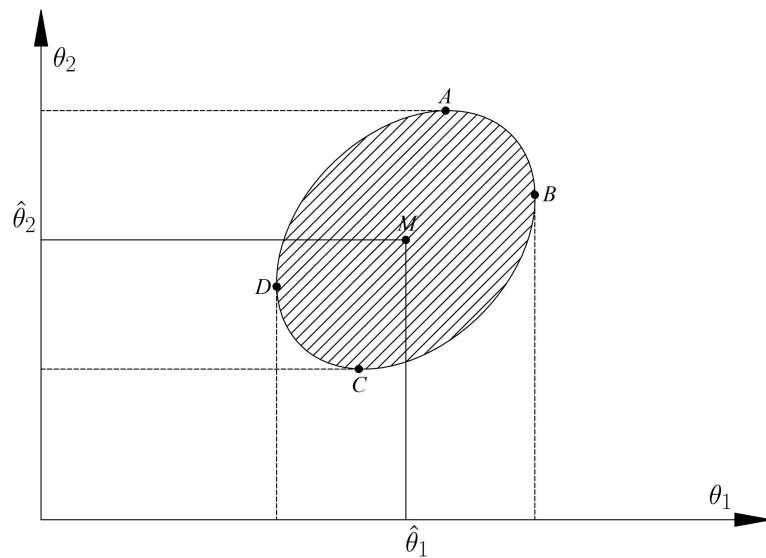

Figure B.3: Example of a confidence region with the extremes *A–D*. $\hat{\theta}_1$ and $\hat{\theta}_2$ describe the likeliest combination of expected value and standard deviation (see [Car90]).

B Statistical Basis

The prefactor of the binomial distribution $\binom{m_j}{k_j}$ can be crossed out here because it drops out due to the later performed normalization to the maximum value of the maximum likelihood function. Thus, the maximum likelihood function becomes:

$$L_{\text{MLM}}(\theta_1, \theta_2) = \prod_{j=1}^{n} (F_{\text{N}}(E_j))^{k_j} \cdot (1 - F_{\text{N}}(E_j))^{w_j} \tag{B.13}$$

The test series in chapter 5.1, in which the complex failure criterion is applied, are evaluated with the help of the MLM 6.1 software developed by the company HIGHVOLT. One example of such an evaluation is given in *figure B.4*. In the chosen measurement series, five groups

Approximation by the normal distribution

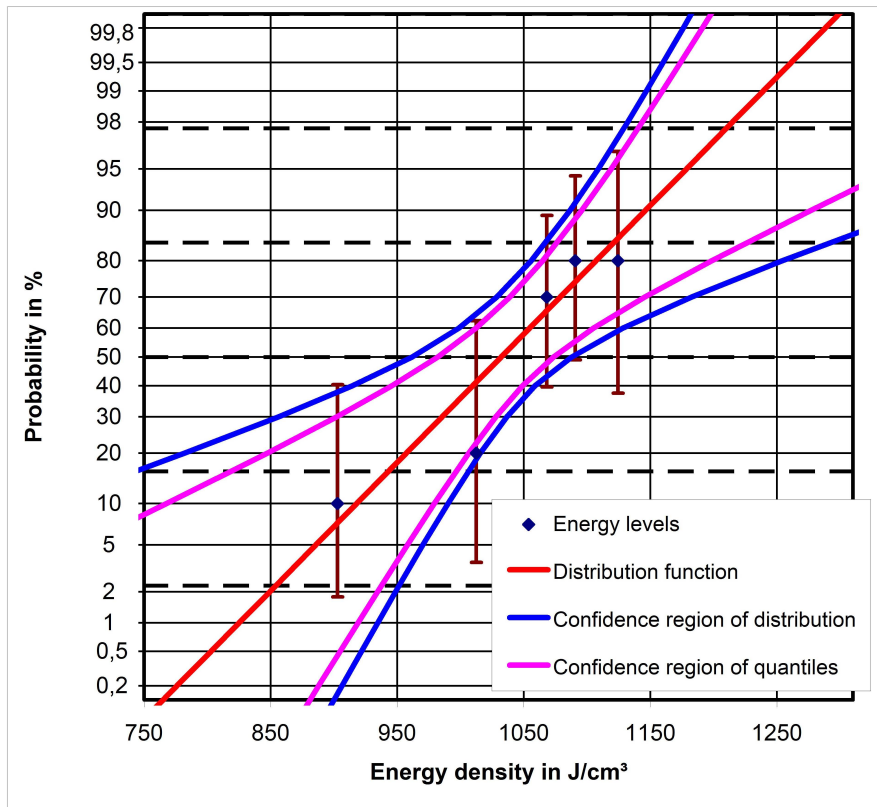| Maximum-Likelihood-Estimation:			
	Point estimate	Confidence estimate (eps=95%)	
		Lower limit	Upper limit
Mean value:	1031,975	981,849	1073,433
Standard deviation:	88,993	54,456	190,072
1% Quantil	824,946	573,436	918,955
Likelihood-ratio:	0,480639		

Figure B.4: Example of an evaluation of a measurement series of chapter 5.1 with the MLM 6.1 software developed by the company HIGHVOLT.

of specimens, each consisting of five respectively ten MOVs, were each stressed with a different energy level. The failure rate inside each group as well as its energy level (referred to the varistor volume) is depicted in the diagram by means of "energy levels". From this data, the likeliest distribution function as well as the confidence intervals, which can also be seen in the diagram, are determined with the help of the point estimation. The point estimation is always used for any further evaluations in chapter 5.

B.4 Progressive Stress Method

The maximum likelihood function for the PSM for n tested specimens each withstanding an energy injection E_i and $m < n$ of which withstanding an energy injection higher than E_i (they do not fail during the tests) is:

$$L_{\mathrm{PSM}}(\theta_1, \theta_2) = \prod_{j=1}^{n-m} f_{\mathrm{N}}(E_j) \cdot \prod_{i=1}^{m}(1 - f_{\mathrm{N}}(E_i)) \tag{B.14}$$

Concerning this thesis, as all measurement series that are evaluated with the PSM fail during the energy injection, the equation can be simplified as follows:

$$L_{\mathrm{PSM}}(\theta_1, \theta_2) = \prod_{i=1}^{n} f_{\mathrm{N}}(E_{\mathrm{i}}) \tag{B.15}$$

The maximum of this function for the expected value reveals the arithmetic mean of $x_1, ..., x_n$:

$$\hat{\theta}_1(x_1, ..., x_n) = \frac{1}{n} \sum_{i=1}^{n} x_n \tag{B.16}$$

The equation for the standard deviation is:

$$\hat{\theta}_2(x_1, ..., x_n) = \frac{1}{n} \sum_{i=1}^{n} (x_i - \hat{\theta}_1)^2 \tag{B.17}$$

Here, the only advantage of choosing the maximum likelihood estimator over a classical estimation is that it is possible to indicate confidence regions with the help of the maximum likelihood function.

The measurement series of chapter 5.1 that were carried out up to the mechanical failure of the specimen during the energy injection are evaluated with the PSM 6.1 software

developed by the company HIGHVOLT. One example of such an evaluation is given in *figure B.5* . Each measurement point describes the failure energy of a stressed specimen

Approximation by the normal distribution

Maximum-Likelihood-Estimation			
	Point estimate:	Confidence estimate (eps=95%)	
		Lower limit	Upper limit
Mean value:	724,295	711,273	737,318
Standard deviation:	43,633	35,965	54,471
1% Quantil:	622,789	593,758	644,047
Kolmogorov test:	Test quantity: 0,0885	Critical value: 0,2024	=> admissible

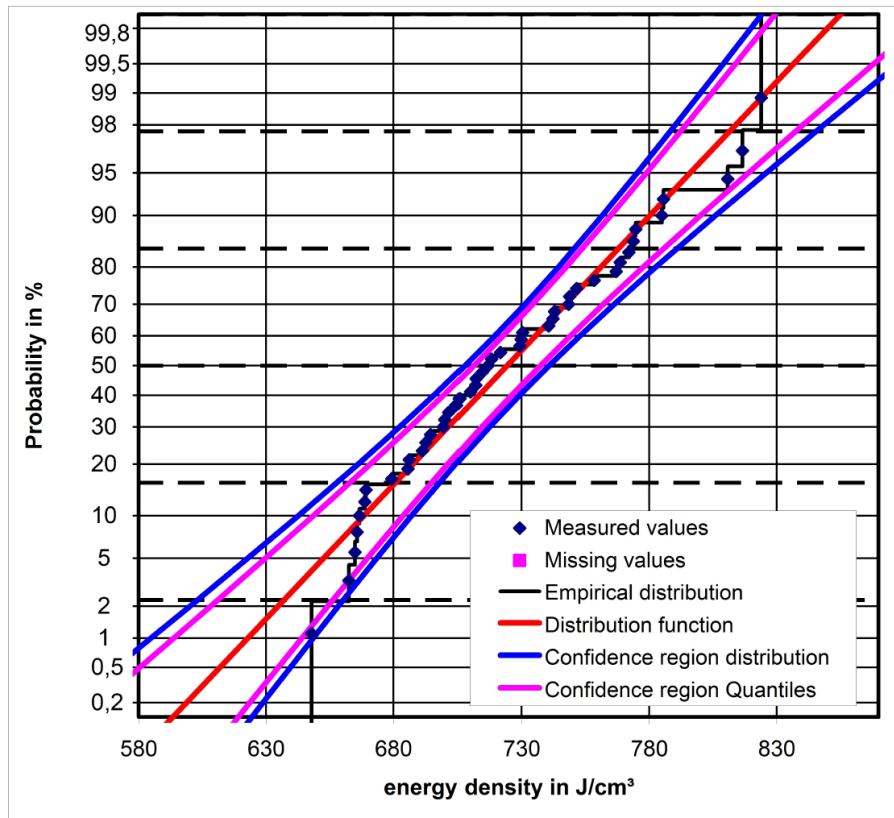**Figure B.5:** Example of an evaluation of a measurement series of chapter 5.1 with the PSM 6.1 software developed by the company HIGHVOLT.

referred to the MOV volume. These measurement points are entered into the normal probability plot sorted by size. The expected value (arithmetic mean of the measurement points) as well as the standard deviation used for further evaluations is determined from the failure energy densities.

Bibliography

[ABB11]   ABB SWITZERLAND LTD. *Overvoltage protection, Metal oxide surge arresters in medium voltage systems – Application guidelines.* 5th edition, 2011

[Aso88]   ASOKAN, T.; NAGABHUSHANA, G. R. and IYENGAR, G. *Improvement of Non-linear Characteristics of Multicomponent ZnO-based Ceramics Containing Nb2O5.* In: IEEE Transactions on Electrical Insulation, volume 23(2): pp. 279–286, 1988. ISSN 0018-9367

[Bar96a]   BARTKOWIAK, M.; COMBER, M. and MAHAN, G. *Energy handling capability of ZnO varistors.* In: Journal of Applied Physics, volume 79(11): pp. 8629–8633, 1996

[Bar96b]   BARTKOWIAK, M.; MAHAN, G.; MODINE, F. and ALIM, M. *Influence of ohmic grain boundaries in ZnO varistors.* In: Journal of Applied Physics, volume 79(1): pp. 273–281, 1996. ISSN 0021-8979

[Bar99]   BARTKOWIAK, M.; COMBER, M. and MAHAN, G. *Failure Modes and Energy Absorption Capability of ZnO Varistors.* In: IEEE Transactions on Power Delivery, volume 14(1): pp. 152–162, 1999. ISSN 0885-8977

[Bar01]   BARTKOWIAK, M.; COMBER, M. and MAHAN, G. D. *Influence of Nonuniformity of ZnO Varistors on Their Energy Absorption Capability.* In: IEEE Transactions on Power Delivery, volume 16(4): pp. 591–598, 2001. ISSN 0885-8977

[Bla86]   BLATTER, G. and GREUTER, F. *Electrical breakdown at semiconductor grain boundaries.* In: Phys. Rev. B, volume 34: pp. 8555–8572, December 1986

[Bog00]   BOGGS, S.; KUANG, J.; ANDOH, I. and NISHIWAKI, S. *Increased Energy Absorption in ZnO Arrester Elements Through Control of Electrode Edge Margin.* In: IEEE Transactions on Power Delivery, volume 15(2): pp. 562–568, 2000. ISSN 0885-8977

Bibliography

[Car82] CARLSON, W. G. and GUPTA, T. K. *Improved varistor nonlinearity via donor impurity doping.* In: Journal of Applied Physics, volume 53(8): pp. 5746–5753, 1982

[Car90] CARRARA, G. and HAUSCHILD, W. *Statistical evaluation of dielectric test results.* Cigré, Electra, 1990

[Cig10] CIGRÉ WORKING GROUP C4.301, TECHNICAL BROCHURE 440. *Use of Surge Arresters for Lightning Protection of Transmission Lines.* Cigré, 2010

[Cig13a] CIGRÉ WORKING GROUP A3.17, TECHNICAL BROCHURE 544. *MO Surge Arresters – Stresses and Test Procedures.* Cigré, 2013

[Cig13b] CIGRÉ WORKING GROUP C4.407, TECHNICAL BROCHURE 549. *Lightning Parameters for Engineering Applications.* Cigré, 2013

[Cla99] CLARKE, D. R. *Varistor Ceramics.* In: Journal of the American Ceramic Society, volume 82(3): pp. 485–502, 1999. ISSN 1551-2916

[Dar94] DARVENIZA, M.; ROBY, D. and TUMMA, L. R. *Laboratory and analytical studies of the effects of multipulse lightning current on metal oxide arresters.* In: IEEE Transactions on Power Delivery, volume 9(2): pp. 764–771, 1994. ISSN 0885-8977

[Dar97] DARVENIZA, M.; TUMMA, L. R.; RICHTER, B. and ROBY, D. A. *Multipulse Lightning Currents and Metal-Oxide Arresters.* In: IEEE Transactions on Power Delivery, volume 12(3): pp. 1168–1175, 1997. ISSN 0885-8977

[Dar98] DARVENIZA, M. and SAHA, T. *Surface Flashovers on Metal-Oxide Varistor Blocks.* In: IEEE 6th International Conference on Conduction and Breakdown in Solid Dielectrics, pp. 406–409. 1998

[Dar00] DARVENIZA, M.; SAHA, T. and WRIGHT, S. *Comparisons of In-Service and Laboratory Failure Modes of Metal-Oxide Distribution Surge Arresters.* In: IEEE Power Engineering Society Winter Meeting, volume 3, pp. 2093–2100. 2000

[Den98] DENGLER, K. *Impulsalterung von Metalloxidableitern und ihre Überwachung im Betrieb.* Dissertation, Universität Stuttgart, 1998

[Eda84] EDA, K. *Destruction mechanism of ZnO varistors due to high currents.* In: Journal of Applied Physics, volume 56(10): pp. 2948–2955, 1984. ISSN 0021-8979

[Eda88]   EDA, K. *Progress in Fabrication Technology of Zinc Oxide Varistors.* In: *Advances in Varistor Technology. Conference Proceedings of the 2nd International Varistor Conference*, pp. 10–21. 1988

[Eda89]   EDA, K. *Zinc Oxide Varistors.* In: IEEE Electrical Insulation Magazine, volume 5(6): pp. 28–30, 1989. ISSN 0883-7554

[Ein79]   EINZINGER, R. *Grain Junction Properties of ZnO Varistors.* In: Applications of Surface Science, volume 3(3): pp. 390–408, 1979. ISSN 0378-5963

[Ein82]   EINZINGER, R. *Nichtlineare elektrische Leitfähigkeit von dotierter Zinkoxid-Keramik.* Dissertation, Technische Universität München, 1982

[FH03]   FERNANDEZ-HEVIA, D.; DE FRUTOS, J.; CABALLERO, A. C. and FERNANDEZ, J. *Bulk-Grain Resistivity and Positive Temperature Coefficient of ZnO-Based Varistors.* In: Applied Physics Letters, volume 82(2): pp. 212–214, 2003. ISSN 0003-6951

[FI08]   FRIGURA-ILIASA, M. and TAMAS, A. *A Few Aspects about the Manufacturing Process of Five and Two Additives Metal Oxides Varistors.* In: Chemical Bulletin of "POLITEHNICA" University of Timisoara, volume 53(67): pp. 282–285, 2008

[Fin02]   VON FINCKENSTEIN, K. G. F.; LEHN, J.; SCHELLHAAS, H. and WEGMANN, H. *Arbeitsbuch Mathematik für Ingenieure, Band II Differentialgleichungen, Funktionentheorie, Numerik und Statistik.* Teubner, 1st edition, August 2002

[Fuj82]   FUJIWARA, Y.; SHIBUYA, Y.; IMATAKI, M. and NITTA, T. *Evaluation of Surge Degradation of Metal Oxide Surge Arrester.* In: IEEE Transactions on Power Apparatus and Systems, volume PAS-101(4): pp. 978–985, 1982. ISSN 0018-9510

[Gre86]   GREUTER, F.; BLATTER, G.; ROSSINELLI, M. and SCHMÜCKLE, F. *Bulk and Grain Boundary Defects in Polycrystalline ZnO.* In: Materials Science Forum, volume 10-12: pp. 235–240, 1986

[Gre88]   GREUTER, F.; BLATTER, G.; ROSSINELLI, M. and STUCKI, F. *Conduction mechanism in ZnO-varistors: an overview.* In: *Advances in Varistor Technology. proc. sec. inter. Varistor conf.*, pp. 31–53. 1988

[Gre90]   GREUTER, F. and BLATTER, G. *Electrical properties of grain boundaries in polycrystalline compound semiconductors.* In: Semiconductor Science and Technology, volume 5(2): p. 111, 1990

Bibliography

[Gup90]   GUPTA, T. K. *Application of Zinc Oxide Varistors.* In: Journal of the American Ceramic Society, volume 73(7): pp. 1817–1840, 1990. ISSN 1551-2916

[Had90]   HADDAD, A.; FUENTES-ROSADO, J.; GERMAN, D. and WATERS, R. *Characterisation of ZnO surge arrester elements with direct and power frequency voltages.* In: IEE Proceedings, volume 137(5): pp. 269–279, September 1990

[Had04]   HADDAD, A. and D.F., W., eds. *Advances in High Voltage Engeineering.* The Institution of Engineering and Technology, 2004

[Had05]   HADDAD, A.; WATERS, R.; GERMAN, D. M. and ABDUL-MALEK, Z. *Current disparity in multi-column surge arresters.* In: IEE Proceedings Generation, Transmission and Distribution, volume 152(6): pp. 945–951, 2005. ISSN 1350-2360

[Har95]   HARTUNG, J.; ELPELT, B. and KLÖSENER, K. *Statistik.* Lehr- und Handbuch der angewandten Statistik. Oldenburg, München, 10th edition, 1995

[Hau84]   HAUSCHILD, W. and MOSCH, W. *Statistik für Elektrotechniker.* VEB Technik Berlin, 1st edition, 1984

[He07]   HE, J. and HU, J. *Discussions on Nonuniformity of Energy Absorption Capabilities of ZnO Varistors.* In: IEEE Transactions on Power Delivery, volume 22(3): pp. 1523–1532, 2007. ISSN 0885-8977

[He11]   HE, J.; LI, C.; HU, J. and ZENG, R. *Deep Suppression of Switching Overvoltages in AC UHV Systems Using Low Residual Arresters.* In: IEEE Transactions on Power Delivery, volume 26(4): pp. 2718–2725, 2011. ISSN 0885-8977

[Hei01]   HEINRICH, C. and HINRICHSEN, V. *Diagnostics and monitoring of metal-oxide surge arresters in high-voltage networkscomparison of existing and newly developed procedures.* In: IEEE Transactions on Power Delivery, volume 16(1): pp. 138–143, 2001. ISSN 0885-8977

[Hie74]   HIEDA, S.; KOBAYASI, M.; FURUYA, N.; KONDO, N.; MITANI, K. and AIZAWA, T. *Gapless Arrester for Power Use.* In: Meiden Jiho, volume 119(6): pp. 65–72, 1974. This paper was originally published in Japanese. The English translation "Gapless Lightning Arresters for Power Systems" was published in Meiden review 46 (1975), No. 2, pp. 17–24.

[Hin07]   Hinrichsen, V.; Reinhard, M. and Richter, B. *Energy Handling Capability of High-Voltage Metal-Oxide Surge Arresters Part 1: A Critical Review of the Standards.* In: *Cigré SCA3 International Technical Colloquium.* 2007

[Hin11]   Hinrichsen, V. *Metalloxid-Ableiter in Hochspannungsnetzen.* Siemens AG, 3rd edition, 2011

[Hof13]   Hofstätter, M.; Nevosad, A.; Teichert, C.; Supancic, P. and Danzer, R. *Voltage polarity dependent current paths through polycrystalline ZnO varistors.* In: Journal of the European Ceramic Society, volume 33(15-16): pp. 3473–3476, 2013. ISSN 0955-2219

[Ish04]   Ishii, M.; Yokoyama, S.; Imai, Y. and Hongo, Y. *Lightning Protection of Pole-Mounted Transformer on Japanese MV Lines.* In: *Cigré Paris Session.* 2004

[Kan83]   Kan, M.; Nishiwaki, S.; Sato, T.; Kojima, S. and Yanabu, S. *Surge Discharge Capability and Thermal Stability of a Metal Oxide Surge Arrester.* In: IEEE Transactions on Power Apparatus and Systems, volume 102(2): pp. 282–289, 1983. ISSN 0018-9510

[Kle04]   Klein, T. *Einflüsse auf das Energieaufnahmevermögen von Metalloxidableitern.* Dissertation, Universität Stuttgart, February 2004

[Lat83]   Lat, M. V. *Thermal Properties of Metal Oxide Surge Arresters.* In: IEEE Transactions on Power Apparatus and Systems, volume 102(7): pp. 2194–2202, 1983. ISSN 0018-9510

[Leh85]   Lehn, J. and Wegmann, H. *Einführung in die Statistik.* Teubner, Stuttgart, 3rd edition, 1985. ISBN 3519020717

[Lev76]   Levinson, L. M. and Philipp, H. R. *High-frequency and high-current studies of metal oxide varistors.* In: Journal of Applied Physics, volume 47(7): pp. 3116–3121, 1976

[Mar96]   Martinez, M. L. B. and Zanetta, L. *Comments on Metal Oxide Surge Arresters Surges Energy Absorption Capacity.* In: *IEEE International Symposium on Electrical Insulation,* volume 2, pp. 498–501. 1996. ISSN 1089-084X

[Mic70]   Michio, M. *Non-Linear Resistor,* February 1970. Pr.: US Ser. Nr. 637492 05/16/1966

Bibliography

[Ols89a] OLSSON, E. and DUNLOP, G. L. *Characterization of individual interfacial barriers in a ZnO varistor material.* In: Journal of Applied Physics, volume 66(8): pp. 3666–3675, 1989

[Ols89b] OLSSON, E. and DUNLOP, G. L. *The effect of Bi2O3 content on the microstructure and electrical properties of ZnO varistor materials.* In: Journal of Applied Physics, volume 66(9): pp. 4317–4324, 1989

[Pik81] PIKE, G. E. *Electronic Properties of ZnO Varistors: A New Model.* In: Proceedings of the Materials Research Society, volume 5: pp. 369–379, January 1981

[Rei08] REINHARD, M. *Experimentelle Untersuchungen zum Einzelimpulsenergieaufnahmevermögen von Metalloxidwiderständen eingesetzt in Hochspannungsnetzen unter Berücksichtigung eines komplexen Fehlerkriteriums.* Dissertation, Technische Universität Darmstadt, December 2008

[Rin97] RINGLER, K. G.; KIRKBY, P.; ERVEN, C.; LAT, M. V. and MALKIEWICZ, T. A. *The Energy Absorption Capability and Time-to-Failure of Varistors Used in Station-Class Metal-Oxide Surge Arresters.* In: IEEE Transactions on Power Delivery, volume 12(1): pp. 203–212, 1997. ISSN 0885-8977

[Roc09] ROCKS, A. *Einsatz von Metalloxid-Varistoren zum Überspannungsschutz pulsumrichtergespeister Drehfeldmaschinen.* Dissertation, Technische Universität Darmstadt, December 2009

[Sak89] SAKSHAUG, E. C.; BURKE, J. and KRESGE, J. *Metal oxide arresters on distribution systems: fundamental considerations.* In: IEEE Transactions on Power Delivery, volume 4(4): pp. 2076–2089, 1989. ISSN 0885-8977

[Sch94] SCHAUMBURG, H. *Werkstoffe und Bauelemente der Elektrotechnik, Keramik.* Teubner, Stuttgart, 5th edition, 1994

[Shi79] SHIRLEY, C. G. and PAULSON, W. M. *The pulse-degradation characteristic of ZnO varistors.* In: Journal of Applied Physics, volume 50(9): pp. 5782–5789, 1979. ISSN 0021-8979

[Stu87] STUCKI, F.; BRÜESCH, P. and GREUTER, F. *Electron Spectroscopic Studies of Electrically Active Grain Boundaries in ZnO.* In: Surface Science, volume 189/190: pp. 294–299, 1987. ISSN 0039-6028

[Stu90] STUCKI, F. and GREUTER, F. *Key role of oxygen at zinc oxide varistor grain boundaries.* In: Applied Physics Letters, volume 57(5): pp. 446–448, 1990. ISSN 0003-6951

[Swe89] SWEETANA, A.; RADFORD, K.; JOHNSON, R. and HENSLEY, S. *High Energy Metal Oxide Valve Blocks.* In: Varistor Technology, volume 3: pp. 240–247, 1989

[Wan98] WANG, H.; BARTKOWIAK, M.; MODINE, F. A.; DINWIDDIE, R. B.; BOATNER, L. A. and MAHAN, G. D. *Nonuniform Heating in Zinc Oxide Varistors Studied by Infrared Imaging and Computer Simulation.* In: Journal of the American Ceramic Society, volume 81(8): pp. 2013–2022, 1998. ISSN 1551-2916

[Wil62] WILKS, S. *Mathematical Statistics.* Wiley, 1962

[Won80] WONG, J. *Sintering and varistor characteristics of ZnO-Bi$_2$O$_3$ ceramics.* In: Journal of Applied Physics, volume 51(8): pp. 4453–4459, 1980

Relevant Standards

[IEC60143-2] *Series capacitors for power systems – Part 2: Protective equipment for series capacitor banks*

[IEC60060-1] *High-voltage test techniques – Part 1: General definitions and test requirements*

[IEC-37/416/FDIS] *IEC 60099-4/Ed3: Surge arresters – Part 4: Metal-oxide surge arresters without gaps for a.c. systems* published as new standard in June 2014

[IEC60099-4] *Surge arresters – Part 4: Metal-oxide surge arresters without gaps for a.c. systems*

[IEC60099-5] *Surge arresters – Part 5: Selection and application recommendations*

[IEC60099-8] *Surge arresters – Part 8: Metal-oxide surge arresters with external series gap (EGLA) for overhead transmission and distribution lines of a.c. systems above 1 kV*

[IEC-37/417/FDIS] *IEC 60099-9/Ed1: Surge arresters – Part 9: Metal-oxide surge arresters without gaps for HVDC converter stations* published as new standard in June 2014

[IEEEC62.22-2009] *IEEE Guide for the Application of Metal-Oxide Surge Arresters for Alternating-Current Systems*

[IEEEC62.11-2012] *IEEE Standard for Metal-Oxide Surge Arresters for AC Power Circuits (>1 kV)*

Publications as Author or Coauthor

[Cig13]   CIGRÉ WORKING GROUP A3.17, HINRICHSEN, V. AND REINHARD, M.
(SUPPORTED BY TUCZEK, M. N.), TECHNICAL BROCHURE 544. *MO Surge
Arresters – Stresses and Test Procedures, Chapter 3: Energy handling capability
of MO surge arresters.* Cigré, 2013

[Den10]   DENZ, F.; GJONAJ, E.; WEILAND, T.; TUCZEK, M. N. and HINRICHSEN, V.
Electric and Thermal Reaction of Zinc Oxide to Current Impulses. In: *30th
International Conference on Lightning Protection, paper 6B-1331.* 2010

[Göh10]   GÖHLER, R.; SCHUBERT, M.; WECK, K. H.; HINRICHSEN, V.; TUCZEK,
M. N.; CLEMENS, M. and APPEL, R. *Special Requirements on Surge Arrester
Design for UHV A.C. Systems above 800 kV System Voltage.* In: *Cigré
Conference, Report A3-104-2010.* Cigré, 2010

[Göh11]   GÖHLER, R.; TUCZEK, M. N. and HINRICHSEN, V. *Optimierung der
Potentialverteilung von MO-Überspannungsableitern durch externe Steuerung.* In:
*ETG-Workshop: Feldsteuernde Isoliersysteme, Werkstoffe, Design, Prüfung und
Simulation. ISBN 978-3-8007-3390-3.* 2011

[Hin09]   HINRICHSEN, V.; TUCZEK, M. N. and REINHARD, M. *Recent Experimental
Findings on the Energy Handling Capability of Metal-Oxide Varistors for
High-Voltage Applications.* In: *World Congress on Insulators, Arresters and
Bushings.* January 2009

[Hin12]   HINRICHSEN, V. and TUCZEK, M. N. *Surge arresters for insulation coordination
in UHV power systems – related problems and solutions.* In: Elektrotechnik und
Informationstechnik: e & i, volume 129(5): pp. 326–331, 2012

[Tuc09]   TUCZEK, M. N.; REINHARD, M. and HINRICHSEN, V.
*Energieaufnahmevermögen von Metalloxidvaristoren eingesetzt in
Überspannungsableitern elektrischer Energieversorgungsnetze.* In: *RCC*

Fachtagung Werkstoffe "Forschung und Entwicklung neuer Technologien zur Anwendung in der elektrischen Energietechnik". May 2009

[Tuc13a] TUCZEK, M. N. and HINRICHSEN, V. *Recent Experimental Findings on the Single and Multi-Impulse Energy Handling Capability of Metal-Oxide Varistors for Use in High-Voltage Surge Arresters*, 2013. IEEE Transactions on Power Delivery, submitted and accepted 09/18/2013. DOI: 10.1109/TPWRD.2013.2283911

[Tuc13b] TUCZEK, M. N. AND HINRICHSEN, V., TECHNICAL BROCHURE OF THE CIGRÉ WORKING GROUP A3.25, CHAPTER. *Energy handling capability of MO surge arresters*, submitted 10/22/2013. Publication planned for 2015.

[Tuc14] TUCZEK, M. N.; BRÖKER, M.; HINRICHSEN, V. and GÖHLER, R. *Experimental investigations on the effects of continuous operating voltage stress and a.c. energy injection on current sharing among parallel connected MO varistor columns (as used in FACTS) in a highly non-linear regime of the voltage-current-characteristic*, 2014. IEEE Transactions on Power Delivery, submitted and accepted 10/18/2014. DOI: 10.1109/TPWRD.2014.2365045

Student Research Papers Supervised by the Author

[Böl10] BÖLKE, M. *Experimentelle Untersuchung der Stromaufteilung parallel belasteter MO-Varistoren eingesetzt in elektrischen Energieversorgungsnetzen.* Bachelor thesis, TU Darmstadt, 2010

[Dür10] DÜREN, A. *Auswirkungen von Temperaturschiefverteilungen auf die thermische Stabilität eines 550 kV-Überspannungsableiters.* Student research project, TU Darmstadt, 2010

[Gie11] GIESSEL, M. *Doppelimpulsenergieaufnahmevermögen von MO"=Varistoren.* Student research project, TU Darmstadt, 2011

[Gol09] GOLDE, K. *Auswirkungen repetierender Wechselstromenergieeinträge auf MO-Varistoren eingesetzt in Überspannungsableitern elektrischer Energieversorgungsnetze.* Student research project, TU Darmstadt, 2009

[Hal12] HALLAS, M. *Temperaturabhängigkeit im Durchbruchsbereich der UI-Kennlinie von kommerziellen MO-Varistoren der Hochspannungsebene.* Diploma thesis, TU Darmstadt, 2012. Winner of the .... IEEE PES Germany Chapter - Werner von Siemens - Best Diploma / Master Thesis Award 2013

[Kac11] KACZMAREK, D. *Experimentelle Untersuchungen zur Abhängigkeit der Temperaturschiefverteilung sowie der thermischen Stabilität ungesteuerter Überspannungsableiter der Hochspannungsebene von der Umgebungstemperatur.* Student research project, TU Darmstadt, 2011

[Mus09] MUSCHALLE, S. *Thermische Untersuchungen an einem Überspannungsableiter der 1200 kV-Ebene.* Student research project, TU Darmstadt, 2009

[Nur11] NUREDINI, M. *Thermische Untersuchungen zur Reduktion des Steuerringsystems von Überspannungsableitern der Hochspannungsebene.* Diploma thesis, TU Darmstadt, 2011

Student Research Papers Supervised by the Author

[Sch13] SCHWERT, M. *Praktische Untersuchung des Energieaufnahmevermögens von temperierten MO-Varistoren.* Bachelor thesis, TU Darmstadt, 2013

[Tsc11] TSCHECHONADSHIJ, D. *Aufbau und Inbetriebnahme eines Versuchsstandes zur beschleunigten Prüfung von Varistoren.* Student research project, TU Darmstadt, 2011

[Ufe11] UFER, M. *Untersuchung der Kennlinienalterung von MO-Varistoren durch Wechselstromenergieeinträge.* Master thesis, TU Darmstadt, 2011